

**INDOLE SYNTHESIS: KNOEVENAGEL\HEMETSBERGER REACTION
SEQUENCE**

**SUZUKI COUPLING REACTIONS OF BASIC NITROGEN CONTAINING
SUBSTRATES**

A Thesis
Presented to
The Academic Faculty

By

William L. Heaner IV

In Partial Fulfillment
Of the Requirements for the Degree
Doctor of Philosophy in Chemistry

Georgia Institute of Technology

August 2013

Copyright © William L. Heaner IV 2013

Indole Synthesis: Knoevenagel/Hemetsberger Reaction Sequence
Suzuki Coupling Reactions of Basic Nitrogen Containing Substrates

Approved by:

Dr. Charles L. Liotta, Advisor
School of Chemistry and Biochemistry
Georgia Institute of Technology

Dr. Stefan A. France
School of Chemistry and Biochemistry
Georgia Institute of Technology

Dr. Wendy L. Kelly
School of Chemistry and Biochemistry
Georgia Institute of Technology

Dr. Charles A. Eckert
School of Chemical and Biochemical
Engineering
Georgia Institute of Technology

Dr. Christopher Jones
School of Chemical and Biochemical
Engineering
Georgia Institute of Technology

Date Approved: June 11, 2013

ACKNOWLEDGEMENTS

I am very grateful for the opportunities I have had at the Georgia Institute of Technology. The instruction I have received here has prepared me well for the challenges that lie ahead. I am also grateful to AMPAC™ Fine Chemical and The Dow Chemical Company for their funding support and research opportunities.

I would like to thank Drs. Charles Liotta and Charles Eckert for the opportunity to be a part of their research team. Because of their leadership and inspiration I have become a better scientist, communicator, and leader. I would especially like to thank Dr. Liotta. He is an extremely gifted individual who has the rare ability to effectively impart his knowledge and wisdom to others. From my interactions and discussions with Dr. Liotta I have become a more proficient chemist. He has taught me how to clearly communicate ideas, whether giving a presentation or writing a manuscript. His example of excellence is something I have strived for and will continue to do so throughout my life. I am very grateful for the time he has devoted to mentoring me, and it was great honor to have worked for him.

I would also like to thank Dr. Pamela Pollet for the insight she has provided to me as well as the encouragement and support. I certainly benefitted from exchanging ideas with her, and she was a great resource for honing my laboratory skills.

Teamwork is a cornerstone of success in research, and I would be remiss to not thank my group members for their work and support, especially Carol Gelbaum. Being able to exchange ideas and laugh together has made this experience very enjoyable. One

of the greatest blessings in life is to be able to do what you enjoy with people you like, and that was certainly the case for me while I was here at Georgia Tech.

Finally, I would like to thank my family for their love and support. My parents and my in-laws have been an immeasurable help to Sarah and me throughout our time in Atlanta. My greatest sense of gratitude, though, is to Sarah, my loving wife. She was a tremendous source of strength and inspiration for me. Graduate school is challenging and demanding, and I was so blessed to have her by my side throughout. As this chapter of my life comes to a close, we both look forward to the first time in our lives together that neither of us is in school!

TABLE OF CONTENTS

ACKNOWLEDGEMENT	iii
LIST OF TABLES	ix
LIST OF FIGURES	x
LIST OF SYMBOLS AND ABBREVIATIONS	xiv
LIST OF SCHEMES	xv
SUMMARY	xviii
CHAPTER 1: Knoevenagel Condensation and Hemetsberger Indolization	1
1.1 Indoles: An Overview	1
1.1.1 The Indole Structure and Its Importance	1
1.1.2 Methods of Indole Synthesis	3
1.2 Hemetsberger-Knittel Indolization	13
1.2.1 Hemetsberger-Knittel Indolization Overview	14
1.2.2 Hemetsberger Indolization: Modifications and Extensions	16
1.3 The Hemetsberger Indolization Process	19
1.3.1 Reaction Sequence	19
1.3.1.1 Synthesis of Alkyl Azidoacetates	21
1.3.2 Improving the Hemetsberger-Hemetsberger Reaction Sequence	22
1.3.2.1 Knoevenagel Condensation	23
1.3.2.2 Prior Art for α -azido- β -arylacrylate Synthesis	26
1.3.3 Circumventing Ester Hydrolysis in the Knoevenagel Condensation	28
1.3.3.1 Strategy 1: Inorganic Base and a Dehydrating Agent	28

1.3.3.2 Strategy 2: Base-stable Benzoxazole Protecting Group	30
1.3.3.3 Sacrificial Electrophiles	32
1.3.3.4 Substrate Screening	37
1.3.4 Stereochemistry of the α -azido- β -arylacrylates	39
1.3.5 Regioselectivity in the Hemetsberger Indolization	43
1.3.5.1 Origins of Regioisomers	43
1.3.5.2 Differential Scanning Calorimetry of the α -azido- β -arylacrylates	44
1.3.5.3 Regioselectivity Results	47
1.3.5.4 Pyrolysis of Crude α -azido- β -arylacrylates	50
1.4 Conclusions	54
1.5 Recommendations	55
1.6 Experimental	55
CHAPTER 2: Suzuki Coupling Reactions	124
2.1 Suzuki Coupling Reactions	124
2.1.1 Overview	124
2.1.1.1 Mechanism	125
2.1.1.1.1 Transmetallation	127
2.1.1.1.2 The Role of Base	128
2.1.2 Challenges and Improvements of the Suzuki Couplings	131
2.1.2.1 Bulky, Electron Rich Ligands Enhance Catalyst Activity	131
2.1.2.2 Phase Behavior and Catalyst Separation and Recycling	132
2.1.2.3 Ligand Free Suzuki Couplings	134
2.1.2.4 Catalyst De-activation by Substrates Containing Basic Nitrogens	136

2.3 In situ Reversible Protection of Basic Nitrogens with CO ₂	140
2.3.1 Properties and Current Applications of CO ₂	140
2.3.1.1 Physical and Chemical Properties of CO ₂	140
2.4 CO ₂ as an <i>In situ</i> , Reversible Protecting Reagent in Suzuki Couplings	142
2.4.1 Overview	142
2.4.1.1 The Effect of Water on Suzuki Couplings	144
2.4.1.2 Base Screening for Suzuki Coupling Reactions that will employ CO ₂	146
2.4.2 Suzuki Couplings of Substrates Containing Basic Nitrogens	149
2.4.2.1 Suzuki Couplings under 30.6 atmospheres of CO ₂ Pressure	149
2.4.2.2 Evaluating mono-, di-, and tribasic potassium phosphates	154
2.4.2.3 Suzuki couplings with 4-amino-2-bromopyridine as a function of P _{CO₂}	156
2.4.2.4 Suzuki couplings with 4-amino-2-chloropyridine at 30.6 atm CO ₂	158
2.4.2.5 Effect of amino-bromopyridine substitution pattern on yield	159
2.4.2.6 Role of CO ₂ in Suzuki couplings	160
2.5 Conclusions	162
2.6 Recommendations	164
2.7 Experimental	165
2.7.1 General Information	165
2.7.1.1 Reactions with Pd(OAc) ₂	165
2.7.1.2 Reactions with Pd(PPh ₃) ₄	166
2.7.1.3 General procedure for Suzuki reactions in a Parr reactor	166
2.7.1.4 Calibration Curves	167
CHAPTER 3: Ligand Free Suzuki Coupling Reactions	171

3.1 Ligand free Suzuki Coupling Reactions in Aqueous Systems	171
3.1.1 Introduction and Motivation	171
3.1.2 Ligand free Suzuki couplings in water	172
3.1.2.1 Temperature Optimization	174
3.1.3 Ligand free Suzuki Couplings in a Water:Co-solvent System	175
3.1.3.1 Ligand free Suzuki Coupling in Tetramethylurea (TMU)	175
3.1.3.2 Evaluation of Effects of Co-solvent...	178
3.1.4 Conclusion and Reccomendations	181
3.1.5 Experimental Procedures	182
3.1.5.1 Suzuki Reactions in Water	182
3.1.5.2 General Procedure for Suzuki Reactions in Water, Water:TMU...	182
3.1.5.3 Calibration Curves	183
REFERENCES	185

LIST OF TABLES

Table 1. Effect of sacrificial electrophiles (SE) on the condensation...	33
Table 2. Stoichiometry and temperature optimization	35
Table 3. Substrate Screening	38
Table 4. Exothermic events of α -azido- β -arylacrylates measured by DSC	46
Table 5. Hemetsberger indolization yields...	48
Table 6. Comparison of Knoevenagel-Hemetsberger process...	51
Table 7. Base strength ($\text{pK}_a(\text{BH}^+)$) relative to pK_a of phenylboronic acid	119
Table 8. Effect of Water (v/v%) on Suzuki coupling reactions	145
Table 9. Organic base screening	148
Table 10. Suzuki coupling under 30.6 atm CO_2 in acetonitrile water...	150
Table 11. Effect of potassium phosphate bases on product yield under 1 atm N_2	151
Table 12. Effect of CO_2 on the coupling of 4-amino-2-phenylpyridine...	158
Table 13. Yield and appearance of aqueous, ligand free Suzuki couplings	174
Table 14. Temperature optimization...	175
Table 15. Optimization of water:TMU Suzuki coupling	177
Table 16. Yield of 4-methoxybiphenyl as a function of co-solvent	179
Table 17. Yield of 4-aminobiphenyl as a function of co-solvent	180

LIST OF FIGURES

Figure 1. Suzuki coupling reaction mechanism	xx
Figure 2. Indole skeleton and pertinent examples	2
Figure 3. Indole skeleton and substituent positions	3
Figure 4. Extensions of the Hemetsberger indolization	18
Figure 5. ^1H (Z)-ethyl- α -azido- β -arylacrylate	40
Figure 6. $^3\text{J}_{\text{C}=\text{O},\text{H}}$ coupling	41
Figure 7. ^1H - ^{13}C Coupled NMR: carbonyl signal from...	42
Figure 8. DSC: (Z)-ethyl α -azido- β -(m-chlorophenyl)acrylate (2d)	45
Figure 9. Stereoisomers of pyrrolindoles	49
Figure 10. ^1H NMR: (Z)-Ethyl α -azido- β -phenylacrylate (2a)	67
Figure 11. ^{13}C NMR: (Z)-Ethyl α -azido- β -phenylacrylate (2a)	68
Figure 12. $^3\text{J}_{\text{C},\text{H}}$ of ^1H - ^{13}C Coupled NMR: (Z)-Ethyl-...	69
Figure 13. ^1H NMR: (Z)-Ethyl <i>meta</i> -methyl- α -azido- β -phenylacrylate (2b)	70
Figure 14. ^{13}C NMR: (Z)-Ethyl <i>meta</i> -methyl- α -azido- β -phenylacrylate (2b)	71
Figure 15. ^1H - ^{13}C Coupled NMR: (Z)-Ethyl <i>meta</i> -methyl-... (2b)	72
Figure 16. $^3\text{J}_{\text{C},\text{H}}$ of ^1H - ^{13}C Coupled NMR: (Z)-Ethyl <i>meta</i> -methyl-...(2b)	73
Figure 17. ^1H NMR: (Z)-Ethyl <i>meta</i> -methoxy- α -azido- β -phenylacrylate (2c)	74
Figure 18. ^{13}C NMR: (Z)-Ethyl <i>meta</i> -methoxy- α -azido- β -phenylacrylate (2c)	75
Figure 19. ^1H - ^{13}C Coupled NMR: (Z)-Ethyl <i>meta</i> -methoxy-...(2c)	76
Figure 20. $^3\text{J}_{\text{C},\text{H}}$ of ^1H - ^{13}C Coupled NMR: (Z)-Ethyl <i>meta</i> -methoxy-...(2c)	77
Figure 21. ^1H NMR: (Z)-Ethyl <i>meta</i> -chloro- α -azido- β -phenylacrylate (2d)	78

Figure 22.	^{13}C NMR: (Z)-Ethyl <i>meta</i> -chloro- α -azido- β -phenylacrylate (2d)	79
Figure 23.	^1H - ^{13}C Coupled NMR: (Z)-Ethyl <i>meta</i> -chloro-...(2d)	80
Figure 24.	$^3\text{J}_{\text{C,H}}$ of ^1H - ^{13}C Coupled NMR: (Z)-Ethyl <i>meta</i> -chloro-...(2d)	81
Figure 25.	^1H NMR: (Z)-Ethyl <i>meta</i> -phenyl- α -azido- β -phenylacrylate (2e)	82
Figure 26.	^{13}C NMR: (Z)-Ethyl <i>meta</i> -phenyl- α -azido- β -phenylacrylate (2e)	83
Figure 27.	^1H - ^{13}C Coupled NMR: (Z)-Ethyl <i>meta</i> -phenyl-...(2e)	84
Figure 28.	$^3\text{J}_{\text{C,H}}$ of ^1H - ^{13}C Coupled NMR: (Z)-Ethyl <i>meta</i> -phenyl-...(2e)	85
Figure 29.	^1H NMR: (Z)-Ethyl <i>meta</i> -nitro- α -azido- β -phenylacrylate (2f)	86
Figure 30.	^{13}C NMR: (Z)-Ethyl <i>meta</i> -nitro- α -azido- β -phenylacrylate (2f)	87
Figure 31.	^1H - ^{13}C Coupled NMR: (Z)-Ethyl <i>meta</i> -nitro-...(2f)	88
Figure 32.	$^3\text{J}_{\text{C,H}}$ of ^1H - ^{13}C Coupled NMR: (Z)-Ethyl <i>meta</i> -nitro-...(2f)	89
Figure 33.	^1H NMR: (Z)-Ethyl <i>para</i> -methyl- α -azido- β -phenylacrylate (2g)	90
Figure 34.	^{13}C NMR: (Z)-Ethyl <i>para</i> -methyl- α -azido- β -phenylacrylate (2g)	91
Figure 35.	^1H NMR: (2Z,2'Z)-diethyl 3,3'-(1,3-phenylene)bis...(2h)	92
Figure 36.	^{13}C NMR: (2Z,2'Z)-diethyl 3,3'-(1,3-phenylene)bis...(2h)	93
Figure 37.	$^3\text{J}_{\text{C,H}}$ of ^1H - ^{13}C Coupled NMR: ... (2h)	94
Figure 38.	^1H NMR: (2Z,2'Z)-diethyl 3,3'-(1,4-phenylene)bis... (2i)	95
Figure 39.	^{13}C NMR: (2Z,2'Z)-diethyl 3,3'-(1,4-phenylene)bis... (2i)	96
Figure 40.	$^3\text{J}_{\text{C,H}}$ of ^1H - ^{13}C Coupled NMR: ... (2i)	97
Figure 41.	^1H NMR: (Z)-ethyl 2-azido-3-(furan-2-yl)acrylate (2j)	98
Figure 42.	^{13}C NMR: (Z)-ethyl 2-azido-3-(furan-2-yl)acrylate (2j)	99
Figure 43.	^1H - ^{13}C Coupled NMR: (2j)	100
Figure 44.	$^3\text{J}_{\text{C,H}}$ of ^1H - ^{13}C Coupled NMR: (Z)-ethyl 2-azido-3-(furan-2-yl)acrylate	101

Figure 45. ¹ H NMR: (Z)-ethyl 2-(3-nitrobenzamido)-3-(3-nitrophenyl)acrylate	102
Figure 46. ¹³ C NMR: (Z)-ethyl 2-(3-nitrobenzamido)-3-(3-nitrophenyl)acrylate	103
Figure 47. Mass Spectroscopy (EI+): (Z)-ethyl 2-(3-nitrobenzamido)-3...	104
Figure 48. ¹ H NMR, 3j	105
Figure 49. ¹³ C NMR, 3j	106
Figure 50. ¹³ C NMR, 124-125 ppm, 3j	107
Figure 51. ¹³ C-DEPT NMR, 3j	108
Figure 52. ¹³ C-DEPT NMR, 124-126 ppm, 3j	109
Figure 53. ¹ H- ¹³ C HMQC, 3j	110
Figure 54. ¹ H- ¹ H COSY and ¹ H- ¹³ C HMQC Overlay, 3j	111
Figure 55. ¹ H- ¹³ C HMBC, 3j	112
Figure 56. DSC: Ethyl azdioaceate (1)	113
Figure 57. DSC: (Z)-Ethyl α-azido-β-phenylacrylate (2a)	114
Figure 58. DSC: (Z)-Ethyl meta-methyl-α-azido-β-phenylacrylate (2b)	115
Figure 59. DSC: (Z)-Ethyl meta-methoxy-α-azido-β-phenylacrylate (2c)	116
Figure 60. DSC: (Z)-Ethyl meta-chloro-α-azido-β-phenylacrylate (2d)	117
Figure 61. DSC: (Z)-Ethyl meta-phenyl-α-azido-β-phenylacrylate (2e)	118
Figure 62. DSC: (Z)-Ethyl meta-nitro-α-azido-β-phenylacrylate (2f)	119
Figure 63. DSC: (Z)-Ethyl para-methyl-α-azido-β-phenylacrylate (2g)	120
Figure 64. DSC: (2Z,2'Z)-diethyl 3,3'-(1,3-phenylene)bis(2-azidoacrylate) (2h)	121
Figure 65. DSC: (2Z,2'Z)-diethyl 3,3'-(1,4-phenylene)bis(2-azidoacrylate) (2i)	122
Figure 66. DSC: (Z)-ethyl 2-azido-3-(furan-2-yl)acrylate (2j)	123
Figure 67. Generalized Suzuki coupling reaction	124

Figure 68. Reductive elimination via pentavalent Pd complex	130
Figure 69. Biarylphosphine ligands	132
Figure 70. Water-soluble ligands used in Suzuki couplings	133
Figure 71. Complexation of Pd catalyst with starting material...	137
Figure 72. Reaction or interaction of CO ₂ with a 4-amino-2-halo-pyridine	143
Figure 73. Yield of 4-amino-2-phenylpyridine as a function of time and % water	154
Figure 74. Suzuki coupling of 4-amino-2-phenylpyridine as a function of P _{CO2}	157
Figure 75. GC-FID Calibration Curve: 4-amino-2-phenylpyridine	167
Figure 76. GC-FID Calibration Curve: 4-amino-2-bromopyridine	168
Figure 77. HPLC Calibration Curve: Biphenyl	168
Figure 78. HPLC Calibration Curve: Bromobenzene	169
Figure 79. HPLC Calibration Curve: 4-Bromotoluene	169
Figure 80. HPLC Calibration Curve: 4-Methylbiphenyl	170
Figure 81. Substrates employed in ligand free Suzuki couplings in water	172
Figure 82. GC/MS Calibration Curve: 4-Methoxybiphenyl	183
Figure 83. GC/MS Calibration Curve: 4-Aminobiphenyl	184
Figure 84. GC/MS Calibration Curve: 4-Bromoaniline	184

LIST OF SYMOBLS AND ABBREVIATIONS

ACN	acetonitrile
atm	atmosphere
Boc	<i>tert</i> -butyloxy carbonyl
Bz	benzyl
CV	cyclic voltammetry
DBU	1,8-diazabicycloundec-7-ene
DIPEA	N,N-diisopropylethylamine
DME	dimethoxyethane
DMF	<i>N,N</i> -dimethylformamide
DMF-DMA	<i>N,N</i> -dimethylformamide dimethylacetal
EF	ethyl formate
ETCIA	ethyl trichloroacetate
ETFA	ethyl trifluoroacetate
HMBC	Heteronuclear Multiple Bond Correlation
HSQC	Heteronuclear Single Quantum Coherence
L	ligand
Ra-Ni	Raney nickel
sc	supercritical
SE	sacrificial electrophile
TM	transition metal
TMG	tetramethylguanidine
TMU	tetramethylurea
TPP	triphenylphosphine
ϵ	dielectric constant

LIST OF SCHEMES

Scheme 1. Knoevenagel-Hemetsberger reaction sequence	xviii
Scheme 2. Regiospecific ormsation of <i>anti</i> -pyrroloindoles	xix
Scheme 3. Indole Syntheses	4
Scheme 4. Fischer indole synthesis	6
Scheme 5. Origins of regioisomers in the Fischer indole synthesis	7
Scheme 6. Japp-Klingemann-Fischer indole synthesis	8
Scheme 7. Pd-catalyzed hydrazone arylation and Fischer indolization	9
Scheme 8. Leimgruber-Batcho and Reissert indole syntheses	11
Scheme 9. Indole syntheses by the Larock, and Madelung reactions	12
Scheme 10. Nenitzescu and Hemetsberger reactions	13
Scheme 11. Mechanism of the Hemetsberger indolization	15
Scheme 12. Origin of regioisomers in the Hemetsberger reaction	16
Scheme 13. Mechanism of Rh-catalyzed indolization	16
Scheme 14. Knoevenagel-Hemetsberger reaction sequence	20
Scheme 15. Ethyl 2-azidoacetate synthesis	22
Scheme 16. Decomposition of ethyl azidoacetate in the presence of sodium ethoxide	24
Scheme 17. Routes of Hydrolysis in the Knoevenagel Condensation	25
Scheme 18. Formation of α -azido- β -hydroxy- β -[2-furyl]propanoic acid side product	25
Scheme 19. Two step synthesis of α -azido- β -arylacrylates	27
Scheme 20. Knoevenagel condensation with inorganic bases	29
Scheme 21. Condensation of ethylazidoacetate and benzaldehyde by Cs_2CO_3	29

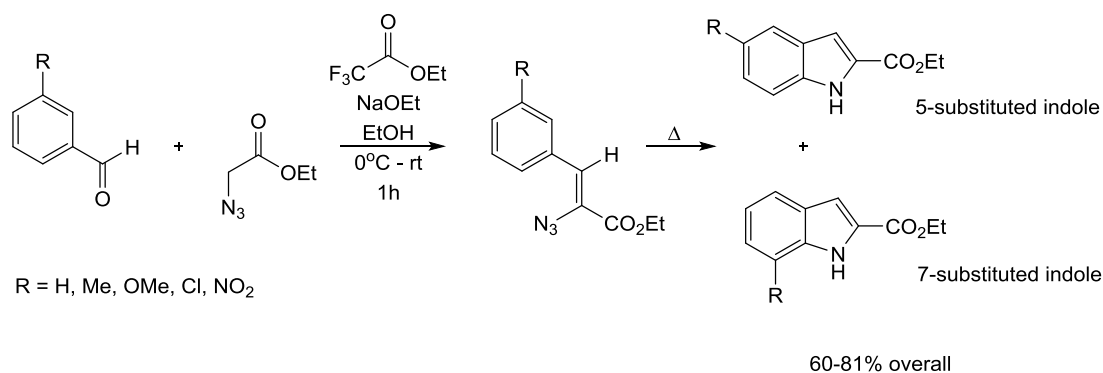
Scheme 22. Reaction sequence utilizing a benzoxazole protecting group	31
Scheme 23. The role of a sacrificial electrophile in a model Knoevenagel reaction	32
Scheme 24. Stereochemistry in the Knoevenagel condensation	39
Scheme 25. Regioisomer formation	44
Scheme 26. Side product formation in thermolysis	53
Scheme 27. Suzuki cross-coupling mechanism	126
Scheme 28. Proposed transmetallation pathways	127
Scheme 29. Aqueous base equilibrium in a Suzuki coupling	129
Scheme 30. Water soluble Suzuki ligand in the arylation of a halonucleoside	134
Scheme 31. Microwave-assisted Suzuki coupling reaction	135
Scheme 32. Suzuki couplings in water and water:DMF	136
Scheme 33. Suzuki coupling of a free amino pyridine under standard conditions	138
Scheme 34. Suzuki coupling with a protected aminopyridine	139
Scheme 35. Reaction of an amine with CO ₂	141
Scheme 36. CO ₂ as a protecting reagent in nucleophilic substitution	142
Scheme 37. Suzuki coupling reactions as a function of water content (v/v %)	145
Scheme 38. Suzuki coupling reaction use in organic base screening	147
Scheme 39. Suzuki coupling of 4-amino-2-bromopyridine under 450 psi CO ₂	149
Scheme 40. Potassium phosphate-carbonic acid equilibrium	152
Scheme 41. Suzuki coupling of 4-amino-2-phenylpyridine using K ₃ PO ₄	153
Scheme 42. Suzuki coupling of 4-amino-2-bromopyridine	155
Scheme 43. Suzuki couplings as a function of CO ₂ pressure	157
Scheme 44. Effect of substitution pattern about aminopyridines	159

Scheme 45. Suzuki coupling volume expansion simulation	161
Scheme 46. Suzuki coupling, decreased dielectric constant simulation	162
Scheme 47. Ligand free Suzuki couplings in water	173
Scheme 48. Suzuki coupling of 4-bromoanisole in water:TMU	177
Scheme 49. Suzuki couplings as a function of co-solvent	179

SUMMARY

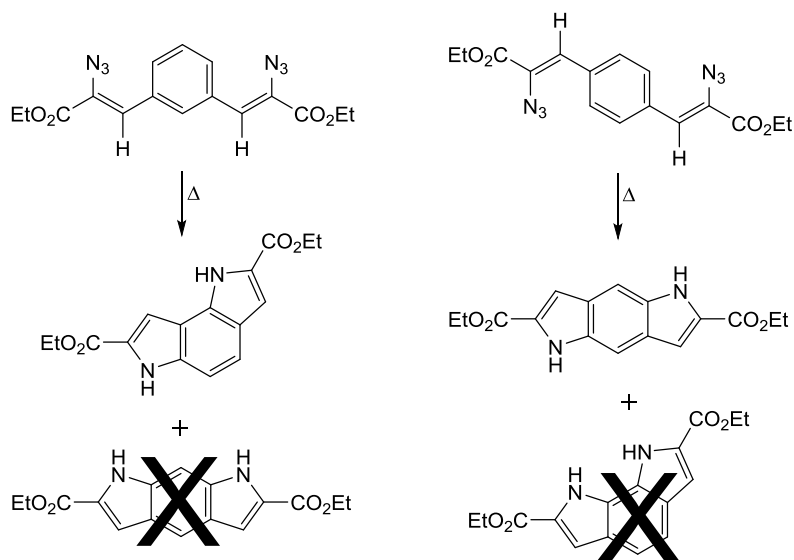
INDOLE SYNTHESIS: KNOEVENAGEL-HEMETSBERGER REACTION SEQUENCE

A series of substituted indoles have been synthesized by the sequential reaction of aromatic aldehydes with ethyl azidoacetate in the presence of sodium ethoxide to form the corresponding ethyl α -azido- β -arylacrylates (Knoevenagel process) followed by a solvent-mediated thermolysis (Hemetsberger process) (Scheme 1). The isolated yields of the ethyl α -azido- β -arylacrylates were significantly increased when employing the sacrificial electrophile ethyl trifluoroacetate. This is the first reported use of a sacrificial species to prevent hydrolysis in a base-catalyzed condensation reaction. This strategy could be applicable to other similar reactions offering potential cost-saving opportunities in additional industrial processes as well. ^1H NMR and coupled ^1H - ^{13}C NMR analysis of the ethyl α -azido- β -arylacrylates indicate that the condensation is stereospecific—only the *Z*-isomer could be detected.



Scheme 1. Knoevenagel-Hemetsberger reaction sequence

Solvent-mediated thermal treatment of the *meta*-substituted ethyl α -azido- β -arylacrylates resulted in the formation of both the 5- and 7- substituted indoles—the 5-regioisomer being slightly favored over the 7-regioisomer. Analogous thermal treatment of (2*Z*, 2*Z'*)-diethyl 3,3'-(1,3-phenylene)bis(2-azidoacrylate) and (2*Z*, 2*Z'*)-diethyl 3,3'-(1,4-phenylene)bis(2-azidoacrylate) exclusively produced pyrroloindoles, diethyl 1,5-dihydropyrrolo[2,3-*f*]indole-2,6-dicarboxylate and diethyl 1,6-dihydropyrrolo[2,3-*e*]indole-2,7-dicarboxylate, respectively (Scheme 2). Results are also reported which indicate that the α -azido- β -arylacrylates can be used in the subsequent Hemetsberger indolization process without prior purification.



Scheme 2. Regiospecific formation of *anti*-pyrroloindoles

SUZUKI COUPLING REACTIONS OF BASIC NITROGEN CONTAINING SUBSTRATES

Organic substrates containing basic nitrogen centers have been problematic in achieving high yields in the Suzuki coupling process. The origin of this issue is attributed to the complexation of the basic nitrogen center with the palladium catalyst. As a consequence, the use of CO₂ at a variety of pressures was evaluated as a reversible protecting/activating reagent for basic nitrogen containing substrates. In general, the Suzuki coupling reaction has many variables associated with it (Figure 1). These include catalyst precursor, the temperature of reaction, base, the solvent system (amount of water), and the specific halogen being substituted (chloro vs. bromo).

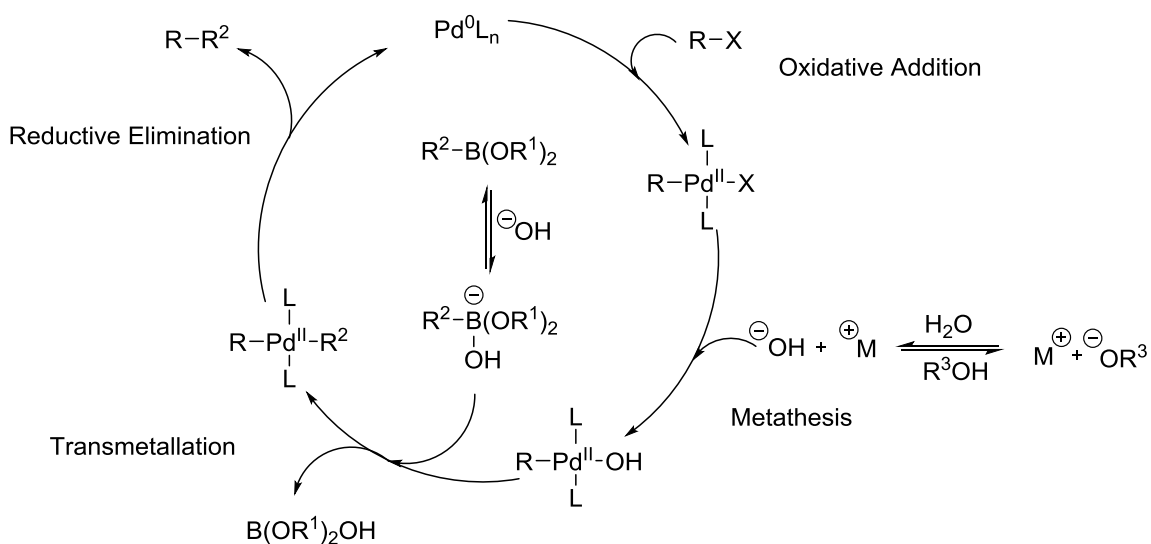


Figure 1. Suzuki coupling reaction mechanism

In the research presented in this thesis, another variable was added to the preceding list, this variable being the CO₂ pressure. Substrates with and without basic nitrogen centers

were explored. The following observations and conclusions were reached. (1) The use of small amounts of water, 2.5 vol%, significantly improves the rate and yield of Suzuki coupling reactions. (2) The presence of water is critical to having an efficient Suzuki coupling reaction in reaction media that exhibit solid-liquid heterogeneity, liquid-liquid heterogeneity, or homogeneity. (3) Organic and inorganic bases were screened in the absence of CO₂, and the most effective bases were found to be K₂CO₃, K₃PO₄, and TEA. However, in the presence of aqueous CO₂, careful selection of the base is essential due to formation of bicarbonate and the associated decrease in the amount water. K₃PO₄ was found to be the most effective base in the presence of CO₂. (4) The yield of product in the Suzuki coupling of 4-amino-2-bromopyridine with phenylboronic acid was evaluated as a function of CO₂ pressure. Compared to reactions in the absence of CO₂, the yield of product increased at all pressures of CO₂ (6.8, 17, and 30.6 atm)—from 15% with no CO₂ to 73% with 30.6 atm of CO₂. (5) The changes CO₂ imparts on the reaction volume and the reaction medium's dielectric constant were independently evaluated. The volume expansion and decrease in dielectric constant of the reaction mixture imparted by CO₂ do not account for the enhanced yields. Even though the concept of CO₂ protection/activation is demonstrated on Suzuki coupling reactions, this strategy could also be applicable to other reactions as well (e.g. Heck cross couplings, selective Buchwald-Hartwig cross couplings, condensation reactions, or Michael additions). Therefore, the use of CO₂ as an *in situ*, reversible protecting reagent could enable a variety of more sustainable reaction processes.

CHAPTER 1: KNOEVENAGEL CONDENSATION AND HEMETSBERGER INDOLIZATION

1.1 Indoles: An Overview

1.1.1 The Indole Structure and Its Importance

The indole skeleton is a key structural component in many molecules. These include natural products, pharmaceutical compounds, dyes, agricultural compounds, cosmetics, nutraceuticals, and flavourings.¹⁻³ A few pertinent examples of compounds containing the indole moiety are below in Figure 1. Melatonin and serotonin are natural product indoles that are important in animal life. Melatonin is a hormone secreted by the pineal gland in the brain. It helps regulate our circadian rhythm, functions as an antioxidant, and some people even take it as a dietary supplement to assist with sleep problems.⁴ Serotonin, derived from the essential amino acid tryptophan, is a neurotransmitter linked to mood and appetite regulation.⁵ Natural product indoles such as these and indoles containing isoprene units are commonly termed indole alkaloids.

Indole-containing compounds are also used in medicine and agriculture. Cediranib is a pharmaceutical candidate that is being evaluated in clinical trials for its anti-brain tumor activity.^{6,7} Vincristine, a Federal Drug Administration-approved medicine, is used to treat cancers such as lymphoma and leukemia. Other approved drugs include indomethacin and frovatriptan.³ Indole-3-carbinol is found in cruciferous vegetables such as broccoli and is thought to help prevent cancers and have antioxidant properties. An agricultural product containing an indole is amisulbrom which is used to

protect grapes and potatoes from fungi.⁸

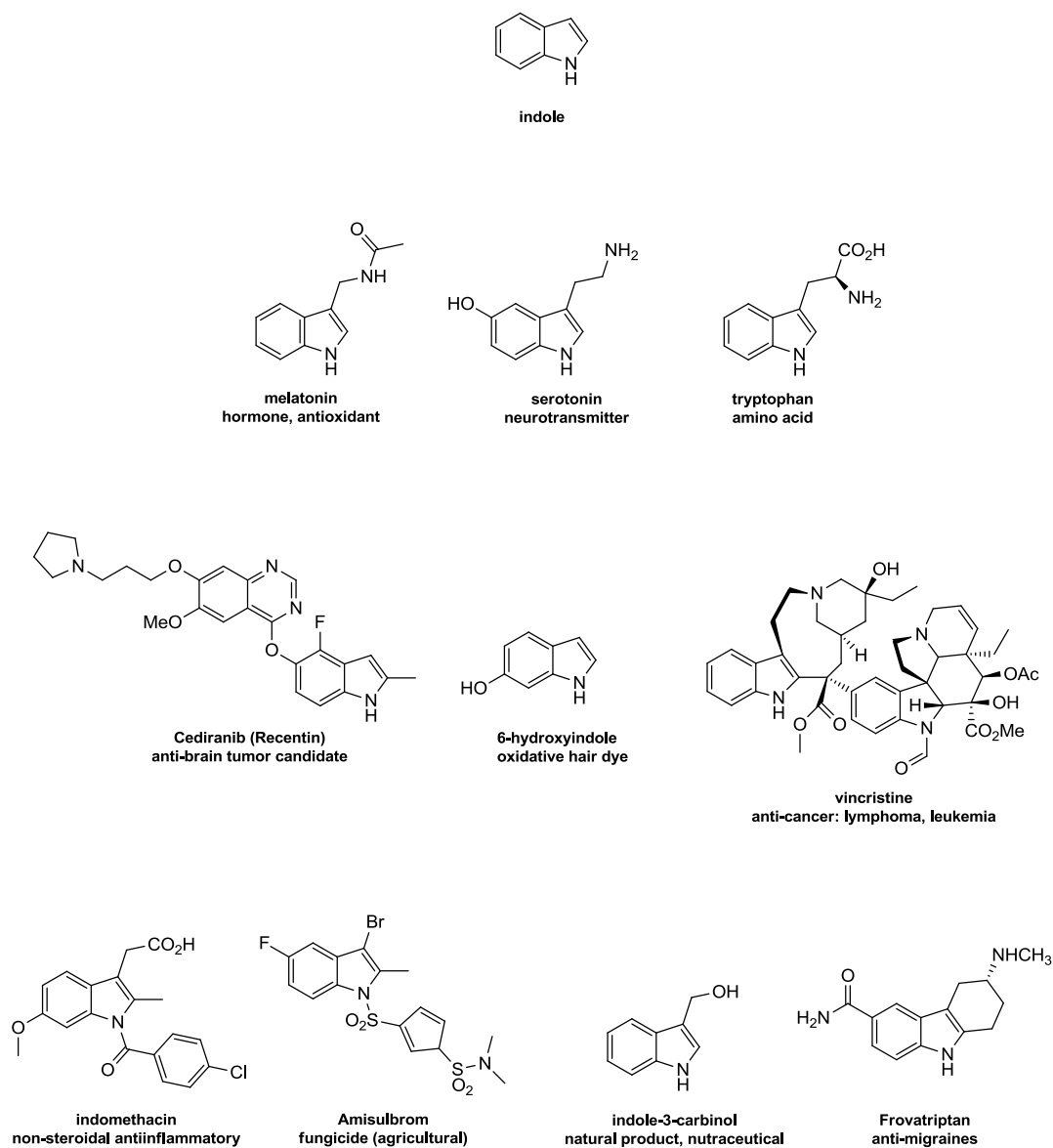


Figure 2. Indole skeleton and pertinent examples

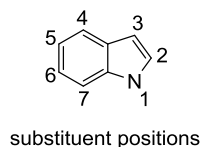


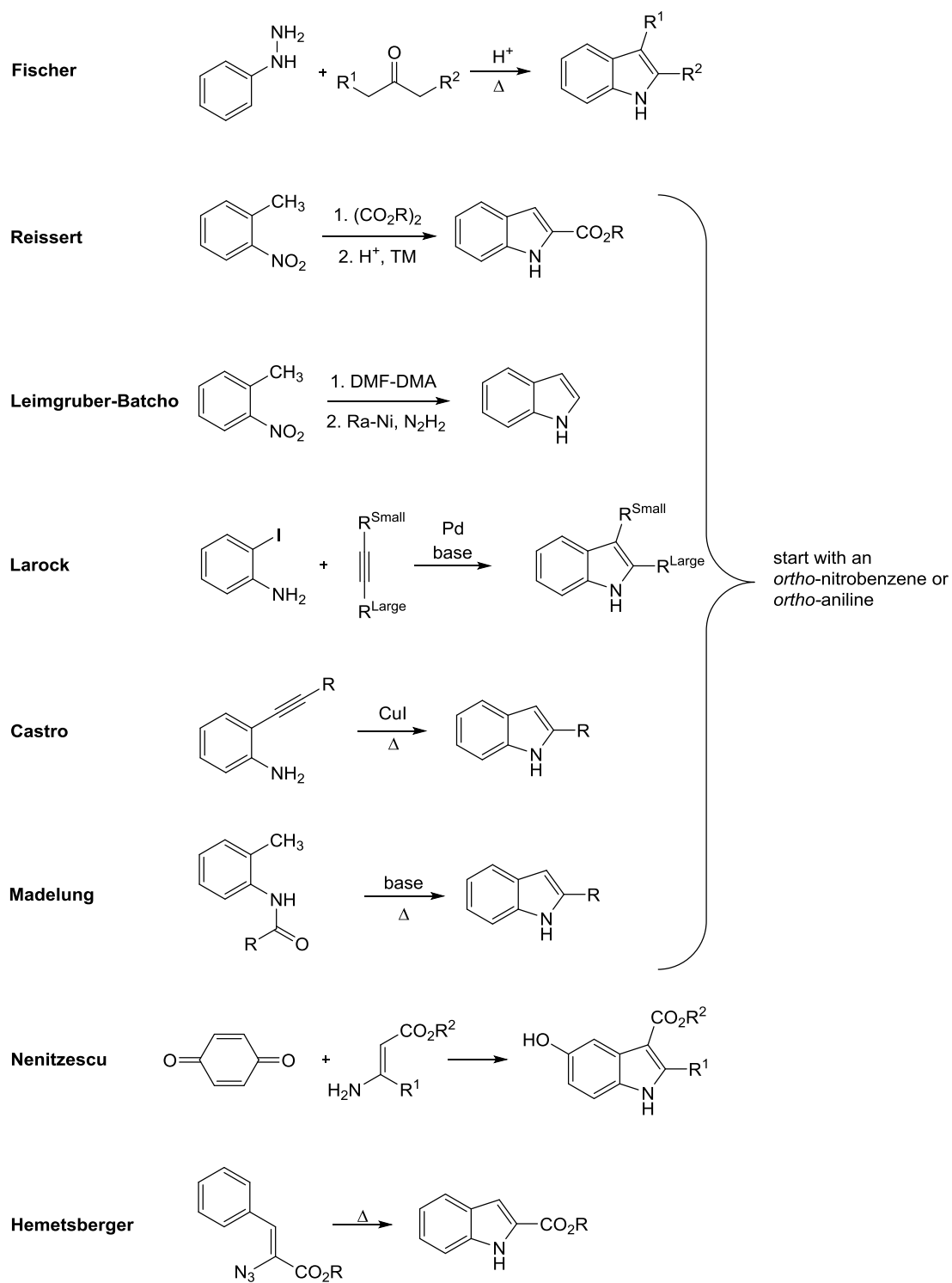
Figure 3. Indole skeleton and substituent positions

The indole skeleton is a fused bicyclic ring with seven substituent positions numbered as in Figure 3. As the few examples in Figure 2 illustrate, the substitution pattern around the indole ring varies greatly, both in complexity and extent. Indoles have ten π -electrons and obey Hückel's rules for aromaticity. The structure is weakly acidic having a pK_a of 20.96 (in dimethylsulfoxide).⁹ The lone pair electrons of the nitrogen are delocalized into the π -system, and the carbon at position three is the most nucleophilic and readily participates in electrophilic aromatic substitution reactions.

1.1.2 Methods of Indole Synthesis

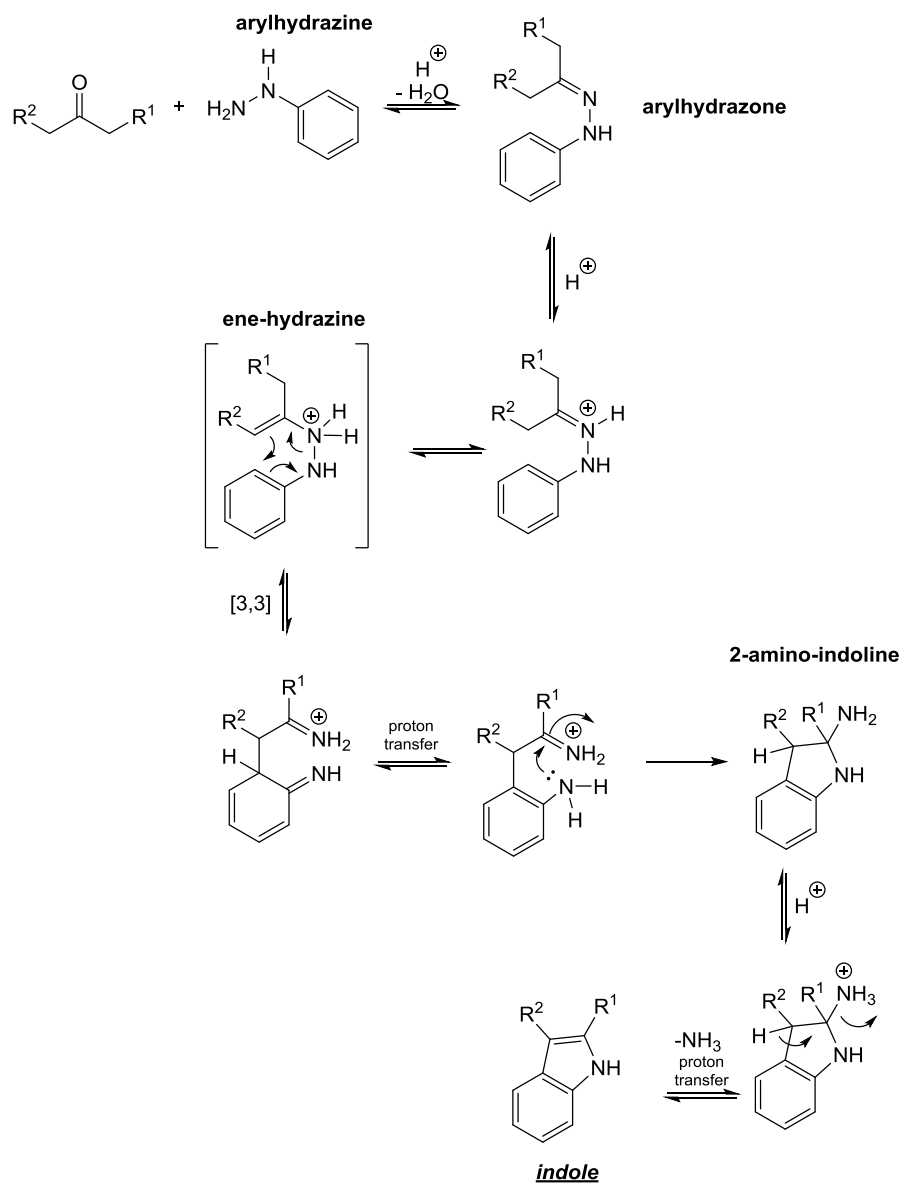
The prevalence of complex indoles has led to the development of a plethora of synthetic routes. Some of these methods include the Fischer¹⁰, Castro¹⁰, Leimgruber-Batcho^{11,12}, Larcok¹³, Reissert^{2,10}, Madelung¹⁴, Hemetsberger-Knittel^{15,16}, and Nenitzescu¹⁰ syntheses. As Moody pointed out, indole syntheses can be grouped into two categories: those that start with *ortho* substituted arenes, typically *o*-nitrobenzenes or *o*-aniline derivatives, and those that don't.² A brief and general summary of these syntheses can be found below in Scheme 3.

Indole Synthesis



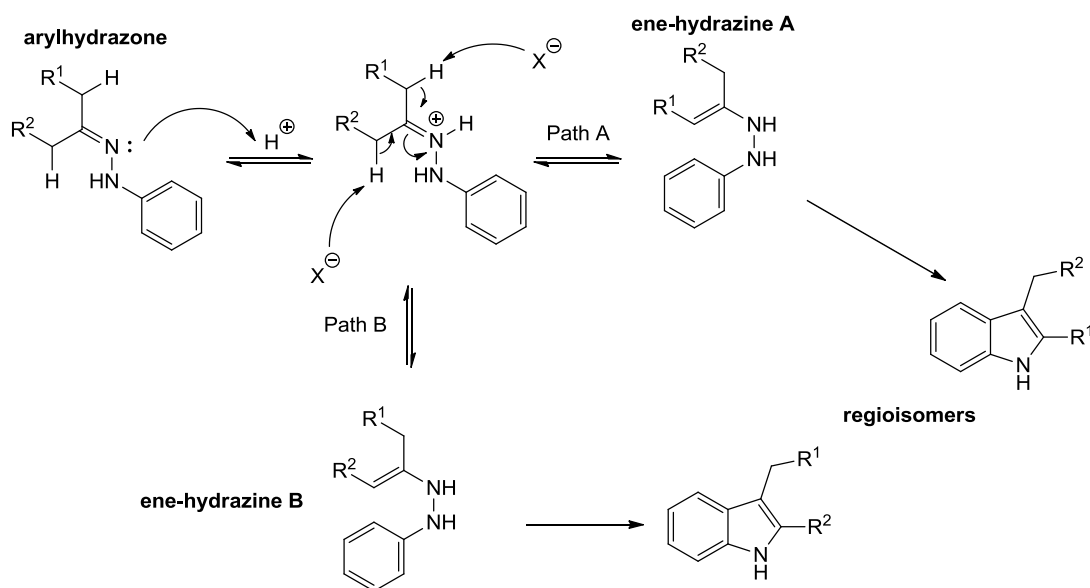
Scheme 3. Indole syntheses^{2,10}

The Fischer indole synthesis is often viewed as the quintessential method to construct an indole, having been around since in 1883 and finding widespread use in the laboratory and in industry.¹⁰ The Fischer mechanism is shown in Scheme 4. The first step is the condensation of an arylhydrazine and a ketone or aldehyde in the presence of an acid (Lewis or Brønsted) to produce an arylhydrazone. In the presence of the acid catalyst, the arylhydrazone then tautomerizes to an ene-hydrazine. The protonated ene-hydrazine then proceeds through a [3,3] sigmatropic rearrangement—an allowed pericyclic process. The driving force becomes re-aromatization and a 5-exo-trig (Baldwin's rules¹⁷) cyclization to form a 2-amino-indoline. The amino group of the indoline then coordinates to the acid catalyst, and the C3 carbon is deprotonated generating the indole with the accompanying loss of ammonia.



Scheme 4. Fischer indole synthesis

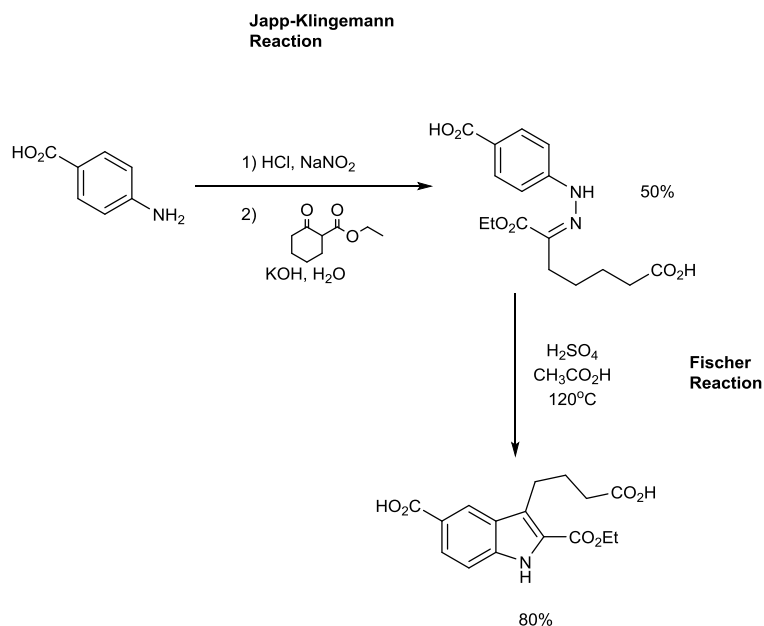
If an unsymmetrical ketone is used regioisomeric indoles are observed. The origins of the regioisomers are found in the tautomerization of the arylhydrazone. The arylhydrazone has two enolizable hydrogens; therefore, two constitutional isomers of the ene-hydrazine can form leading to the two regioisomeric indoles (Scheme 5).



Scheme 5. Origins of regioisomers in the Fischer indole synthesis

The Fischer synthesis is an attractive method because it employs mild reaction conditions, tolerates most functional groups, and the arylhydrazone intermediates do not require isolation.¹⁰ The aryl ring is often functionalized, but electron withdrawing groups may slow the reaction by increasing the activation energy necessary for the [3,3] rearrangement.¹⁸ One limitation that is frequently referred to in the literature is the lack of commercially available arylhydrazines; although, arylhydrazines may be synthesized

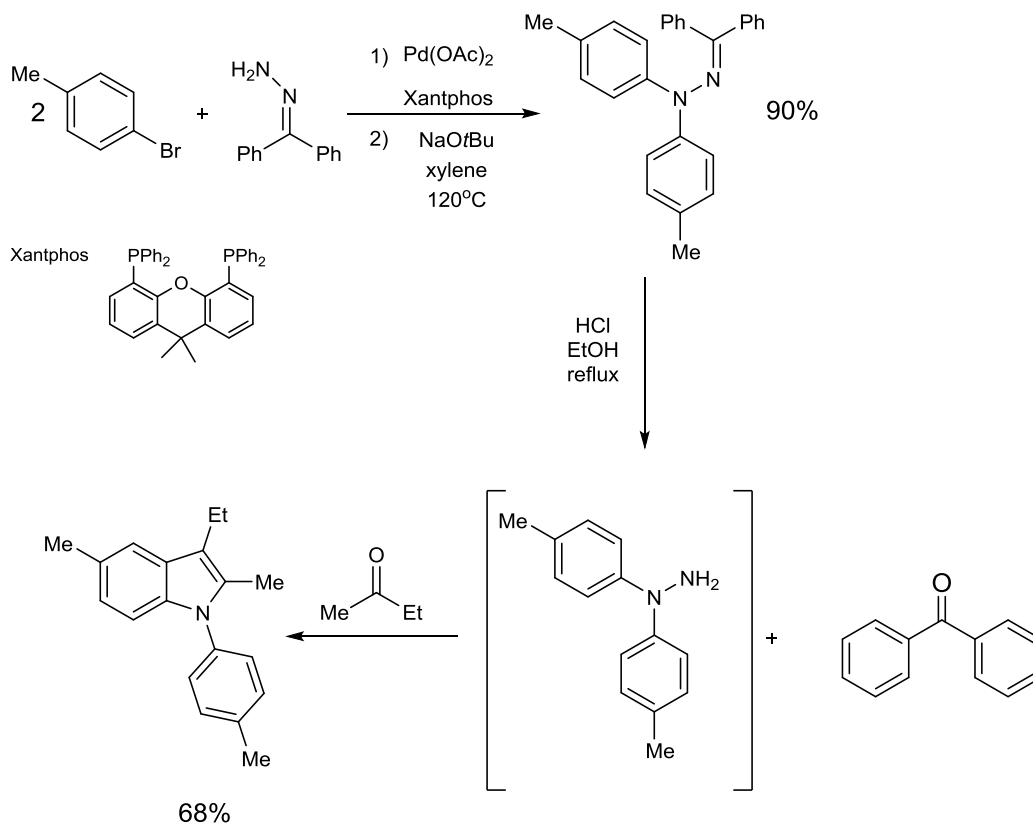
by the diazotization of anilines with nitrous acid followed by reduction with stannous chloride.¹⁹ Variations to the Fischer method have been developed to get around this lack of availability through alternative syntheses of the arylhydrazone intermediates. One such method is the Japp-Klingemann reaction in which an arylhydrazone is synthesized directly from β -keto-acids/esters and aryl diazonium salts thereby avoiding the need to synthesize an arylhydrazine all together. Scheme 6 shows the tandem use of the Japp-Klingemann and Fischer syntheses for the synthesis of an intermediate to a metabolite of vilazodone.²⁰



Scheme 6. Japp-Klingemann-Fischer indole synthesis

The first step is diazotization of the aniline to an aryl diazonium salt. Next, addition of ethyl 2-oxocyclohexane carboxylate led to the ring opening condensation to form the arylhydrazone which was then subjected to the Fischer indole synthesis in

sulfuric acid at 120°C. Another variation includes the palladium catalyzed Buchwald-Hartwig cross-coupling formation of functionalized arylhydrazones (Scheme 7).²¹



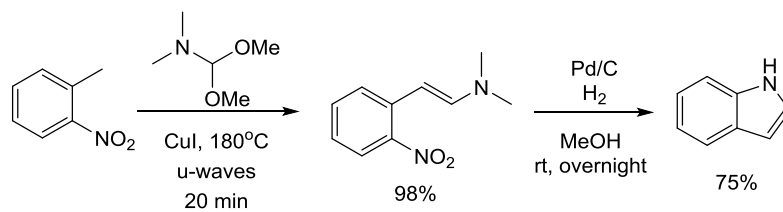
Scheme 7. Pd-catalyzed hydrazone arylation and Fischer indolization

Arylhydrazones can be thought of as protecting groups for arylhydrazines. Thus, an arylhydrazone can be functionalized then deprotected *in situ* to make the aryl hydrazine for the Fischer reaction. In this example, benzophenone hydrazone is arylated in the presence of Pd(OAc)₂ and the ligand Xantphos. The second step of the reaction

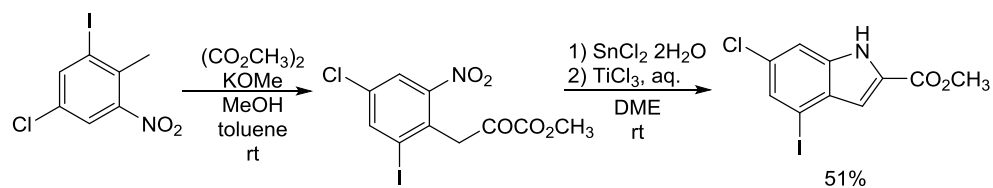
involved the *in situ*, acid promoted hydrolysis of the benzophenone arylhydrazone in the presence of 2-butanone generating the enolizable hydrazone which then afforded the indole. A more direct synthesis of this product would have started with methyl-ethylhydrazone instead of benzophenone hydrazone; however, the investigators selected the use of benzophenone hydrazone owing to its commercial availability, lower cost, increased stability²², and efficiency in their protocol.

The Leimbgruber-Batcho^{11,12,23} and Reissert^{2,24} indole syntheses, both start with an *ortho*-nitrotoluene (Scheme 8). The premise of both of these strategies is very similar. The *ortho* nitro group activates the methyl group for nucleophilic attack to create a new carbon-carbon bond. In the Leimgruber-Batcho reaction, the electrophile is commonly dimethylformamide dimethyl acetal. In the specific example shown, the investigators used a Lewis acid, copper iodide, and microwave heating to generate the enamine in twenty minutes with a 98% yield. The same reaction, but instead using conventional heating (110°C) and no Lewis acid, took twenty-two hours to achieve the same yield. In the Reissert reaction the electrophile is a di-alkyl oxalate. The next step in each method is a reductive cyclization forming a new carbon-nitrogen bond. Raney Nickel and hydrazine or H₂ in the presence of Pd/C are commonly employed to afford the cyclization in the Leimgruber-Batcho reaction. The Reissert synthesis employs a transition metal catalyst (Zn, Pt, Pd, Sn, Ti) and a proton source. These methods are advantageous because they allow for the specific formation of one indole isomer since the carbon-carbon and carbon-nitrogen bonds of the benzene ring are already present. This, however, is also a limitation because the method is completely reliant on *ortho*-nitrotoluenes.

Leimgruber-Batcho reaction



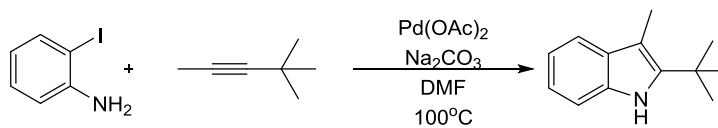
Reissert reaction



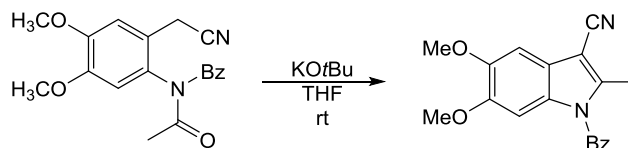
Scheme 8. Leimgruber-Batcho and Reissert indole syntheses^{23,24}

Indoles can also be constructed from anilines or phenylamides as in the Castro and Larock reactions or the Madelung reaction, respectively.^{13,25-27} An illustrative example of the Larock and Madelung reactions are below in Scheme 9.

Larock heteroannulation



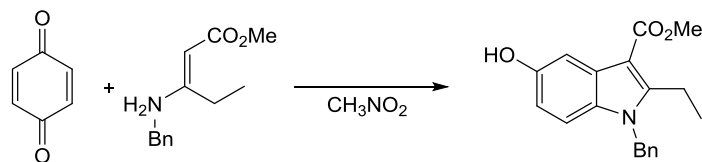
Madelung reaction



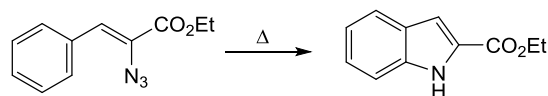
Scheme 9. Indole syntheses by the Larock and Madelung reactions

All of the previously discussed indole syntheses employ a starting material with a nitrogen atom already connected to the benzene ring (arylhazines, *o*-nitrobenzenes, or anilines).²⁸ In contrast, the Nenitzescu and Hemetsberger reactions (Scheme 10) install the C_{ring}-N bond.

Nenitzescu reaction



Hemetsberger reaction



Scheme 10. Nenitzescu and Hemetsberger reactions

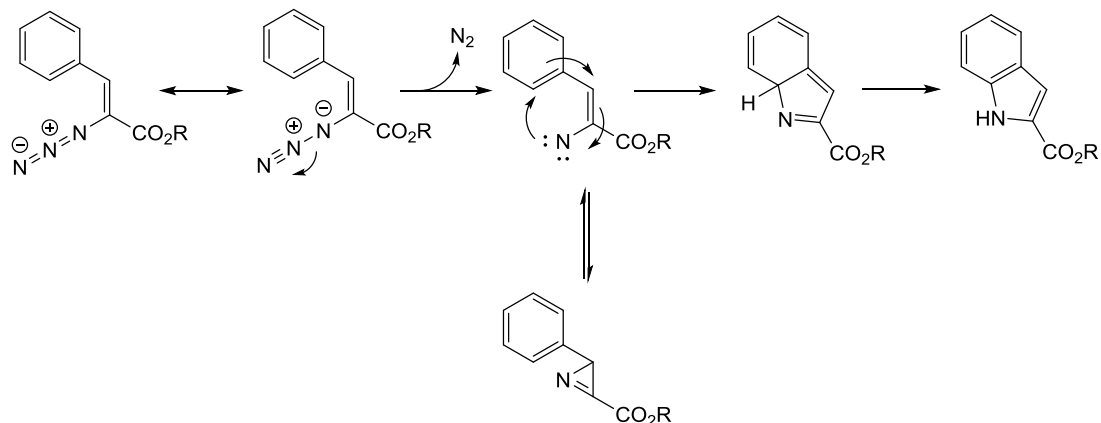
The Nenitzescu reaction is a condensation reaction between 3-aminocrotonates or enamines with 1,4-benzoquinone. This methodology is limited in scope compared to other syntheses because it only constructs 5-hydroxyindoles due to the requisite use of 1,4-benzoquinone. The Hemetsberger-Knittel indolization (henceforth referred to as the Hemetsberger indolization or Hemetsberger reaction) is the intramolecular cyclization of an α -azido- β -arylacrylate.¹⁵ With respect to other indole syntheses, this synthesis may be the simplest since it only requires heat to promote the cyclization of α -azido- β -arylacrylates via a nitrene.²⁹

1.2: Hemetsberger-Knittel Indolization

1.2.1 Hemetsberger-Knittel Indolization Overview

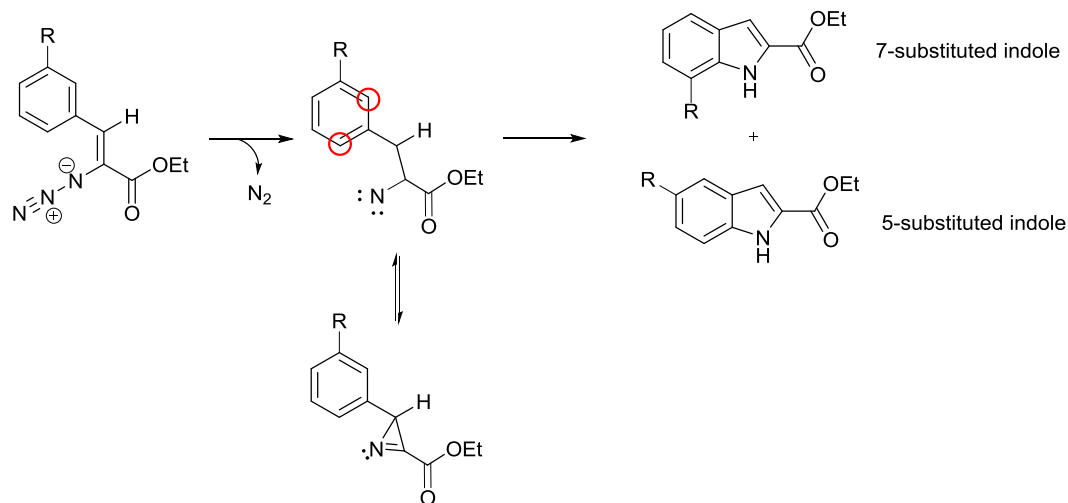
H. Hemetsberger and D. Knittel reported the thermally catalyzed intramolecular cyclization of α -azido- β -arylacrylates to indoles in near quantitative yields in 1970.¹⁵ The Hemetsberger-Knittel indolization is performed in solvents at temperatures of ~110°C - 150°C. The typical solvents that are used are toluene (bp 110°C), xylenes (bp 138-144°C), mesitylene (bp 165°C), and *ortho*-dichlorobenzene (bp 180°C). The benzene ring can have multiple substituents and they may include halogens, cyano, nitro, alkyl, aryl, alkoxy, carbonyl, and/or amino groups.^{15,16,30-32} Thus, this reaction is well suited for both laboratory and industrial uses. Moreover, from an industrial point of view, it can be conducted by a continuous flow process.³¹

The Hemetsberger indolization is based on nitrene chemistry. The first step in the mechanism is the thermal degradation of the α -azido- β -arylacrylate generating molecular nitrogen and a nitrene (Scheme 11). The nitrene is believed to be in equilibrium with an azirine intermediate. The final steps are insertion of the nitrene into the aromatic ring followed by a [1,5] hydrogen shift and re-aromatization forming the indole skeleton.



Scheme 11. Mechanism of the Hemetsberger indolization

D. Knittel isolated and characterized the azirine species formed from the thermolysis of α -azido- β -arylacrylates in cyclohexane at 80°C .¹⁶ It was shown that this species can subsequently be cyclized to the indole by heating in refluxing xylenes. If a *meta* substituent is present on the aromatic ring, then regioisomeric indoles are possible: a 7-substituted indole and a 5-substituted indole (Scheme 12).

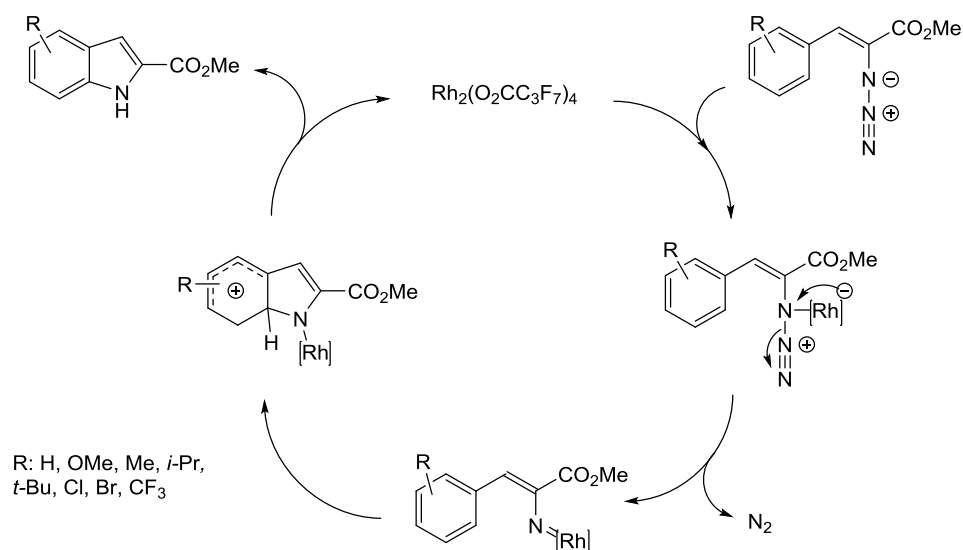


Scheme 12. Origin of regioisomers in the Hemetsberger reaction

The regioselectivity of the Hemetsberger reaction as not been established in the literature; therefore, part of my research includes investigating electronic and steric effects on the regioselectivity of indole formation.

1.2.2 Hemetsberger Indolization: Modifications and Extensions

In addition to the thermally induced reaction of α -azido- β -arylacrylates to indoles, a transition metal catalyzed process has also been published.^{33,34} Stokes reported that the use of rhodium(II) perfluorobutyrate allows for the cyclization to occur at lower temperatures of 40°C and 60°C (Scheme 13).³⁵



Scheme 13. Mechanism of Rh-catalyzed indolization³⁵

In the proposed mechanism, the rhodium catalyst coordinates to the vinyl nitrogen of the azide driving the loss of molecular nitrogen and formation of a nitrenoid intermediate. The nitrenoid then participates in an electrophilic attack on the aromatic ring generating the indole via the Wheland intermediate. The authors also reported that when a *meta*-chloro substituent was on the ring, the 5-indole was selectively formed over the 7-indole in a ratio of 87:13; and steric effects appeared to dominate the regioselectivity. As pointed out above, the regiochemistry accompanying the thermally induced Hemetsberger process has not, as yet been reported.

The insertion of nitrenes into sp^2 C-H bonds is well known.^{32,36,37} Consequently, the Hemetsberger indolization has been extended to include the synthesis of many heterocyclic compounds from α -azido- β -heteroaromatic-acrylates (Figure 4). These include but are not limited to pyrrolopyridines, furopyrroles, thienopyrroles, pyrrolopyrroles, pyrroloindoles, benzathiazines, isoquinolines, and benzoazepines.

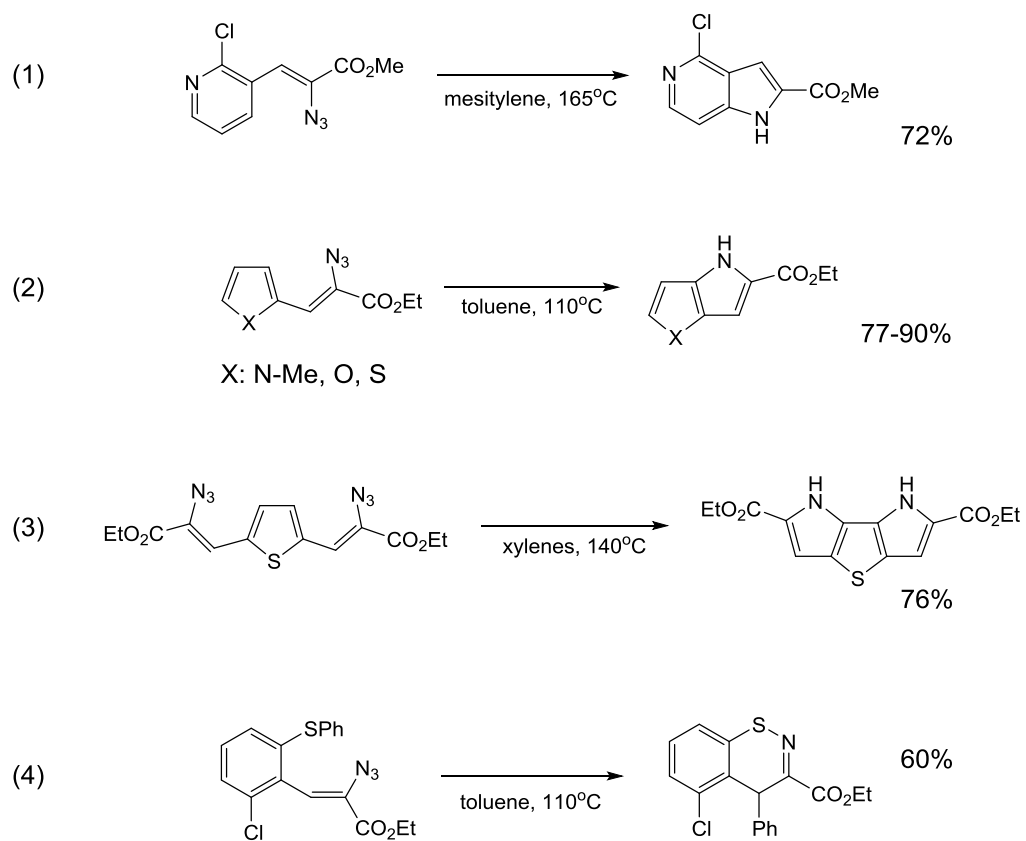


Figure 4. Extensions of the Hemetsberger indolization [(1)³⁸, (2)³⁹⁻⁴¹, (3)⁴⁰, (4)³²]

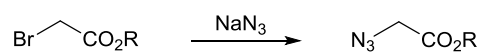
The Hemetsberger indolization and its modifications exhibit high regio- and chemoselectivity for nitrene insertion leading to various pyrrolo cycles. A major accomplishment of the Hemetsberger indolization process over other indole syntheses is that it provided the foundation for facile access to many heterocyclic skeletons.

1.3 The Hemetsberger Indolization Process

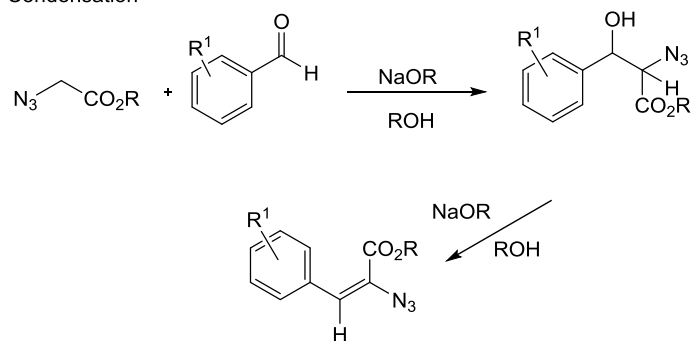
1.3.1 Reaction Sequence

The overall process to form an indole by the Hemetsberger-Knittel indolization involves three steps: (1) the synthesis of an alkyl azidoacetate, (2) a base-promoted Knoevenagel condensation between an azidoacetate and an aromatic aldehyde to form an α -azido- β -arylacrylate, and finally (3) the thermolysis of the α -azido- β -arylacrylate in an intramolecular cyclization to form the indole skeleton (Scheme 14).

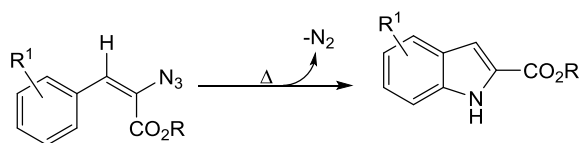
Alkyl Azidoacetate Synthesis



Knoevenagel
Condensation



Hemetsberger Indolization

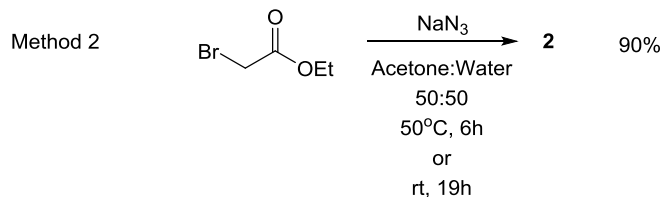
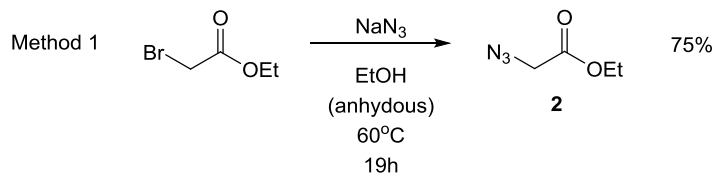


Scheme 14. Knoevenagel-Hemetsberger reaction sequence

1.3.1.1 *Synthesis of alkyl azidoacetates*

Alkyl azidoacetates can be synthesized from an alkyl haloacetate and sodium azide. This substitution reaction requires appropriate safety precautions.⁴² First, alkyl haloacetates are lachrymators; as such they should always be handled in a fume hood. Second, sodium azide (or solutions containing it) should not be allowed to come into contact with metal either in handling, use, or disposal in order to prevent the formation of unstable metal azide salts. In addition, azide solutions should not be exposed to heat and/or Brønsted acids or halogenated solvents, such as dichloromethane or chloroform, which may result in the formation of explosive compounds (hydrazoic acid and azides of low carbon content).

The synthesis of alkyl azidoacetates may be performed under anhydrous or aqueous conditions, with or without heating.⁴³⁻⁴⁶ These substitution reactions are usually heterogeneous. Anhydrous systems have solid-liquid heterogeneity due to the low solubility of sodium azide in organic solvents, and aqueous systems have liquid-liquid heterogeneity because of the low solubility of the alkyl bromoacetates in water. The alkyl azidoacetate employed in this body of work was ethyl 2-azidoacetate (**2**, ethyl azidoacetate) which was synthesized from ethyl bromoacetate and sodium azide. Anhydrous and aqueous conditions were both used for its synthesis (Scheme 15).



Scheme 15. Ethyl 2-azidoacetate synthesis

The aqueous conditions (Method 2, above) gave a higher isolated yield, 90%, of the product at both 50°C and room temperature compared to the 75% yield in anhydrous ethanol at 60°C.

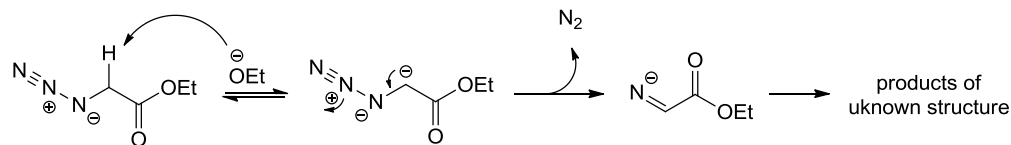
1.3.2 Improving the Knoevenagel-Hemetsberger Reaction Sequence

There are two major issues dealing the Knoevenagel-Hemetsberger reaction sequence which must be addressed in order to control the outcomes of the overall process. First, the yields in the Knoevenagel condensation to form α -azido- β -arylacrylates are often poor to moderate. Typical yields have been reported to range from 10% to 64%.^{30,31,35,47,48} Second, the regiochemistry associated with the thermally induced indolization of *meta*-substituted α -azido- β -arylacrylates has not been explored.

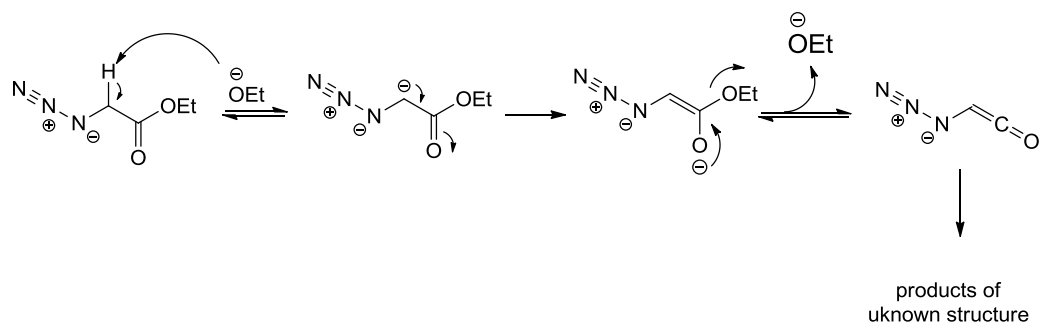
1.3.2.1 Knoevenagel Condensation

A serious limitation in the laboratory use and industrial implementation of the Hemetsberger indozliation is the low to moderate yields ($\leq 55\%$) associated with the base promoted Knoevenagel condensation of the α -azido- β -arylacrylates precursors. There are at least two primary reasons for these relatively low yields. First, alkyl azidoacetates are unstable in the presence of base. The decomposition of ethyl azidoacetate is visible in two ways: (1) the solution changes from colorless to yellow-orange and (2) an effervescence is observed. One suggested decomposition pathway involves, the deprotonation of ethyl azidoacetate followed by elimination of molecular nitrogen (Scheme 16, Path 1). A second decomposition pathway is also possible in which an azidoketene is formed (Scheme 16, Path 2). Both conjectured pathways involve the direct interaction of ethyl azidoacetate with base, and both lead to products of unknown structure.

Decomposition Path 1

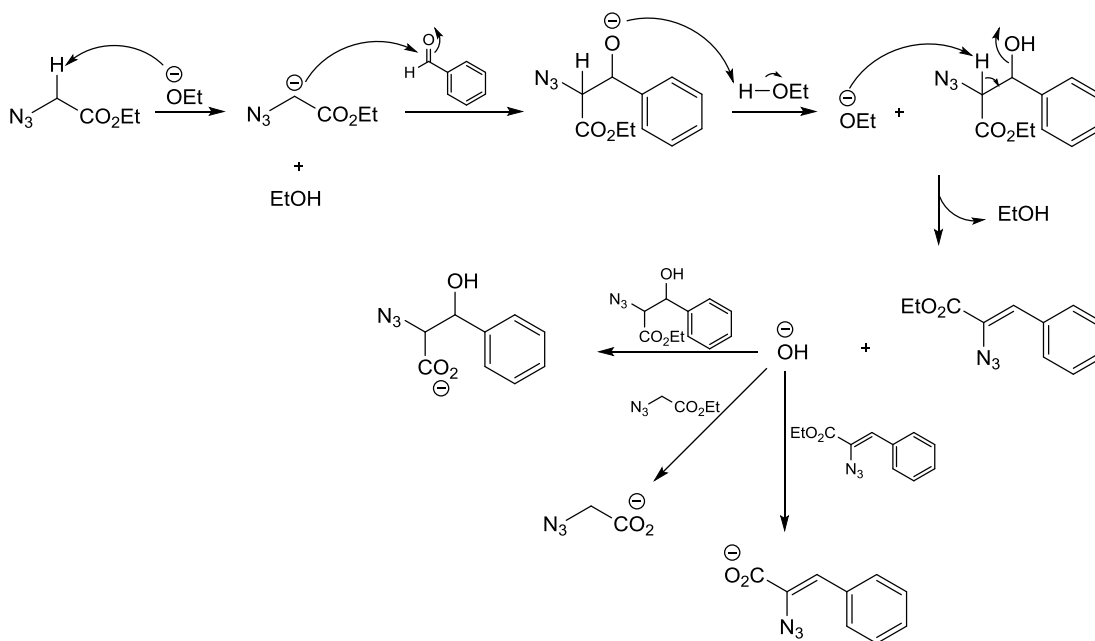


Decomposition Path 2



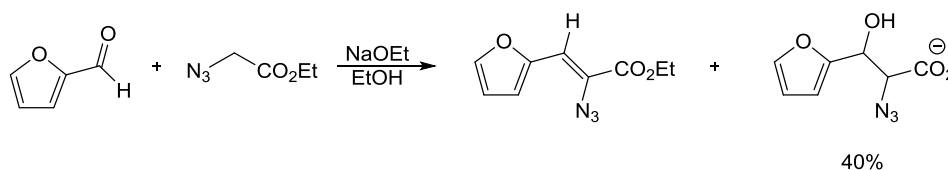
Scheme 16. Decomposition of ethyl azidoacetate in the presence of sodium ethoxide

The second and more critical side reaction which affects the yield of the α -azido- β -arylacrylates is hydrolysis of the ester group by hydroxide during the Knoevenagel condensation reaction; specifically, the ester functionality of the alkyl azidoacetate reagent, the azido alcohol intermediate, and/or the α -azido- β -arylacrylate product (Scheme 17).



Scheme 17. Routes of Hydrolysis in the Knoevenagel Condensation of α -azido- β -arylacrylate

In particular, it was discovered that in the Knoevenagel condensation of furfural and ethyl azidoacetate the intermediate azidoalcohol was being hydrolyzed (Scheme 18). The undesired ester hydrolysis product of the azido alcohol intermediate (α -azido- β -hydroxy- β -[2-furyl]propanoic acid) occurred in yields as high as 40%.⁴⁹ Additionally, the acid by-product did not undergo dehydration to afford the α -azido- β -[2-furyl]acrylic acid.



Scheme 18. Formation of α -azido- β -hydroxy- β -[2-furyl]propanoic acid side product

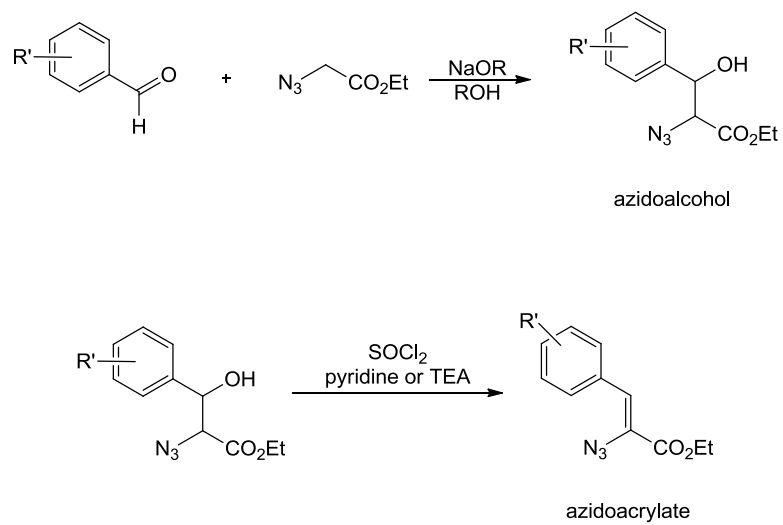
In principle, the azido alcohol intermediate could be re-esterified and subsequently dehydrated but this would add additional steps and complexity to the overall process. Therefore, it is highly desirable to develop strategies that would prevent the hydrolysis of the intermediate or any other ester functionality in the process.

1.3.2.2 Prior Art for α -azido- β -arylacrylate Synthesis

Standard experimental protocols in the literature maximize the yields of α -azido- β -arylacrylates by minimizing the decomposition of the alkyl azidoacetate by performing the condensations at temperatures of -10°C to 5°C . They also employ an excess of the alkyl azidoacetate (up to four equivalents) to compensate for the decomposition.^{16,30,35,48,50} The typical procedure requires the addition of a solution of alkyl azidoacetate (2-4 equivalents) and benzaldehyde (1 equivalent) to a solution of sodium ethoxide in ethanol (0.1 – 0.5M). The isolated yields achieved in these reactions were approximately 50%.³⁰

The highest yields of the α -azido- β -arylacrylates were reported by Kondo and Murakami et al. using a two step approach (Scheme 19). This approach involved first reacting the aryl aldehyde with the alkyl azidoacetate at -30°C to produce the azidoalcohol intermediate which was then treated with thionyl chloride and triethyl amine to promote the elimination of water in order to produce the alkyl α -azido- β -arylacrylates. With this two-step strategy the authors successfully increased the yields for two specific substrates, *ortho*- and *para*-methoxybenzaldehyde, reporting yields of 78% and 80%, respectively. However, the yields associated with other substituted benzaldehydes, particularly those with electron withdrawing groups were low-to-moderate; the yields

ranged from 9% - 55% .^{50,51}



R'	Azidoalcohol Yield (%)	Azidoacrylate Yield (%)	Overall Yield (%)
H	69	77	53
2-Me	74	48	35
2-OMe	90	87	78
4-OMe	70	75	53
2-Cl	38	82	31
2-CF ₃	11	80	9

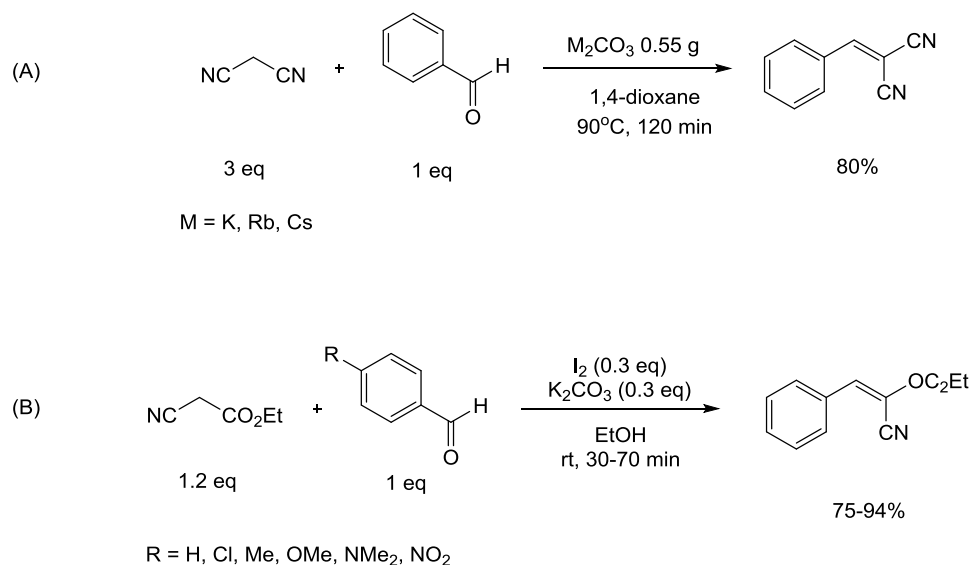
Scheme 19. Two step synthesis of α -azido- β -arylacrylates

1.3.3 Circumventing Ester Hydrolysis in the Knoevenagel Condensation

High yields of Knoevenagel condensation products are essential for developing a viable process for the synthesis of indoles via the Hemetsberger indolization. Three strategies were investigated to prevent ester hydrolysis in the Knoevenagel condensation. One strategy investigated the replacement of the base, sodium ethoxide, with the inorganic bases K_2CO_3 or Cs_2CO_3 which could also function as dehydrating agents. The next strategy explored involved replacing the ester group of ethyl azidoacetate with the base-stable benzoxazole group—an ester equivalent. The third strategy employed sacrificial electrophiles to scavenge the hydroxide produced in the condensation.

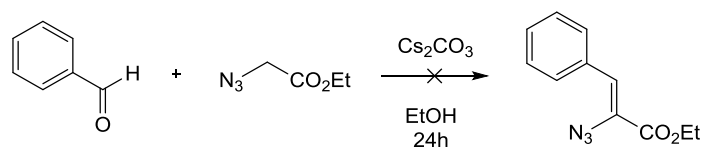
1.3.3.1 Strategy 1: Inorganic Base and a Dehydrating Agent

It has been reported in the literature that carbonate can be an effective base in Knoevenagel condensations. Aramendia et al. evaluated a variety of carbonate bases in the condensations of malonitrile and benzaldehyde in 1,4-dioxane at 90°C concluding that the potassium, rubidium, and cesium salts provided the best results, yields ~80% (Scheme 20, A). In another example, Ren et al. surveyed a number of substituted benzaldehydes in condensations with malonitrile or ethyl cyanoacetate in the presence of catalytic iodine and potassium carbonate at room temperature in ethanol, yields 75-95% (Scheme 20, B). It was found that the weakly Lewis acidic iodine improved the yields and rates of their condensations.



Scheme 20. Knoevenagel condensations with inorganic bases

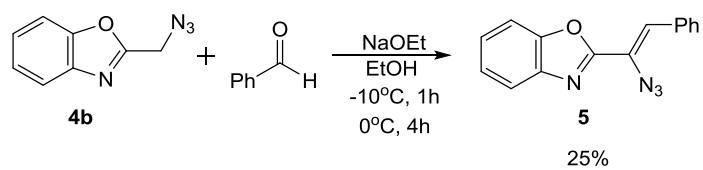
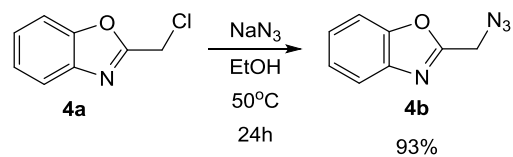
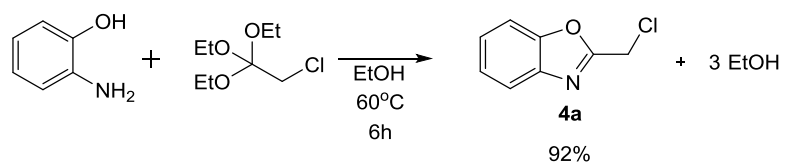
Unfortunately, when Cs₂CO₃ and K₂CO₃ were employed in the condensation of ethyl azidoacetate and benzaldehyde no product formed (Scheme 21). Additionally, no product was detected in separate reactions which included the use of the phase transfer catalyst tetra-butylammonium bromide (10 mol%) and catalytic iodine (10 mol%), as well as heating the reaction mixture to 58°C or 75°C for twenty-four hours. Thus, it was concluded that ethyl azidoacetate is not sufficiently acidic to react under these conditions.



Scheme 21. Condensation of ethyl azidoacetate and benzaldehyde by Cs₂CO₃

1.3.3.2 Strategy 2: Base-stable Benzoxazole Protecting Group

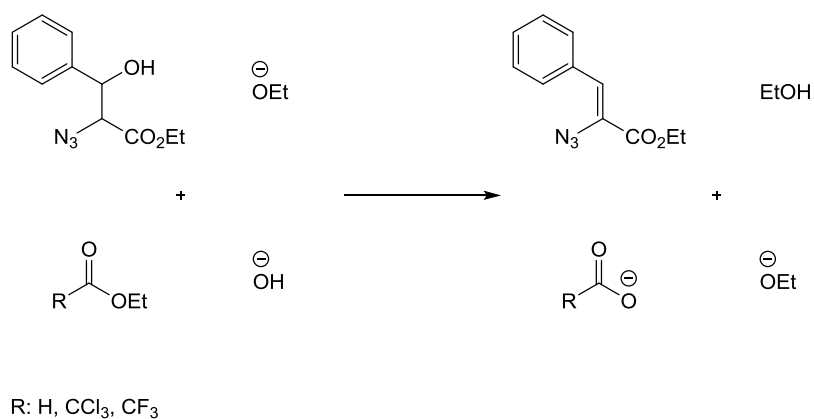
The ester group of ethyl azidoacetate was replaced by a benzoxazole group which is stable in base. The 2-azidomethylbenzoxazole **4b** was synthesized in a two step process. First 2-chloro-1,1,1-triethoxy ethane was reacted with *o*-aminophenol at 60°C for six hours to afford 2-chloromethylbenzoxazole **4a** as a colorless oil in a 92% yield after distillation. A substitution reaction of the chloride for azide provided **4b** as a faint yellow oil in a 93% yield after distillation. Unfortunately when **4b** was employed in the base-promoted Knoevenagel condensation with benzaldehyde only a 25% isolated yield of the desired product was obtained (Scheme 22). The crude ¹H NMR of the reaction mixture indicated a significant amount of unreacted benzaldehyde. It was observed that **4** undergoes a competitive degradation in the presence of base to form products of unknown structures. Upon addition of **4b** to a solution of sodium ethoxide, the solution turns dark green accompanied by the evolution of gas, presumably molecular nitrogen. As a consequence, the oxazole protecting group strategy was not a viable means for generating the corresponding azido-arylacrylate for use in the Hemetsberger indolization process.



Scheme 22. Reaction sequence utilizing a benzoxazole protecting group

1.3.3.3 Sacrificial Electrophiles

Hydrolysis of the ester group during the condensation may be prevented by adding a sacrificial electrophile in the reaction. To be successful, the sacrificial electrophile must be highly electrophilic, react faster with hydroxide than the ester of the intermediate, and it must generate a weak base/nucleophile upon reaction with hydroxide. Moreover, it must not possess an enolizable hydrogen which could, in principle, take part in unwanted condensation reactions. Three candidates that potentially possessed these properties are: ethyl formate, ethyl trichloroacetate, and ethyl trifluoroacetate (Scheme 23).

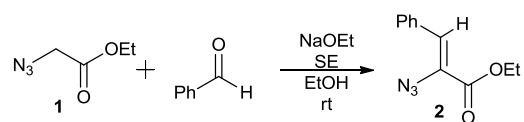


Scheme 23. The role of a sacrificial electrophile in a model Knoevenagel condensation

Ethyl formate (EF) was chosen primarily on steric grounds while ethyl trichloroacetate (EtClA) and ethyl trifluoroacetate (EtFA) were chosen based on their highly electrophilic carbonyl carbons. The electron-withdrawing properties of trichloromethyl and

trifluoromethyl are reflected in their σ^* -values: +2.65 and +2.60, respectively. This new strategy was first applied to the condensation of ethyl 2-azidoacetate **1** and benzaldehyde to yield ethyl α -azido- β -phenylacrylate **2**. A solution of benzaldehyde, ethyl azidoacetate, and a sacrificial electrophile were added to a 0.35 M solution of sodium ethoxide in ethanol at room temperature. Table 1 summarizes the isolated yields of product obtained when employing these sacrificial electrophiles at various stoichiometries of base and sacrificial electrophile at room temperature.

Table 1. Effect of sacrificial electrophiles (SE) on the condensation of benzaldehyde and ethyl azidoacetate

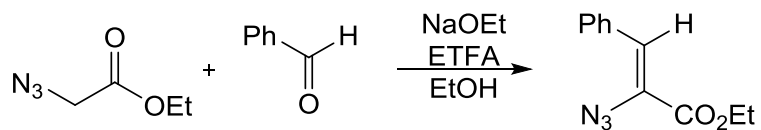


Entry	1		SE		NaOEt	Yield, Isolated
	(eq)		(eq)	(eq)	(eq)	
1	2	none	n/a	2	48%	
2	2	EF	1	2	45%	
3	3	EF	1	3	51%	
4	2	EF	2	2	50%	
5	2	ETCIA	1	2	48%	
6	2	ETCIA	2	2	58%	
7	2	ETFA	1	2	53%	
8	2	ETFA	2	2	74%	
9	3	ETFA	2	3	76%	

All results are compared to the yields when no sacrificial electrophile is present (48%). From Table 1 it can be concluded that ethyl formate (entries 2-4) and ethyl trichloroacetate (entries 5, 6) had little to no effect on the yield. In contrast, the presence of two equivalents of ethyl trifluoroacetate (Entries 7-9) resulted in a substantial increase in yield (74-76%) of product **2**. Although the trichloromethyl group has a slightly larger σ^* -value compared to the trifluoromethyl group (+2.65 vs. +2.60), the latter is smaller giving it a kinetic advantage which is reflected in its effectiveness as a sacrificial electrophile. The use of three equivalents of base and ethyl azidoacetate marginally increases the yield of product (Entries 2 and 3; 8 and 9, respectively).

Reported experimental protocols for analogous Knoevenagel reactions call for reaction temperatures $\leq 0^\circ\text{C}$ for up to 6 hours.^{16,30,47,50,51} To our knowledge only a single literature example can be found in which the reaction was performed at ambient temperature, and the reactions proceeded for 30 minutes. The yields ranged from 6 to 80% depending on the substituent.¹⁶ This clearly put into question the need for reduced temperatures and prompted us to investigate the reaction of ethyl azidoacetate with benzaldehyde as a function of temperature, time, and reagent stoichiometry. These results are summarized in Table 2, and the yields are averages from two to three trials.

Table 2. Stoichiometry and temperature optimization



Entry	NaOEt (eq)	1 (eq)	ETFAs (eq)	Temp (°C)	Time	Isolated Yields
1	2	2	2	RT	15min	76 ±3%
2	1.5	1.5	1.5	RT	15min	71 ±1%
3	1.25	1.25	1.25	RT	15min	65 ±2%
4	2	2	2	0°C	4h	71 ±2%
5	1.5	1.5	1.5	0°C	4h	74%
6	1.25	1.25	1.25	0°C	4h	70%
7	2	2	2	0°C-RT	1h	70 ± 4%
8	1.5	1.5	1.5	0°C-RT	1h	73%
9	1.25	1.25	1.25	0°C-RT	1h	66 ± 2%

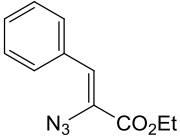
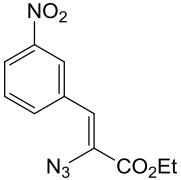
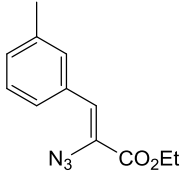
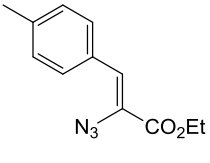
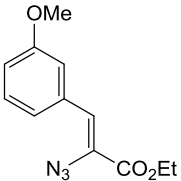
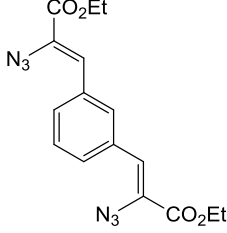
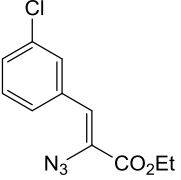
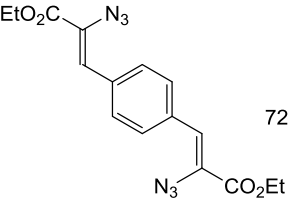
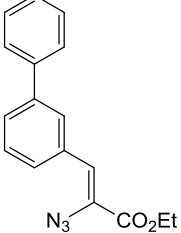
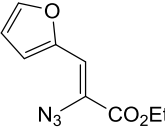
At ambient temperature and with two equivalents of ethyl trifluoroacetate, the reaction was complete within 15 minutes with isolated yields after recrystallization of $76 \pm 3\%$ (Table 2, entry 1). When the condensation was performed at 0°C for 4 hours, comparable isolated yields of $71 \pm 2\%$ were obtained (Table 2, entry 4). Experimentally, it was observed that the reaction solution at ambient temperature goes through a series of color changes—colorless to yellow to orange (attributed to the decomposition of ethyl azidoacetate). In contrast, at 0°C the reaction solution never gets darker than a yellow color. It was believed that the difference in intensity of the color change corresponded to the amount of decomposition. Indeed, the NMR spectra of the crude reaction products showed fewer impurities at 0°C than at ambient temperatures. In light of these observations—the reaction protocol employed in subsequent experiments involved adding the reactants and the sacrificial electrophile to the sodium ethoxide solution at 0°C and then allowing the reaction mixture to warm to room temperature for a period of one hour. After recrystallization in ethanol and water isolated yields of $70 \pm 4\%$ were obtained. This protocol was further improved by investigating the relative stoichiometries of ethyl azidoacetate, NaOEt, and ETFA. It was found that the optimized number of equivalents of base and ETFA could be reduced to 1.5 while maintaining an isolated, recrystallized yield of 73% (entry 8). However, a further decrease to 1.25 equivalents resulted in a slight decrease in yield (66%) (Table 2, entry 9). Thus, an enhanced protocol for the Knoevenagel condensation was developed based upon the use of ethyl trifluoroacetate as a sacrificial electrophile.

1.3.3.4 Substrate Screening

The optimized procedure using 1.5 equivalents of ethyltrifluoroacetate was applied to a variety of substituted benzaldehydes, heteroaromatic aldehydes, and alicyclic aldehydes in order to establish the scope of the methodology. The crude yields of the products averaged 90% and contained approximately 10% impurity by ^1H NMR. The relatively high purity of the crude products indicated that they could potentially be subjected to the Hemetsberger reaction without prior purification. This would be very advantageous from a process view point, and this topic will be revisited later in the thesis. The isolated, recrystallized yields are tabulated in Table 3 and are averages from three to five trials.

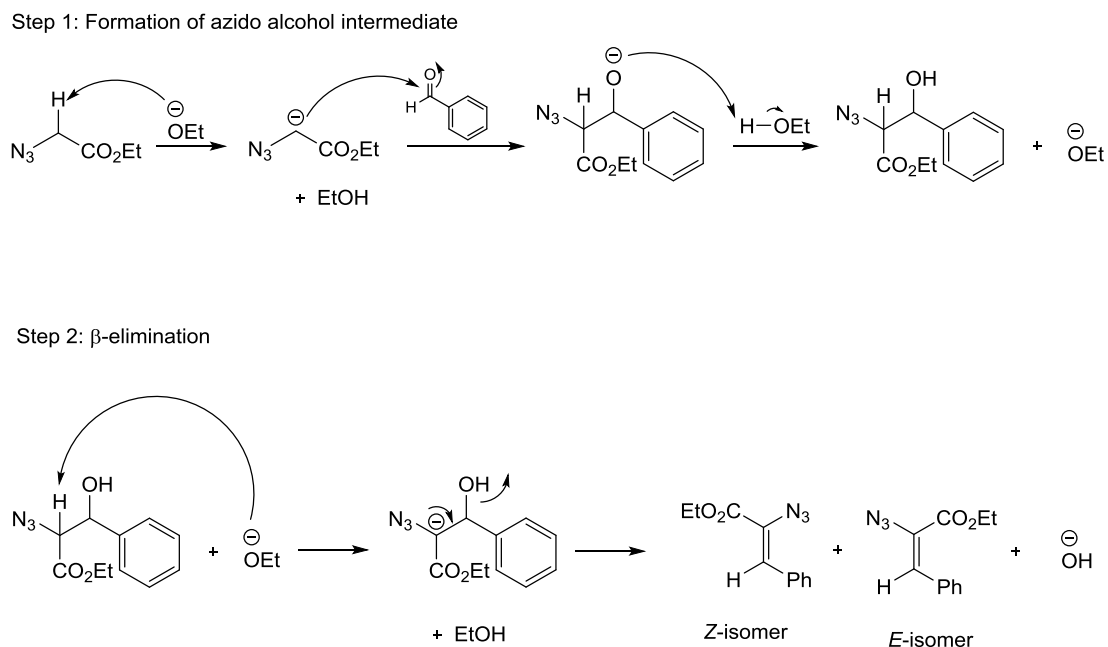
The isolated, recrystallized yields from the substituted benzaldehydes were good to excellent ($> 70\%$) with the exception of *m*-nitrobenzaldehyde (**2f**, Table 3) which afforded $60 \pm 5\%$ yield.⁵³ *Iso*- and *terephthal*aldehydes not only gave high yields (**2h** $77 \pm 2\%$, **2i** $72 \pm 1\%$) but, quite surprisingly, the products precipitated during reaction—allowing for simple isolation via filtration; the products were analytically pure. The heteroaromatic, furfural, also produced high yields (**2j**, $83 \pm 1\%$). In contrast, however, *N*-methylpyrrole-2-carboxaldehyde (not shown in Table 3) gave very poor yields, $\sim 10\%$. Pyrrole-2-carboxaldehyde, cyclopentanecarboxaldehyde, and cyclohexanecarboxaldehyde failed to yield any products using the above protocol.

Table 3. Substrate Screening⁵²

Substrate	Isolated Yield	Substrate	Isolated Yield
<p>2a</p> 	76 ± 3%	<p>2f</p> 	60 ± 5%
<p>2b</p> 	70 ± 3%	<p>2g</p> 	77 ± 2%
<p>2c</p> 	78 ± 3%	<p>2h</p> 	77 ± 2%
<p>2d</p> 	72 ± 4%	<p>2i</p> 	72 ± 1%
<p>2e</p> 	70 ± 2%	<p>2j</p> 	83 ± 1%

1.3.4 Stereochemistry of the α -azido- β -arylacrylates

In the process of optimizing the yields of indole products, it was of interest to understand the stereochemistry of the α -azido- β -arylacrylates products and the relationship of the stereochemistry to the yields and regioselectivity associated with the Hemetsberger process. In principle, both the *Z* and *E* configurations of ethyl α -azido- β -arylacrylates can be obtained (Scheme 24). The first step of the condensation leads to the formation of the azido-alcohol intermediate. There are four possible stereoisomers of the intermediate, and these are diastereomeric sets of enantiomers; (*R,R*) | (*S,S*) and (*R,S*) | (*S,R*). The next step is β -elimination in which the carbon-carbon double bond is formed.



Scheme 24. Stereochemistry in the Knoevenagel condensation of α -azido- β -arylacrylates

Quite unexpectedly, only one vinyl hydrogen was observed in the ^1H NMR spectra for all of the products listed in Table 3 indicating the formation of only one stereoisomer. As an example, the ^1H NMR of ethyl- α -azido- β -phenylacrylate is illustrated below in Figure 5. The ethyl ester signals are at 1.41 ppm (3H's, CH_3 , triplet) and 4.37 ppm (2H's, CH_2 , quartet). The aromatic protons are at 7.34 (3-H's, multiplet), and 7.83 (2H, doublet). The signal at 6.93 ppm corresponds to the vinyl hydrogen, and it is clearly a single peak.

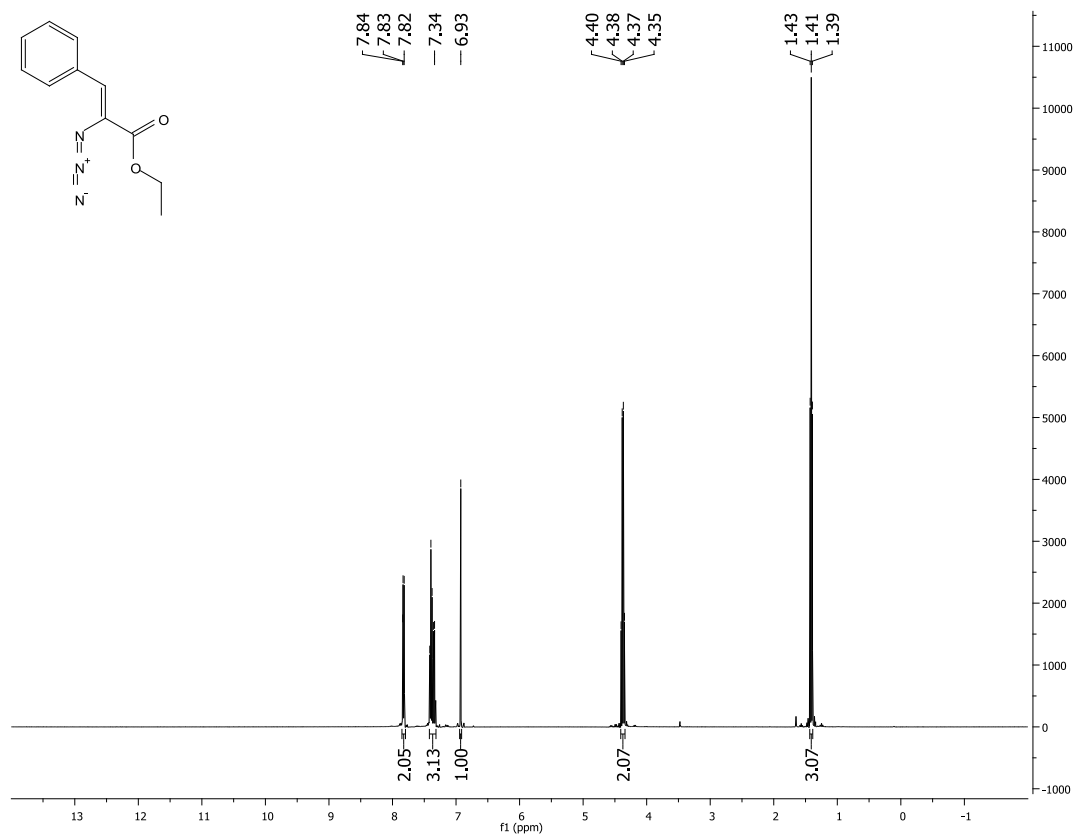


Figure 5. ^1H (Z)-ethyl- α -azido- β -phenylacrylate

The question remained as to which stereoisomer was present. It has been reported in the literature that the coupling constant between the *cis* and *trans* β -vinyl hydrogens and the carbonyl carbon in α,β -unsaturated esters have substantially different coupling constants. A ${}^3J_{C=O,H}$ value ~ 5 Hz is associated with a *cis* relationship whereas a ${}^3J_{C=O,H}$ value greater than 10 Hz is associated with the *trans* relationship (Figure 6).⁵³

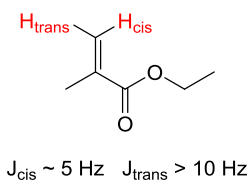


Figure 6. ${}^3J_{C=O,H}$ coupling

In these substrates, the ${}^1\text{H}$ - ${}^{13}\text{C}$ coupled signal should appear as a doublet of triplets (Figure 7). The carbonyl carbon will couple with the vinylic hydrogen as well as with the methylene group of the ester. The signals for all of the products were indeed a doublets of triplets, and ${}^3J_{C=O,H}$ was < 5 Hz for all of products reported in Table 3. These results support that the products formed in the Knoevenagel reaction are of the *Z* configuration. Density functional theory calculations (B3LYP-6-31G*) on molecule **2a** indicated that the *Z*-isomer is thermodynamically more stable than the *E*-isomer by 6.86 kcal/mole. In fact, the calculations indicate that the equilibrium geometry for the *Z*-isomer showed that all the atoms in the molecule were essentially in one plane. In contrast, the equilibrium geometry of the *E*-isomer clearly showed that the interaction of the bulky carboethoxy

group with the phenyl group resulted in a distorted, non-planar structure. Based on these calculations it was concluded that the energy of the transition state leading to the *Z*-isomer is substantially lower than that leading to the *E*-isomer, the origin of the difference being steric in nature.

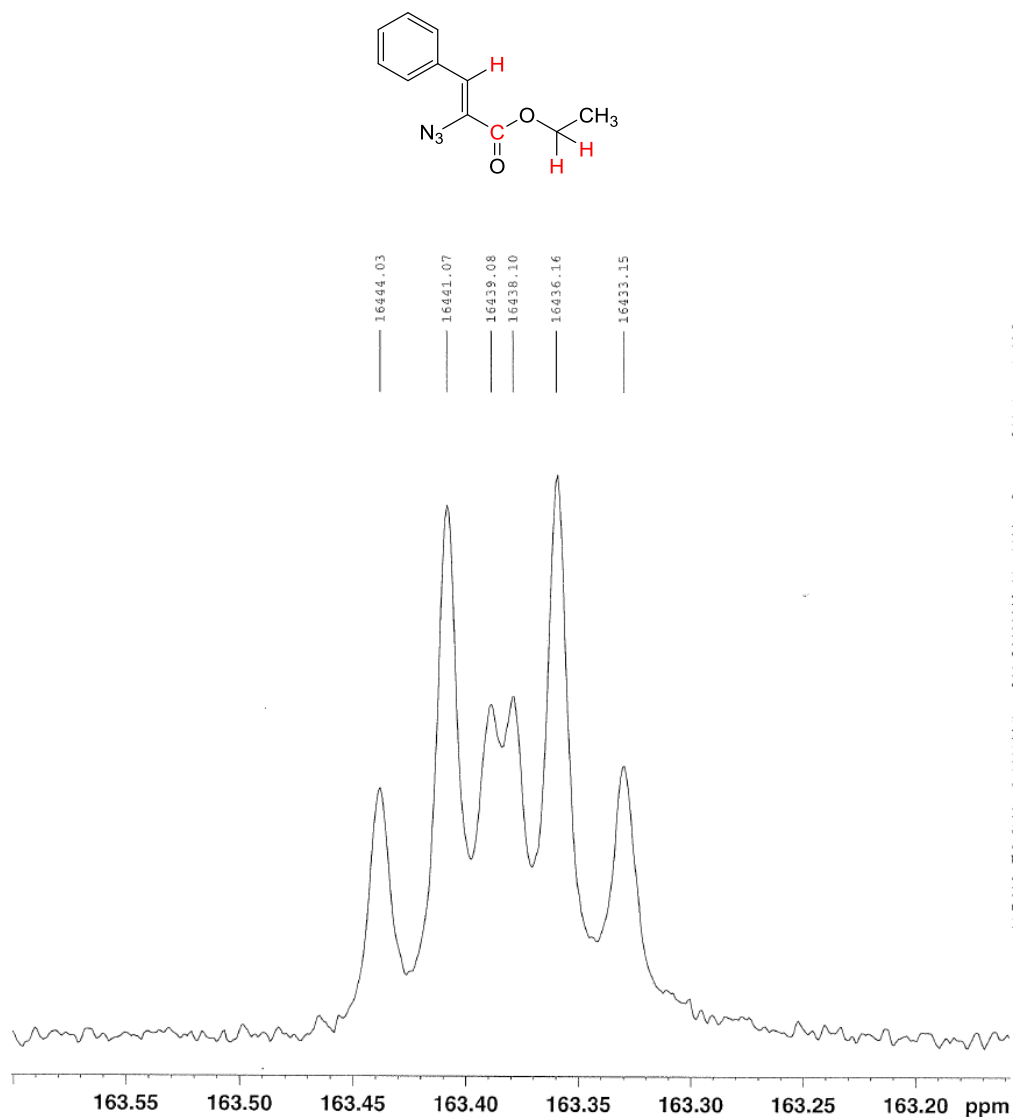
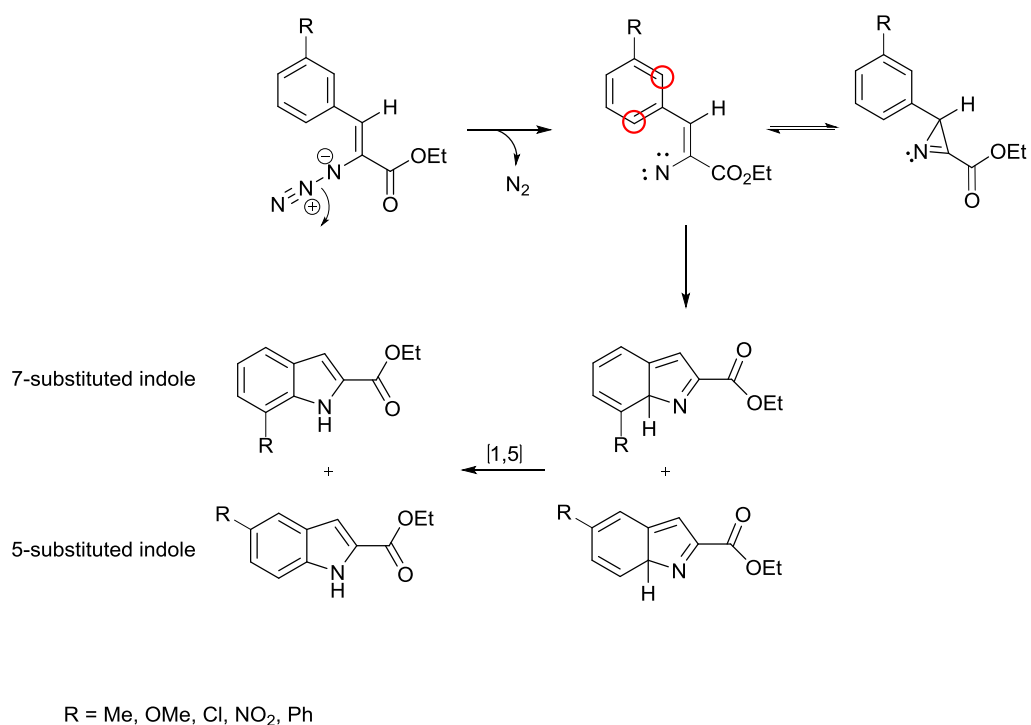


Figure 7. ^1H - ^{13}C Coupled NMR: carbonyl signal from (*Z*)-ethyl α -azido- β -phenylacrylate

1.3.5 Regioselectivity in the Hemetsberger Indolization

1.3.5.1 Origins of Regioisomers

The thermally-induced Hemetsberger indolization is typically carried out in refluxing *p*-xylene or mesitylene (bp 138 °C and 165 °C, respectively), with yields ranging from 50% - 100%.^{16,47,50,51,54,55} The mechanism is believed to proceed in a stepwise fashion; as pointed out previously. It is not clear if the azirine is an intermediate on the pathway to the indole or a side product in equilibrium with the nitrene intermediate. While the literature contains several reports regarding the yields associated with the thermally induced Hemetsberger indolization, there have been no reports discussing the regiochemical outcome in the cyclization of *meta*-substituted ethyl α -azido- β -phenylacrylates. It was of interest, therefore, to explore the regiochemistry associated with indole formation and to determine the potential role of electronic and/or steric factors in controlling the outcome. When a *meta*-substituent is present on the aromatic ring both 5- and 7-substituted regioisomeric indoles are possible (Scheme 25).



Scheme 25. Regioisomer formation

1.3.5.2 Differential Scanning Calorimetry of the α -azido- β -arylacrylates

In order to provide guidance for optimal reaction conditions for the thermal cyclization process, as well as for safety purposes, differential scanning calorimetric (DSC) analyses were conducted on all of the α -azido- β -arylacrylates reported in this study. As an example, the DSC for (*Z*)-ethyl α -azido- β -(*m*-chlorophenyl)acrylate **2d** is presented in Figure 8. The first is an endothermic transformation at 48°C which corresponds to the melting point of **2d**. The two subsequent exothermic events are attributed to the formation of the azirene intermediate (134°C) followed by cyclization to the indole (166°C). Two distinct exothermic events were observed for most molecules listed in Table 3 except for the ethyl esters of α -azido- β -(*m*-nitrophenyl)acrylate, α -azido-

β -furylacrylate, *p*-phenylene-bis(α -azidoacrylate), and *m*-phenylene-bis(α -azidoacrylate) (Table 4). Since in each of these cases the indole products were also formed upon thermally induced cyclization, both DSC exothermic events were assumed to take place at temperatures too close to resolve.

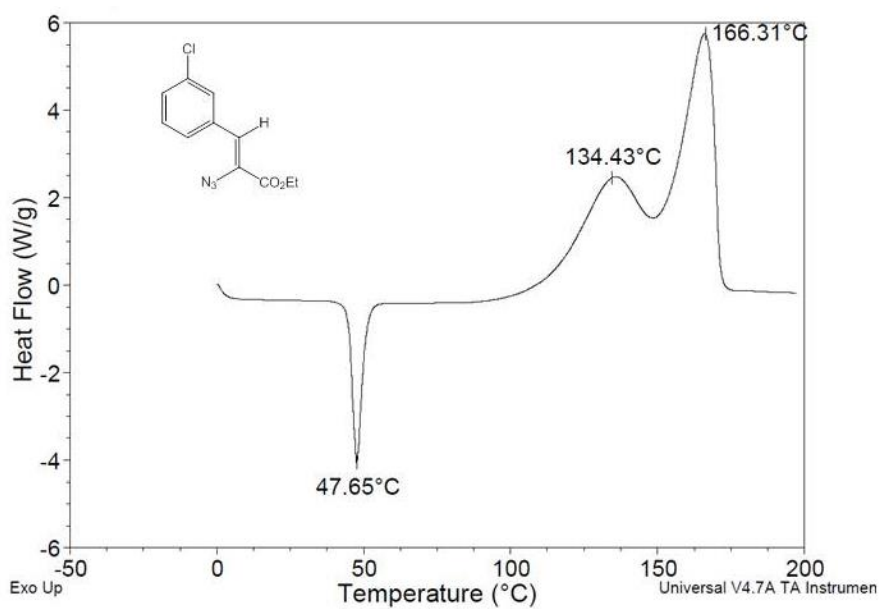


Figure 8. DSC: (Z)-ethyl α -azido- β -(*m*-chlorophenyl)acrylate (2d)

Table 4. Exothermic events of α -azido- β -arylacrylates measured by DSC

α -azido- β -arylacrylate	<u>Exothermic Events °C</u>	
	First	Second
2a	136.8	159.5
2b	136.2	160.7
2c	137.2	158.9
2d	134.4	166.3
2e	136.3	160.8
2f	136.2 ^a	
2g	134.6	154.6
2h	139.4 ^a	
2i	129.7 ^a	
2j	129.0 ^a	

^a Only one exothermic event observed.

1.3.5.3 Regioselectivity Results

The α -azido- β -arylacrylates listed in Table 3 (**2a-2j**) were subjected to the Hemetsberger indolization in *o*-dichlorobenzene at 150°C for 30 minutes. The isolated yields (obtained from column chromatography) of the indoles (**3a-3j**) were consistently in the 75% range suggesting that neither electronic nor steric effects influence the efficacy of the cyclization. Table 5 summarizes the isolated yields from the Hemetsberger indolization and the regiochemical ratio (5-substituted/7-substituted) associated with each of the indole products. It is obvious that there is no overwhelming preference for either the 5- or the 7-substituted indole products. Although no significant electronic effects were observed, steric effects appeared to more strongly influence the regiochemistry of the reaction. Specifically, it was found that, in the thermolysis of ethyl α -azido- β -(*m*-phenylphenyl)acrylate, ethyl 5-phenyl-indole-2-carboxylate was favored by a 2:1 ratio over the ethyl 7-phenyl-indole-2-carboxylate implying that steric factors may play a role. The significance of the steric factors in the thermally induced Hemetsberger process is consistent with the observations for the Rh-catalyzed process.

Table 5. Hemetsberger indolization: yields and regioselectivities

α -azido- β -arylacrylate	Yield (%) (from the aldehyde)	Regioisomer Ratio (5- vs. 7- substitution)
2a	78	n/a
2b	60	1.1:1 ^a
2c	71	1:1 ^a
2d	68	1.2:1 ^b
2e	63	2:1 ^b
2f	62	1.1:1 ^a
2g	80	n/a
2h	n/a	3h only
2i	n/a	3i only
2j	76	n/a

^adetermined by ¹H NMR, ^b5- and 7- isomers separated by column chromatography.

In contrast to the *meta*-substituted ethyl α -azido- β -phenylacrylates, the thermal cyclization of *m*-phenylene-bis(α -azidoacrylate) and *p*-phenylene-bis(α -azidoacrylate) (**2h** and **2i**, respectively) showed exclusive preferences; only one regioisomer was detected in each case. Figure 9 shows the two possible regioisomers which can be formed from **2h** and **2i**.

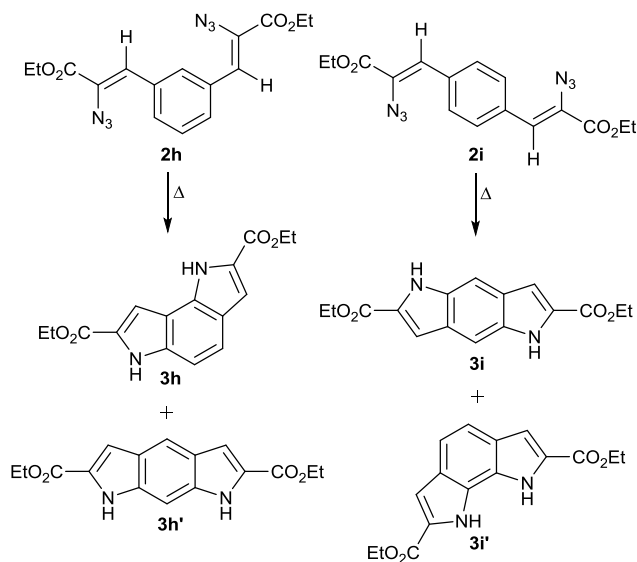


Figure 9. Stereoisomers of pyrrolindoles

Thermolysis of *m*-phenylene-bis(α -azidoacrylate) (**2h**) could result in the formation of **3h** and/or **3h'**. These isomers can be easily distinguished from each other using ^{13}C NMR. **3h'** has a mirror plane of symmetry; whereas, **3h** possesses no symmetry. Experimentally, ten aromatic/vinyl carbons were observed which is consistent with the regioisomer **3h**. In contrast, the thermolysis of **2i** could result in regioisomers, **3i** and **3i'**, which cannot be distinguished by one-dimensional NMR as both possess symmetry

elements, a C_2 -axis and σ_v elements, respectively. Therefore, two-dimensional ^1H - ^{13}C -HMBC NMR experiments were used to determine the identity of the product. The relationships of interest were the correlations between the protons on the nitrogens and the carbons possessing hydrogens within a distance of three bonds. Regioisomer **3i** would exhibit two three-bond correlations while only one such correlation would be expected in **3i'**. Two three-bond correlations were observed in the ^1H - ^{13}C -HMBC experiment. It was concluded that regioisomer **3i** had been formed. Thus, the pyrroloindoles⁵⁶⁻⁵⁹ formed in the thermolysis of **2h** and **2i** were specific towards those regioisomers in which the nitrogens are *anti* to each other (**3h** and **3i** respectively).⁶⁰

1.3.5.4 Pyrolysis of Crude α -azido- β -arylacrylates

The crude yields of the α -azido- β -arylacrylates ranged from 84 – 95% with purities of ~90% by ^1H NMR, indicating that the crude α -azido- β -arylacrylates could, in principle, be used in the subsequent Hemetsberger indolization process. To proceed from the directly to the indoles without prior purification of the vinylazide precursors would simplify the synthetic process and potentially have great industrial appeal. The high purity of the crude α -azido- β -arylacrylates obtained from our methodology (~90%) would enable the realization of a Knoevenagel-Hemetsberger sequence without intermediary purification. Operationally, the condensation reaction was quenched with three to five milliliters of saturated aqueous NH_4Cl . The solvent from the condensation reactions (ethanol) was removed *in vacuo*, and the α -azido- β -arylacrylates were extracted from the condensation reaction mixture with *o*-dichlorobenzene and filtered to remove salts formed when the reaction was quenched. The resulting *o*-dichlorobenzene solution

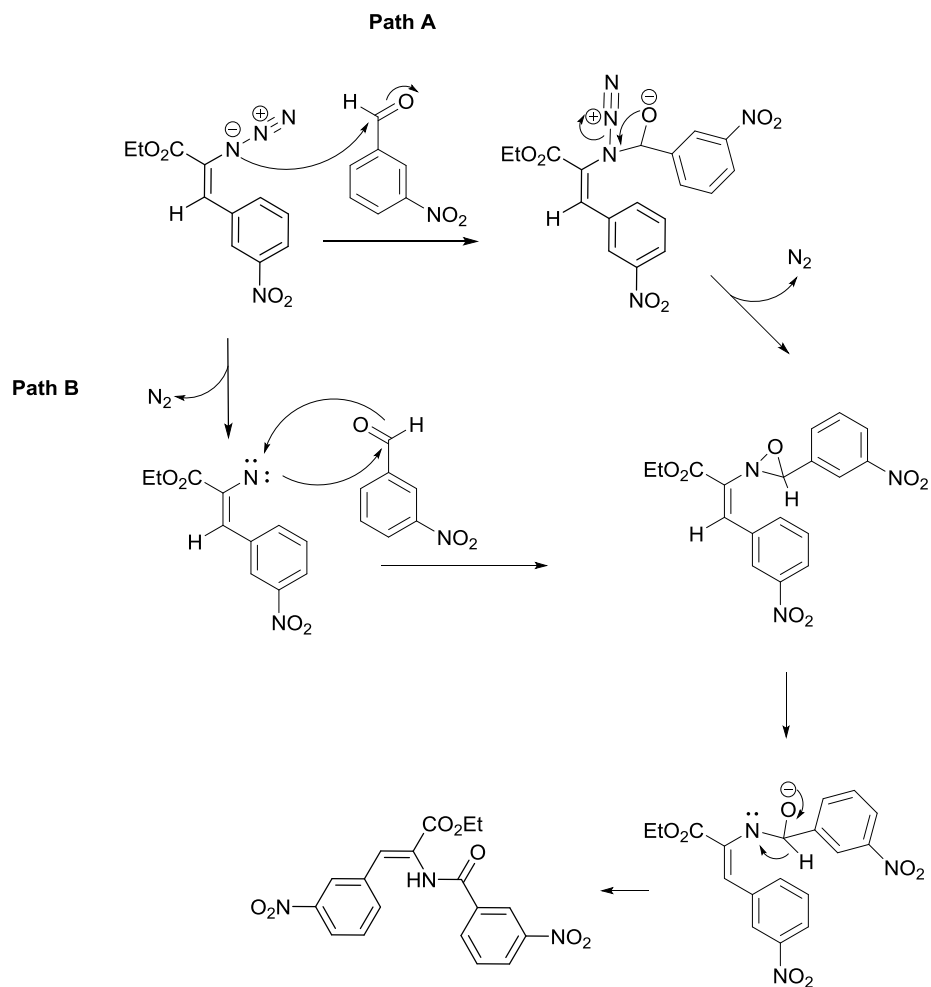
was heated to 150°C to perform the Hemetsberger reaction. The results are tabulated in Table 6 and are compared to those from the step-wise approach in which the α -azido- β -arylacrylates were isolated and purified.

Table 6. Comparison of Knoevenagel-Hemetsberger processes with and without purification of ethyl α -azido- β -arylacrylates (yields calculated from the aldehyde)

α -azido- β -arylacrylate	Yield (%) w/o Intermediate Purification	Yield (%) w/ Intermediate Purification
2a	81	78
2b	76	60
2c	78	71
2d	72	68
2e	74	63
2f	56	62
2g	--	80
2h	64	n/a
2i	70	n/a
2j	80	76

^adetermined by ¹H NMR, ^b5- and 7- isomers separated by column chromatography.

In all examples, the isolated yields are very good (>70%) with the exception of the nitro-substituted indoles. In this case, the major impurity was determined to be an amide, (*Z*)-ethyl 2-(3-nitrobenzamido)-3-(3-nitrophenyl)acrylate, a by-product from the reaction of *m*-nitrobenzaldehyde and the (*Z*)-ethyl *m*-nitro- α -azido- β -phenylacrylate (Scheme 26). Analysis of the crude starting material revealed the presence of approximately 10% *m*-nitrobenzaldehyde. Thus, it is postulated that when the crude (*Z*)-ethyl *m*-nitro- α -azido- β -phenylacrylate was used directly in the Hemetsberger indolization process the nucleophilic nitrogen of the azide (Path A) or the nitrene (Path B) reacted with the aldehyde impurity in the reaction mixture to form an oxaziridine which ring-opens to form the amide. Thus, with the exception of the nitro-substituted azido-arylacrylate, it can be concluded that it is not necessary to have a purification step between the condensation and the thermolysis; the yields of the products are essentially the same.



Scheme 26. Side product formation in thermolysis of crude (*Z*)-ethyl meta-nitro- α -azido- β -arylacrylate

1.4 Conclusions

In conclusion, the utility of the Knoevenagel-Hemetsberger sequence for the formation of substituted indoles has been significantly improved. The use of the sacrificial electrophile, ethyl trifluoroacetate, in the Knoevenagel condensation increases the yield of α -azido- β -arylacrylates, the Hemetsberger precursors, from an average of approximately 45% to 72%. The subsequent indolization step, conducted in *o*-dichlorobenzene at 150°C, also resulted in relatively high yields (75%). In most cases, the crude α -azido- β -arylacrylates were successfully taken through the indolization step without prior isolation and purification. This observation has positive implications for both laboratory and industrial scale processes. Finally, it was observed that (1) the stereochemistry associated with the Knoevenagel process produces only one stereoisomer—the *Z* ethyl α -azido- β -arylacrylates and (2) the regioselectivity associated with the Hemetsberger process from *meta*-substituted ethyl α -azido- β -arylacrylates is not strongly influenced by either electronic or steric effects—the exceptions being the cyclization of the ethyl esters of *m*- and *p*-phenylene-bis(α -azidoacrylate).

1.5 Recommendations

The Hemetsberger reaction has many advantages that make it a great candidate for use in the laboratory or on the industrial scale. It is fast, chemoselective, atom economical,⁶¹ the intermediate azido-arylacrylates precursors do not necessarily require purification, it can be used in a continuous flow reactor,³¹ and it can be applied to a variety of heterocycles in addition to the indole. Nonetheless, the thermally induced Hemetsberger indolization is only slightly regioselective. When synthesizing complex molecules it is important to control the regiochemical outcome of the products. The results of the work from Stokes³⁵—Rh^{II}(O₂CC₃F₇)₄ catalyst afforded regioselectivity (≥ 87:13) and lowered temperature from 150°C to 40°C—and O'Brien³¹ (who demonstrated Hemetsberger reaction in a continuous flow reactor) can be combined with those contained herein to create a more sustainable Hemetsberger process.

The Knoevenagel condensation of ethyl α -azido- β -arylacrylates is stereospecific to the formation of only the *Z* isomer. It is not clear why this reaction is specific. Density functional theory calculations of transition states for the azidoalcohol intermediate and the azido-acrylates may provide insights into our understanding of the overall process.

1.6 Experimental

All solvents and reagents were purchased from commercial sources in “reagent”

grade form and were used without further purification. Nuclear magnetic resonance spectra were measured on a 400 MHz Varian (1-D measurements) and a Bruker AVIII HD 500 MHz (2-D measurements). Mass spectrometry measurements were performed by electron impact (EI) on a Micromass (Waters) Autospec M. Differential scanning calorimetry experiments were performed on a TA Instruments Q20; samples were heated at a rate of 10°C/minute. Infrared spectroscopy measurements were performed with neat samples on a Shimadzu FTIR Prestige-21 equipped with a Specac Golden Gate ATR cell. Elemental analyses were performed by Atlantic MicroLab, Inc.

2-(chloromethyl)benzo[d]oxazole.⁶² 2-chloro-1,1,1-triethoxy ethane (10.31 g, 0.5242 mol) was added to a solution of *o*-aminophenol (5.454 g, 0.4998 mol) in 70 mL of anhydrous ethanol under an inert atmosphere. The reaction mixture was heated, with stirring to 60°C for four hours and subsequently cooled and concentrated *in vacuo*. The crude organic product was purified by distillation, 68°C at 11 mmHg, yielding a colorless oil, 79% yield (6.615 g). ¹H NMR (CDCl₃, δ ppm): 4.66 (2 H, s), 7.17 (2 H, m), 7.34 (1 H, m), 7.58 (1 H, m). ¹³C NMR: 36.37, 110.53, 120.22, 124.45, 125.58, 140.69, 150.80, 160.57.

2-(azidomethyl)benzo[d]oxazole (4). NaN₃ (1.42 g, 0.0218 mol) was added to a solution of 2-(chloromethyl)benzo[d]oxazole (2.09 g, 0.0125 mol) in 80 mL anhydrous ethanol under an inert atmosphere. The reaction mixture was heated at reflux overnight. Approximately 20 mL of water and 40 mL of EtOAc were added to the heterogeneous reaction mixture. The organic layer was separated and the aqueous layer was extracted with EtOAc (2 x 20 mL). The combined organic fractions were dried over MgSO₄ and concentrated *in vacuo* to give a dark green oil. The crude organic product was purified

by distillation, 95°C 11 mmHg, to give a colorless oil, 97% yield (2.10 g). ¹H NMR (CDCl₃, δ ppm): 4.55 (2 H, s), 7.33 (2 H, m), 7.52 (1 H, m), 7.71 (1 H, m). ¹³C NMR: 47.19, 110.83, 120.46, 124.78, 125.72, 140.75, 151.00, 160.54. MS (m/z): 174.0 [M⁺], 146 [M⁺ - N₂], 132 [M⁺ - N₃].

(Z)-2-(1-azido-2-phenylvinyl)benzo[d]oxazole (5). A freshly prepared solution of sodium ethoxide (50 mL, 0.35M) was transferred to a round bottom flask under an atmosphere of argon or nitrogen and cooled to -10°C. In a separate flask, under an inert atmosphere, were added 2-(azidomethyl)benzo[d]oxazole (1.00 g, 0.00574 mol) and benzaldehyde (0.203 g, 0.00191 mol). The resulting solution was added drop-wise to the stirring solution of sodium ethoxide over the period of one hour. The reaction mixture was allowed to warm to 0°C, and after four hours, the reaction was quenched with 3 mL of NH₄Cl_(sat.). The ethanol was removed *in vacuo*. Approximately 20 mL of EtOAc and 20 mL of H₂O were added to the slurry. The organic phase was separated, and the aqueous phase was extracted with additional EtOAc (2 x 25 mL). The combined organic layers were washed with brine (25 mL), dried with MgSO₄, and concentrated *in vacuo*. The crude organic product was purified by short column silica, 60Å, 60-200 μm, chromatography, hexanes:ethyl acetate, 85:15, and recrystallization in ethanol:water yielding yellow-white crystals, 25% yield (0.125 g). ¹H NMR (CDCl₃, δ ppm): 7.02 (1 H, s), 7.38 (5 H, m), 7.57 (1 H, m), 7.79 (1 H, m), 7.89 (2 H, d, *J* = 7.4 Hz). ¹³C NMR: 110.49, 120.57, 122.90, 122.92, 124.87, 128.55, 129.05, 130.27, 133.66, 141.56, 150.22, 158.57. MS: 263 [M+1], 235 [M+1, - N₂]. IR: 2122 cm⁻¹(N_{3, str}).

Ethyl azidoacetate (1).⁴⁴ Ethyl bromoacetate (15.0 mL, 0.135 mol) was added to a solution of sodium azide (17.91 g, 0.276 mol) in 50:50 acetone:water (100 mL). The

reaction mixture was allowed to stir at room temperature overnight. The organic layer was separated and the aqueous layer was extracted with EtOAc (2 x 25 mL). The combined organic layers were washed with brine (25 mL), dried over MgSO₄, and concentrated *in vacuo* to give a colorless oil, 89% yield (15.52 g) yield. The compound was stored in brown glass and in the refrigerator to prevent discoloration. ¹H NMR (CDCl₃, δ ppm): 1.06 (3 H, t, *J* = 8.0 Hz), 3.65 (2 H, s), 4.00 (2 H, q, *J* = 8.0 Hz). ¹³C NMR: 13.58, 49.81, 61.37, 168.11. HRMS: (calc) 129.0538, (found) 129.0539. IR: 1740 cm⁻¹ (C=O_{str}), 2102 cm⁻¹(N_{3, str}).

meta-phenylbenzaldehyde.⁶³ Pd(OAc)₂ (0.313 g, 1.7 mol%), triphenylphosphine (0.885 g, 4.1 mol%), phenyl boronic acid (11.127 g, 0.0913 mol, 1.12 eq), K₂CO₃ (25.002 g, 0.18090 mol, 2.2 eq) and *meta*-bromobenzaldehyde (15.046 g, 0.0813 mol, 1 eq) were added to a flask containing 100 mL THF and 50 mL H₂O. The reaction mixture was heated at 65°C, and then cooled after 24h. The organic layer was separated, and the aqueous layer was extracted with EtOAc (2 x 40 mL). The combined organic layers were washed with brine (25 mL), dried over MgSO₄, and concentrated *in vacuo*. The resulting crude organic product was purified by distillation, 150°C at 3 mmHg, yielding a colorless oil, 95% yield (14.08 g). ¹H NMR (CDCl₃, δ ppm): 7.42 (1 H, m) 7.47 (2 H, m), 7.60 (3 H, m), 7.85 (2 H, t, *J* = 7.49 Hz), 8.09 (1 H, s), 10.06 (1 H, s). ¹³C NMR: 126.94, 127.85, 127.96, 128.45, 128.84, 129.32, 132.84, 136.71, 139.44, 141.88, 192.14. MS: 182.0 [M⁺].

Knoevenagel Condensations. A freshly prepared solution of sodium ethoxide (50 mL, 0.35M) was transferred to a round bottom flask under an atmosphere of argon or nitrogen and cooled to 0°C. In a separate flask under an inert atmosphere was added ethyl

azidoacetate (1.4119 g, 0.0109 mol), ethyl trifluoroacetate (1.5533 g, 0.0109 mol), and the appropriate amount of aldehyde (0.00727 mol). The resulting solution was added with stirring to the solution of sodium ethoxide in a single portion. The ice bath was then removed, and after one hour, the reaction was quenched with 3 mL of $\text{NH}_4\text{Cl}_{(\text{sat.})}$. The ethanol-water was removed *in vacuo*. Approximately 20 mL of EtOAc and 20 mL of H_2O were added to the slurry. The organic phase was separated, and the aqueous phase was extracted with additional EtOAc (2 x 25 mL). The combined organic layers were washed with brine (25 mL), dried with MgSO_4 , and concentrated *in vacuo*.

(Z)-ethyl α -azido- β -phenylacrylate (2a). Crude product appears as wet orange crystals, 90% yield. Recrystallization (3x) with ethanol:water yields pale yellow crystals, 79% yield (1.253 g). ^1H NMR (CDCl_3 , δ ppm): 1.41 (3 H, t, $J = 8.0$ Hz), 4.38 (2 H, q, $J = 8.0$ Hz), 6.92 (1 H, s), 7.37 (3 H, m), 7.81 (2H, m). ^{13}C NMR: 14.04, 62.08, 125.18, 125.51, 128.30, 129.20, 130.43, 133.14, 163.32; $^3J_{\text{C,H}}$: 4.2 Hz. MS: 217.1 [M^+]. IR: 1713 cm^{-1} ($\text{C}=\text{O}_{\text{str}}$), 2110 cm^{-1} (N_3_{str}). EA (calc.): C, 60.82; H, 5.10; N, 19.34. (found): C, 61.08; H, 5.14; N, 18.68. mp 37-41 $^\circ\text{C}$.

(Z)-ethyl α -azido- β -(*m*-methylphenyl)acrylate (2b). Crude product appears as red-orange oil, 92% yield. Silica chromatography ethyl acetate:hexanes (10:90), 73% yield yellow oil (1.235 g). ^1H NMR (CDCl_3 , δ ppm): 1.41 (3 H, t, $J = 8.0$ Hz), 2.39 (3H, s), 4.37 (2 H, q, $J = 8.0$ Hz), 6.91 (1 H, s), 7.37 (3 H, m), 7.20 (2H, d, $J = 8.0$ Hz), 7.72 (2H, d, $J = 8.0$ Hz). ^{13}C NMR: 14.04, 21.24, 62.05, 125.13, 125.36, 127.60, 128.18, 130.09, 131.04, 132.99, 137.85, 163.38; $^3J_{\text{C,H}}$: 4.9 Hz. HRMS: (calc) 231.1008, (found) 231.0998. IR: 1707 cm^{-1} ($\text{C}=\text{O}_{\text{str}}$), 2110 cm^{-1} (N_3_{str}).

(Z)-ethyl α -azido- β -(*m*-methoxyphenyl)acrylate (2c). Crude product appears as wet orange crystals, 93% yield. Recrystallization with ethanol:water (3x) yields pale yellow-white crystals 78% yield (1.410 g). ^1H NMR (CDCl_3 , δ ppm): 1.40 (3 H, t, $J = 8.0$ Hz), 3.84 (3H, s), 4.37 (2 H, q, $J = 8.0$ Hz), 6.88 (2 H, m), 7.31 (2 H, m), 7.44 (1H, s). ^{13}C NMR: 14.21, 55.29, 62.30, 115.26, 115.43, 123.38, 125.11, 125.74, 129.36, 134.40, 159.42, 163.47; $^3\text{J}_{\text{C,H}}$: 4.9 Hz. MS: M^+ , 247.1. IR: 1707 cm^{-1} ($\text{C}=\text{O}_{\text{str}}$), 2102 cm^{-1} (N_3_{str}). EA (calc.): C, 58.29; H, 5.30; N, 17.00. (found): C, 58.35; H, 5.30; N, 17.02. mp 49.6°C .

(Z)-ethyl α -azido- β -(*m*-chlorophenyl)acrylate (2d). Crude product appears as wet yellow-orange crystals, 99% yield. Recrystallization with ethanol:water (3x) yields pale yellow-white crystals 76% yield (1.408g). ^1H NMR (CDCl_3 , δ ppm): 1.40 (3 H, t, $J = 8.0$ Hz), 4.37 (2 H, q, $J = 8.0$ Hz), 6.80 (2 H, m), 7.28 (2 H, m), 7.63 (1H, s), 7.85 (1 H, s). ^{13}C NMR: 14.12, 62.41, 123.17, 126.69, 128.63, 129.11, 129.54, 130.00, 134.28, 134.83, 163.10; $^3\text{J}_{\text{C,H}}$: 4.9 Hz. MS [M^+]: 262.0. IR: 1708 cm^{-1} ($\text{C}=\text{O}_{\text{str}}$), 2119 cm^{-1} (N_3_{str}). EA (calc.): C, 52.49; H, 4.01; Cl, 14.08; N, 16.70. (found): C, 52.81; H, 4.09; Cl, 14.08; N 16.52. mp 47.7°C .

(Z)-ethyl α -azido- β -(*m*-phenylphenyl)acrylate (2e). Crude product appears as wet orange crystals, 86% yield (1.546 g). Recrystallization with ethanol:water (3x) yields pale yellow-white crystals 72% yield. ^1H NMR (CDCl_3 , δ ppm): 1.42 (3 H, t, $J = 8.0$ Hz), 4.39 (2 H, q, $J = 8.0$ Hz), 6.99 (1 H, s), 7.31 (2 H, m), 7.44 (1H, s), 7.38 (1 H, m) 7.47 (3 H, m) 7.61 (3 H, m) 7.83 (1 H, d, $J = 8.0$ Hz) 8.03 (1 H, s). ^{13}C NMR: 14.21, 62.32, 125.09, 125.81, 127.16, 127.52, 128.15, 128.81, 128.87, 129.29, 133.63, 140.62, 141.45, 163.49; $^3\text{J}_{\text{C,H}}$: 4.9 Hz. MS, exact mass: 293.1164. IR: 1707 cm^{-1} ($\text{C}=\text{O}_{\text{str}}$), 2118 cm^{-1} (N_3_{str}). EA (calc): C, 69.61; H, 5.15; N, 14.33. (found): C, 69.74; H, 5.09; N, 13.96. mp 88.1°C .

(Z)-ethyl α -azido- β -(*m*-nitrophenyl)acrylate (2f).

2 equivalents of ethyl azidoacetate, sodium ethoxide, and ethyl trifluoroacetate were used in this condensation. Crude product appears as a wet, red solid, 89% yield (1.239 g). Flash column chromatography with ethyl acetate: hexanes (15:85) yields white solid, 65% yield (0.91g). ^1H NMR (CDCl_3 , δ ppm): 1.40 (3 H, t, $J = 7.14$ Hz), 4.38 (2 H, q, $J = 7.15$ Hz), 6.88 (1H, s), 7.54 (1H, t, $J = 7.89$ Hz), 8.09 (1H, d, $J = 7.86$), 8.16 (1 H, dd, $J = 8.23$), 8.66 (1H, m). ^{13}C NMR: 14.10, 62.70, 121.52, 123.43, 124.80, 128.20, 129.33, 134.71, 135.91, 148.18, 162.81; $^3\text{J}_{\text{C,H}}$: 4.9 Hz. HRMS: (calc) 262.0702 (found) 262.0713. IR: 1711 cm^{-1} ($\text{C}=\text{O}_{\text{str}}$), 2112 cm^{-1} (N_3 , str). mp 58.6°C .

(Z)-ethyl α -azido- β -(*p*-methylphenyl)acrylate (2g). Crude product appears as wet orange crystals, 89% yield. Recrystallization with ethanol:water (3x) yields pale yellow-white crystals 77% yield (1.307 g). ^1H NMR (CDCl_3 , δ ppm): 1.40 (3 H, t, $J = 8.0$ Hz), 2.37 (3H, s), 4.36 (2 H, q, $J = 8.0$ Hz), 6.90 (1 H, s), 7.37 (3 H, m), 7.20 (2H, d, $J = 8$ Hz), 7.72 (2H, d, $J = 8.0$ Hz). ^{13}C NMR: 14.21, 21.47, 62.14, 124.63, 125.52, 129.20, 130.58, 139.75, 163.62. MS: 231.1 [M^+]. IR: 1707 cm^{-1} ($\text{C}=\text{O}_{\text{str}}$), 2112 cm^{-1} (N_3 , str). EA (calc.): C, 60.82; H, 5.10; N, 19.34. (found): C, 61.08; H, 5.14; N, 18.68. mp $47\text{-}53^\circ$.

(2Z,2'Z)-diethyl 3,3'-(1,3-phenylene)bis(2-azidoacrylate) (2h). Product precipitates as a white solid, 77% yield (1.995 g). No purification. ^1H NMR (CDCl_3 , δ ppm): 1.41 (6 H, t, $J = 8.0$ Hz), 4.38 (4 H, q, $J = 8.0$ Hz), 6.90 (2 H, s), 7.38 (2 H, 2), 7.40 (1H, t, $J = 8.0$ Hz), 7.81 (2 H, d, $J = 8.0$ Hz), 8.18 (1 H, s). ^{13}C NMR: 14.19, 62.36, 124.51, 126.14, 128.58, 131.07, 132.65, 133.41, 163.34; $^3\text{J}_{\text{C,H}}$: 5.0 Hz. HRMS: (calc) 356.1233, (found) 356.1240. IR: 1707 cm^{-1} ($\text{C}=\text{O}_{\text{str}}$), 2108 cm^{-1} (N_3 , str). mp 106.0°C .

(2Z,2'Z)-diethyl 3,3'-(1,4-phenylene)bis(2-azidoacrylate) (2i). Product precipitates as a pale yellow solid, 72% yield (1.865 g). No purification. The product should be stored under N₂ because it turns brown in air within 2h. The decomposition is limited to the exposed surfaces. ¹H NMR (CDCl₃, δ ppm): 1.42 (6 H, t, *J* = 8.0 Hz), 4.38 (4 H, q, *J* = 8.0 Hz), 6.90 (2 H, s), 7.83 (4 H, s). ¹³C NMR: 14.21, 62.39, 124.13, 126.35, 130.53, 133.99, 163.36. ³J_{C,H}: 4.9 Hz. HRMS: (calc.) 356.1233, (found) 356.1240. IR: 1703 cm⁻¹ (C=O_{str}), 2102 cm⁻¹ (N_{3, str}). mp decomposes at 129.7°C.

(Z)-ethyl 2-azido-3-(furan-2-yl)acrylate (2j). Crude product is a dark brown oil, 90% yield. Purified by silica plug (ethyl acetate:hexanes, 10/90) and recrystallization in ethanol:water, 83% yield (1.254 g). ¹H NMR (CDCl₃, δ ppm): 1.35 (3 H, t, *J* = 8.0 Hz), 4.31 (2 H, q, *J* = 8.0 Hz), 6.50 (1 H, m), 6.84 (1 H, m), 7.08 (1 H, d, *J* = 4.0 Hz), 7.46 (1 H, m). ¹³C NMR: 14.02, 62.01, 112.44, 113.23, 115.02, 122.73, 143.71, 149.39, 162.96. ³J_{C,H}: 4.6 Hz. HRMS: (calc) 207.0644, (found) 207.0643. IR: 1703 cm⁻¹ (C=O_{str}), 2104 cm⁻¹ (N_{3, str}) mp 30.5°C.

Hemetsberger Indolization. A flask containing 1g of crude or pure α-azido-β-arylacrylate in 50 mL of *ortho*-dichlorobenzene was heated to 150°C. The reaction is cooled after 30 minutes, and the solvent is removed *in vacuo*. The regioisomeric indoles are purified by silica column chromatography. The 60Å, 60-200 μm silica particles were stirred in hexanes:triethylamine 98:2 overnight, and the mobile phase used was hexanes:ethyl acetate, 85:15.

Ethyl 1*H*-indole-2-carboxylate (3a). White-beige crystals, 81% yield (0.706 g). ¹H NMR (CDCl₃, δ ppm): 1.43 (3H, t, *J* = 8.0 Hz), 4.42 (2H, q, *J* = 8.0Hz), 7.16 (1H, dt, *J* =

8.0 Hz), 7.25 (1H, dd), 7.33 (1H, dt, $J = 8.0$ Hz), 7.44 (2H, dd, $J = 8.0$ Hz), 7.70 (1H, dd, $J = 8.0$ Hz), 9.27 (1H, s). ^{13}C NMR: 14.34, 61.01, 108.57, 111.88, 120.68, 122.51, 125.24, 127.41, 127.84, 136.86, 162.14. HRMS: (calc) 189.0790, (found) 189.0795. EA: (calc.) C, 69.83; H, 5.86; N, 7.40; (found) C, 69.81; H, 5.85; N, 7.40.

Ethyl 5-methyl-1H-indole-2-carboxylate and ethyl 7-methyl-1H-indole-2-

carboxylate (3b).⁶⁴ White crystals, mixture of regioisomers 1.1:1 respectively by ^1H NMR of the –Me signals, 76% yield (0.668 g). ^1H NMR (CDCl_3 , δ ppm): 1.40 (3H, t, $J = 7.12$ Hz), 1.41 (3H, t, $J = 7.12$ Hz), 2.42 (3H, s), 2.51 (3H, s), 4.41 (4H, p, $J = 7.19$ Hz), 7.04-7.14 (4H, m), 7.23 (1H, d, $J = 2.04$ Hz), 7.30 (1H, d, $J = 8.44$ Hz), 7.44 (1H, s), 7.53 (1H, d, $J = 7.68$), 9.12 (1H, s), 9.25 (1H, s). ^{13}C NMR: 14.40, 16.71, 21.41, 60.95, 61.04, 108.07, 109.19, 111.59, 120.16, 120.98, 121.29, 121.77, 125.52, 125.56, 127.06, 127.20, 127.24, 127.45, 127.71, 129.97, 135.37, 136.79, 162.25, 162.34. MS: 203 [M^+]. EA: (calc.) C, 70.92; H, 6.45; N, 6.89; (found) C, 71.00; H, 6.50; N, 6.86.

Ethyl 5-methoxy-1H-indole-2-carboxylate and ethyl 7-methoxy-1H-indole-2-

carboxylate (3c). Mixture of regioisomers 1:1 respectively, by ^1H NMR of the –OMe signals. White crystals, 78% yield (0.692 g). ^1H NMR (CDCl_3 , δ ppm): 1.42 (3H, 7.13 Hz), 3.86 (3H, s), 3.96 (3H, s), 4.42 (4H, q, $J = 7.13$ Hz), 7.00 (1H, dd, $J = 8.94$ Hz, $J = 1.56$ Hz), 7.06 (2H, m), 7.14 (1H, dd, $J = 2.14$ Hz), 7.20 (1H, d, $J = 2.29$), 7.27 (1H, d, $J = 8.17$ Hz), 7.31 (1H, d, $J = 8.92$ Hz), 9.08, (1H, s), 9.19 (1H, s). ^{13}C NMR: 14.34 (2C), 55.31, 55.59, 60.90 (2C), 102.42, 104.01, 108.10, 108.78, 112.75, 114.71, 116.87, 121.08, 127.16, 127.74, 127.80, 128.02, 128.57, 132.23, 146.40, 154.59, 161.79, 162.00. MS [M^+]: 219.0. IR: 1684 cm^{-1} ($\text{C}=\text{O}_{\text{str}}$), 3226 cm^{-1} ($\text{N}-\text{H}_{\text{str}}$). EA: (calc.) C, 65.74, H, 5.98, N, 6.39; (found) C, 65.97, H, 5.99, N, 6.26.

Ethyl 5-chloro-1*H*-indole-2-carboxylate (3d-5).⁶⁴ White crystals, 39% yield (0.347 g). ¹H NMR (CDCl₃, δ ppm): 1.42 (3H, t, *J* = 7.12 Hz), 4.41 (2H, q, *J* = 7.13 Hz), 7.15 (1H, d, *J* = 2.09), 7.28 (1H, dd, *J* = 8.75), 7.35 (1H, m, *J* = 8.79), 7.66 (1H, d, *J* = 1.92) 9.18 (1H, s). ¹³C NMR: 14.35, 61.27, 107.92, 112.97, 121.71, 125.79, 126.40, 128.35, 128.70, 135.06, 161.78. HRMS: (calc) 223.0400, (found) 223.0393. EA: (calc.) C, 59.07; H, 4.51; N, 6.26; Cl, 15.85 (found) C, 58.99; H, 4.67; N, 6.18; Cl, 15.58.

Ethyl 7-chloro-1*H*-indole-2-carboxylate (3d-7). White crystals, 33% yield (0.293 g). ¹H NMR (CDCl₃, δ ppm): 1.43 (3H, t, *J* = 7.13 Hz), 4.44 (2H, q, *J* = 7.13 Hz), 7.07 (1H, t, *J* = 8.03 Hz), 7.25 (1H, d, *J* = 2.22 Hz), 7.31 (1H, d, *J* = 7.59 Hz), 7.58 (1H, d, *J* = 8.05 Hz) 9.23 (1H, s). ¹³C NMR: 14.31, 61.23, 109.22, 117.15, 121.05, 121.35, 124.32, 128.21, 128.64, 134.18, 161.49. HRMS: (calc) 223.0400, (found) 223.0400.

Ethyl 5-phenyl-1*H*-indole-2-carboxylate (3e-5).⁶⁵ White crystals, 49% yield (0.443 g). ¹H NMR (CDCl₃, δ ppm): 1.45 (3H, t, *J* = 7.14), 4.46 (2H, q, *J* = 7.14), 7.30 (1H, dd, *J* = 2.09), 7.35 (1H, dt, *J* = 7.37), 7.45 (4H, m), 7.60 (2H, dd, *J* = 8.61), 7.66 (2H, dd, *J* = 8.40), 7.91 (1H, s), 9.22 (1H, s). ¹³C NMR: 14.34, 61.01, 108.96, 121.27, 121.73, 124.95, 126.40, 127.71, 127.75, 127.93, 128.12, 129.23, 134.82, 138.32, 161.87. HRMS: (calc) 265.1103, (found) 265.1009.

Ethyl 7-phenyl-1*H*-indole-2-carboxylate (3e-7). White crystals, 25% yield (0.226 g). ¹H NMR (CDCl₃, δ ppm): 1.42 (3H, t, *J* = 7.12), 4.40 (2H, q, *J* = 7.13), 7.27 (1H, m), 7.32 (1H, d, *J* = 2.15), 7.36 (1H, dd, *J* = 7.21, 1.13), 7.43 (1H, dt, *J* = 7.41), 7.55 (2H, t, *J* = 7.31), 7.65 (2H, m), 7.71 (1H, d, *J* = 8.00Hz), 9.08 (1H, s). ¹³C NMR: 14.37, 61.10, 108.90, 112.13, 120.76, 125.33, 126.62, 127.27, 128.69, 134.27, 136.31, 141.80, 162.03.

MS (EI): 265 [M^+]. EA: (calc.) C, 76.96; H, 5.70; N, 5.28; (found) C, 77.03 H, 5.78; N, 5.19.

Ethyl 5-nitro-1*H*-indole-2-carboxylate and ethyl 7-nitro-1*H*-indole-2-carboxylate (3f).⁶⁶ Mixture of regioisomers 1.1:1, by ^1H NMR of the N-H signals. Yellow-white crystals, 62% yield (0.553 g). ^1H NMR (acetone- d_6 , δ ppm): 1.37-1.42 (6H, 2-t), 4.38-4.44 (4H, 2-q), 7.39 (1H, t, $J = 7.97$ Hz), 7.44-7.46 (2H, m), 7.71 (1H, d, $J = 9.13$ Hz), 8.17 (1H, dd, $J = 9.13$ Hz, $J = 2.27$ Hz), 8.23 (1H, d, $J = 7.88$ Hz), 8.32 (1H, d, $J = 8.03$ Hz), 8.73 (1H, d, $J = 2.23$ Hz), 10.74 (1H, s), 11.58 (1H, s). ^{13}C NMR: 13.43, 13.65, 60.96, 61.14, 109.17, 109.84, 112.89, 119.40, 119.47, 120.24, 121.92, 128.71, 130.55, 130.86, 131.10, 131.17, 160.32. MS: 234 [M^+].

Ethyl 6-methyl-1*H*-indole-2-carboxylate (3g). White crystals, 80% yield (0.703 g). ^1H NMR (CDCl_3 , δ ppm): 1.42 (3H, t, $J = 7.14$ Hz), 2.47 (3H, s), 4.41 (2H, q, $J = 7.15$ Hz), 6.99 (1H, d, $J = 8.22$ Hz), 7.20 (2H, m, $J = 6.69$ Hz), 7.57 (1H, d, $J = 8.21$ Hz), 8.88 (1H, s). ^{13}C NMR: 14.30, 21.88, 60.84, 108.55, 111.54, 122.01, 122.74, 125.24, 126.76, 135.33, 137.47, 162.23. MS: 203.1 [M^+].

Diethyl 1,5-dihydropyrrolo[2,3-*f*]indole-2,6-dicarboxylate (3h).⁵⁸ White/beige crystals, 64% yield (0.590 g). ^1H NMR (DMSO, δ ppm): 1.32-1.36 (6H, 2-q), 4.30-4.36 (4H, 2-t), 7.19-7.21 (2H, m), 7.47 (1H, d, $J = 8.84$ Hz), 7.60 (1H, d, $J = 1.27$ Hz), 12.09 (1H, s), 12.29 (1H, s). ^{13}C NMR: 14.34, 14.40, 59.99, 60.18, 106.48, 107.88, 110.00, 113.29, 119.88, 120.00, 123.98, 124.87, 131.35, 136.20, 161.16, 161.30. HRMS: (calc.) 300.1110, (found) 300.1118.

Diethyl 1,6-dihydropyrrolo[2,3-*e*]indole-2,7-dicarboxylate (3i). Yellow/beige crystals, 70% yield (0.645 g). ^1H NMR (DMSO, δ ppm): 1.34 (6H, t, $J = 6.98$ Hz), 4.34 (4H, q, J

= 6.93 Hz), 7.23 (2H, s), 7.31 (2H, s), 11.58 (2H, s). ^{13}C NMR: 14.33, 60.40, 109.64, 115.65, 124.12, 124.14, 124.81, 161.09. HRMS: (calc.) 300.1110, (found) 300.1101.

Ethyl 4H-furo[3,2-b]pyrrole-5-carboxylate (3j). Brown needle-like crystals, 80% yield (0.692 g). ^1H NMR (CDCl_3 , δ ppm): 1.37 (3H, t, $J = 7.12$ Hz), 4.35 (2H, q, $J = 7.13$ Hz), 6.45 (1H, dd, $J = 2.21$ Hz), 6.80 (1H, m, $J = 1.69$), 7.51 (1H, d, $J = 2.22$ Hz), 8.84 (1H, s). ^{13}C NMR: 14.45, 60.48, 96.81, 98.88, 124.20, 128.66, 147.97, 148.56, 162.16. HRMS: (calc) 179.0582, (found) 179.0580. EA: (calc.) C, 60.33; H, 5.06; N, 7.82; (found) C, 60.31; H, 5.07; N, 7.81.

1.7 ^1H , ^{13}C , and ^1H - ^{13}C -coupled NMR spectra, ethyl α -azido- β -arylacrylates (2a-2j)

Nuclear magnetic resonance spectra were measured on a 400 MHz Varian (1-D measurements) and a Bruker AVIII HD 500 MHz (2-D measurements); chloroform-d was used as the solvent except where noted otherwise.

Figure 10. ^1H NMR: (Z)-Ethyl α -azido- β -phenylacrylate (2a)

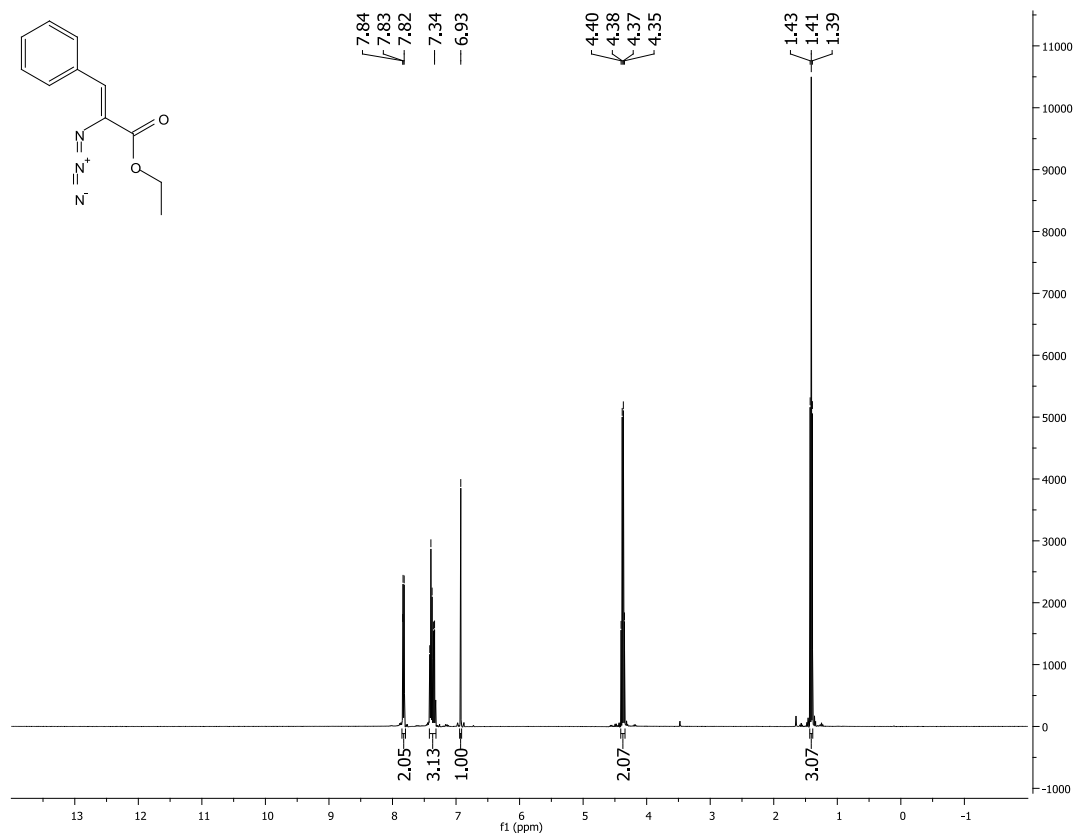
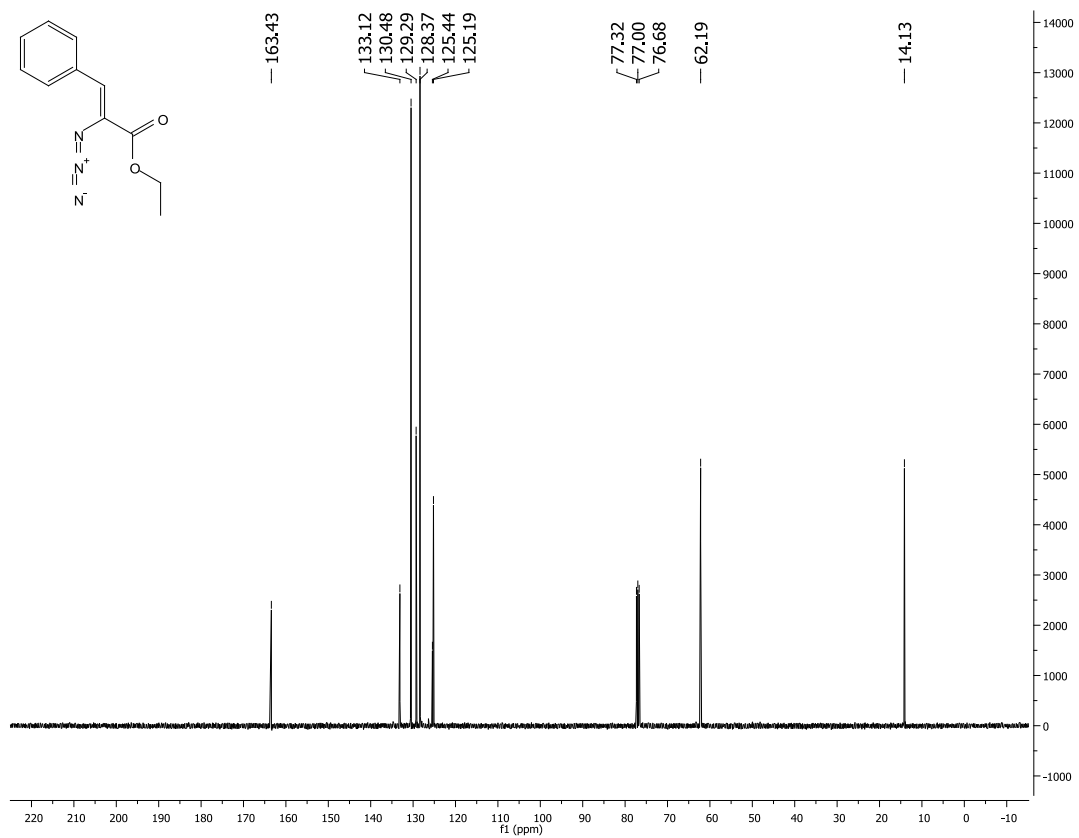


Figure 11. ^{13}C NMR: (Z)-Ethyl α -azido- β -phenylacrylate (2a)



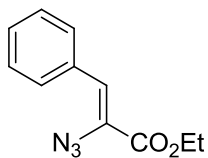


Figure 12. $^3J_{C,H}$ of 1H - ^{13}C Coupled NMR: (Z)-Ethyl α -azido- β -phenylacrylate (2a)

Standard C13

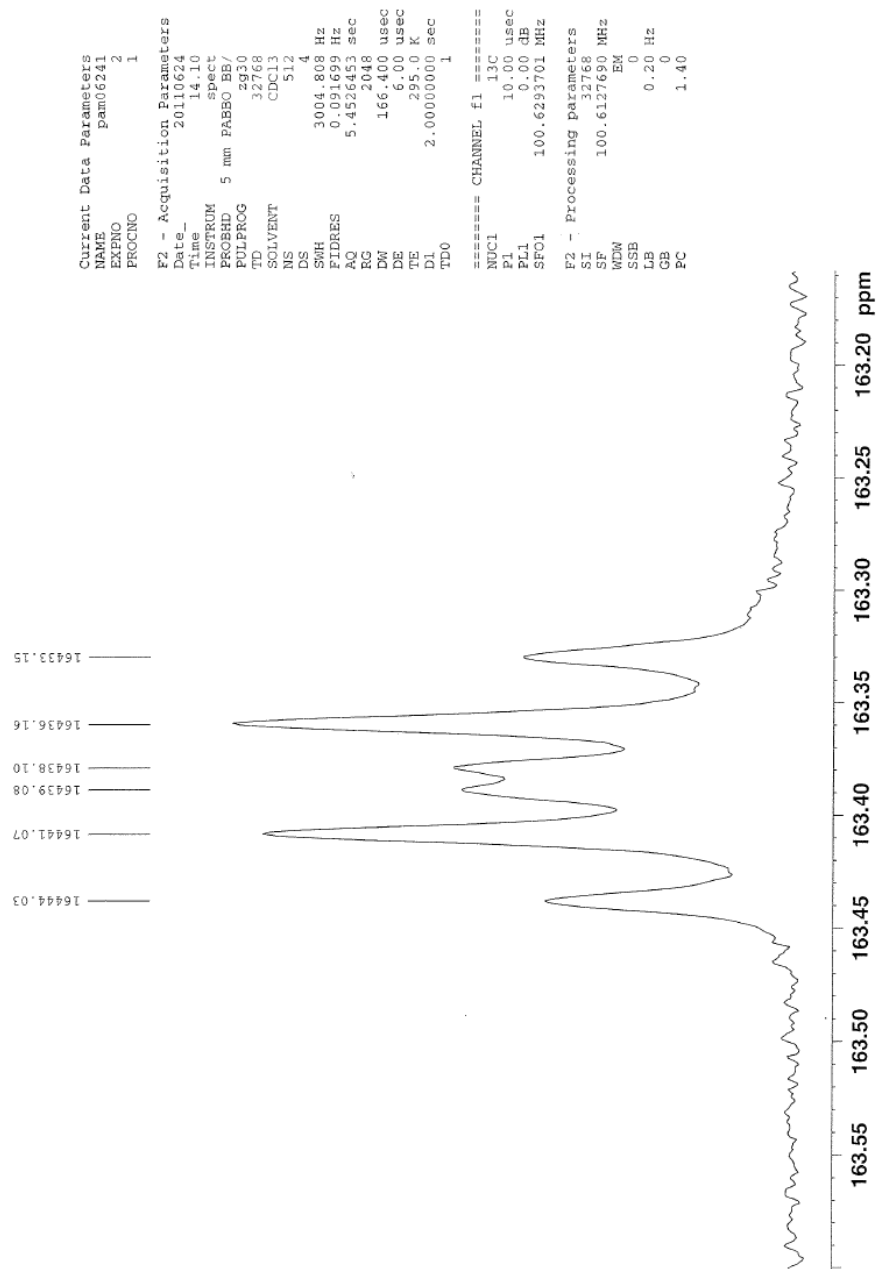


Figure 13. ^1H NMR: (Z)-Ethyl *meta*-methyl- α -azido- β -phenylacrylate (2b)

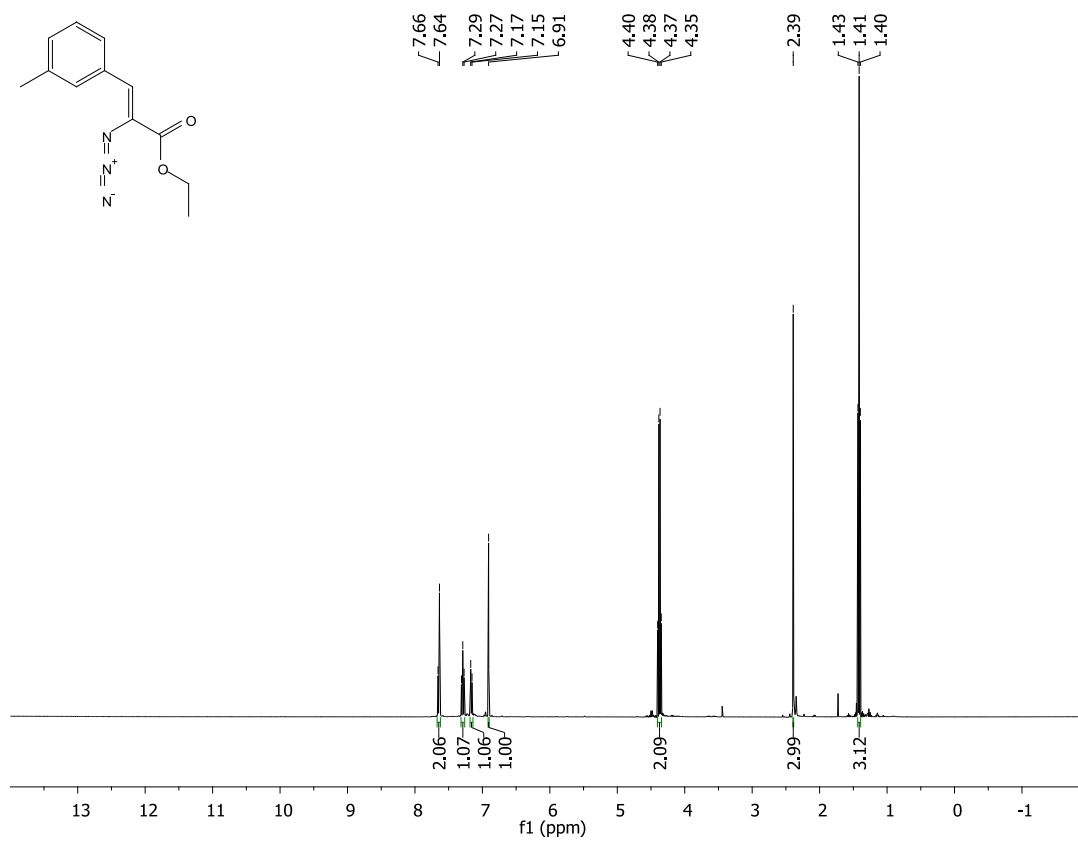


Figure 14. ^{13}C NMR: (Z)-Ethyl *meta*-methyl- α -azido- β -phenylacrylate (2b)

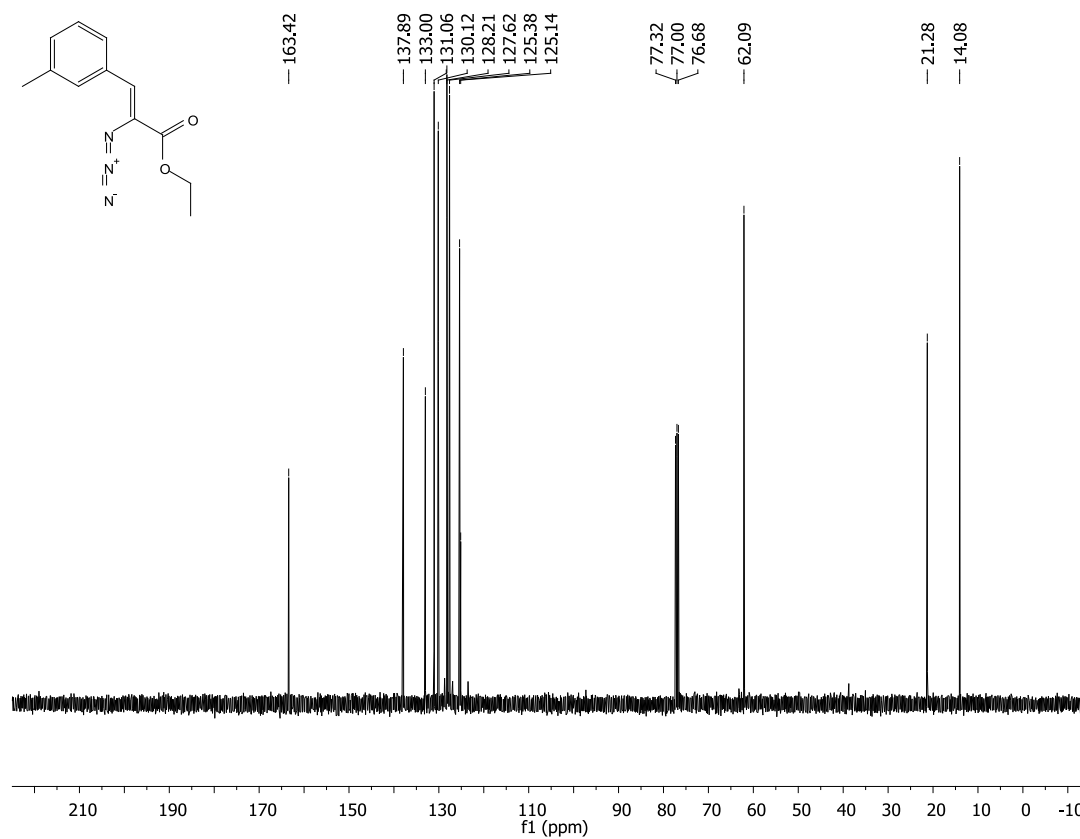


Figure 15. ^1H - ^{13}C Coupled NMR: (Z)-Ethyl *meta*-methyl- α -azido- β -phenylacrylate (2b)

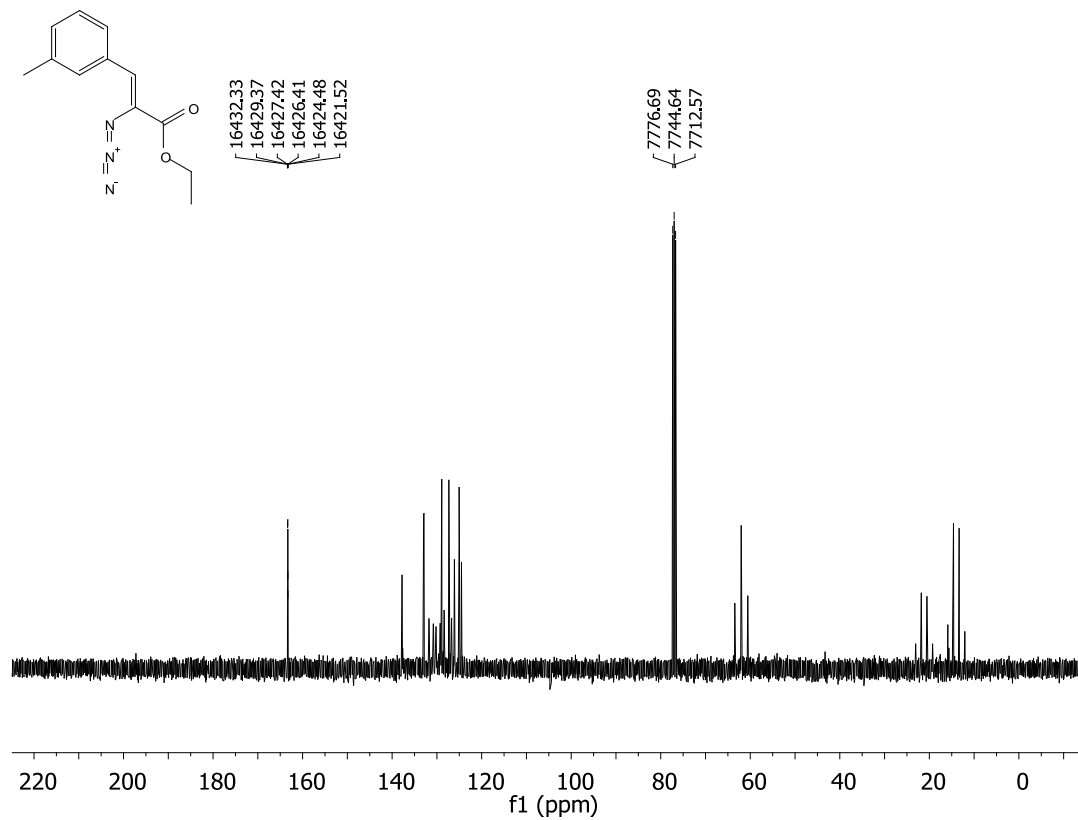


Figure 16. $^3J_{C,H}$ of 1H - ^{13}C Coupled NMR: (Z)-Ethyl *meta*-methyl- α -azido- β -phenylacrylate (2b)

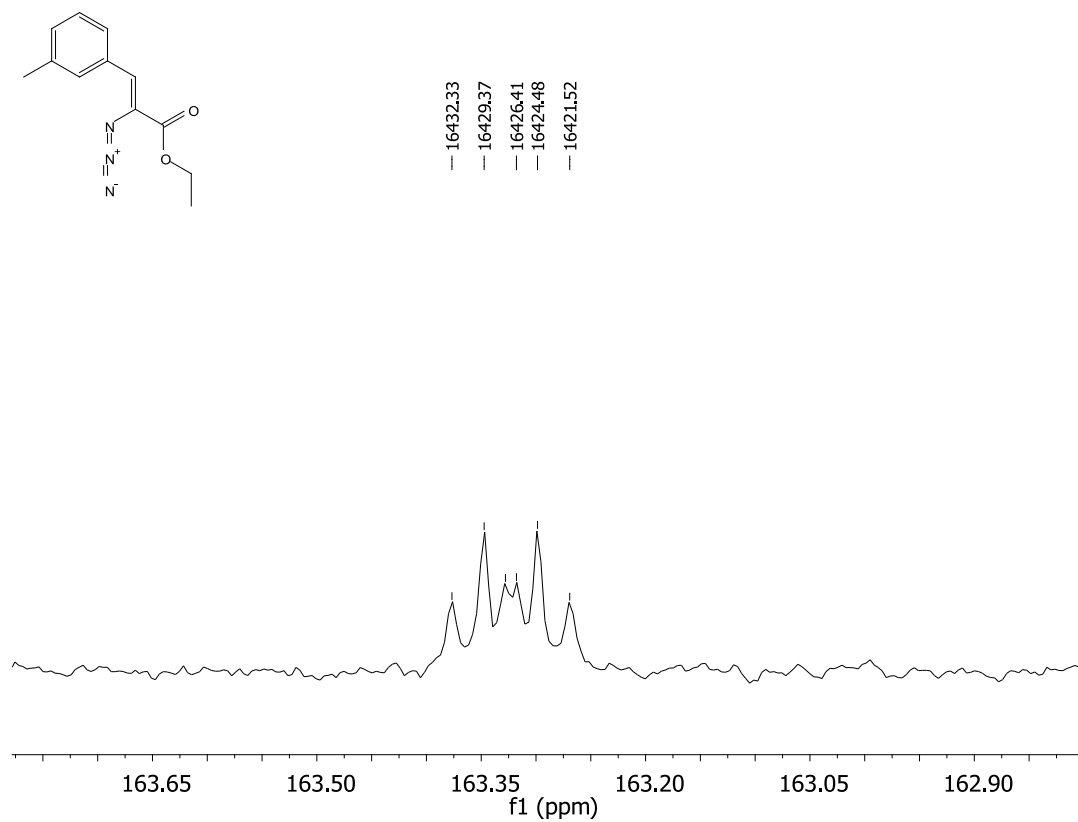


Figure 17. ^1H NMR: (Z)-Ethyl *meta*-methoxy- α -azido- β -phenylacrylate (2c)

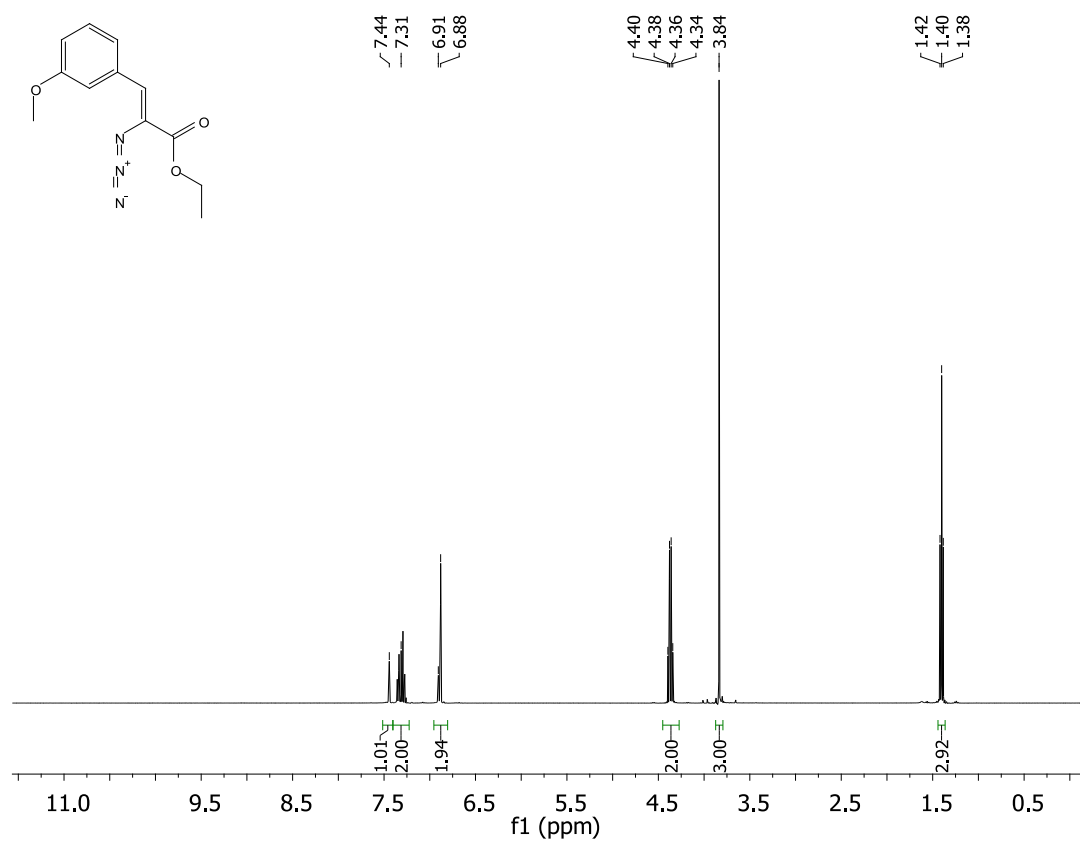


Figure 18. ^{13}C NMR: (Z)-Ethyl *meta*-methoxy- α -azido- β -phenylacrylate (2c)

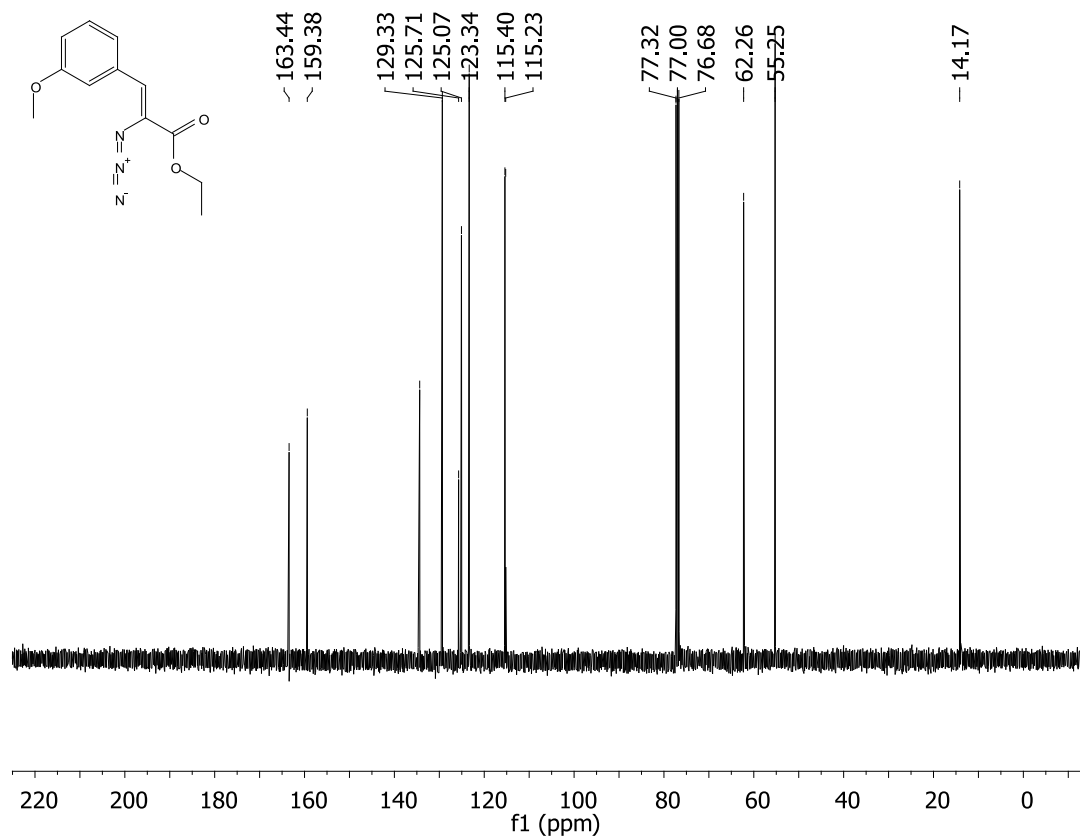


Figure 19. ^1H - ^{13}C Coupled NMR: (Z)-Ethyl *meta*-methoxy- α -azido- β -phenylacrylate (2c)

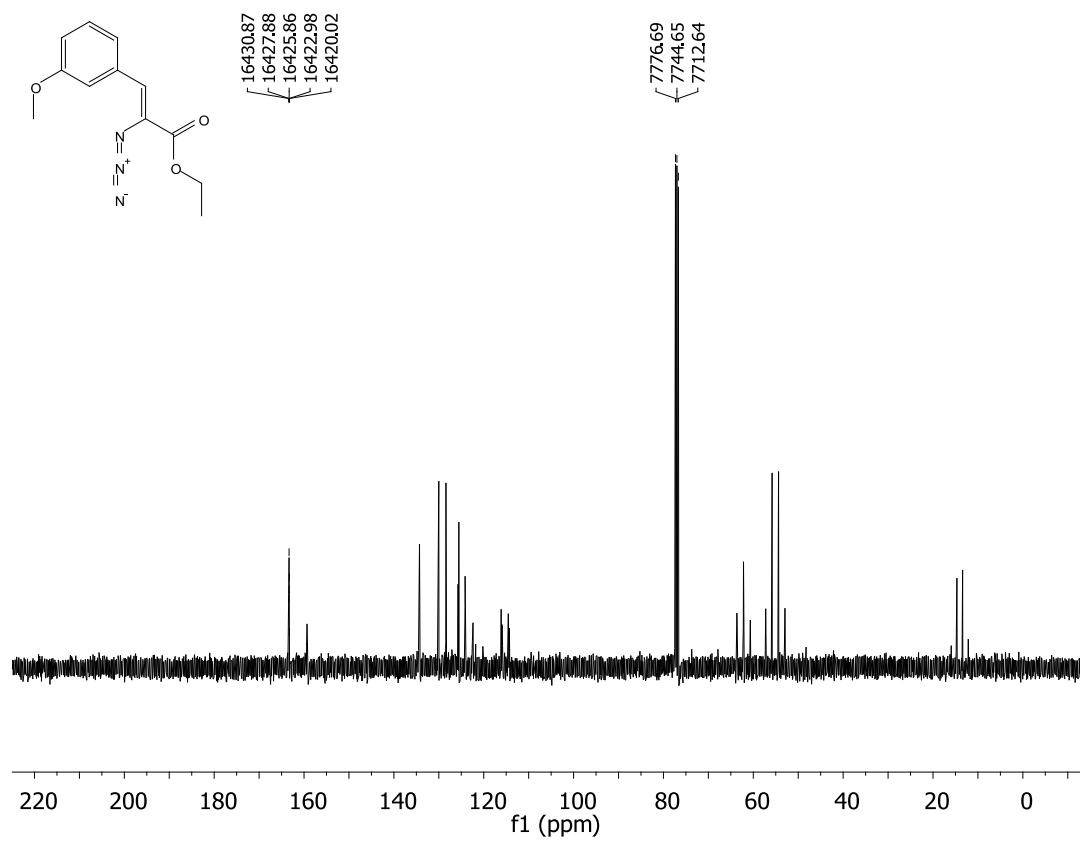


Figure 20. $^3J_{C,H}$ of 1H - ^{13}C Coupled NMR: (Z)-Ethyl *meta*-methoxy- α -azido- β -phenylacrylate (2c)

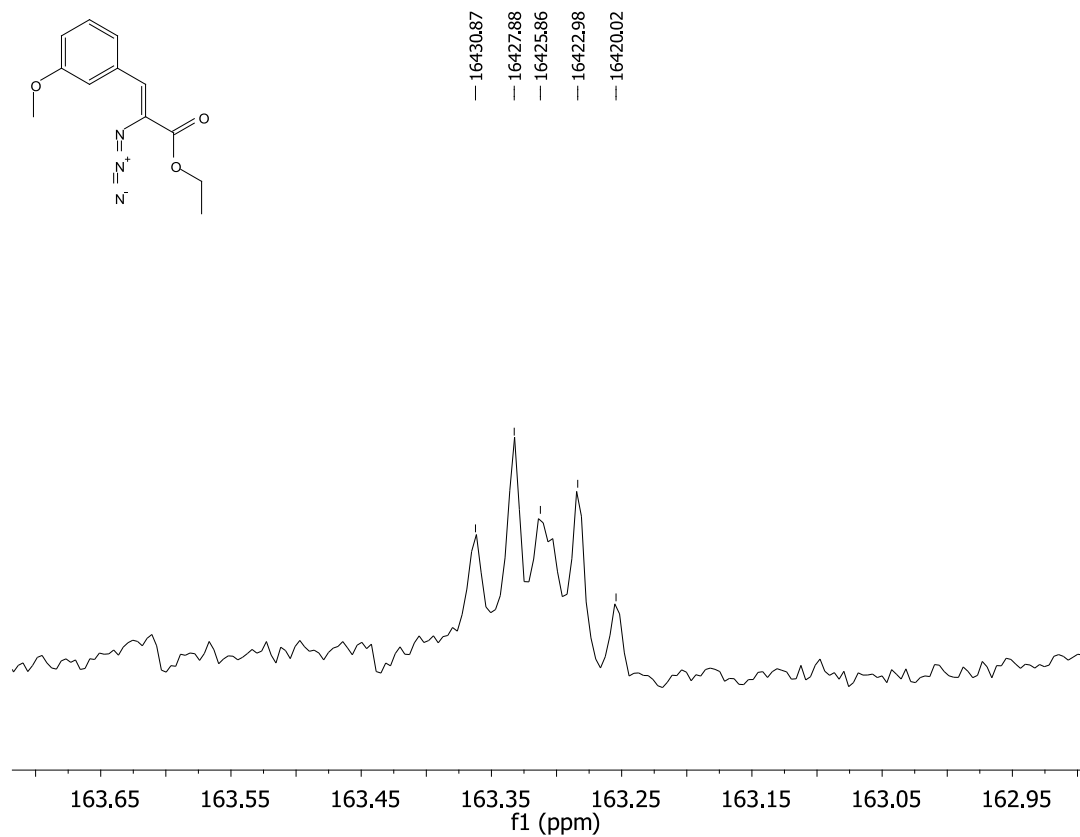


Figure 21. ^1H NMR: (Z)-Ethyl *meta*-chloro- α -azido- β -phenylacrylate (2d)

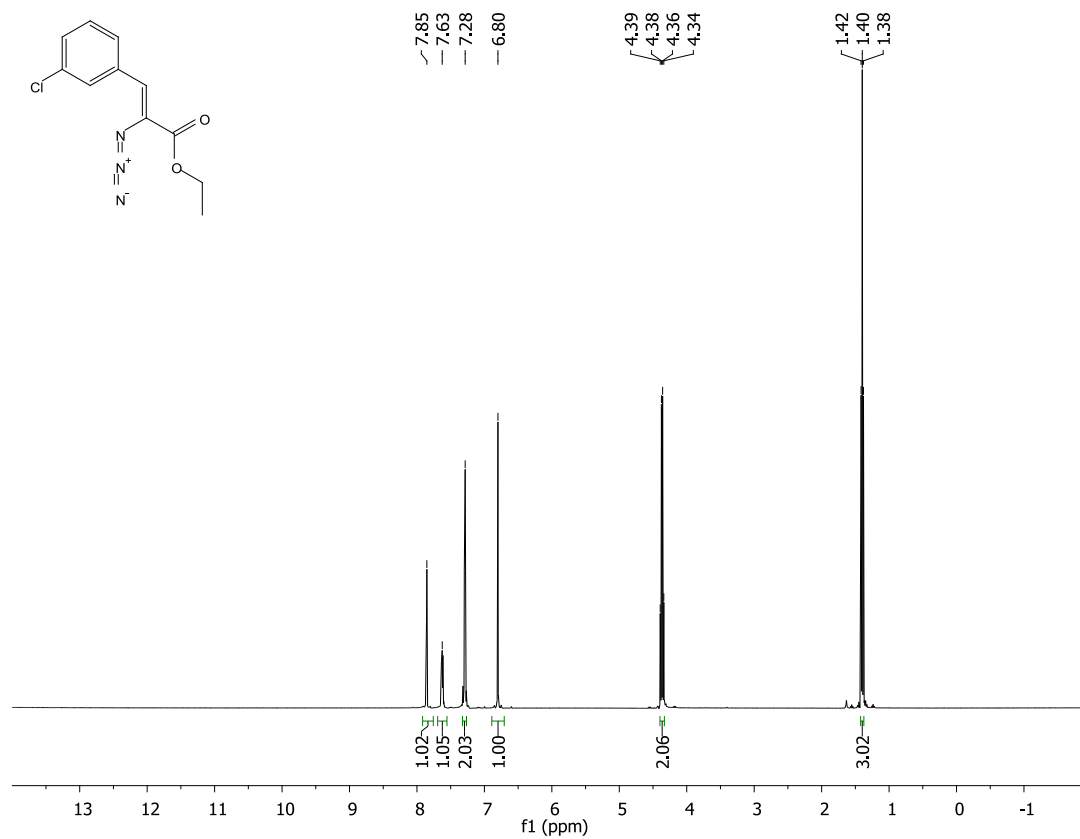


Figure 22. ^{13}C NMR: (Z)-Ethyl *meta*-chloro- α -azido- β -phenylacrylate (2d)

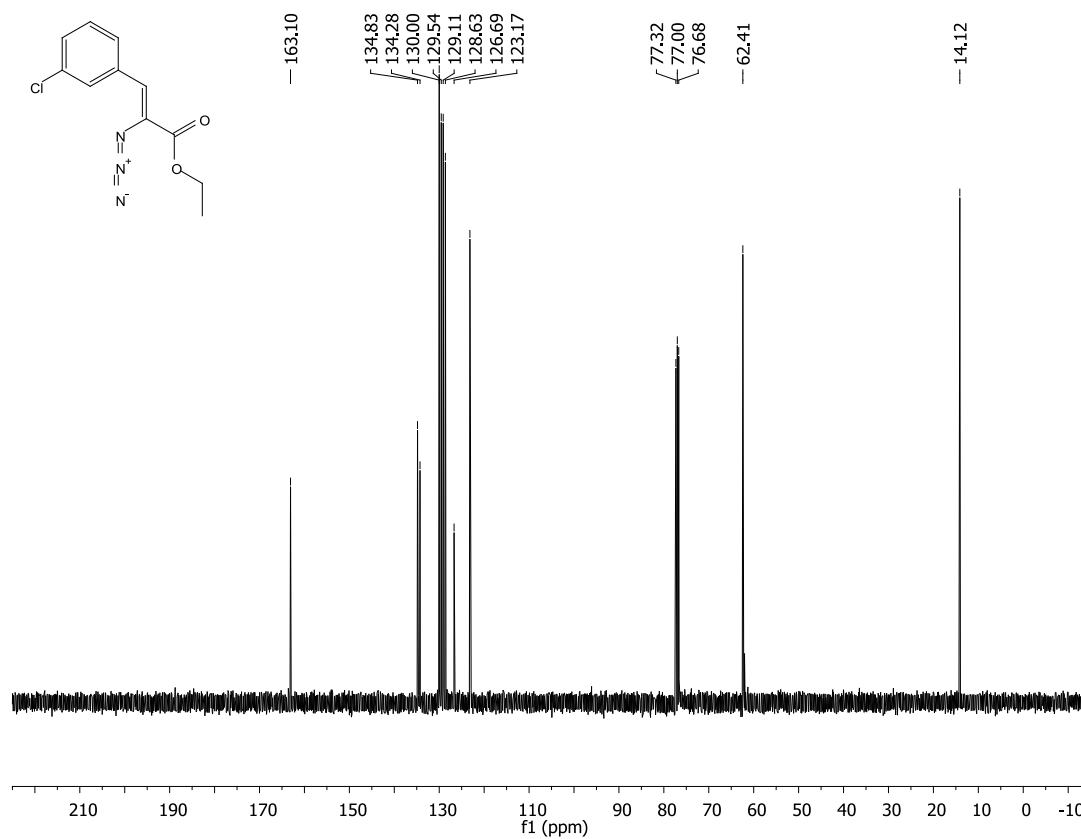


Figure 23. ^1H - ^{13}C Coupled NMR: (Z)-Ethyl *meta*-chloro- α -azido- β -phenylacrylate (2d)

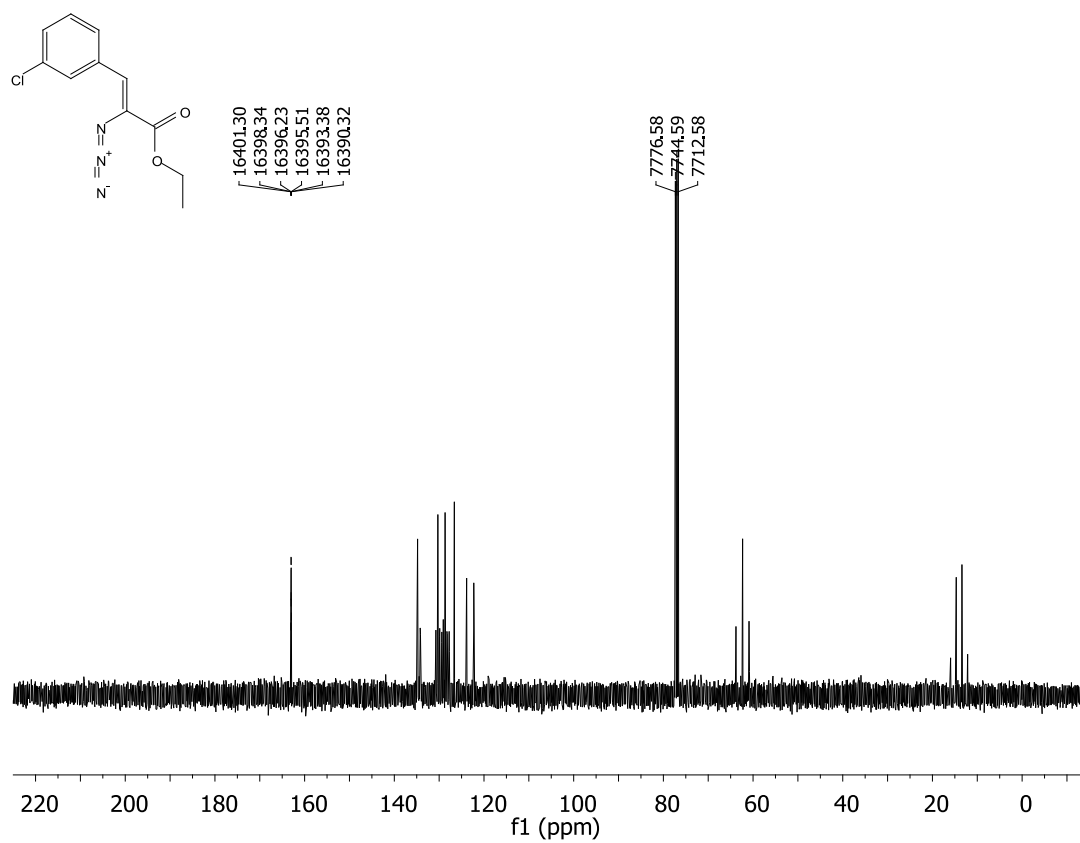


Figure 24. $^3J_{C,H}$ of 1H - ^{13}C Coupled NMR: (Z)-Ethyl *meta*-chloro- α -azido- β -phenylacrylate (2d)

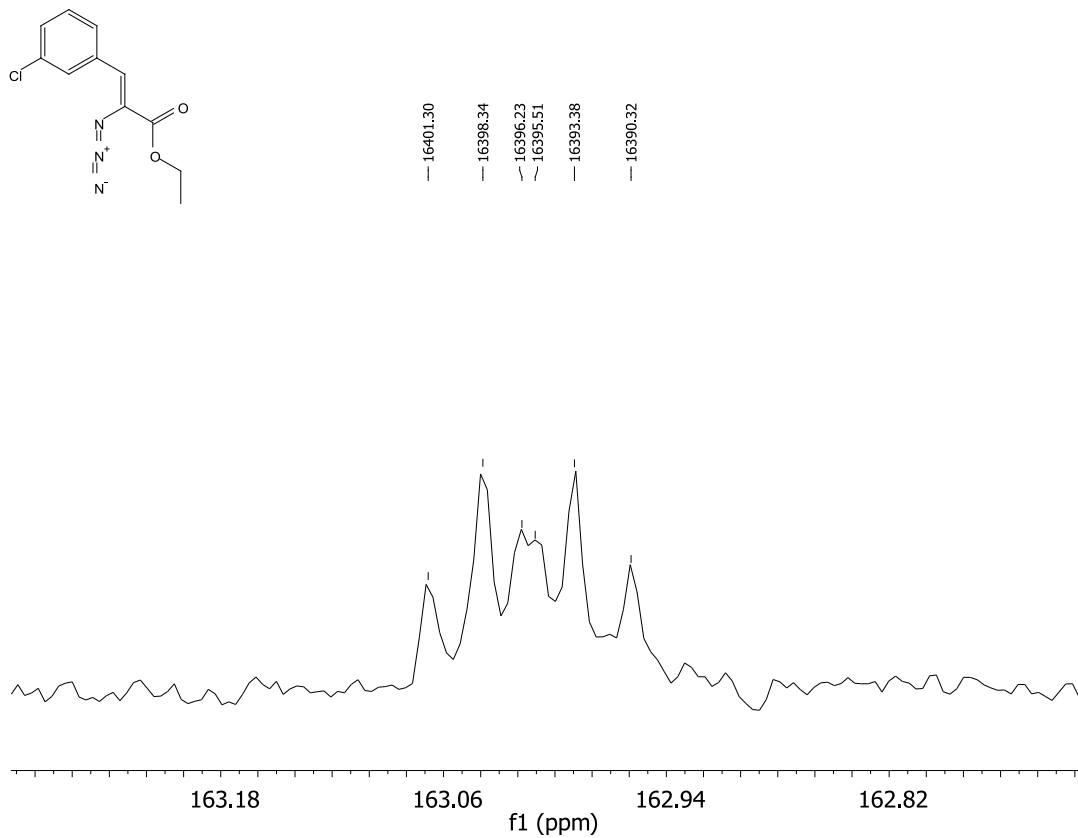


Figure 25. ¹H NMR: Z)-Ethyl *meta*-phenyl- α -azido- β -phenylacrylate (2e)

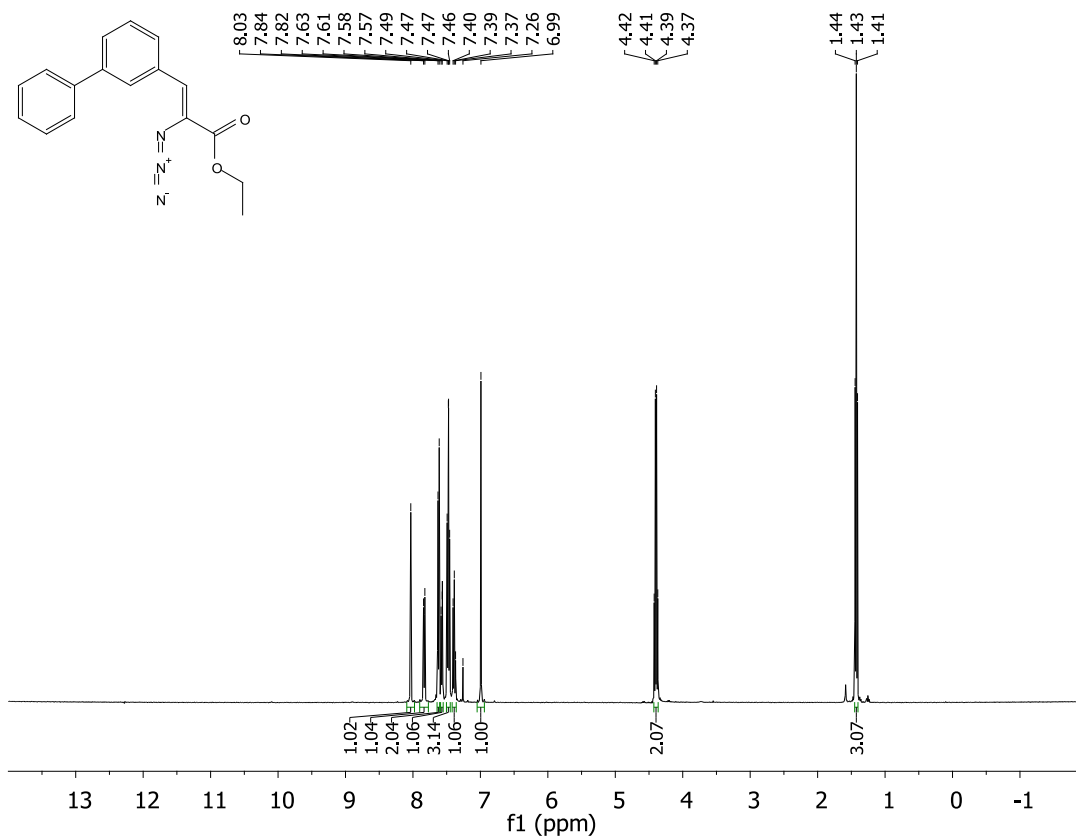


Figure 26. ^{13}C NMR: *Z*-Ethyl *meta*-phenyl- α -azido- β -phenylacrylate (2e)

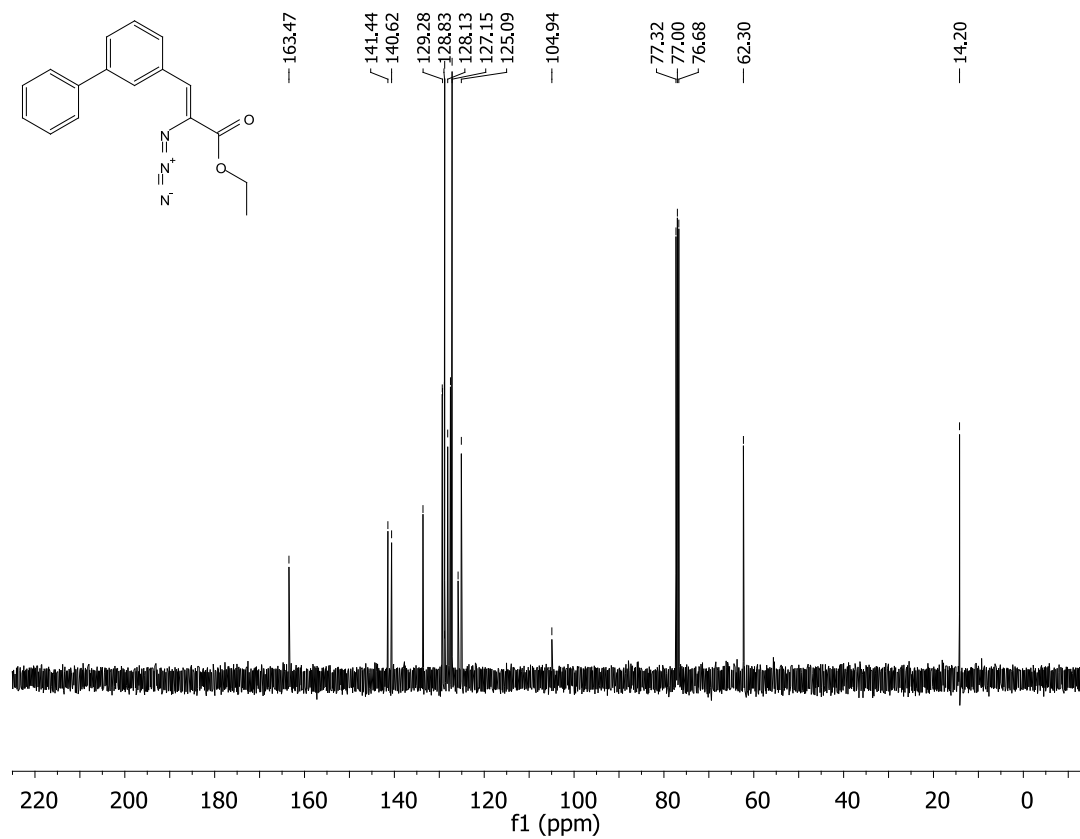


Figure 27. ^1H - ^{13}C Coupled NMR: *Z*-Ethyl *meta*-phenyl- α -azido- β -phenylacrylate (2e)

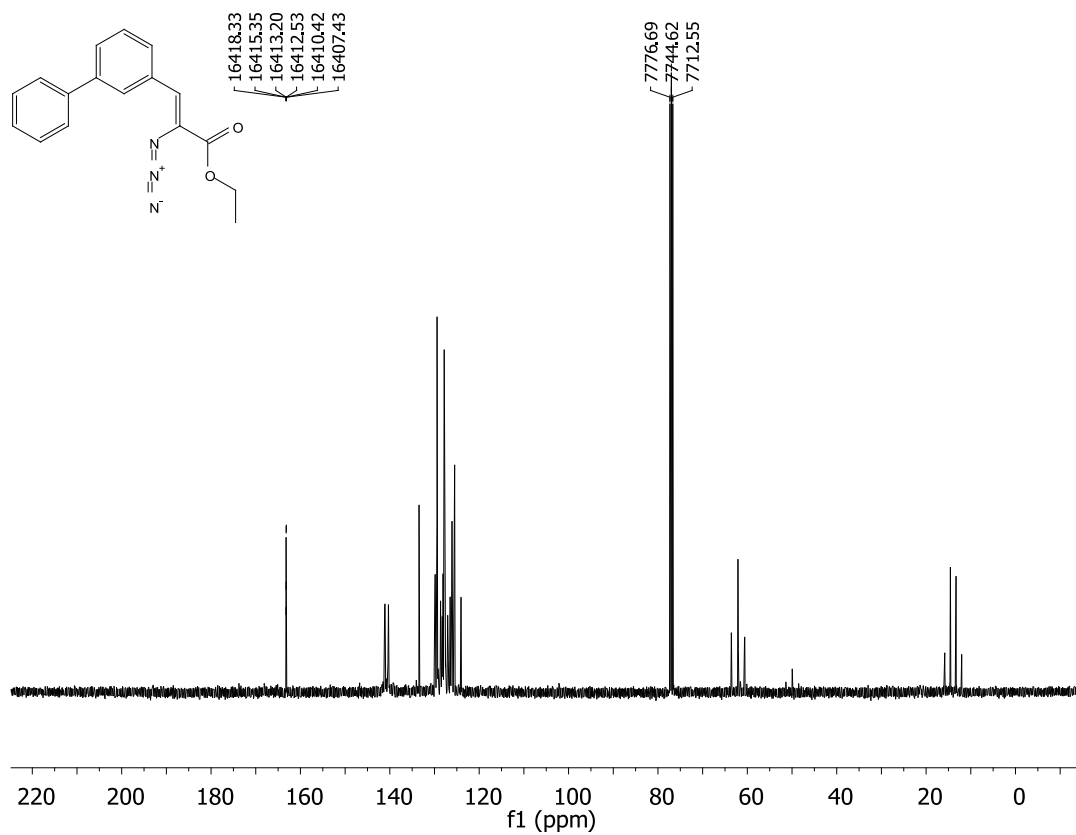


Figure 28. $^3J_{C,H}$ of 1H - ^{13}C Coupled NMR: (Z)-Ethyl *meta*-phenyl- α -azido- β -phenylacrylate (2e)

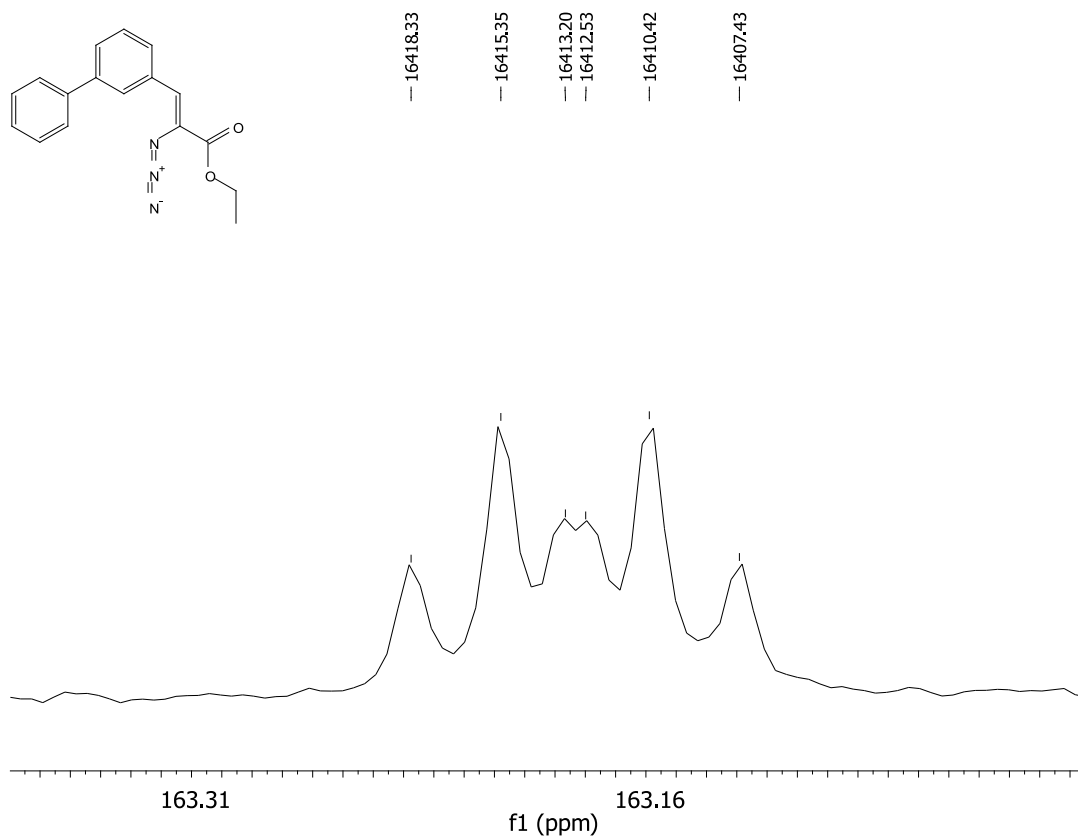


Figure 29. ^1H NMR: (Z)-Ethyl *meta*-nitro- α -azido- β -phenylacrylate (2f)

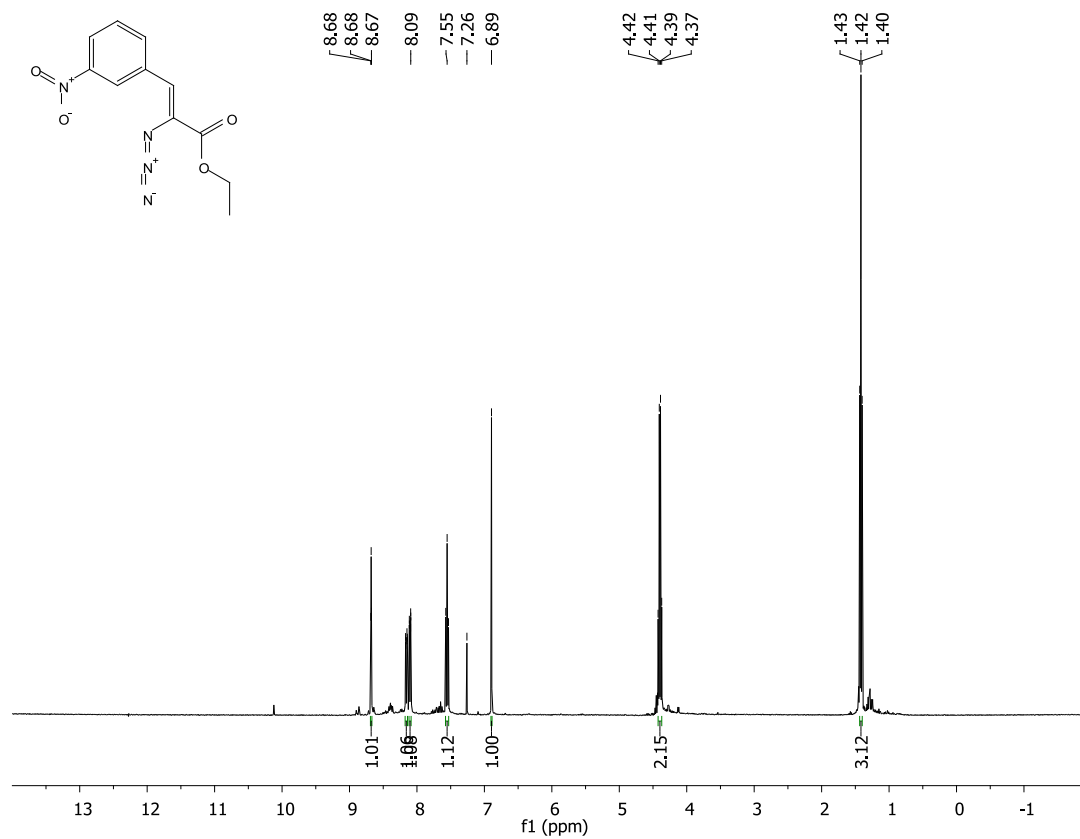


Figure 30. ^{13}C NMR: (Z)-Ethyl *meta*-nitro- α -azido- β -phenylacrylate (2f)

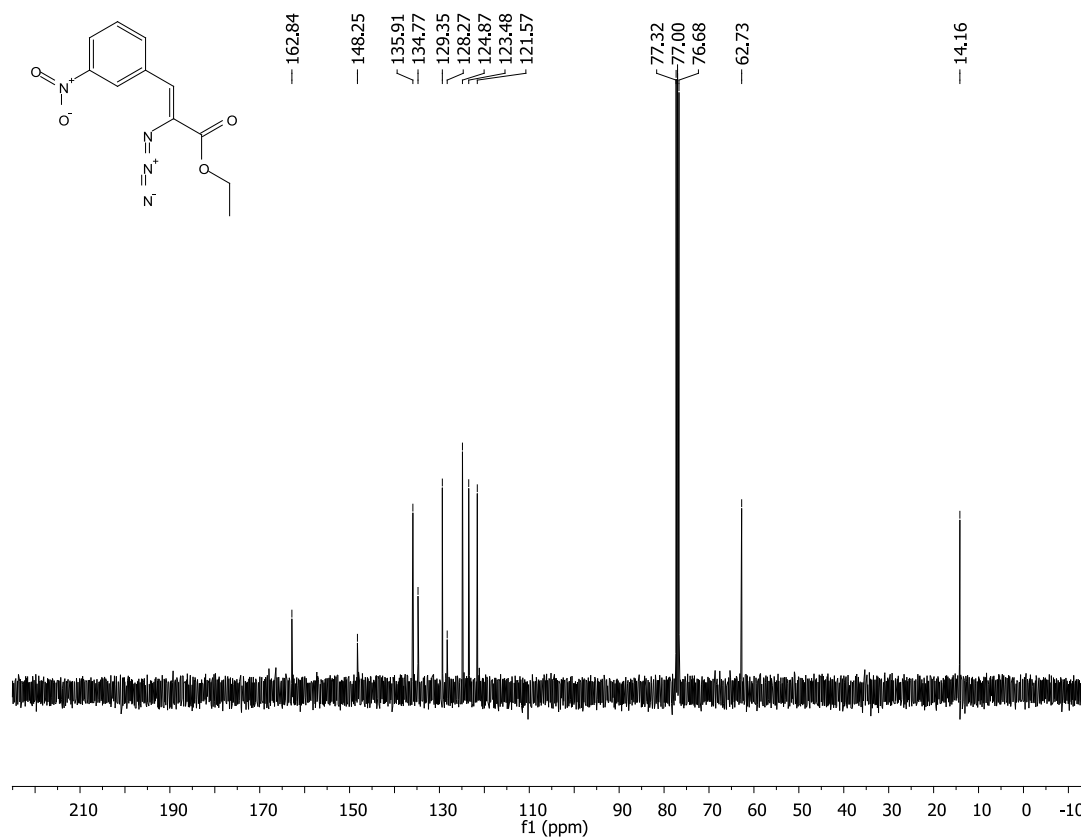


Figure 31. ^1H - ^{13}C Coupled NMR: (Z)-Ethyl *meta*-nitro- α -azido- β -phenylacrylate (2f)

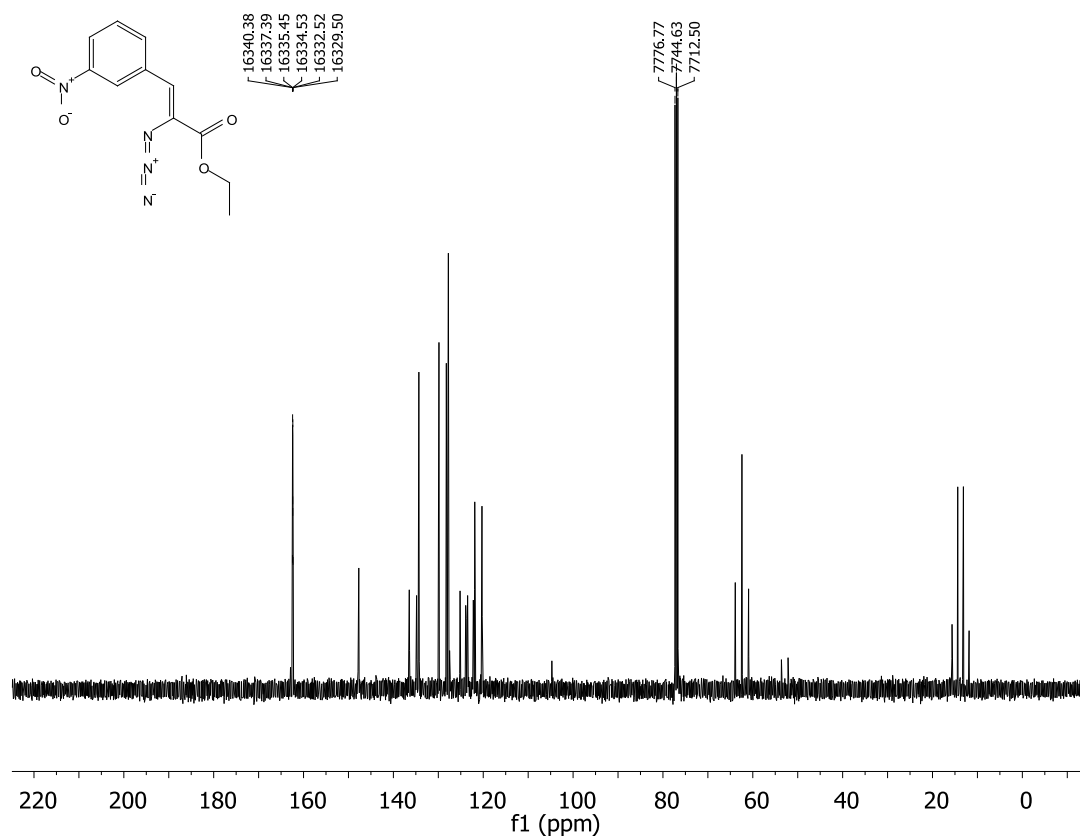


Figure 32. $^3J_{C,H}$ of 1H - ^{13}C Coupled NMR: (Z)-Ethyl *meta*-nitro- α -azido- β -phenylacrylate (2f)

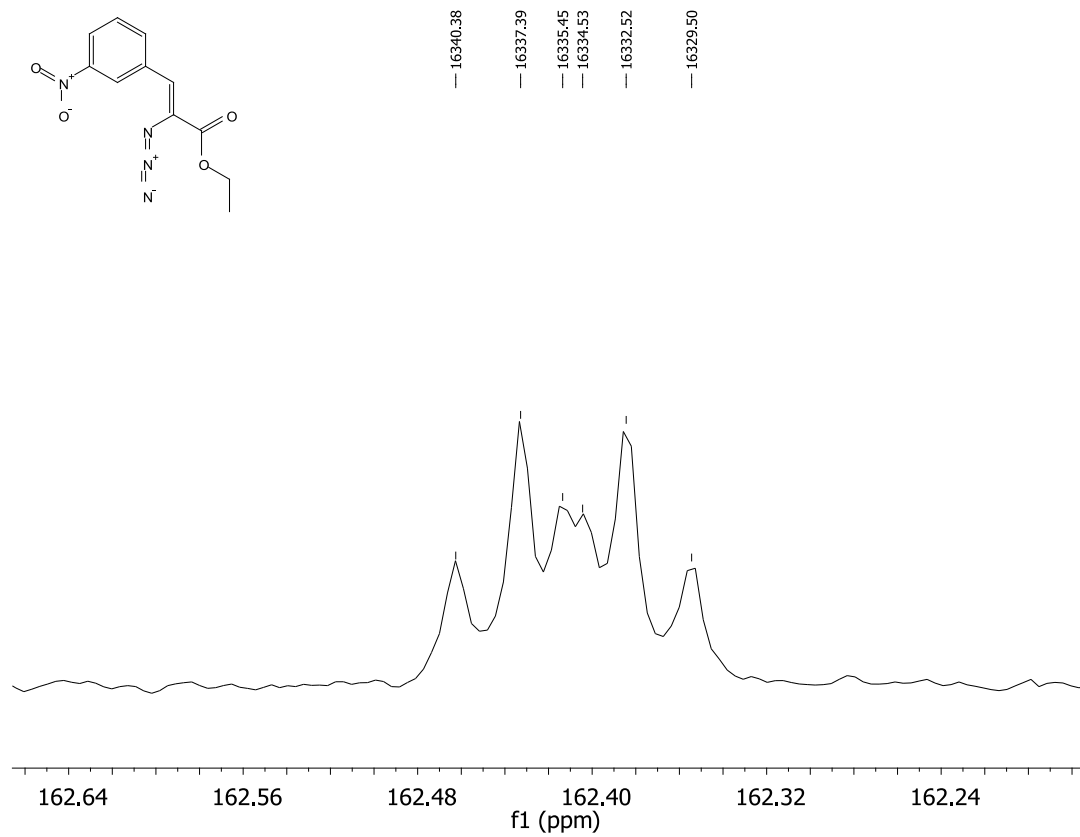


Figure 33. ^1H NMR: (Z)-Ethyl *para*-methyl- α -azido- β -phenylacrylate (2g)

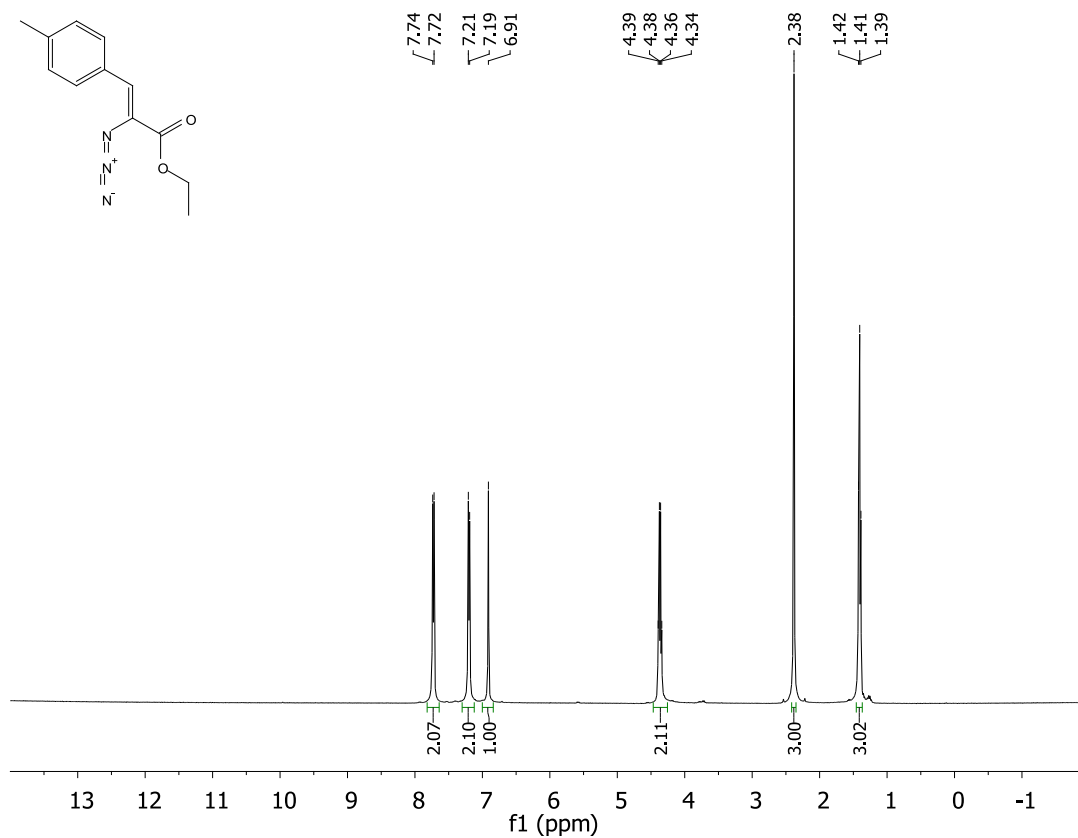


Figure 34. ^{13}C NMR: (Z)-Ethyl *para*-methyl- α -azido- β -phenylacrylate (2g)

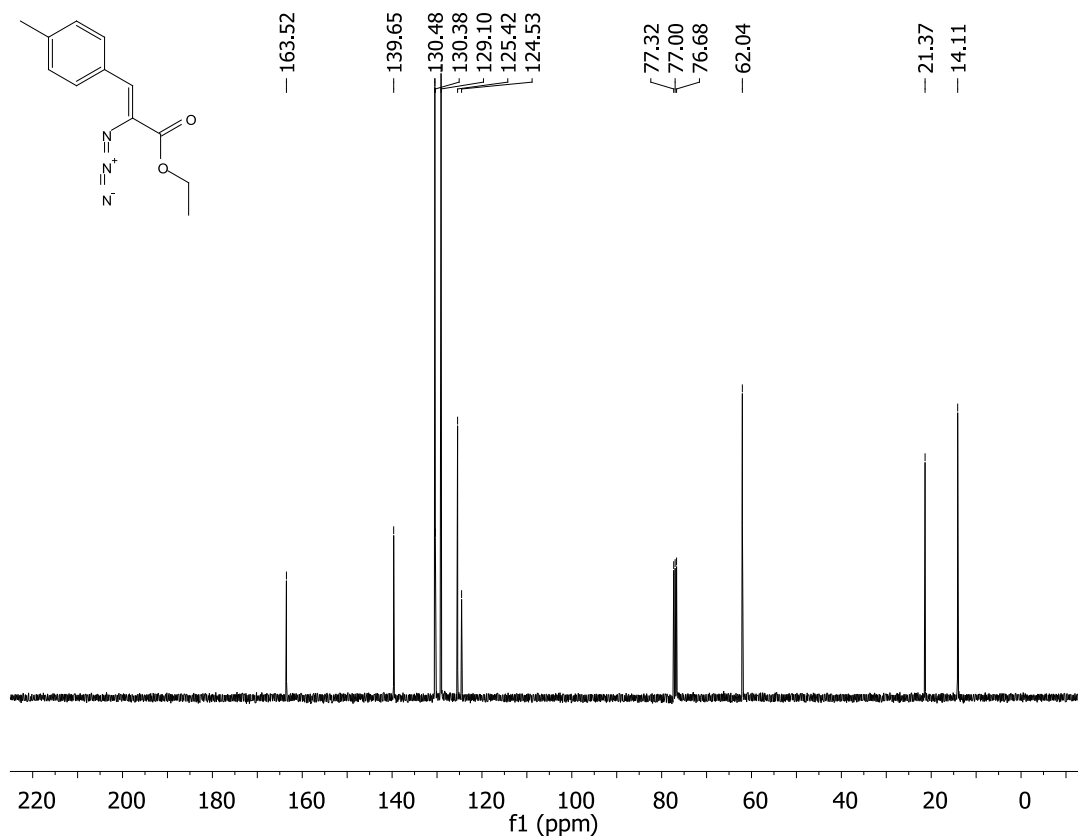


Figure 35. ^1H NMR: (2Z,2'Z)-diethyl 3,3'-(1,3-phenylene)bis(2-azidoacrylate) (2h)

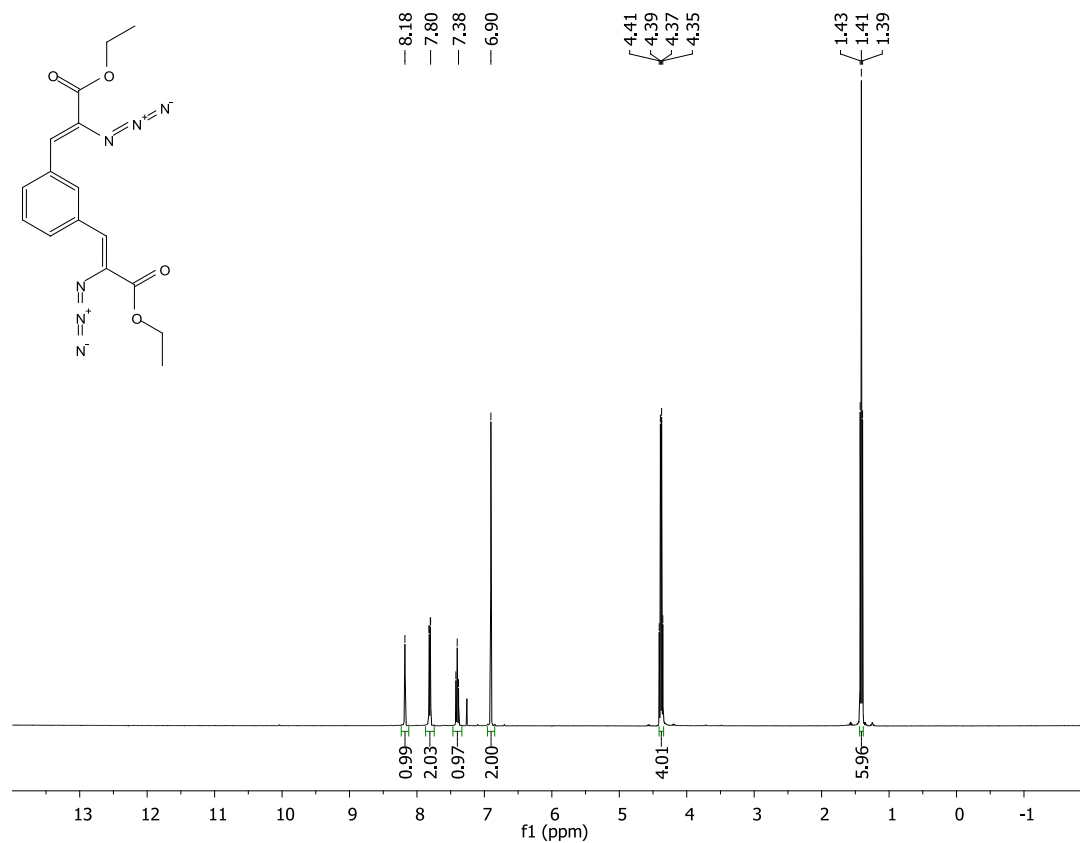


Figure 36. ^{13}C NMR: (2Z,2'Z)-diethyl 3,3'-(1,3-phenylene)bis(2-azidoacrylate) (2h)

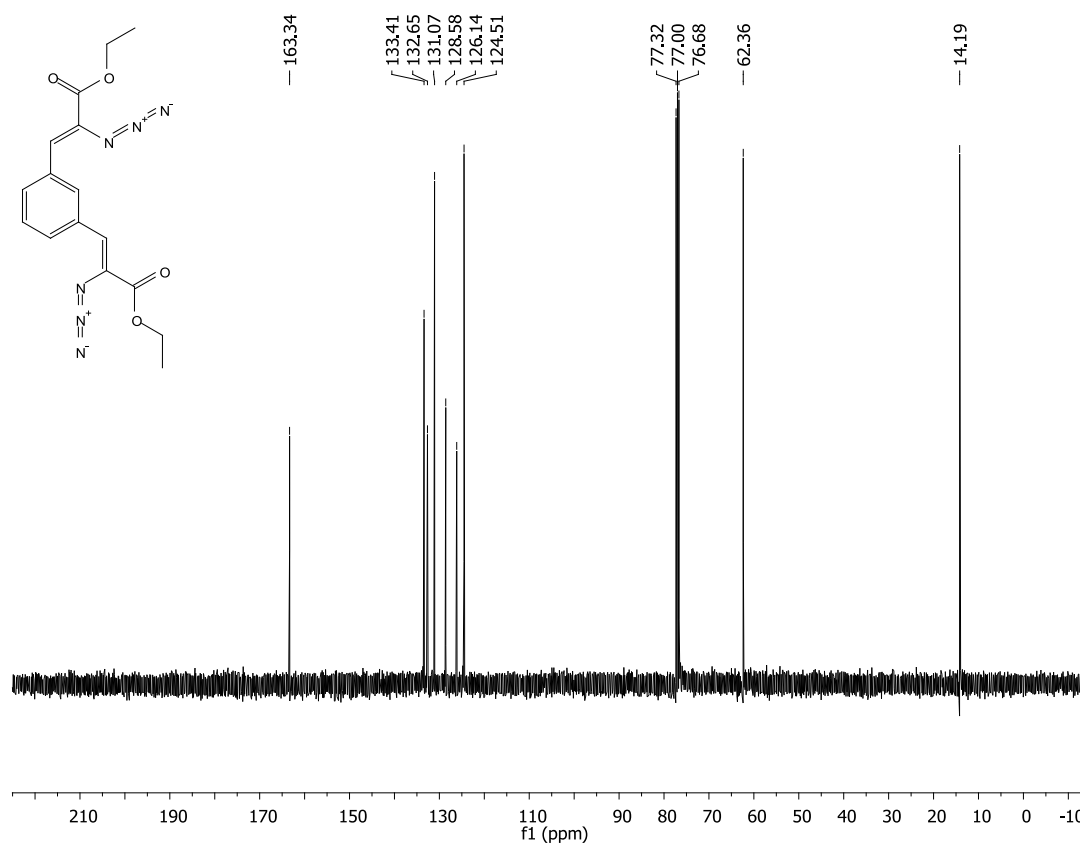


Figure 37. $^3J_{C,H}$ of 1H - ^{13}C Coupled NMR: (2Z,2'Z)-diethyl 3,3'-(1,3-phenylene)bis(2-azidoacrylate) (2h)

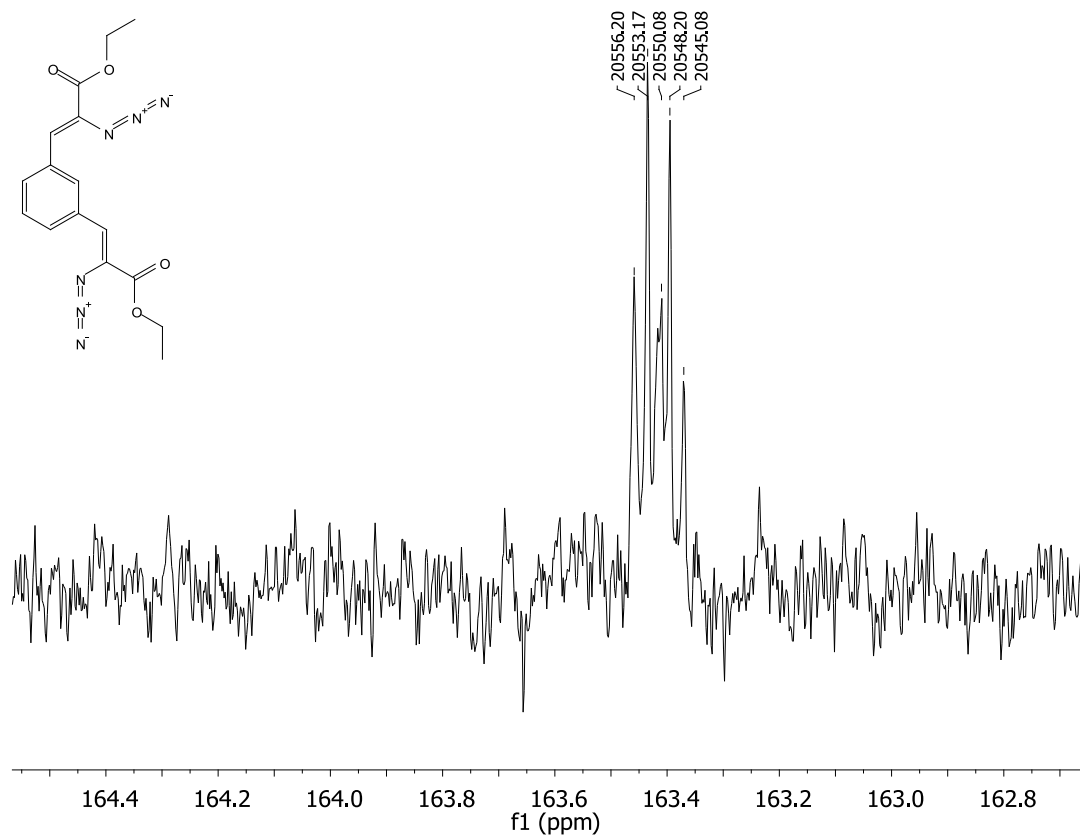


Figure 38. ^1H NMR: (2Z,2'Z)-diethyl 3,3'-(1,4-phenylene)bis(2-azidoacrylate) (2i)

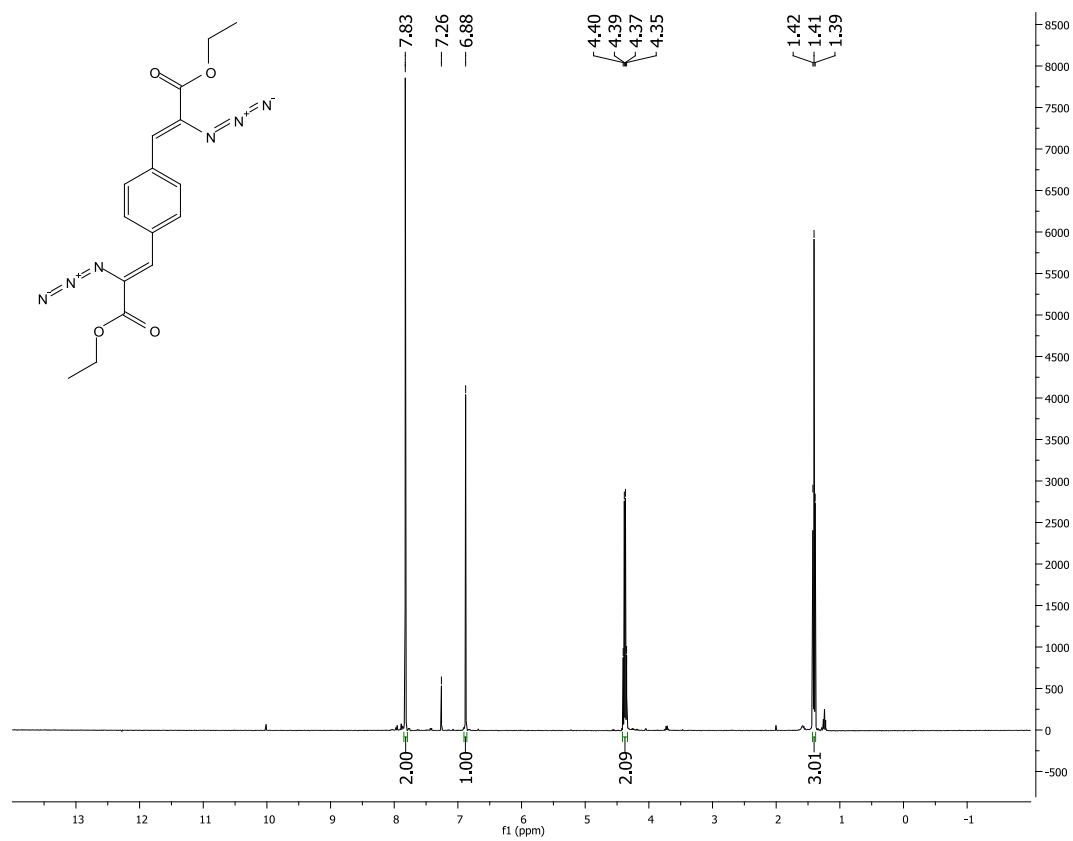


Figure 39. ^{13}C NMR: (2Z,2'Z)-diethyl 3,3'-(1,4-phenylene)bis(2-azidoacrylate) (2i)

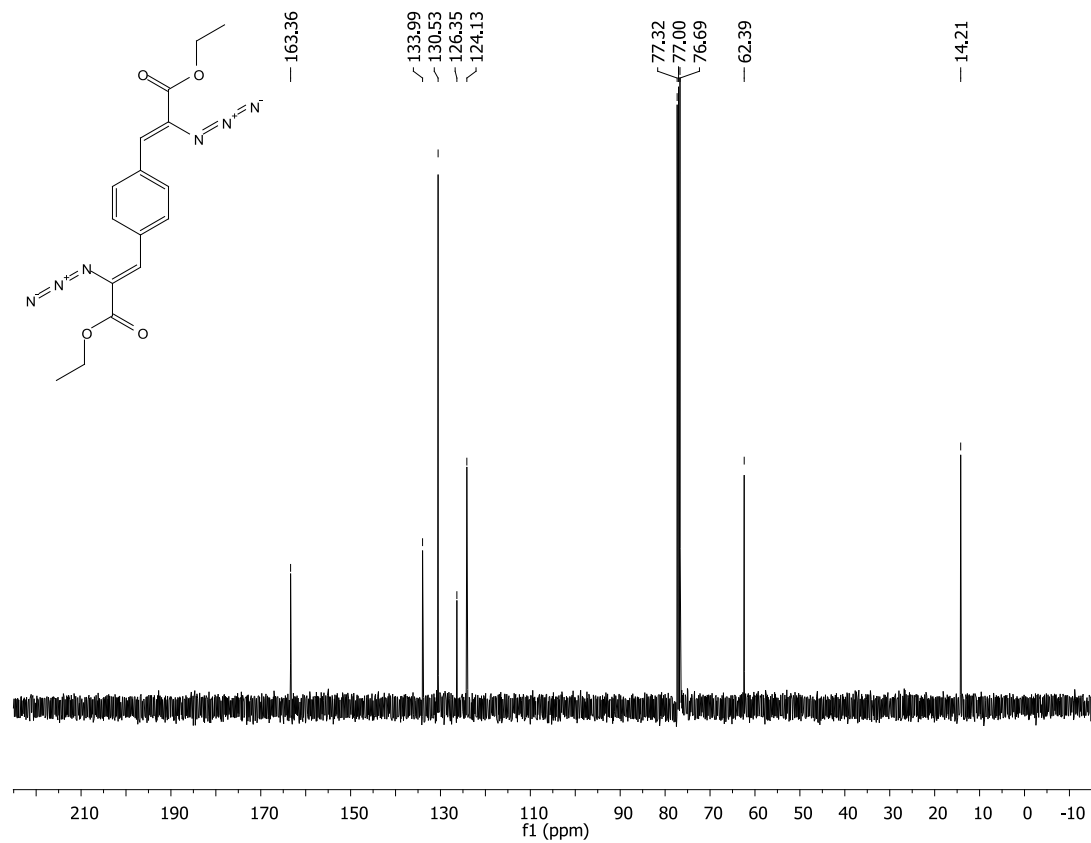


Figure 40. $^3J_{C,H}$ of 1H - ^{13}C Coupled NMR: (2Z,2'Z)-diethyl 3,3'-(1,4-phenylene)bis(2-azidoacrylate) (2i)

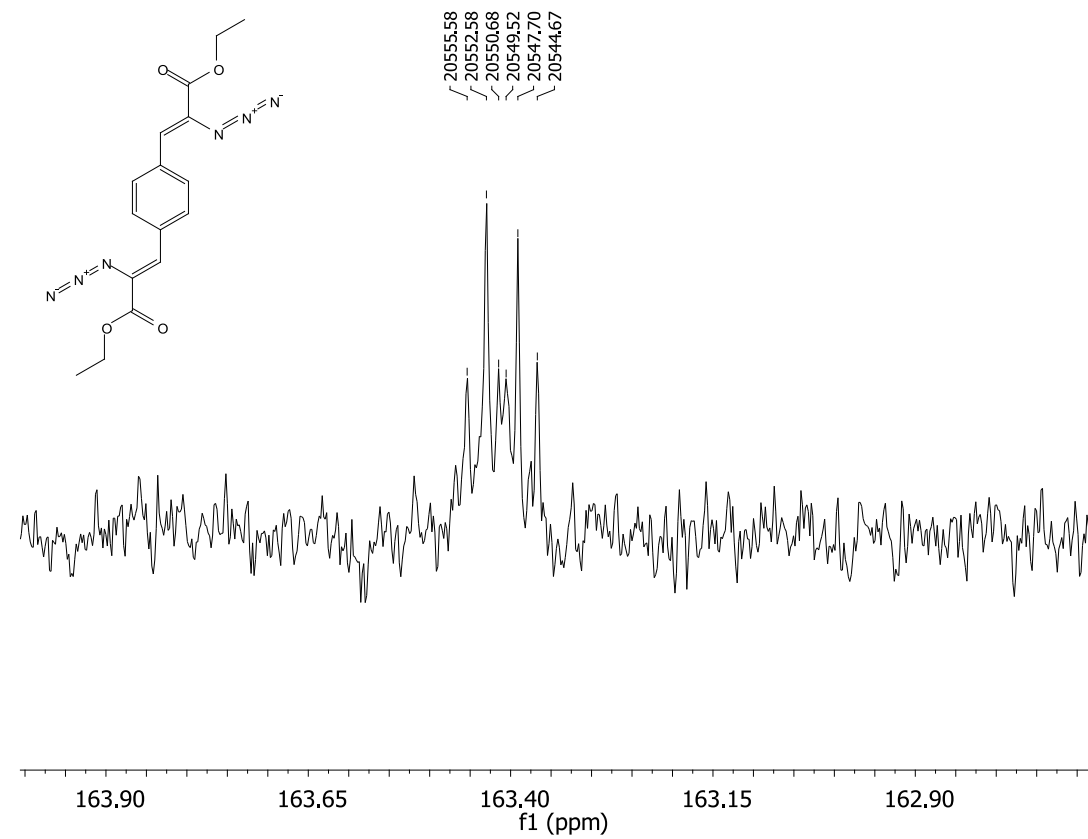


Figure 41. ¹H NMR: (Z)-ethyl 2-azido-3-(furan-2-yl)acrylate (2j)

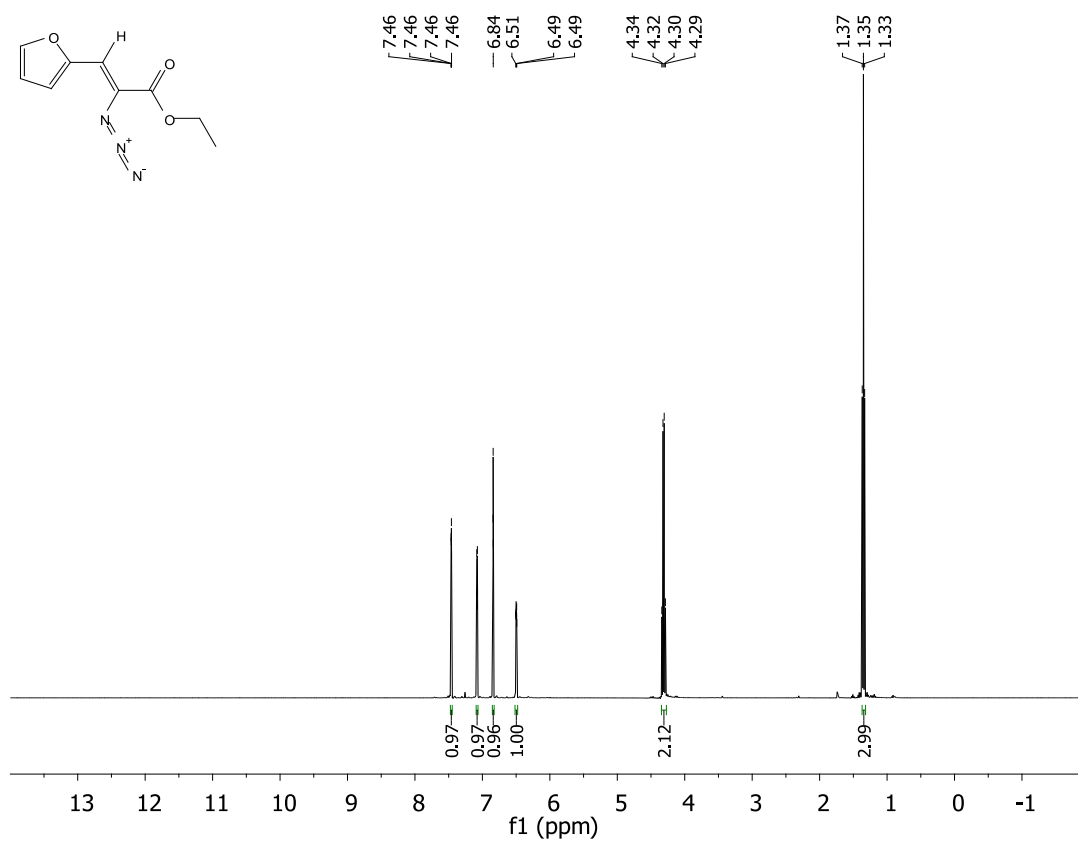


Figure 42. ^{13}C NMR: (Z)-ethyl 2-azido-3-(furan-2-yl)acrylate (2j)

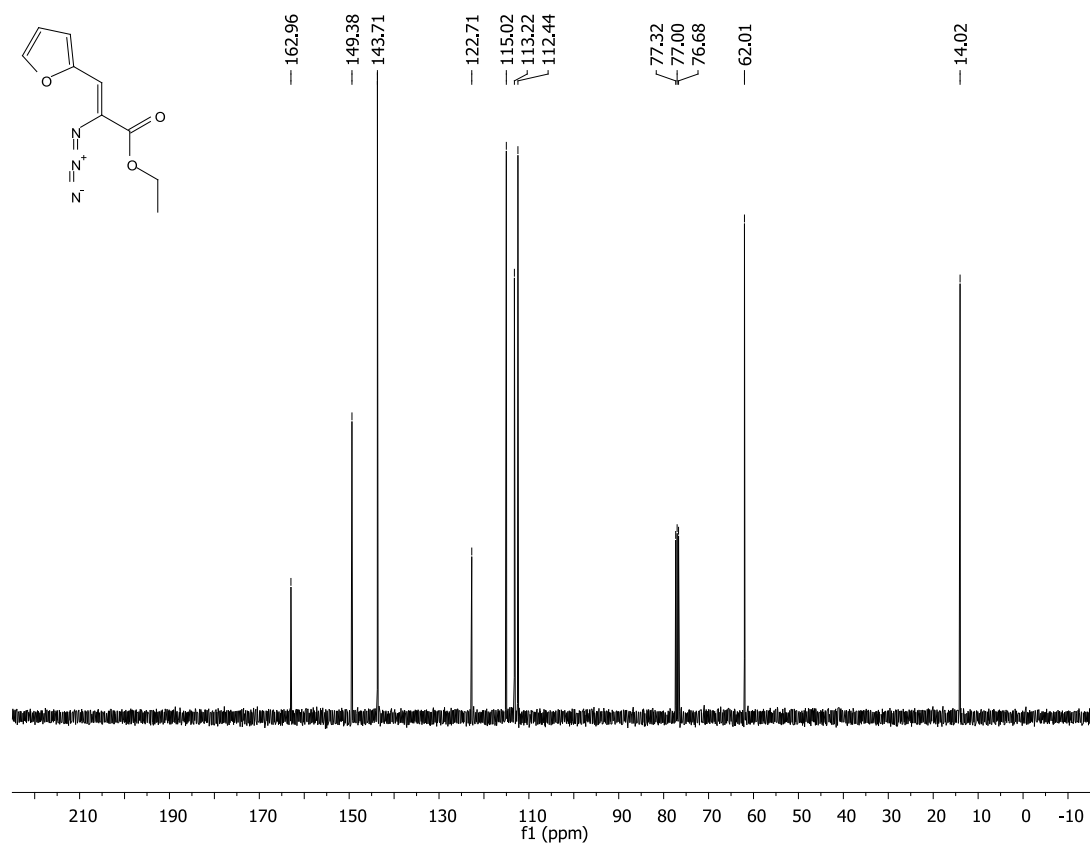


Figure 43. ^1H - ^{13}C Coupled NMR: (Z)-ethyl 2-azido-3-(furan-2-yl)acrylate (2j)

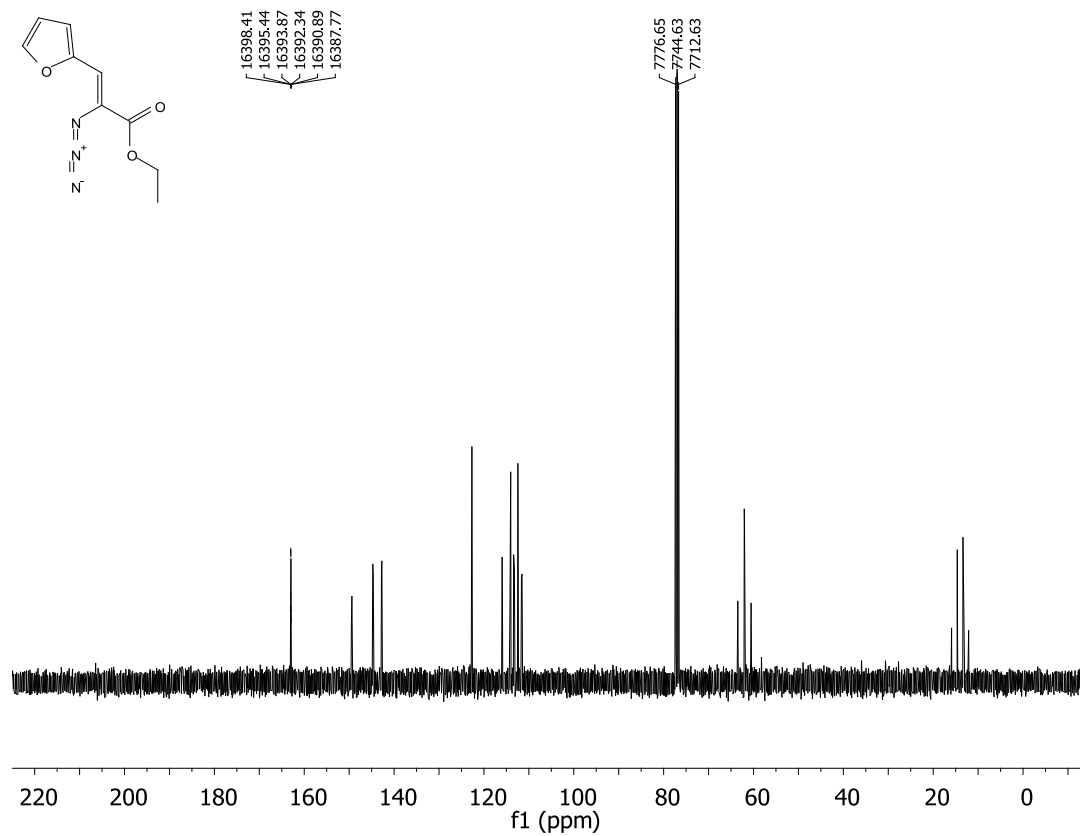
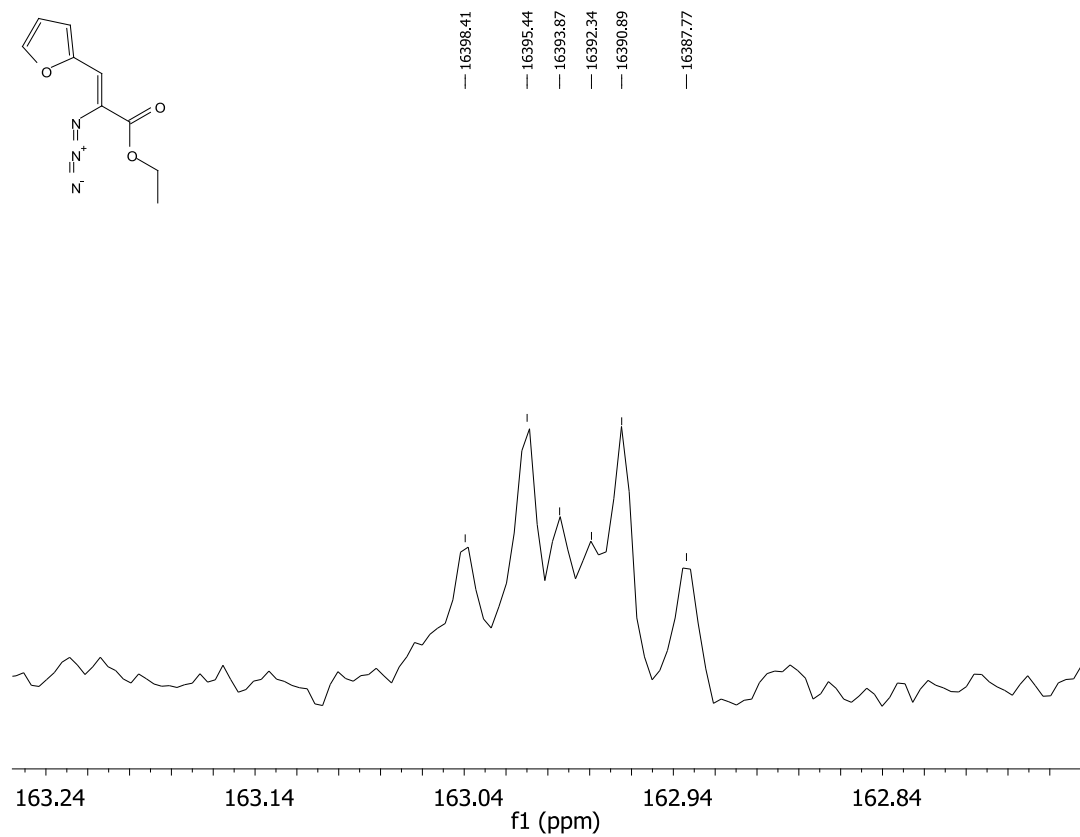


Figure 44. $^3J_{C,H}$ of 1H - ^{13}C Coupled NMR: (Z)-ethyl 2-azido-3-(furan-2-yl)acrylate (2j)



NMR and Mass Spectroscopy of

(Z)-ethyl 2-(3-nitrobenzamido)-3-(3-nitrophenyl)acrylate

Figure 45. ¹H NMR (Z)-ethyl 2-(3-nitrobenzamido)-3-(3-nitrophenyl)acrylate

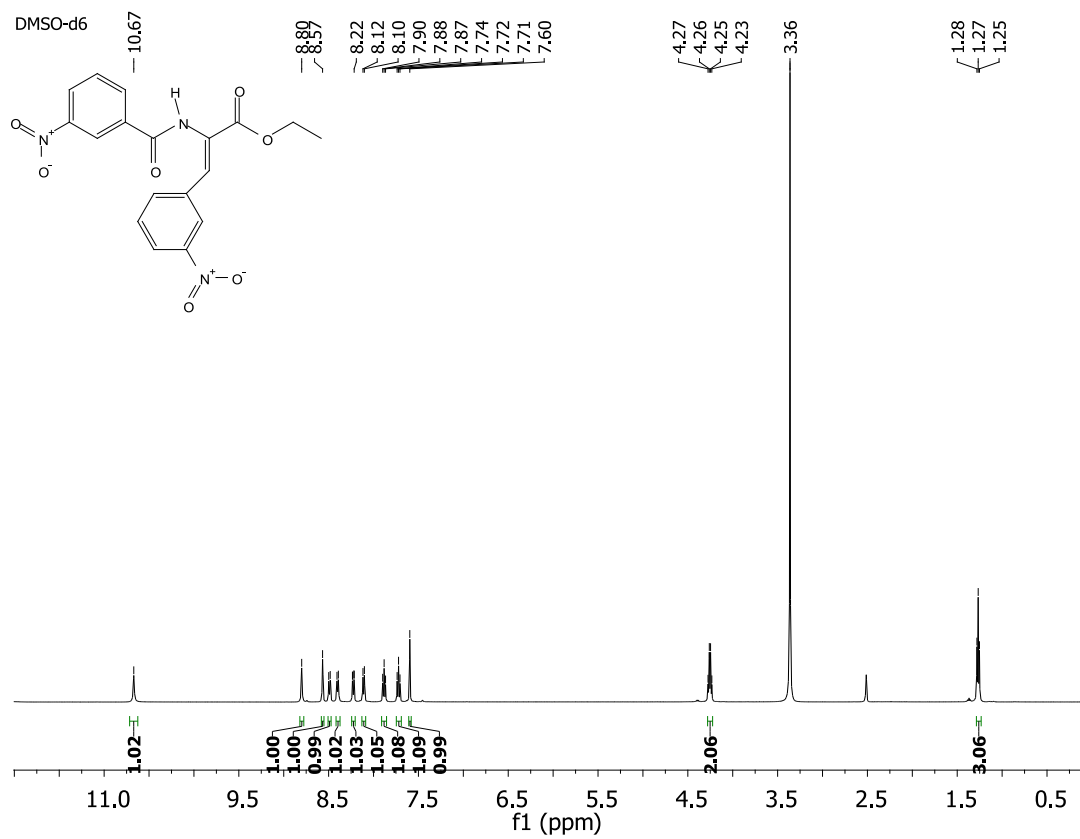


Figure 46. ^{13}C NMR: (Z)-ethyl 2-(3-nitrobenzamido)-3-(3-nitrophenyl)acrylate

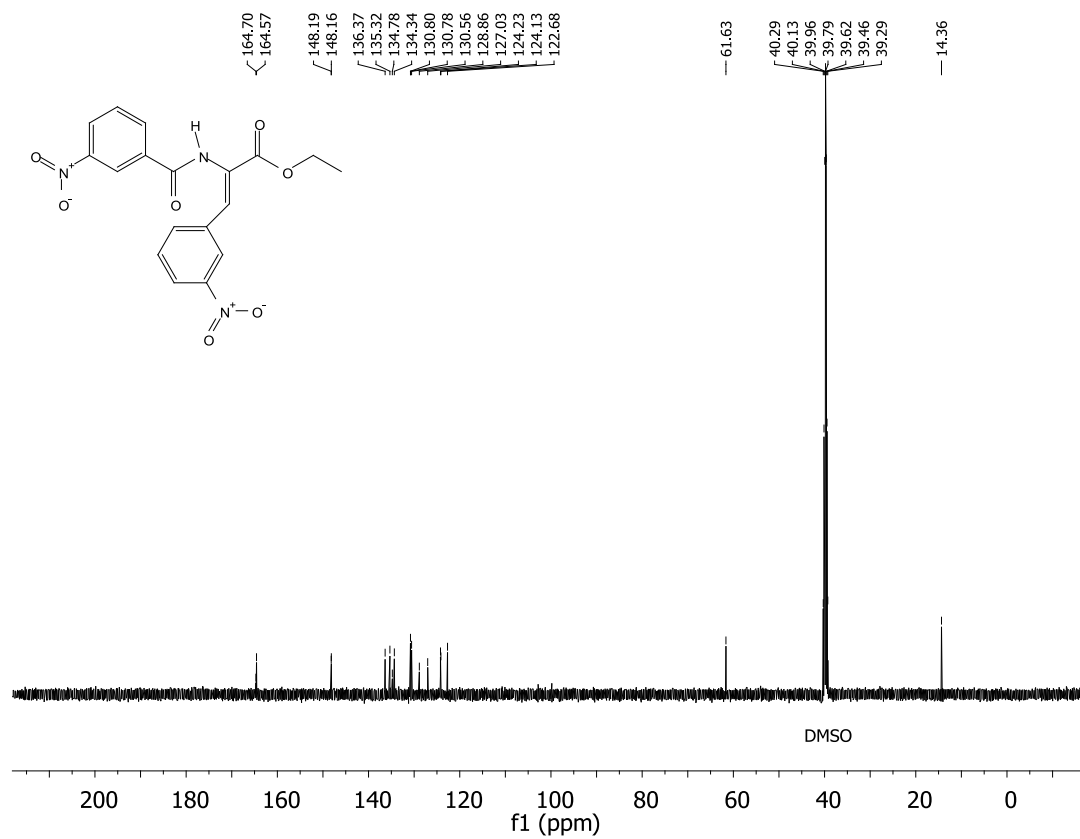
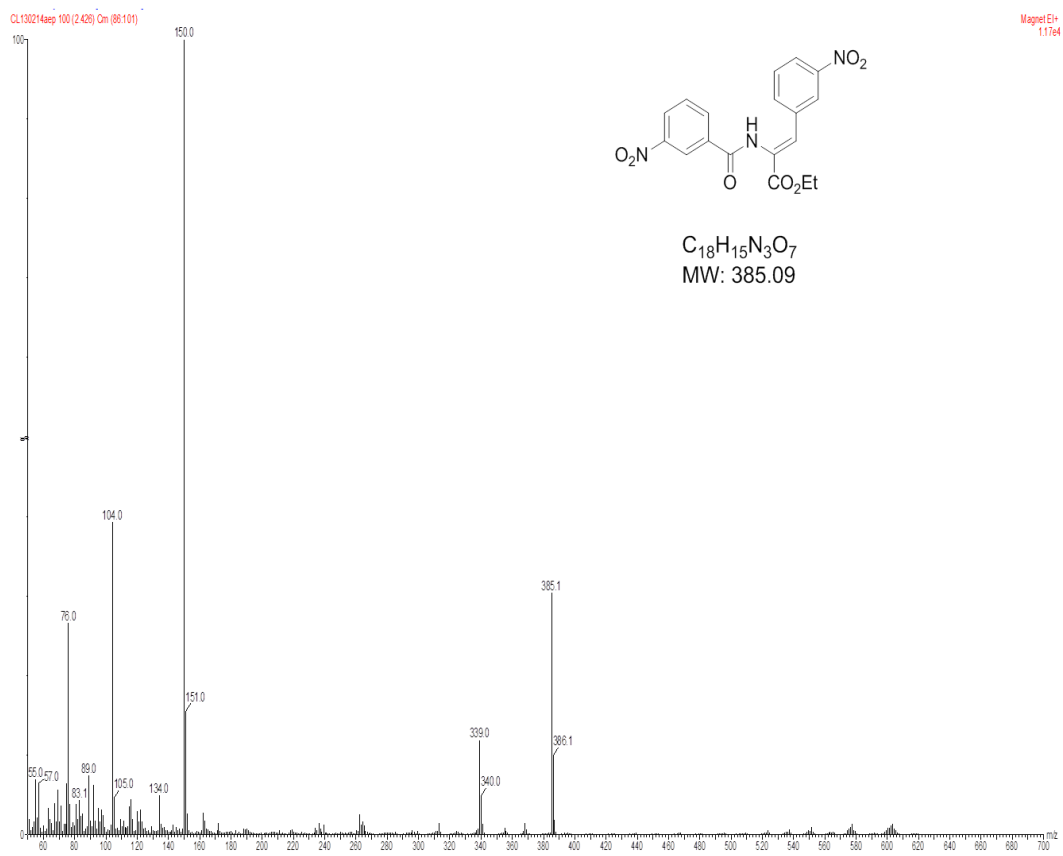


Figure 47. Mass Spectroscopy (EI+): (Z)-ethyl 2-(3-nitrobenzamido)-3-(3-nitrophenyl)acrylate



NMR (1-D and 2-D) of diethyl 1,6-dihydropyrrolo[2,3-e]indole-2,7-dicarboxylate, 3j

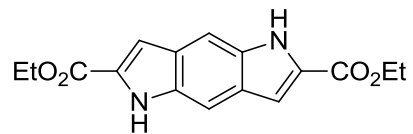
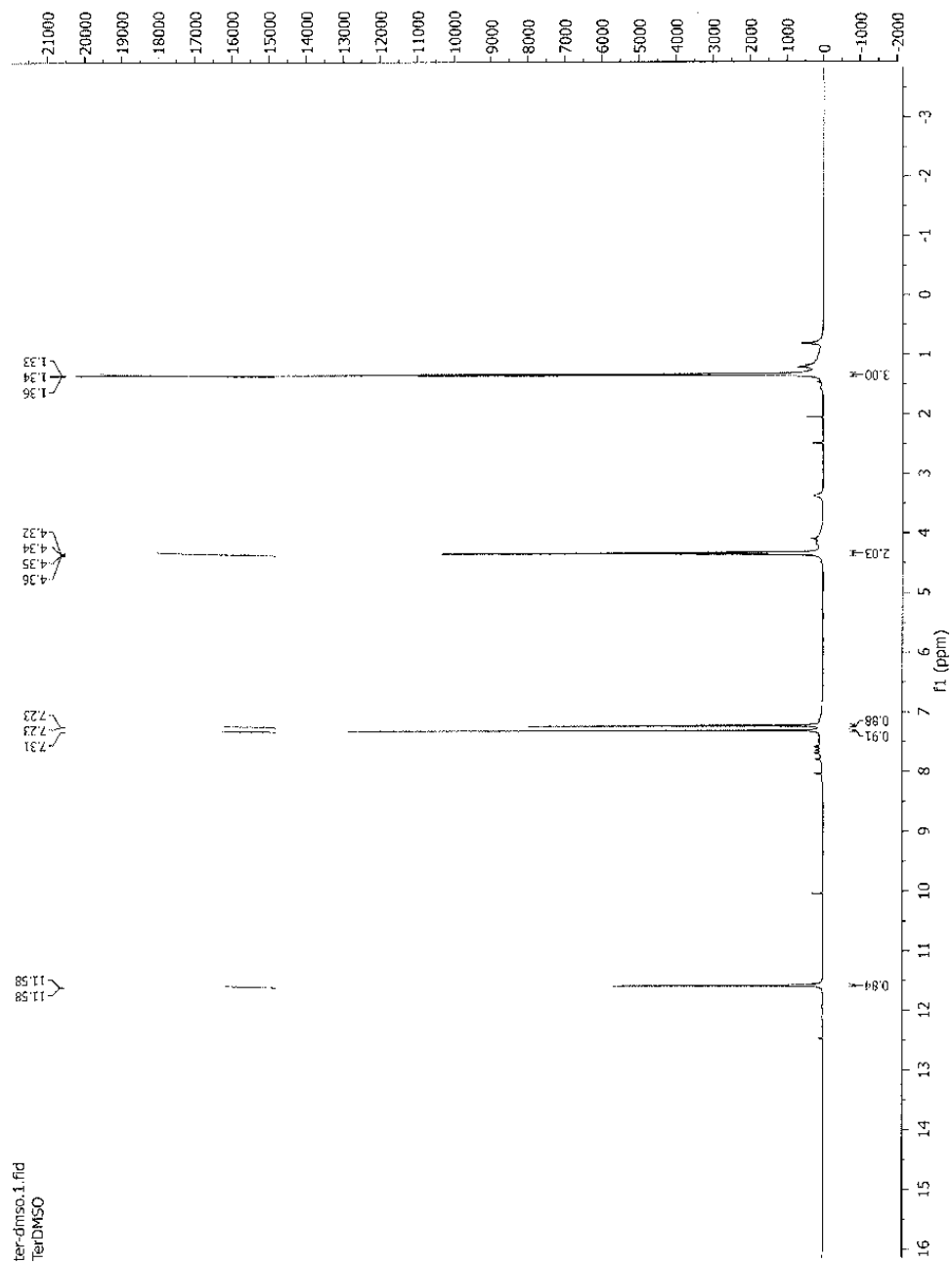


Figure 48. ¹H NMR,3j



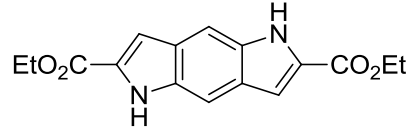
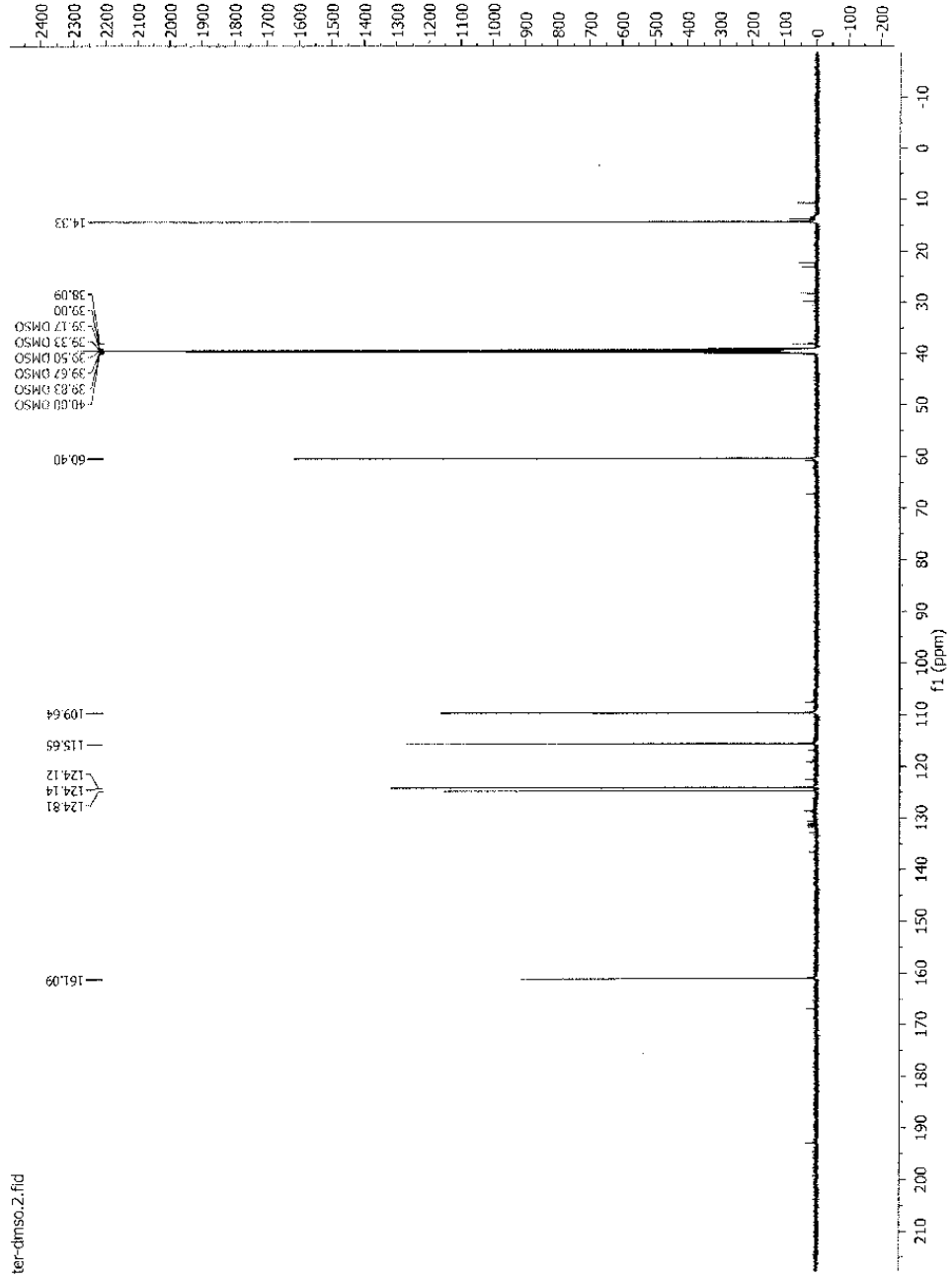


Figure 49. ^{13}C NMR, 3j



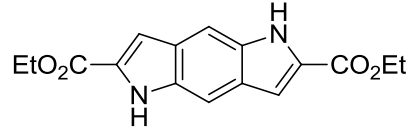
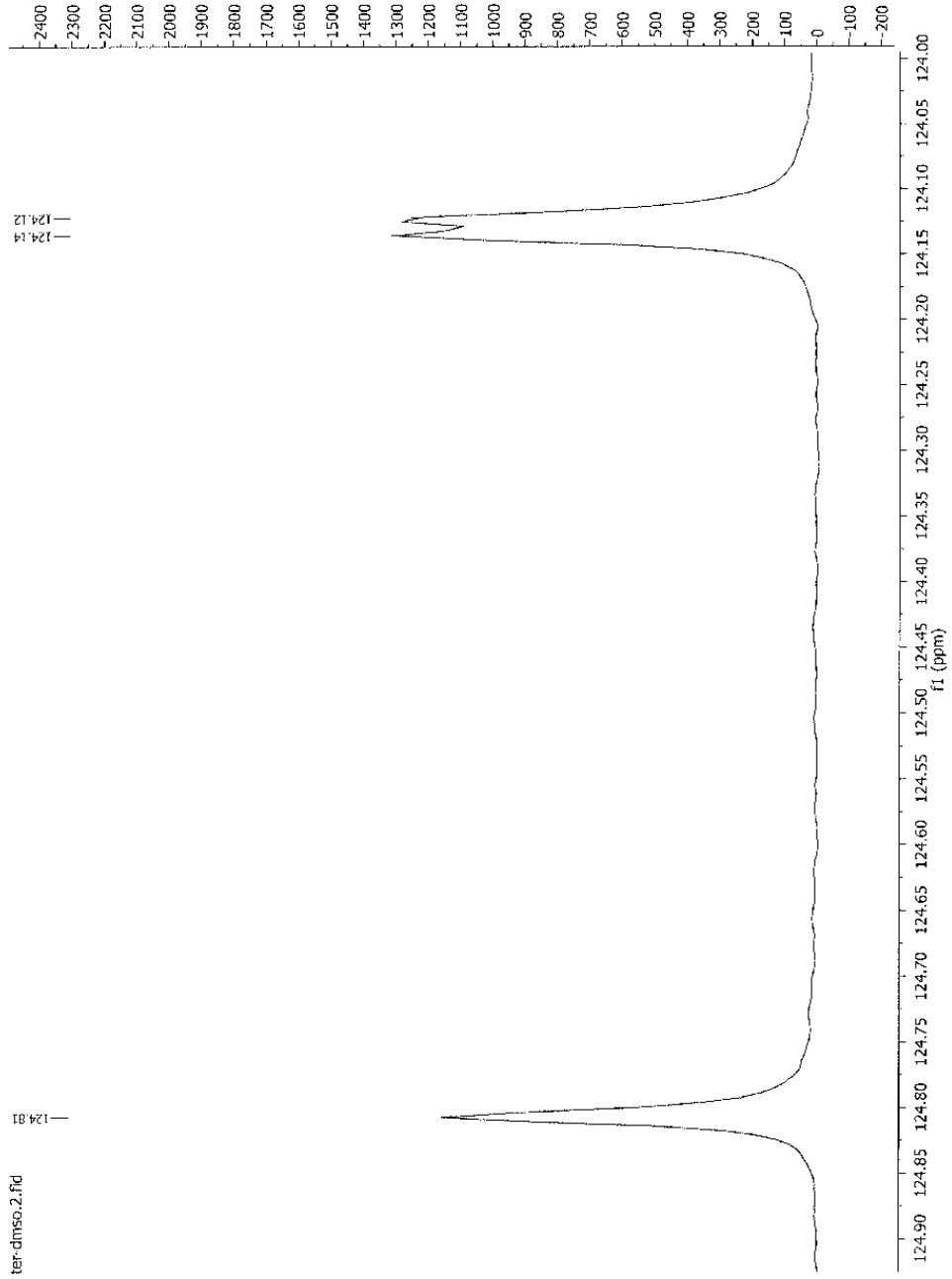


Figure 50. ^{13}C NMR, 124-125 ppm, 3j



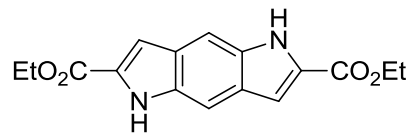
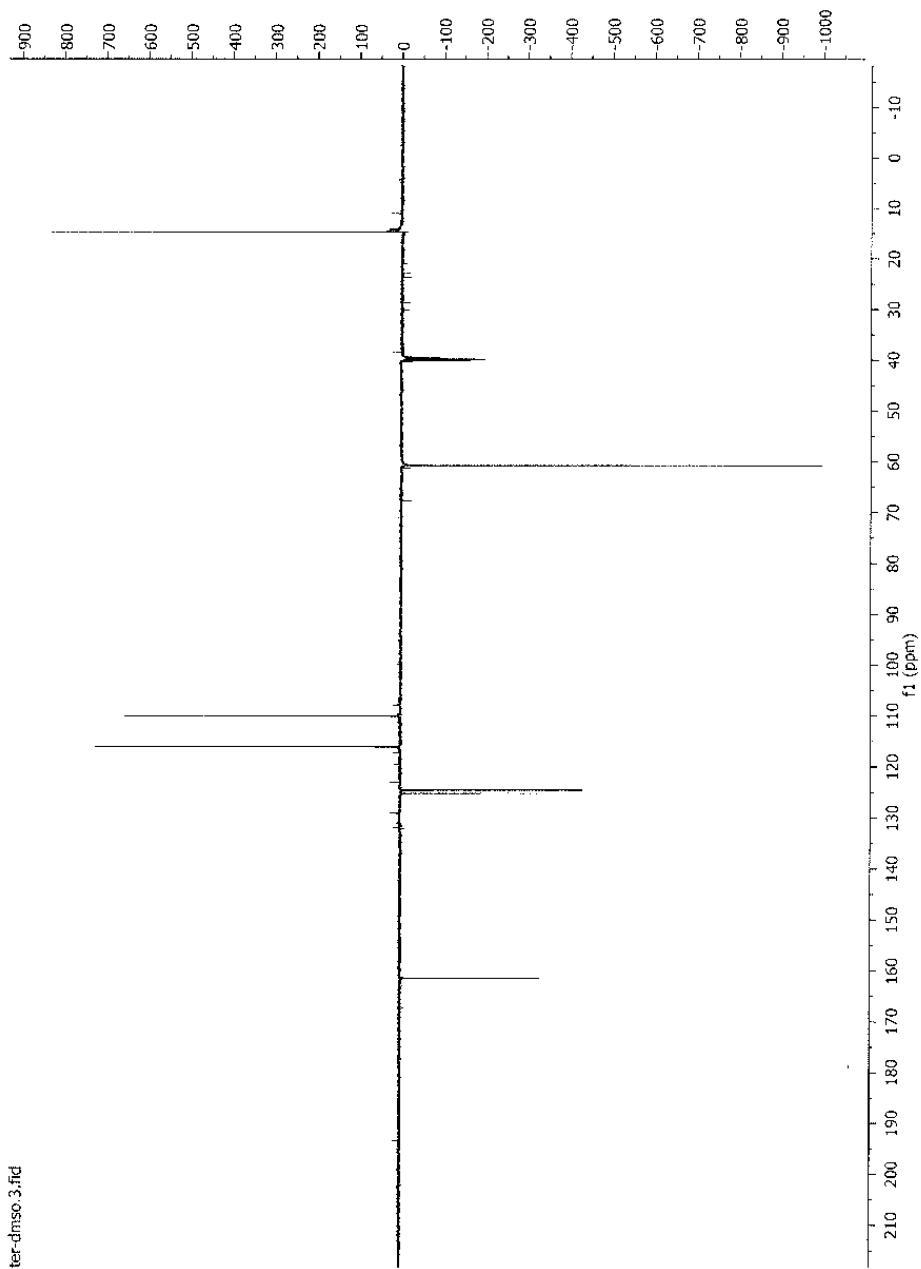


Figure 51. ^{13}C -DEPT NMR, 3j



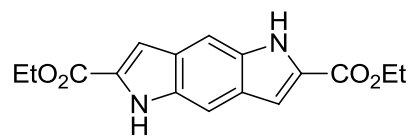
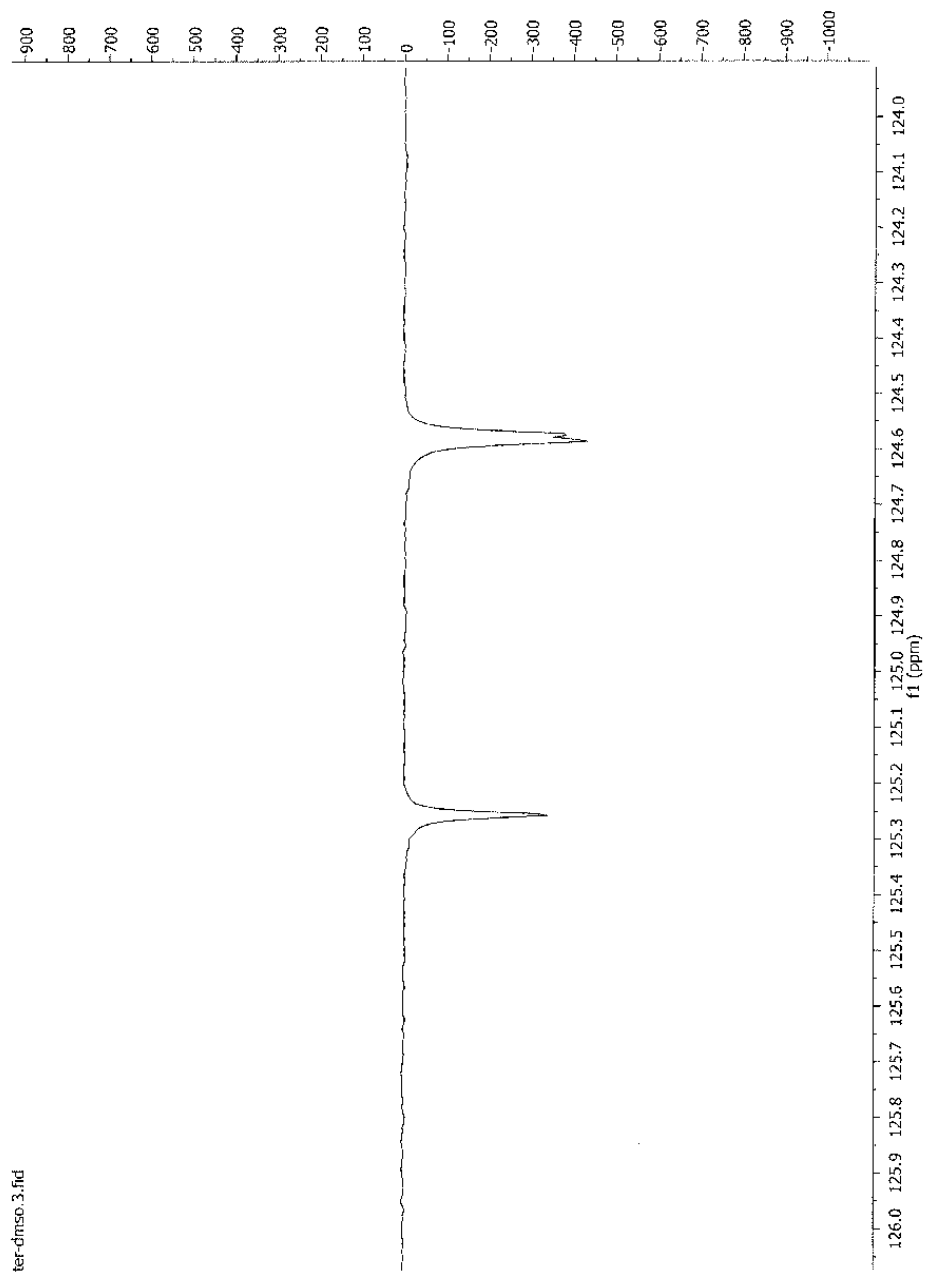


Figure 52. ^{13}C -DEPT NMR, 124-126 ppm,3j



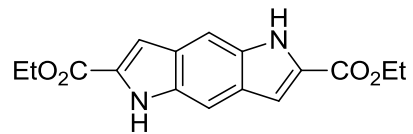
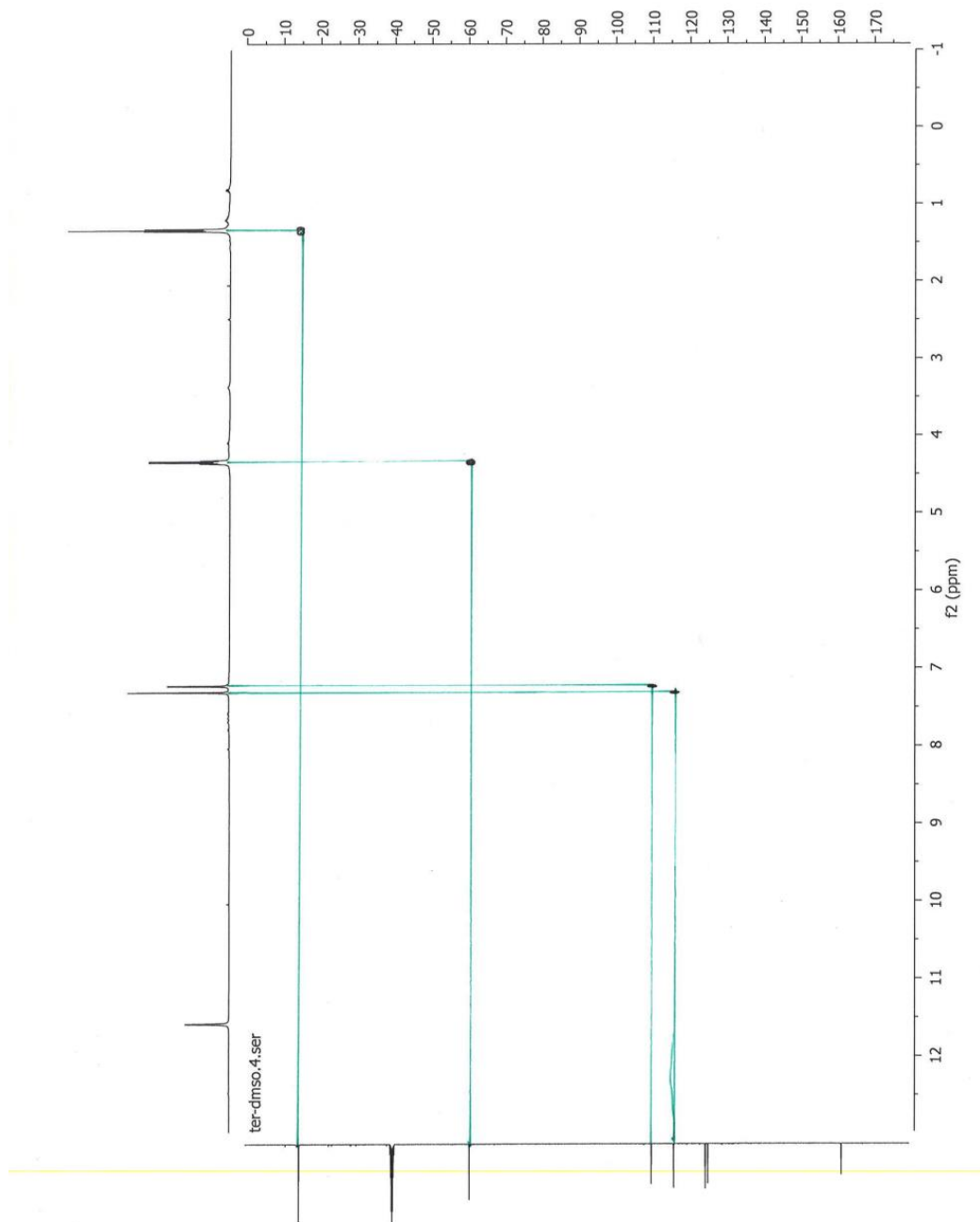


Figure 53. ^1H - ^{13}C HMQC,3j



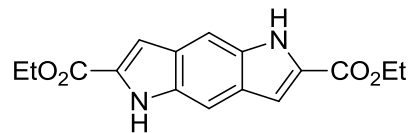
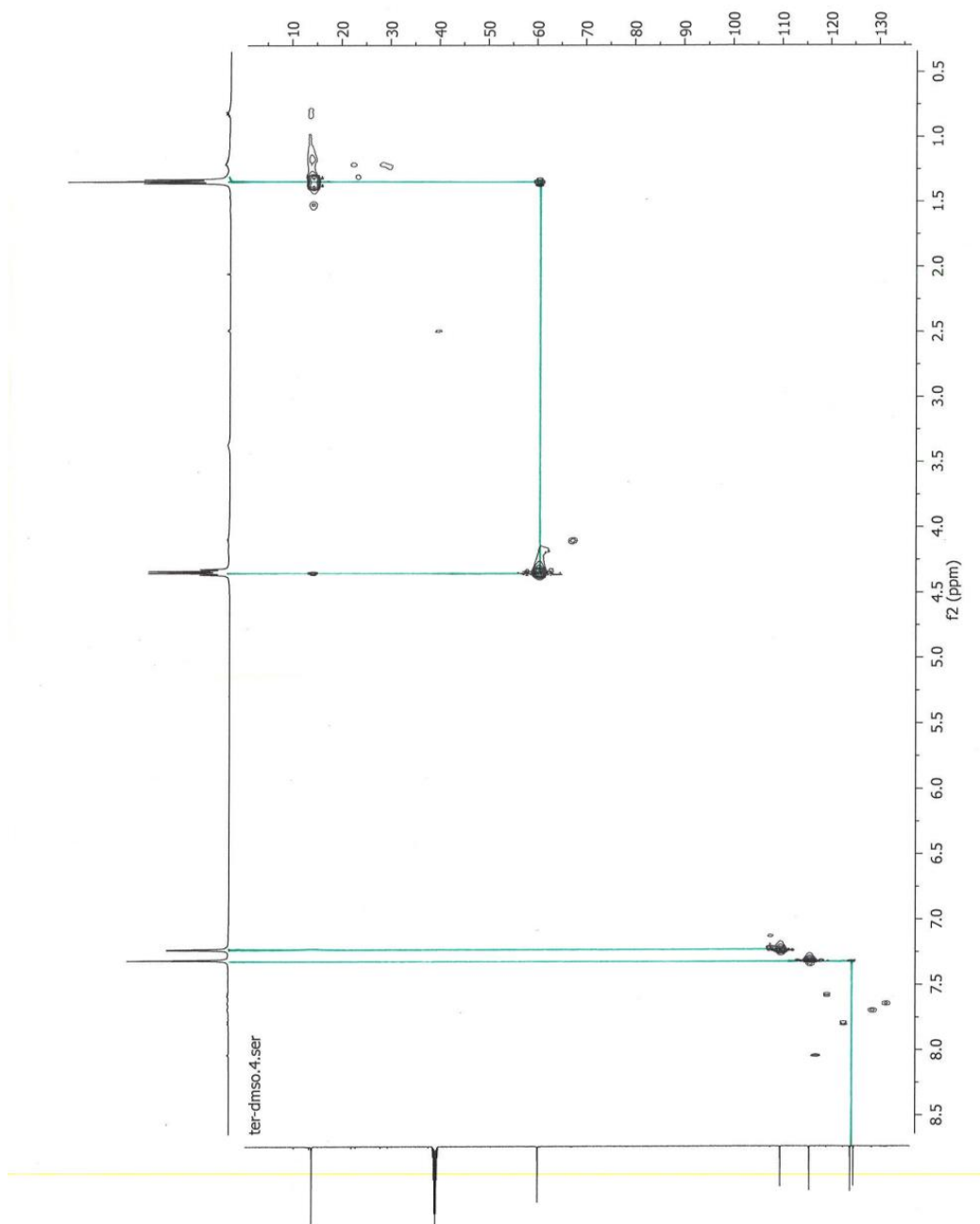


Figure 54. ^1H - ^1H COSY and ^1H - ^{13}C HMQC Overlay, 3j



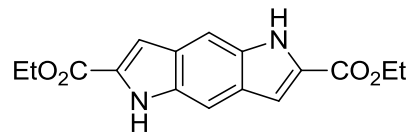
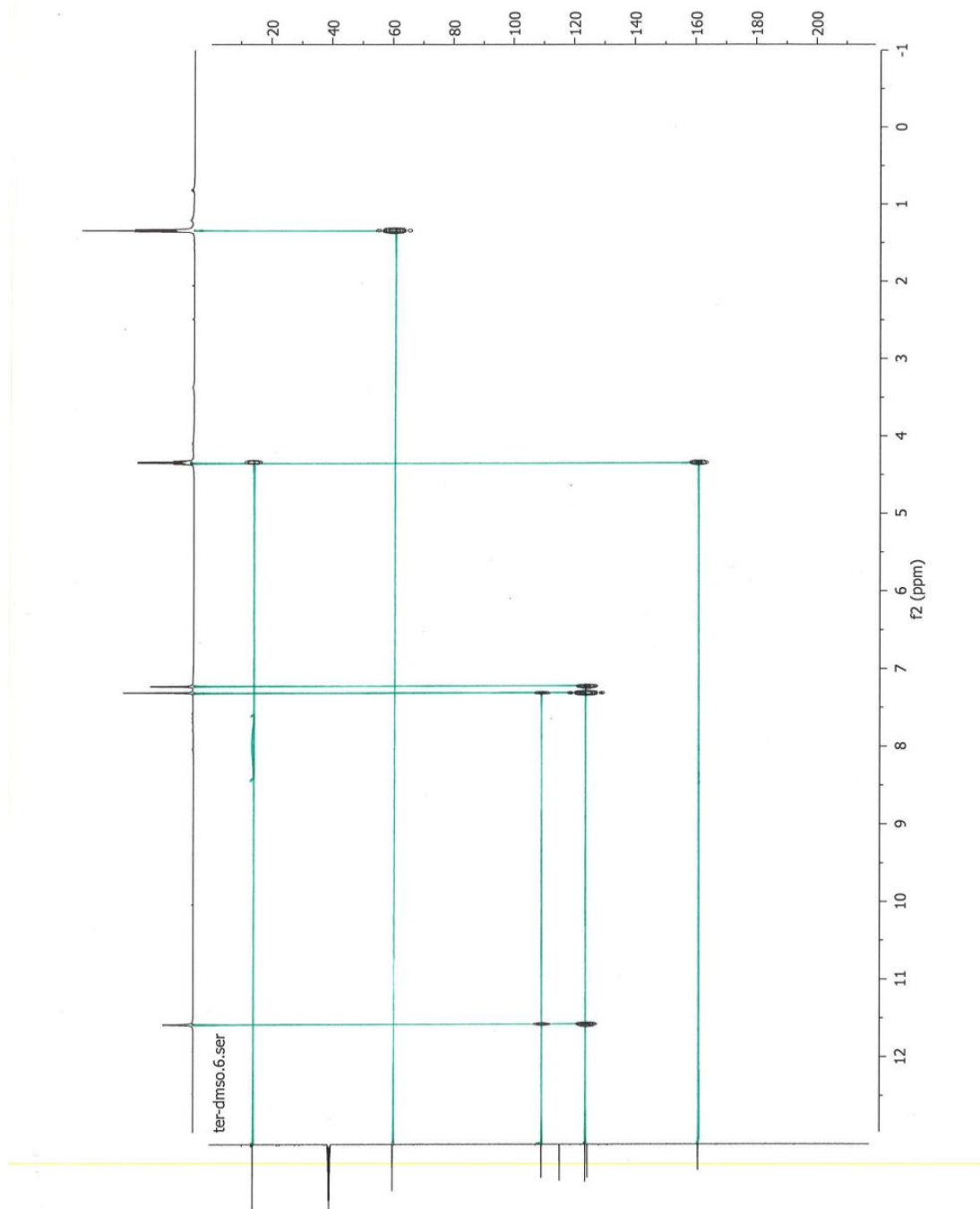


Figure 55. ^1H - ^{13}C HMBC, 3j



Section 4:

Differential Scanning Calorimetry of ethyl azidoacetate (1) and ethyl α -azido- β -acrylates (2a-2j)

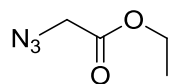
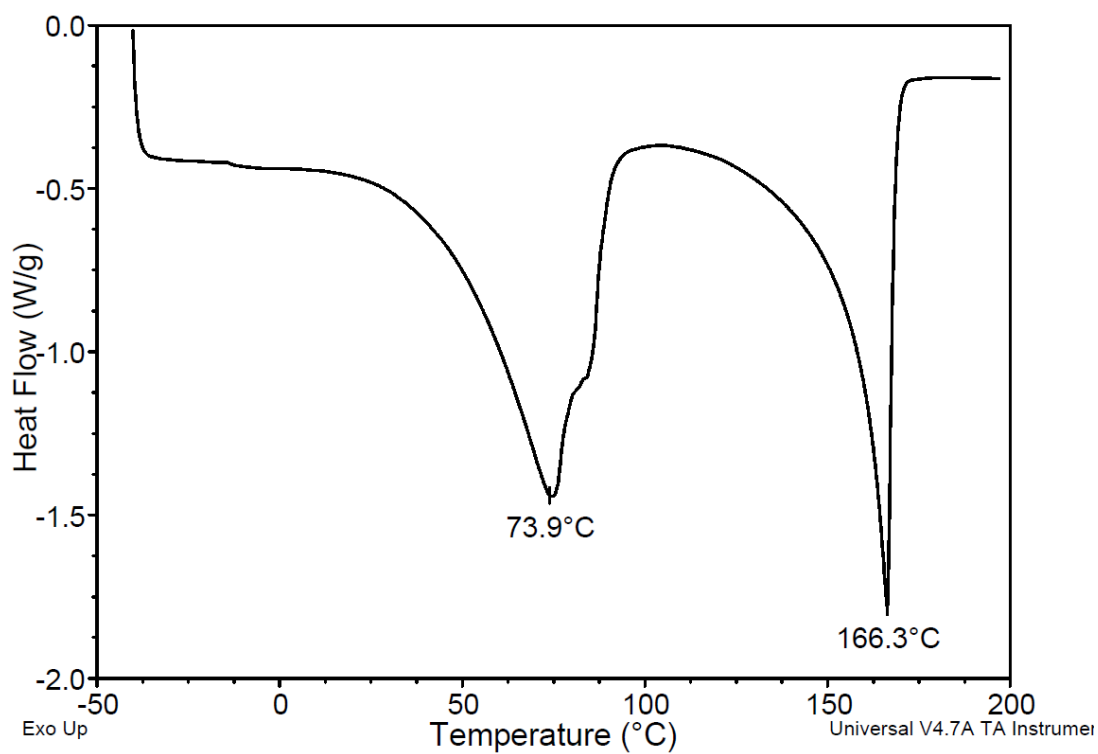


Figure 56. DSC: Ethyl azidoacetate (1)



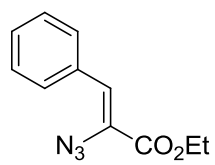
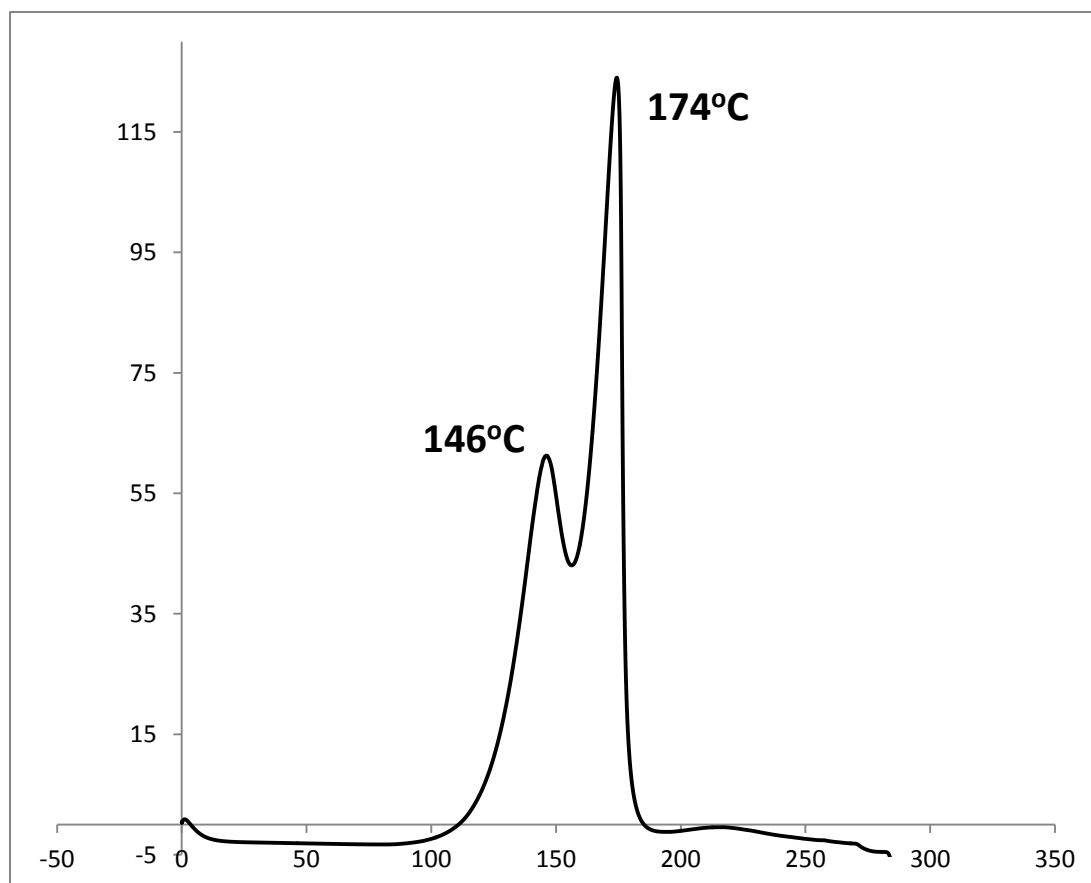


Figure 57. DSC: (Z)-Ethyl α -azido- β -phenylacrylate (2a)



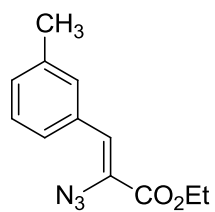
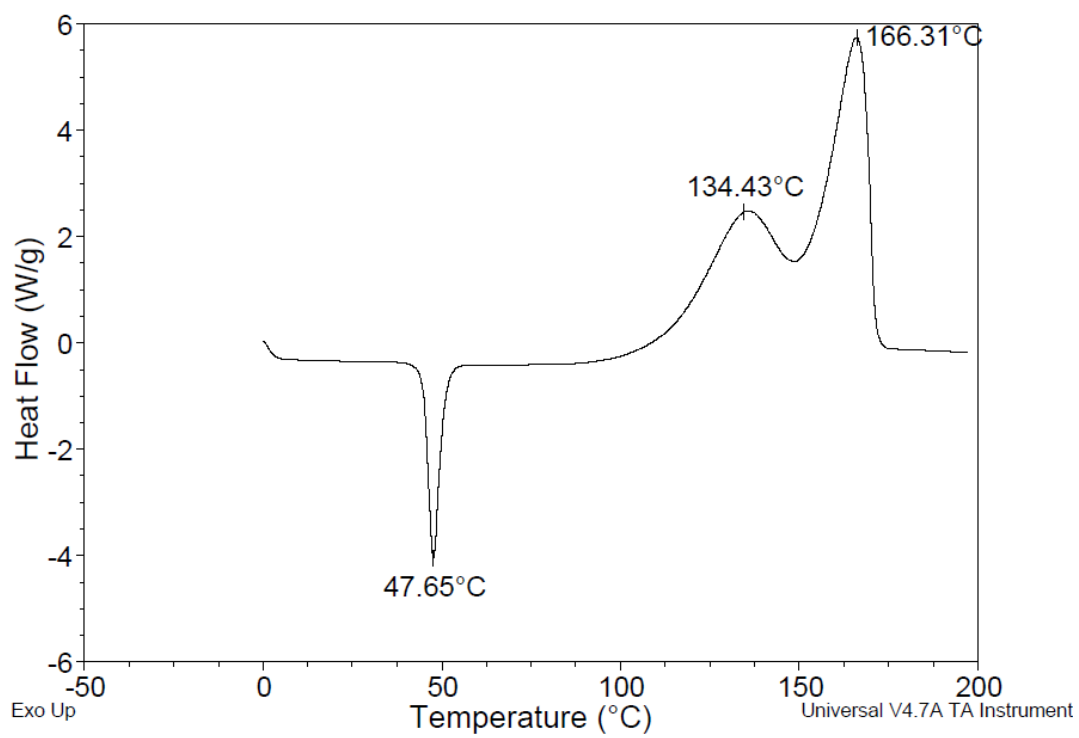


Figure 58. DSC: (Z)-Ethyl *meta*-methyl- α -azido- β -phenylacrylate (2b)



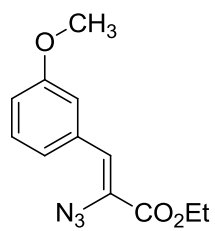
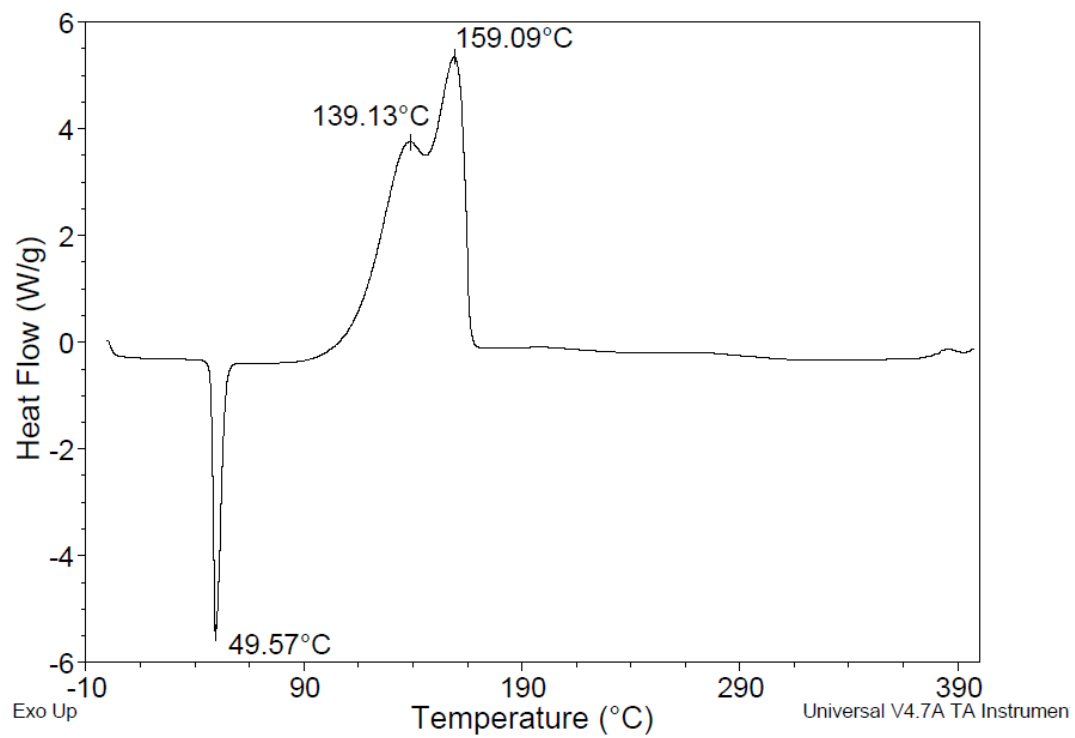


Figure 59. DSC: (Z)-Ethyl *meta*-methoxy- α -azido- β -phenylacrylate (2c)



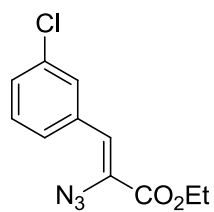
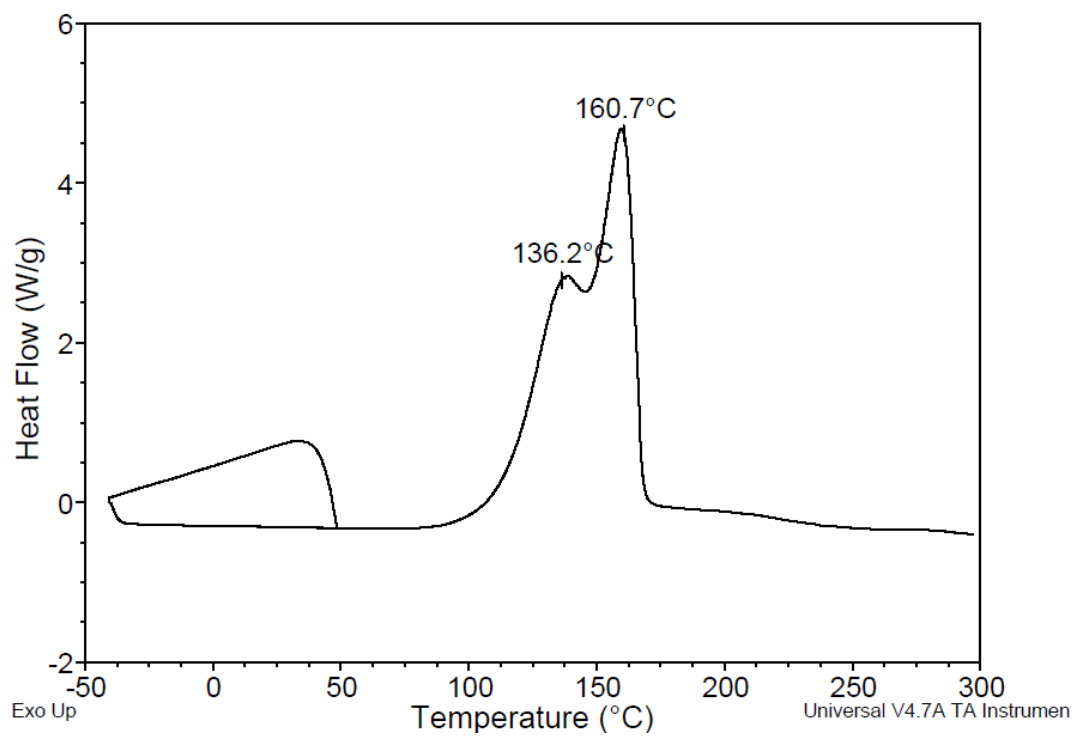


Figure 60. DSC: (Z)-Ethyl *meta*-chloro- α -azido- β -phenylacrylate (2d)



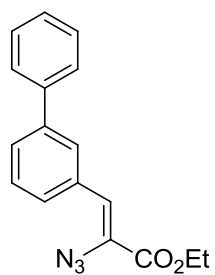
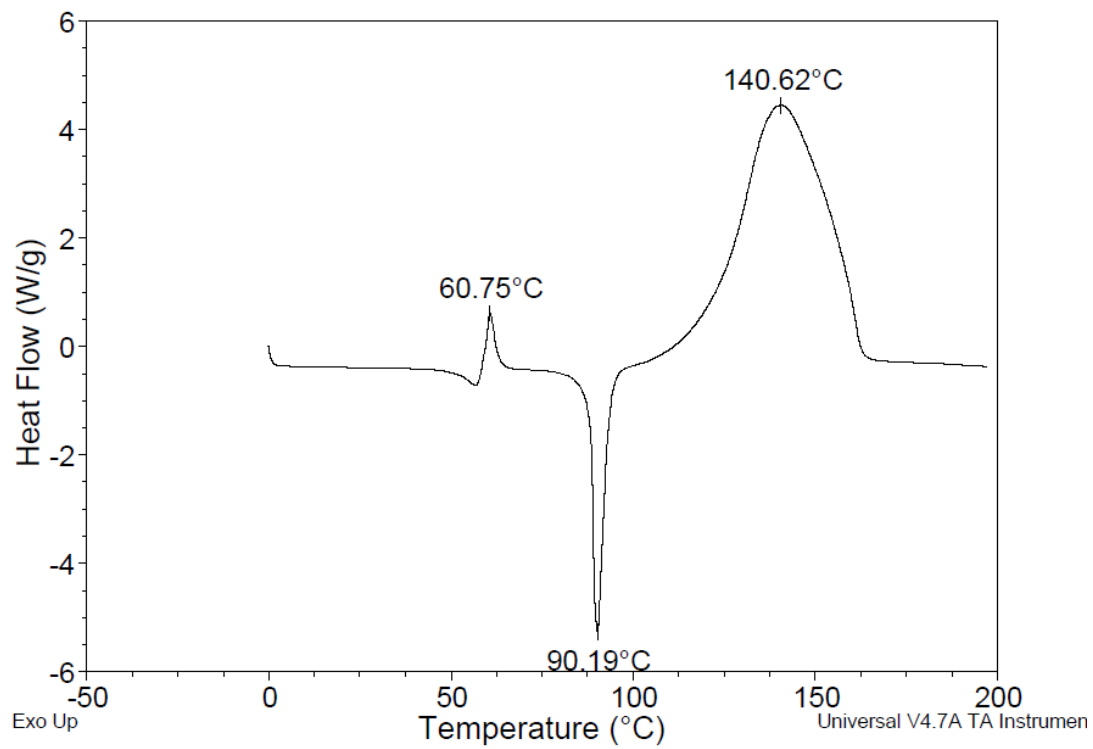


Figure 61. DSC: (Z)-Ethyl *meta*-phenyl- α -azido- β -phenylacrylate (2e)



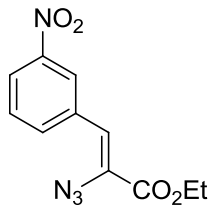
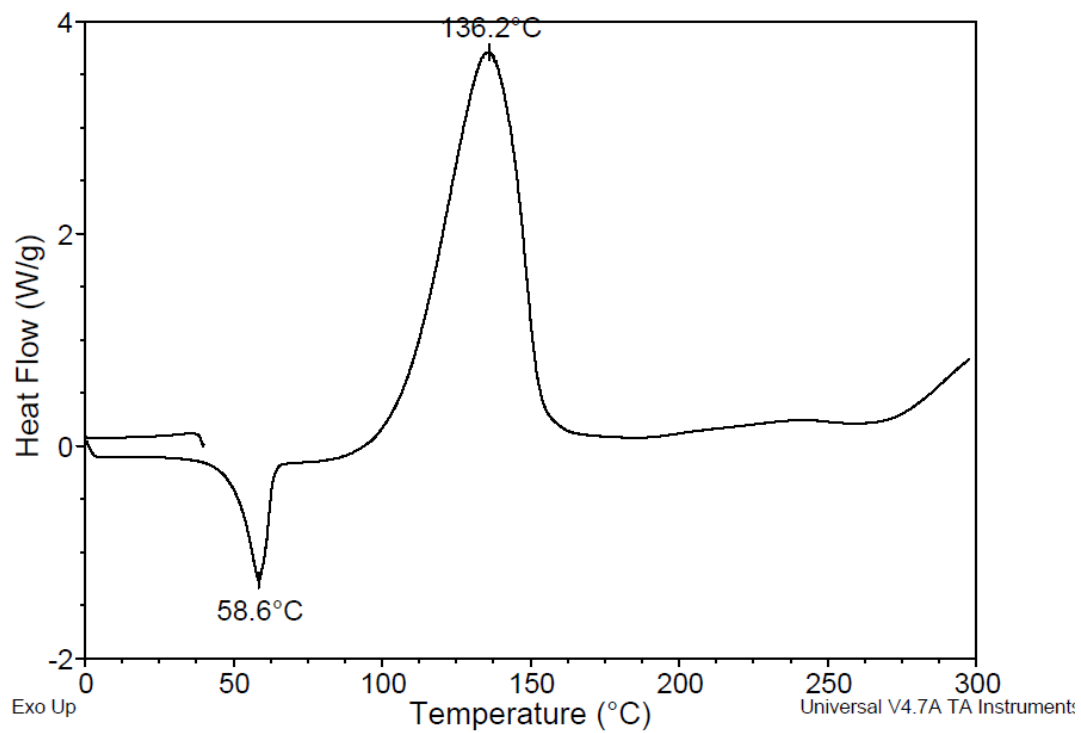


Figure 62. DSC: (Z)-Ethyl *meta*-nitro- α -azido- β -phenylacrylate (2f)



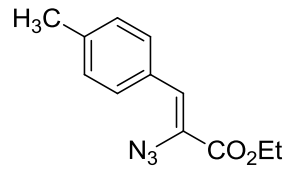
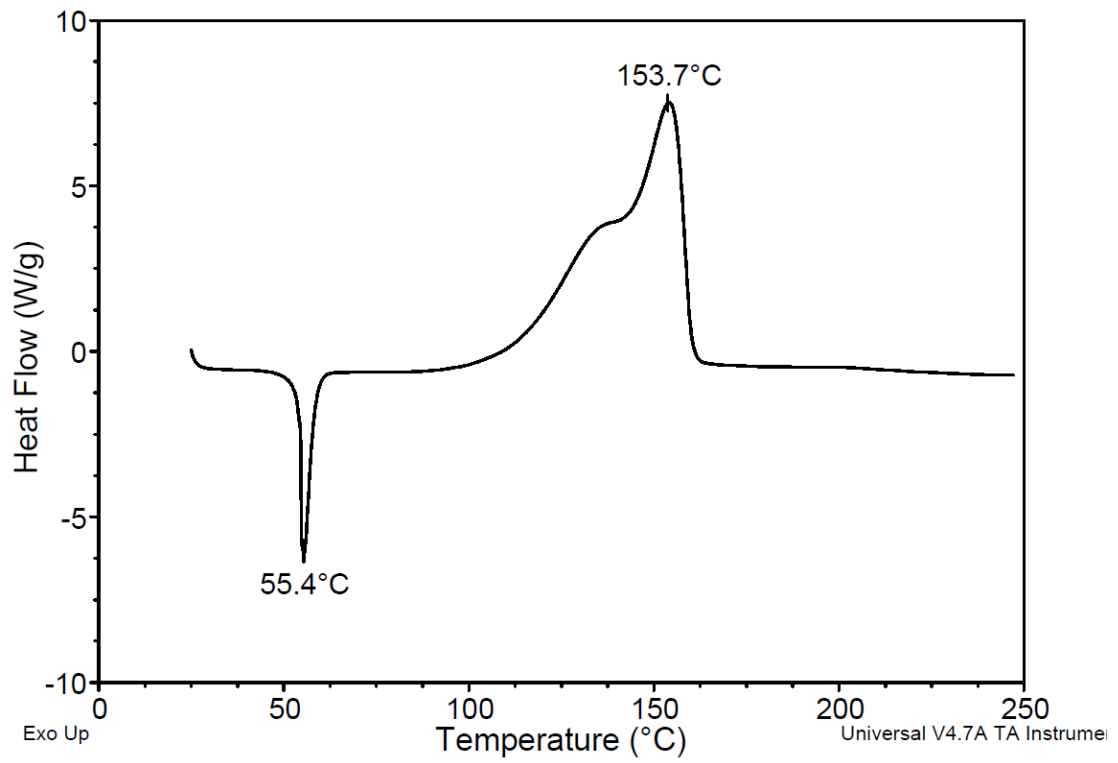


Figure 63. DSC: (Z)-Ethyl *para*-methyl- α -azido- β -phenylacrylate (2g)



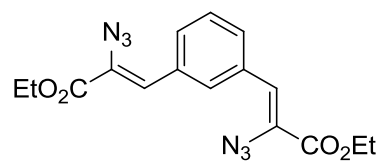
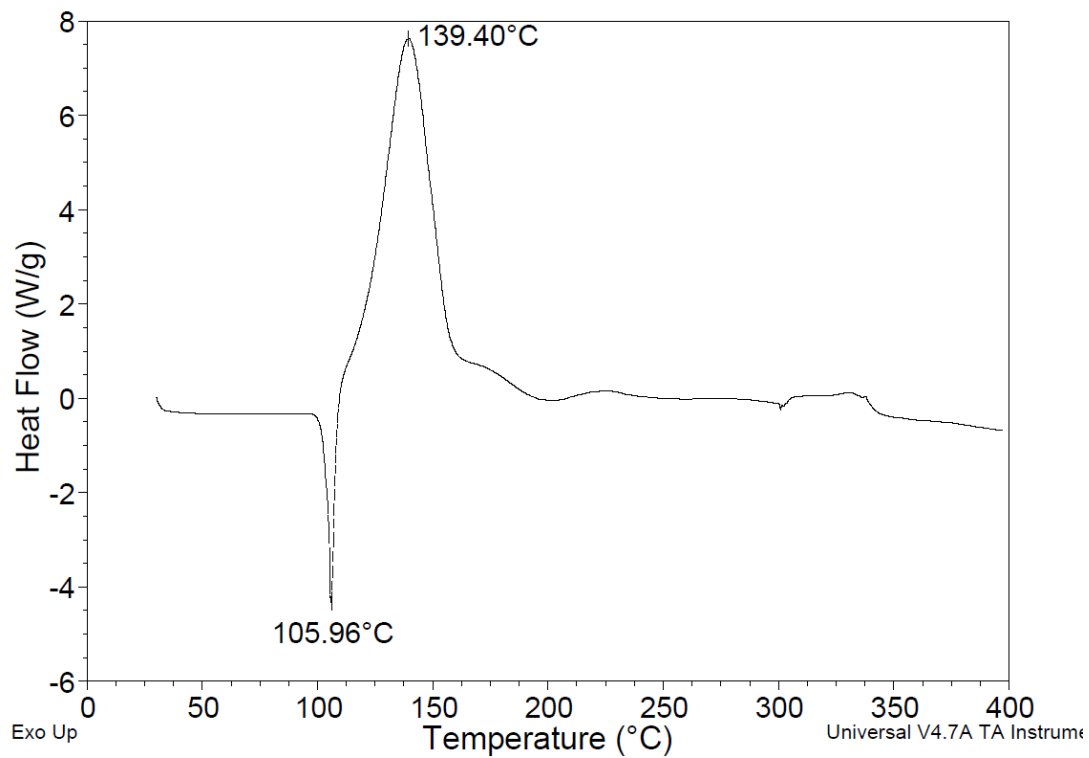


Figure 64. DSC: (2Z,2'Z)-diethyl 3,3'-(1,3-phenylene)bis(2-azidoacrylate) (2h)



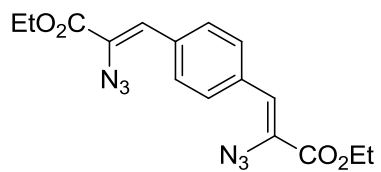
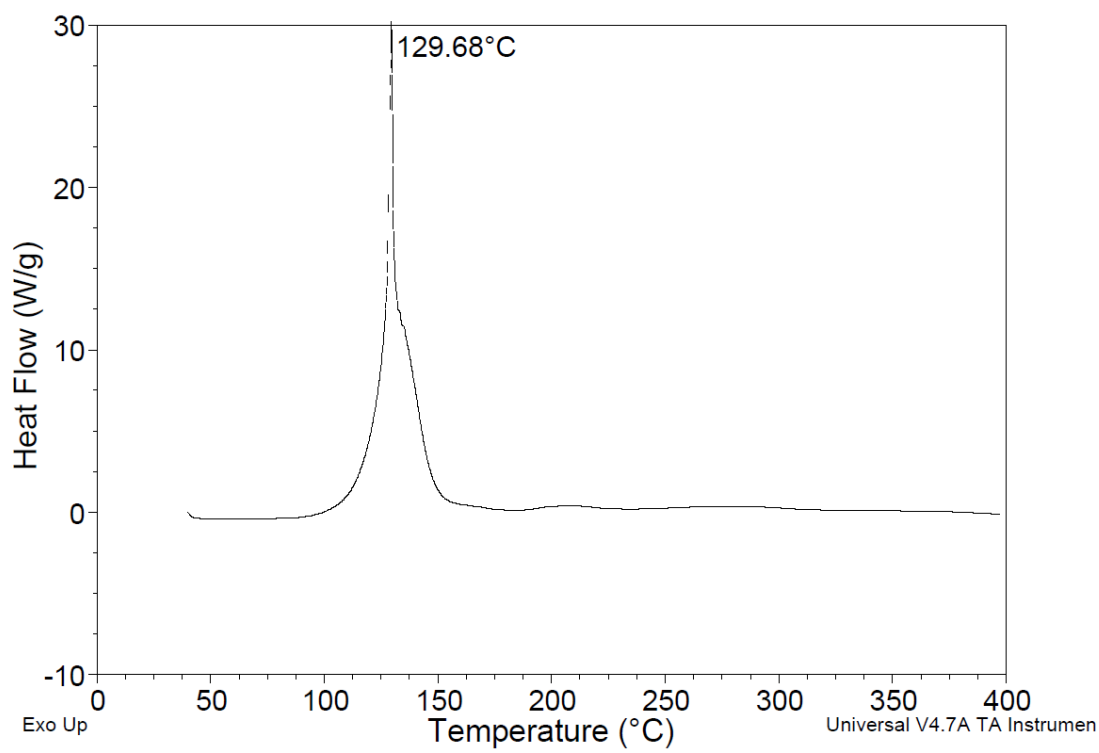


Figure 65. DSC: (2Z,2'Z)-diethyl 3,3'-(1,4-phenylene)bis(2-azidoacrylate) (2i)



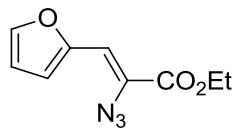
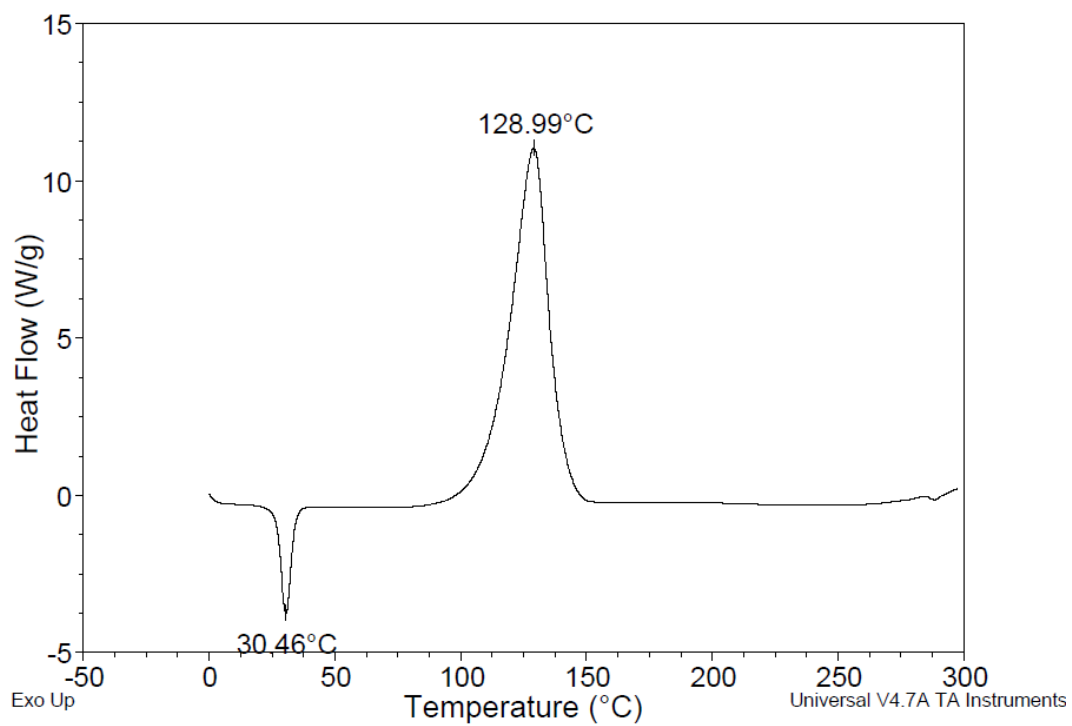


Figure 66. DSC: (Z)-ethyl 2-azido-3-(furan-2-yl)acrylate (2j)

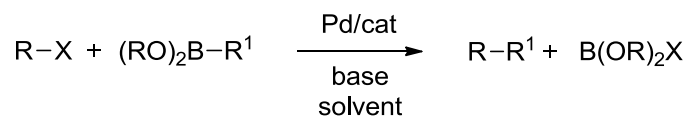


CHAPTER 2

2.1 Suzuki Coupling Reactions

2.1.1 Overview

Carbon-carbon bond forming reactions are critical in the construction of complex organic molecules. The Suzuki-Miyaura cross coupling reaction represents a particularly important carbon-carbon bond forming methodology that is widely used in both academia and industry. For his landmark discovery, Suzuki was awarded the Nobel Prize in 2010.⁶⁷ This versatile and robust reaction is the palladium-catalyzed coupling of organoboron compounds with organic halides in the presence of a base, a generalized illustration is shown in Figure 67.



R: alkyl, alkenyl, aryl,

X: Cl, Br, I, CF₃SO₃

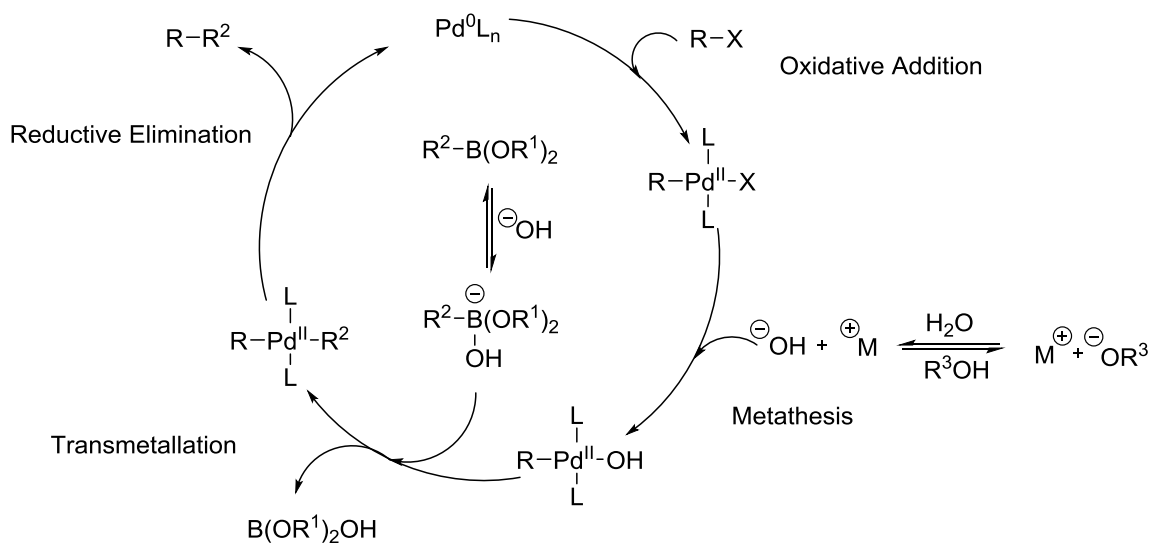
R¹: alkyl, alkenyl, alkynyl, aryl

Figure 67. Generalized Suzuki coupling reaction

The versatility of the Suzuki coupling is reflected in the variety of organoboron compounds that can be coupled with functionalized aryl, vinyl, or alkyl halides or triflates. These include organoboranes in which the boron is attached to an sp -, sp^2 -, or sp^3 -carbon. It is a robust reaction and is tolerant of a wide variety of solvent media and bases. Typical solvent systems are organic-aqueous mixtures. The organic solvents can be miscible with water, such as tetrahydrofuran (THF) and dimethylformamide (DMF), or they can be immiscible with water such as toluene and benzene. Less common solvent systems include super critical carbon dioxide ($scCO_2$), anhydrous organic solvents, or water alone. The most general method employs mild temperatures, $\leq 110^\circ C$, and an inorganic base. The solvent system, base and temperature strongly influence the phase behavior of the reaction. Both homogeneous and heterogeneous reaction conditions have been used successfully. The bottom line is that the Suzuki coupling is at the forefront in the construction of complex molecules.^{68,69}

2.1.1.1 Mechanism

It is well accepted that the general order of reactivity of the organohalides follows $I > OTf > Br \gg Cl$. Because of the variety of acceptable reaction conditions, the optimum parameters—including solvent, co-solvent(s), palladium precatalyst, ligand, base, temperature, concentration, and stoichiometry—have often proved substrate dependent. Additionally, it is believed that the mechanism as well as the rate-determining step in the reaction sequence could also be substrate dependent.⁶⁸ The generally accepted mechanism for the Suzuki coupling reaction is shown in Scheme 27.



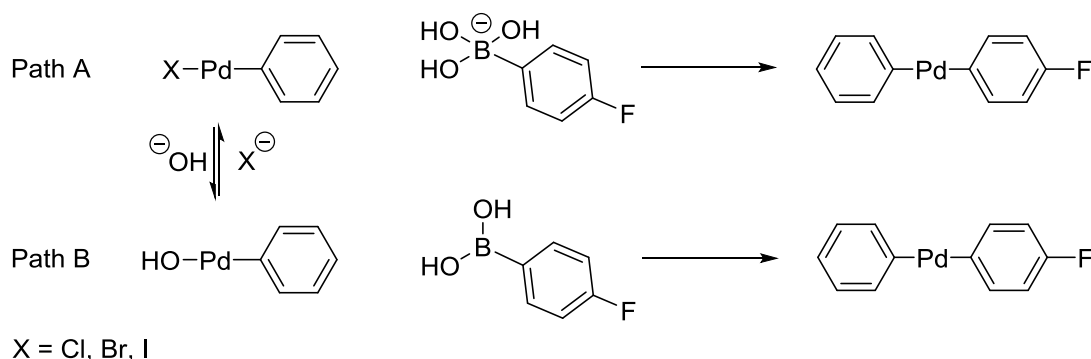
Scheme 27. Suzuki cross-coupling mechanism

The first step is the oxidative addition of the organohalide to the active, ligand-stabilized Pd^0L_n catalyst forming a Pd^{II} complex. Initially, oxidative addition results in a *cis* geometry about the palladium center; however, this complex rapidly reorients to a *trans* $\text{R-Pd(L)}_2\text{-X}$ complex. This is followed by metathesis in which the base displaces the halogen on the palladium metal center. The next step is a transmetalation process in which the organic group of an *in situ* generated organoboronate transfers to the Pd^{II} complex exchanging with the base. The final step is reductive elimination in which the new carbon-carbon bond is formed and the Pd^{II} metal center is reduced regenerating the active Pd^0 catalyst. Two aspects of the catalytic cycle have received particular attention in the literature—the mechanism of the transmetalation step and the role of base.

2.1.1.1.1 Transmetallation

Transmetallation has frequently been found to be the rate determining step in couplings involving organic bromides, iodides and triflates; whereas, with organochlorides the oxidative addition is commonly the rate determining step.⁶⁸ In the mechanism shown above, the transmetallation step occurs once an anionic borate species is generated. Because of the empty *p* orbital of boron, it has long been thought that it was necessary to activate the boron with a Lewis or Brønsted base. However, it has also been proposed that transmetallation can proceed through a neutral boronic species as well as a hydroxy-palladium complex.⁷⁰⁻⁷²

Carrow et al. compared kinetic and equilibrium data from reactions involving the transmetallation between a preformed arylpalladium hydroxy complex (Scheme 28, Path A) or a preformed arylpalladium halo complex (Scheme 28, Path B) with *para*-fluoroboronic acid.⁷²



Scheme 28. Proposed transmetallation pathways

The kinetic and equilibrium data were derived from ^{31}P , ^{11}B , and ^{19}F nuclear magnetic resonance (NMR). The equilibrium between the palladium complexes in Scheme 2 were evaluated in mixed solvent systems—25:1 and 50:1 THF-water mixtures—by ^{31}P NMR at -40°C . It was found that the equilibrium between the Ph-Pd-X and Ph-Pd-OH favored the bromo- and chloro-complexes in both solutions ($K_{\text{Pd-Br}} = 9.3$ and 1.3 , $K_{\text{Pd-Cl}} = 23$ and 3.2 respectively) but the iodo complex was only slightly favored in the 25:1 mixture ($K_{\text{Pd-I}} = 1.1$) and slightly disfavored in the 50:1 mixture ($K_{\text{Pd-I}} = 0.17$). These equilibrium data suggest that an anionic boronate is the favored boronic species in the transmetallation step. However, transmetallation with the Ph-Pd-OH complex was found to occur 14,000 times faster than with the Ph-Pd-X complexes. Therefore, it was concluded that the rate of transmetallation with a Ph-Pd-OH complex is the preferred pathway. The same conclusion was drawn by Amatore et al. from CV and NMR experiments manipulating the equilibria of Pd-X:Pd-OH and $\text{RB}(\text{OR})_2:\text{[RB}(\text{OR})_2\text{OH]}^-$ in aqueous DMF. Though neither path is mutually exclusive, path B was favored over path A.⁷⁰

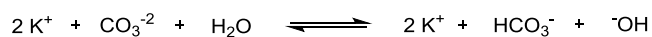
2.1.1.1.2 The Role of Base

The Suzuki coupling reaction cannot occur without a base. Most reactions employ at least two equivalents of aqueous base relative to the organohalide. Organic and inorganic bases have both been successfully used, and the $\text{p}K_{\text{a}}$'s of the conjugate acids are typically within three orders of magnitude greater than the $\text{p}K_{\text{a}}$ of phenylboronic acid (Table 7).

Table 7. Base strength (pK_a (BH^+)) relative to pK_a of phenylboronic acid⁷³

Phenylboronic acid	$pK_a = 8.9$
Base	pK_a (BH^+)
CO_3^{2-}	10.3
PO_4^{3-}	12.4
F^-	3.17
TEA	10.7
DIPEA	11.4

Carbonate and phosphate, usually as their potassium salts, are the most commonly used bases. Fluoride is a much weaker base compared to the others; however, CsF has proven to be an effective base in some Suzuki reactions. When using an aqueous base, hydroxide anion will usually be present in the equilibrium (Scheme 29).



Scheme 29. Aqueous base equilibrium in a Suzuki coupling

It has been suggested that the hydroxide anion can play multiple roles in the catalytic cycle. Amatore et al. used cyclic voltammetry (CV) to measure and track the oxidation and reduction potentials of palladium species in a coupling reaction.⁷⁰ By

comparing the potentials observed to standard potentials of palladium-hydroxide and palladium-halide complexes they determined that hydroxide can participate in three steps in the catalytic cycle: metathesis, transmetallation, and reductive elimination. In metathesis, hydroxide exchanges with the halogen after oxidative addition. The discussion in the previous section highlighted the role the base performs in transmetallation, and the results Amtore et al. found by CV are in agreement with the conclusions made by Carrow et al. in their NMR studies. The investigators also postulated that reductive elimination rapidly occurs through a pentavalent transition structure, illustrated below in Figure 68, when hydroxide is present in the reaction. Although they did not provide structural evidence for this intermediate, it was postulated because as the hydroxide concentration increased the rate of reduction of Pd^{II} to Pd⁰ also increased.

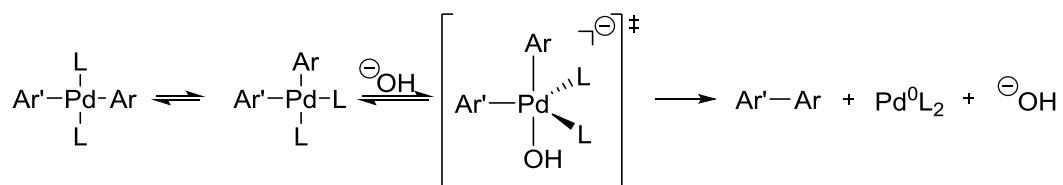


Figure 68. Reductive elimination via pentavalent Pd complex

2.1.2 Challenges and Improvements of the Suzuki Coupling

The volume of literature, ~ 10,000 articles in thirty-four years⁷⁴, not only shows the importance of the Suzuki coupling reaction but also points to on-going challenges as its scope has expanded. In addition to the development in breadth of suitable coupling partners, other areas of exploration and advancement include catalyst and ligand design, catalyst/ligand recovery and recycling, use of *green* solvents, use of microwave technology to accelerate the reaction, aqueous couplings, ligand-free couplings, and process engineering.

Ligand/catalyst design has arguably received the most attention. The traditional role of a ligand has been to stabilize the Pd⁰ catalyst. However, ligand design has been undertaken to: generate a more active Pd⁰L_n catalyst to overcome the slow reactivity of chloro-substrates and sterically challenging compounds⁷⁵⁻⁷⁸, enhance aqueous solubility of the catalyst⁷⁹⁻⁸², and also **prevent catalyst deactivation from undesired complexation by coupling substrates containing basic nitrogens.**^{78,83,84} Ligands are usually aryl phosphines with triphenylphosphine (TPP) being the standard, although alkyl phosphines, nitrogen-based ligands, and several recent reports of couplings with no ligand have also been reported.⁸⁵⁻⁹³

2.1.2.1 Bulky, electron rich ligands enhance catalyst reactivity

Buchwald has reported extensive work on the synthesis and use of bulky, electron-rich ligands.⁷⁸ These ligands have been found to be highly effective for couplings involving the classically challenging chlorinated substrates and some nitrogen-

containing substrates such as pyridine, anilines, and aminopyridines. Figure 69 shows a selection of some of these ligands.

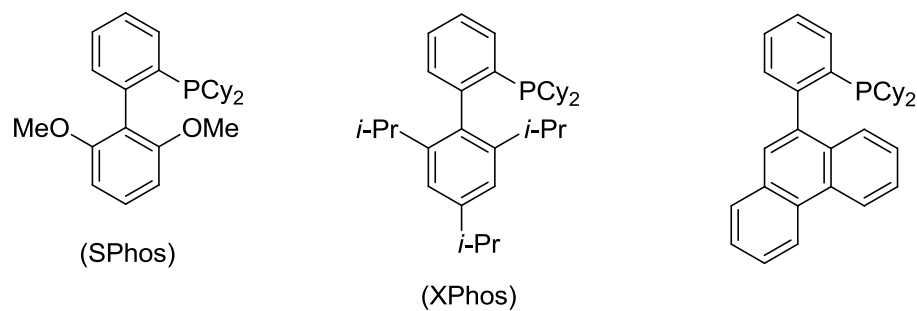


Figure 69. Biarylphosphine ligands

Bulky, electron rich ligands impart an increased reactivity on the palladium catalyst. The first step in the catalytic cycle is oxidative addition. In a most simplistic view, the palladium can be thought of as a nucleophile that substitutes for the halogen atom at the site of insertion. Thus, by increasing the electron density of the Pd catalyst and by creating bulk around it to prevent undesired coordination (e.g. by a basic nitrogen on a substrate) an increased activity of the catalyst can be achieved.

2.1.2.2. Phase Behavior and Catalyst Separation and Recycling

Given that many Suzuki couplings are biphasic, a second area of ligand development has involved increasing catalyst solubility in the aqueous phase through ligand functionalization. These include sulfonation of phosphine ligands, use of

phosphoryl ammonium salts, and phosphoryl-guanidinium species (Figure 70). There are multiple reasons cited in the literature for increasing the aqueous solubility of ligands. These include enhancing yields from highly water soluble substrates (e.g. halonucleosides, Scheme 30) or couplings in aqueous media,^{81,82} as well as catalyst recycling and enhancing separation of the catalyst from organic products.^{79,80,94,95}

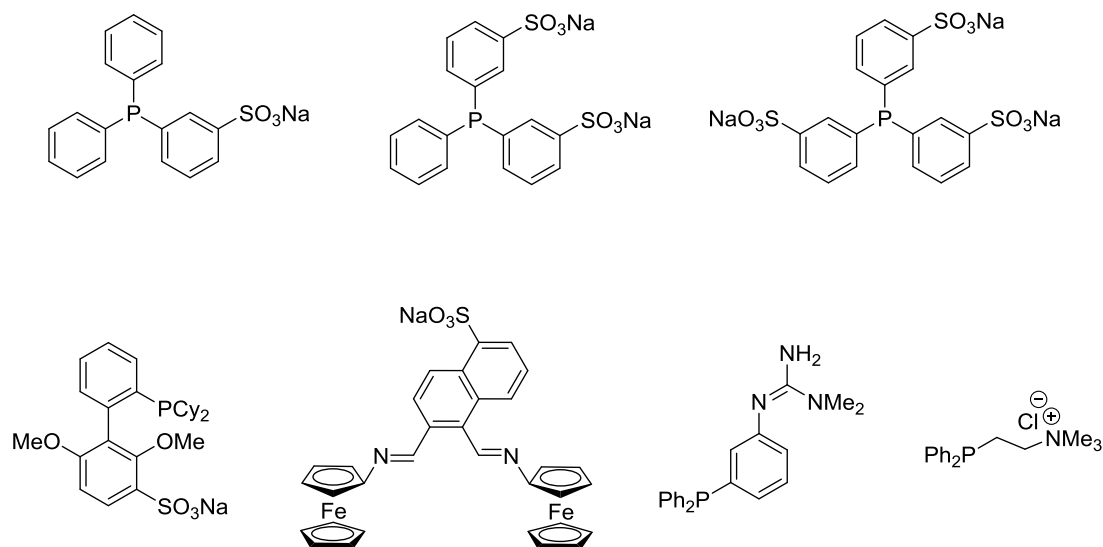
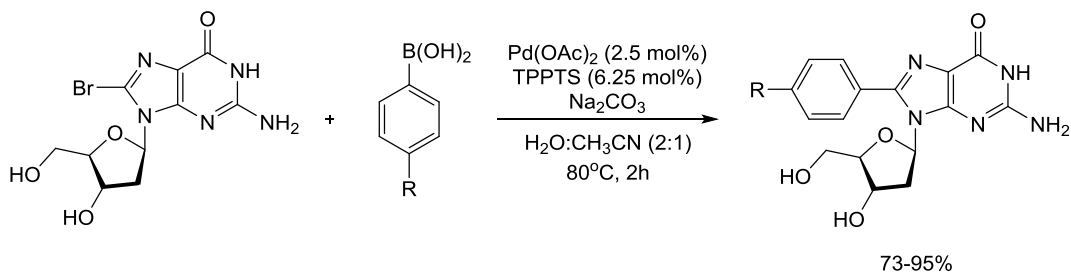
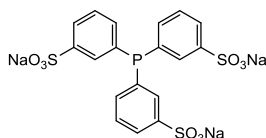


Figure 70. Water-soluble ligands used in Suzuki couplings



R = H, CH₃, CH₂OH, OCH₃, F, CO₂Na

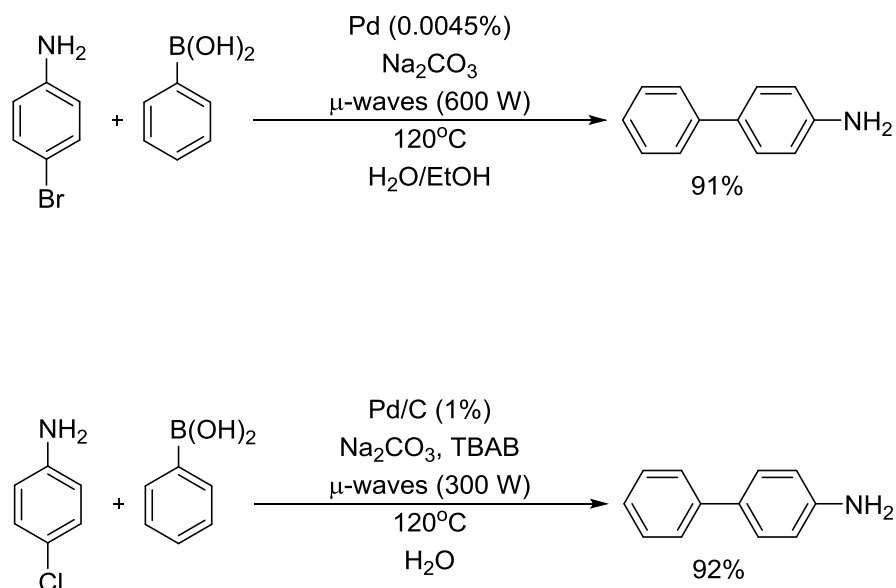
TPPTS



Scheme 30. Water soluble Suzuki ligand in the arylation of a halonucleoside

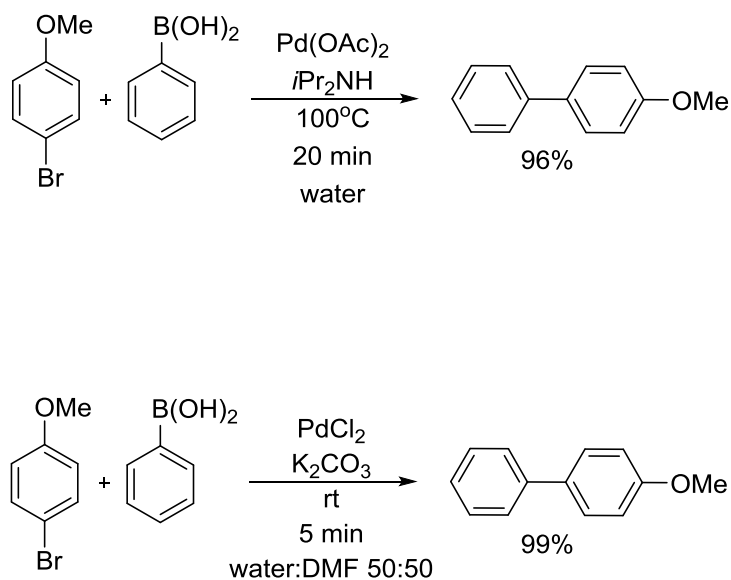
2.1.2.3 Ligand Free Suzuki Couplings

Because phosphine ligands can be toxic and some are costly to synthesize, ligand-free Suzuki couplings have been investigated as a *green* or sustainable alternative. However, it must be pointed out that the toxicity and/or cost of a ligand can be a simple nuance in a reaction process as they are used in very small concentrations. Leadbeater et al. and Liu et al. have reported several conditions in which Suzuki couplings can be run in the absence of a ligand under aqueous conditions.^{85,88,89,96-100} Leadbeater et al. employed microwaves to rapidly heat reaction solutions and achieve near quantitative yields of product in as little time as five minutes with low catalyst loadings (50 ppb – 1% Pd). Also, by using microwave heating and a phase transfer catalyst (tetrabutylammonium bromide, TBAB), they demonstrated high yielding couplings from typically problematic species such as chloroarenes and N-heteroarenes (Scheme 31).



Scheme 31. Microwave-assisted Suzuki coupling reaction

Liu et al. reported couplings in water or various 50:50 water:organic solvent systems at temperatures ranging from ambient temperature to 100°C (Scheme 32). At room temperature and within 5 minutes they achieved a quantitative yield of 4-methoxybiphenyl in a 50:50 mixture of water:dimethyl formamide (DMF).⁸⁸ The same yield could be achieved in water with di-*isopropylamine* at 100°C in twenty minutes.¹⁰¹



Scheme 32. Suzuki couplings in water and water:DMF

2.1.2.4 Catalyst De-activation by Substrates Containing Basic Nitrogens

Since many pharmaceutical and agrochemical compounds contain basic nitrogen functionalities, constructing these complex molecules under standard Suzuki coupling conditions has proven problematic. This is especially true for large scale batch processes employed in industry. The lone pair electrons on the nitrogens can ligate with the Pd catalyst resulting in extremely low turnover and/or catalyst deactivation. In addition, such interactions can create difficulties in separating product from catalyst (Figure 71) which can be extremely problematic in the synthesis of pharmaceutical and agrochemical intermediates.

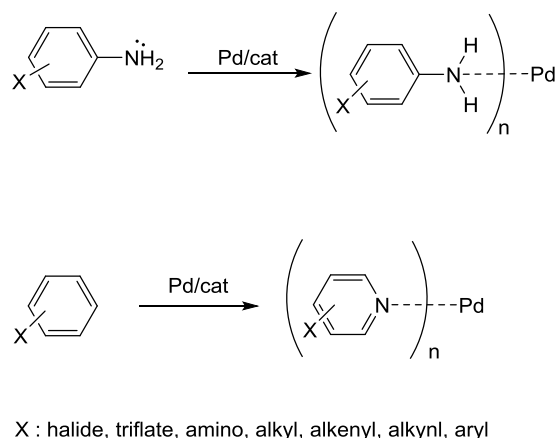
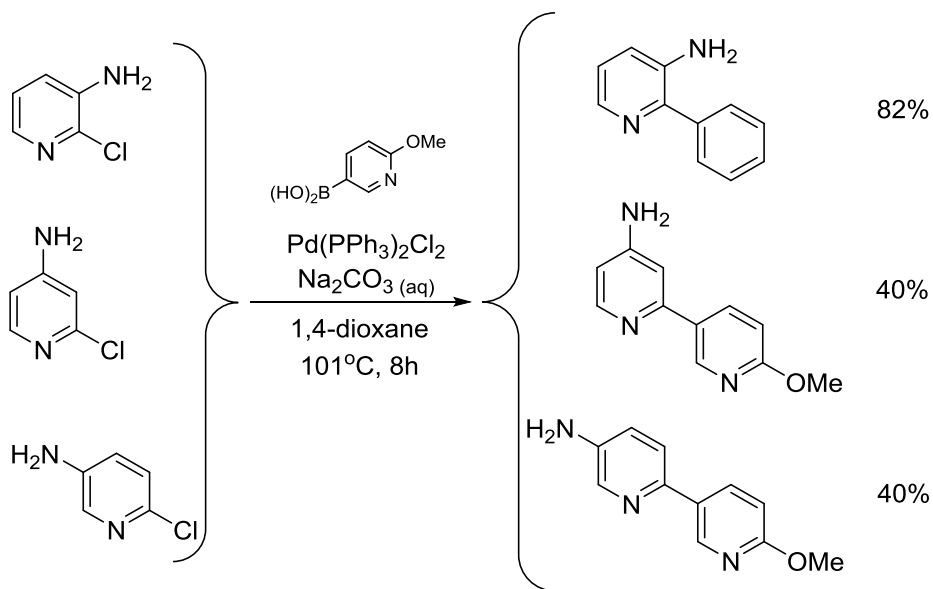


Figure 71. Complexation of Pd catalyst with starting material or product containing a basic nitrogen

The challenge with such substrates goes beyond the mere presence of a basic nitrogen, for the substitution pattern around the ring can greatly influence the outcome of a coupling reaction. For example, Thompson et al. reported this observation in a survey of chloro-aminopyridines coupling with 2-methoxy-5-pyridylboronic acid under standard Suzuki conditions—i.e. TPP as the ligand, no protecting groups (Scheme 33).¹⁰² The 3-amino-2-chloropyridine yielded twice the amount of product as either the 4-amino-2-chloropyridine or the 5-amino-2-chloropyridine within the same period of reaction time. While this statement is factually true, the explanation as to “why” remains a challenge. For instance, one would expect the ring nitrogen on the 4-amino-2-chloropyridine to have greater electron density compared to the 3-amino and the 5-amino isomers. Thus, a lower yield for the 4-amino-2-chloropyridine could be simply rationalized in terms of coordinating ability of the ring nitrogens. In contrast, however, if the coordination of the

Pd takes place primarily at the amino nitrogens then the opposite prediction would be true. To make things even more complicated, the electrophilicity of the *ipso* carbon bonded to the chlorine substituent plays a role in the relative reactivities. Based on resonance and inductive arguments it can be postulated that the electrophilicity of the carbon in question is greatest for the 4-amino isomer. Clearly, there are a variety of factors, none of which present a clear picture of what is causing the experimental observations.

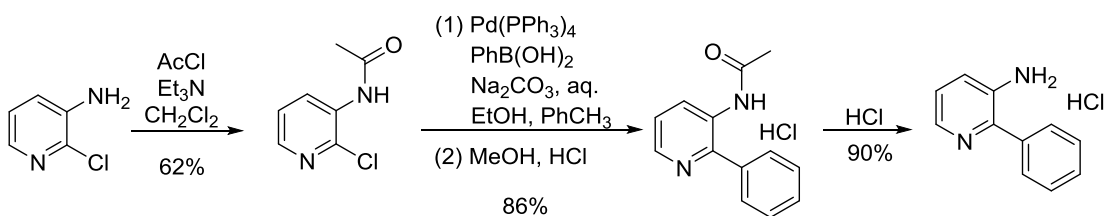


Scheme 33. Suzuki coupling of a free amino pyridine under standard conditions

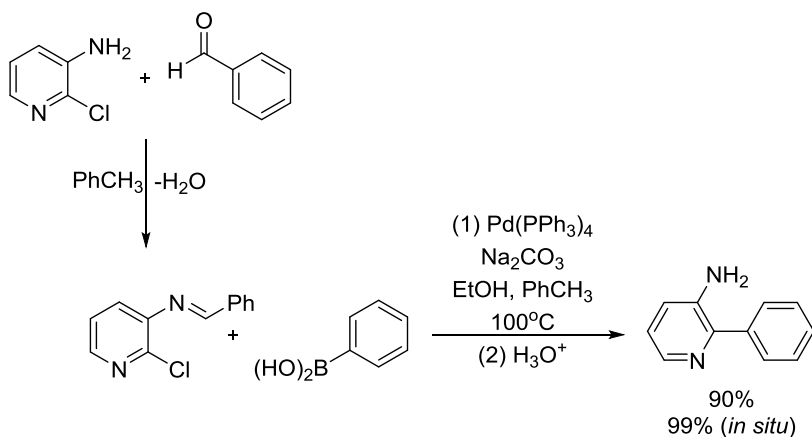
Practical solutions to these challenges have been the use of bulky ligands (see section 2.1.2.1) or protecting groups. Caron et al. reported high yields for the Suzuki

coupling of 3-amino-2-chloropyridine with phenylboronic acid when the amino group was protected as an acetamide or an imine (Scheme 34).¹⁰³ The acetamide protection strategy gave an overall yield of 48%. The imine protection was more effective and provided a 90% yield in a step-wise sequence and a 99% yield when the protection was performed *in situ*. While these results present a chemical solution to the reactivity issues, protecting and deprotecting strategies are not attractive from an industrial view point.

Acetamide protection



Phenylimine protection



Scheme 34. Suzuki coupling with a protected aminopyridine

The synthesis of commercial products employing a Suzuki coupling reaction with substrates containing basic nitrogen substituents presents an important and on-going challenge for the chemical industry, especially reactions involving halo-pyridines, halo-anilines, and halo-aminopyridines. Complexation of the palladium catalyst with basic nitrogens, from either the product or the starting materials, usually results in catalyst deactivation and low yields. Current strategies that are reported in the literature to overcome catalyst deactivation by basic nitrogens include the use of sophisticated ligands or employing separate protection and deprotection reactions—both approaches being quite costly. Thus, the development of an efficient, economical, and general solution is necessary. As a consequence, we initiated studies in the use of CO₂ as an *in situ*, reversible protecting/activating reagent in order to overcome catalyst inhibition by basic nitrogens in Suzuki couplings.

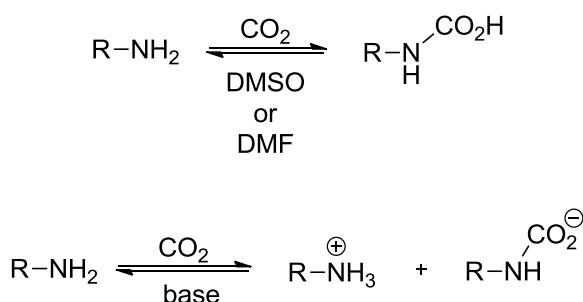
2.3 *In situ* Reversible Protection of Basic Nitrogens with CO₂

2.3.1 Properties and Current Applications of CO₂

2.3.1.1 Brief Overview of Some Physical and Chemical Properties of CO₂

Carbon dioxide (CO₂) is abundant, inexpensive, and non-toxic. It is a gas and does not have a liquid state until ~5 atm. Its critical point can be reached at a relatively low temperature, 31.1°C at 79.2 atm. It is nonpolar and an extremely poor solvent; its dielectric constant is ~1. Although CO₂ is nonpolar, the carbon atom is electrophilic. As

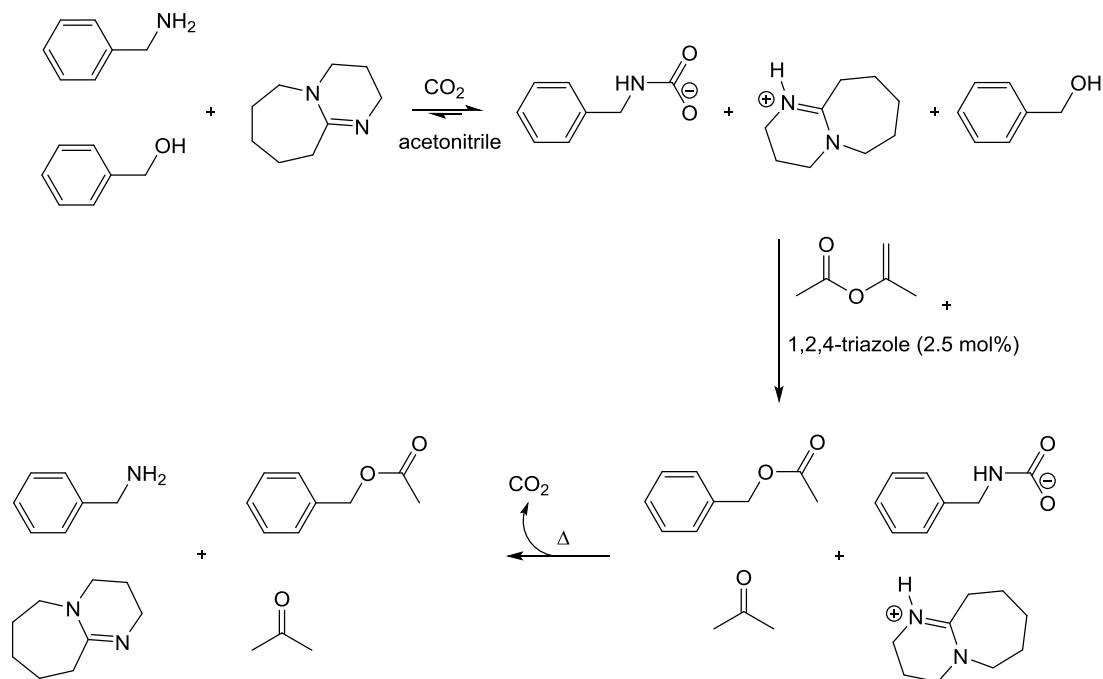
a consequence, it readily coordinates with basic nitrogen species to form the corresponding ammonium carbamate species (Scheme 35). The position of the equilibrium is controlled by the basicity of the amine, the temperature, and the pressure of CO₂.



Scheme 35. Reaction of an amine with CO₂

The reaction of CO₂ with amines has led to its use as a protecting reagent (Scheme 36)¹⁰⁴ and as a CO₂ capture system for coal-fired power plants.^{105,106} Peeters et al. demonstrated the use of CO₂ as a protecting reagent in the competitive acylation between benzylamine and benzyl alcohol in the presence of the organic base 1,8-diazabicycloundec-7-ene (DBU) and a catalytic amount of 1,2,4-triazole. Under one atmosphere of CO₂ in acetonitrile, the benzylamine reacted with the CO₂ in the presence of DBU generating the benzylcarbamate and protonated DBU ion pair. Isopropenyl acetate, the Michael acceptor, was added and it preferentially acylated the benzyl alcohol

in the presence of the 1,2,4-triazole catalyst. After reaction, the protection of the benzylamine was reported to be reversed by heating to 60°C.



Scheme 36. CO₂ as a protecting reagent in nucleophilic substitution

2.4 Data and Results: *In situ*, Reversible Application of CO₂ in Suzuki Couplings

2.4.1 Overview

The application of CO₂ as an *in situ*, reversible protecting group potentially offers an efficient solution to Suzuki coupling reactions where a basic nitrogen is present in at least one of the reaction partners. The substrates of particular interest are halo-anilines,

halo-pyridines, and halo-aminopyridines. Moreover, the reaction or interaction of CO₂ with basic nitrogens could, in principle, activate the haloarene for Pd insertion by decreasing the electron density and thus increasing the electrophilicity at the ipso position of the carbon-halogen bond. Some possible interactions of 4-amino-2-halo-pyridines with CO₂ are illustrated in Figure 72. The structures drawn in the figure are meant to show that CO₂ may be forming covalent bonds with the basic nitrogens present in the substrate or may be strongly solvating these atomic centers. In principle, both models could be means of protecting the basic nitrogens and preventing their coordination with the Pd catalyst.

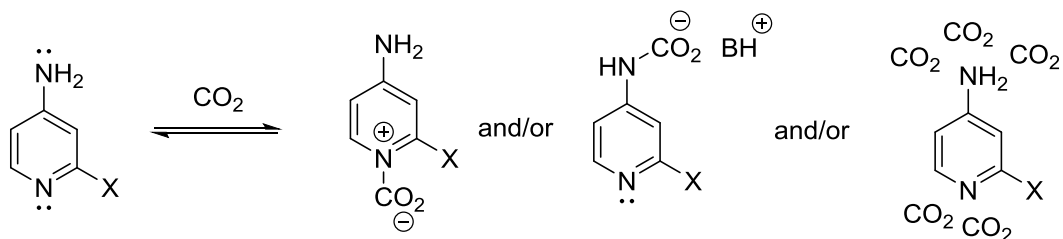


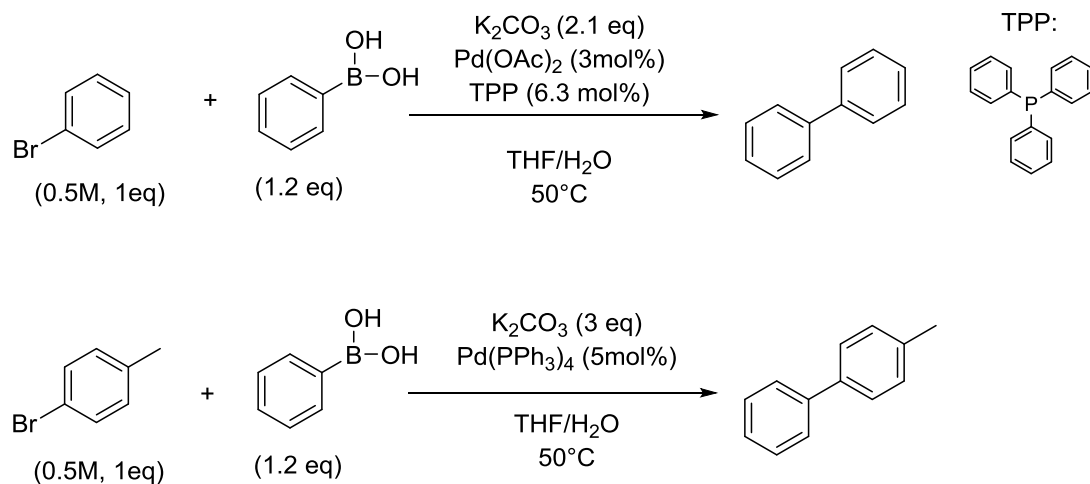
Figure 72. Reaction or interaction of CO₂ with a 4-amino-2-halo-pyridine

As previously discussed, there are many variables which must be addressed in performing a successful Suzuki coupling reaction. The investigation of this strategy is focused first on three facets: (1) the effect of water on Suzuki couplings, (2) the effect of P_{CO₂} on the yield in Suzuki couplings involving anilines, pyridines, and aminopyridines,

and (3) the role of CO₂ in Suzuki couplings involving anilines, pyridines, and aminopyridines.

2.4.1.1 The Effect of Water on Suzuki Couplings

It was already mentioned that the use of water in Suzuki couplings significantly improves the reactions' kinetics and yields compared to anhydrous conditions. Water serves as a source of hydroxide¹⁰⁷ and as a solvent for the inorganic base. However, the use of water in reactions with CO₂ present may affect the coupling. There will be competitive reactions between CO₂ with water in the basic medium and interactions of CO₂ with the substrate. Specifically, in basic media, the formation of carbonate and bicarbonate will result in a reduced concentration of hydroxide; this could seriously affect the transmetallation step. Therefore it was important to understand how the amount of water used affects the product yield and the reaction rate in the absence and presence of CO₂. In order to provide a baseline for this particular investigation, the initial reactions were conducted with substrates which did not contain basic nitrogen atoms. In particular, the couplings of 4-bromotoluene or bromobenzene with phenylboronic acid were studied as a function of the water content (v/v %) in the reaction system (Scheme 37). Potassium carbonate (2-3 eq), Pd(OAc)₂ (3 mol%) and triphenylphosphine (6.3 mol%) or Pd(PPh₃)₄ (3 mol%) were employed. The organic solvent was tetrahydrofuran and the reaction temperature was 50°C. In each of the experiments the phase behavior of the system was assessed since this could be an important contributor to both the yield of product as well as the reaction rate. The progress of the reactions was followed by quantitative GC/MS or HPLC. The results are summarized in Table 8.



Scheme 37. Suzuki coupling reactions as a function of water content (v/v %)

Table 8. Effect of Water (v/v%) on Suzuki coupling reactions

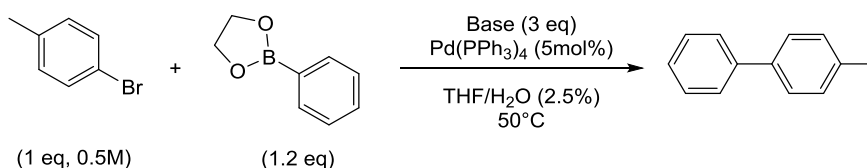
Haloarene	Volume of		Time (h)	Yield	Method
	% Water	Water (mL)			
bromobenzene	0%	0	4.5	9%	GC/MS
bromobenzene	2.5%	0.625	4.5	87%	GC/MS
bromobenzene	4%	1	4.5	100%	GC/MS
bromobenzene	30%	7.5	2	100%	GC/MS
4-bromotoluene	0%	0	4	9%	HPLC
4-bromotoluene	0%	0	24	37%	HPLC
4-bromotoluene	2.5%	0.625	4	100%	HPLC
4-bromotoluene	2.5%	0.625	24	98%	HPLC

In the absence of added water both bromobenzene and 4-bromotoluene produce minute amounts of product over a 4 to 4.5 hour time period. Indeed, allowing 4-bromotoluene to react for 24 hours in the absence of added water results in only a 37% yield. Clearly, the reaction rates are slow in the absence of water. The addition of only 2.5 vol% water increases the yield and accompanying rate of reaction quite dramatically. A further increase in the amount of water marginally affected the product yield. It is important to note that the reactions containing 0-5% water exhibited solid-liquid heterogeneity (one liquid phase); the reactions with 30% water exhibited liquid-liquid heterogeneity. These experiments suggest that the phase behavior differences are not major contributors to the yield and rate differences. A minimum amount of water is all that is necessary for high yields and reaction rates. It should be emphasized that this conclusion is specific for the substrates and reaction conditions employed in this study.

2.4.1.2 Base Screening for Suzuki Coupling Reactions that will employ CO₂

Even though inorganic bases are dominant in Suzuki protocols, organic bases have also been shown to be effective. It has also been reported that a homogeneous Suzuki coupling can be possible using an organic base. Since one of the important goals of this research is to determine the effects of CO₂ in Suzuki coupling reactions on substrates containing basic nitrogen centers, experiments employing organic instead of inorganic bases under homogeneous conditions are important benchmarks. It is well-known that tertiary amines do effectively coordinate with CO₂. Therefore, organic bases would be free to participate in the catalytic Suzuki cycle. In this particular series of experiments, the initial screening was performed with 2-phenyl-1,3,2-dioxaboralane

(phenylboronic ester), 5 mole percent Pd(PPh₃)₄, and three equivalents of base in the presence of 2.5% water in tetrahydrofuran for twenty-four hours at 50°C (Scheme 38). The water was used in the reaction to enhance the rate, and a phenylboronic ester was used to ensure its solubility in the THF-water solvent system. When organic bases were used the reaction mixture was homogeneous, but when an inorganic base was employed the reactions exhibited solid-liquid heterogeneity. The organic bases employed were 1,8-diazabicycloundec-7-ene (DBU), triethylamine (TEA), diisopropylethylamine (DIPEA), pyridine, and tetramethylguanidine (TMG). Table 9 summarizes the results.



Scheme 38. Suzuki coupling reaction use in organic base screening

Less than 10% product was formed in the reactions employing DBU, pyridine, and TMG. However, the reaction using TEA produced a $75 \pm 9\%$ yield of 4-methylbiphenyl. It was determined that the use of DBU, pyridine, or TMG was inhibiting the reaction—one hypothesis being catalyst deactivation via a non-productive coordination of the Pd catalyst with the organic base. Therefore, three equivalents of K₂CO₃ were used in conjunction with three equivalents of TEA or DBU. The reactions employing K₂CO₃ were run for four to four and one half hours since it had previously

been established that this time was sufficient for full conversion with K_2CO_3 alone (see section 2.4.1.1). It was found that the combination of TEA and K_2CO_3 produced a high yield, $88 \pm 12\%$, which was similar to the reaction with TEA alone ($75 \pm 9\%$) but slightly lower than the use of K_2CO_3 alone ($99 \pm 1\%$). In contrast, the combined use of DBU and K_2CO_3 produced 4-methylbiphenyl in a very low yield, 1-2%, similar to the case where DBU was used alone. Clearly DBU is inhibiting the reaction. The yields accompanying the use of diisopropylethylamine, pyridine, and tetramethylguanidine was negligible—results similar to DBU. It was concluded that under the conditions employed in Table 9 organic bases can be detrimental to the Suzuki coupling of 4-bromotoluene with phenylboronic ester. Triethylamine proved to be the only exception.

Table 9. Performance of organic bases compared to K_2CO_3

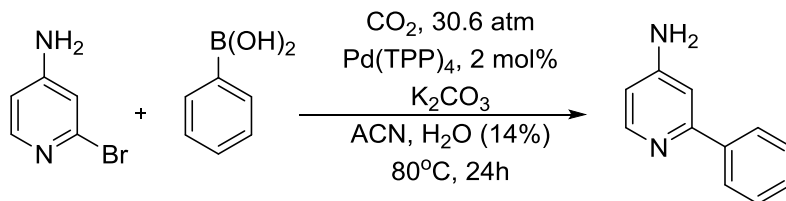
Base	Reaction Time (h)	Yield HPLC, (%)
K_2CO_3	4	99 ± 1
DBU	24	2
DBU/ K_2CO_3	4.5	1
TEA	24	75 ± 9
TEA/ K_2CO_3	4	88 ± 12
DIPEA	24	2
Pyridine	24	7 ± 1
TMG	24	4 ± 1

2.4.2 Suzuki Couplings of Substrates Containing Basic Nitrogens

The application of CO₂ as a protecting/activating species in Suzuki couplings was first investigated with 4-amino-2-bromopyridine and 4-amino-2-chloropyridine. The comparison of these two substrates is important since it is well-known that bromo arenes are inherently more reactive than their chloro counterparts. Both substrates were subjected to Suzuki coupling conditions in the absence and in the presence of CO₂.

2.4.2.1 Suzuki Couplings under 30.6 atmospheres of CO₂ Pressure

Initial experiments employing CO₂ investigated the coupling of 4-amino-2-bromopyridine with phenylboronic acid in the presence of two mole percent Pd(TPP)₃₄ and two equivalents of potassium carbonate under a constant pressure of 30.6 atm of CO₂ for twenty-four hours at 80°C (Scheme 39).¹⁰⁸ The reaction was performed in acetonitrile containing fourteen percent water. This amount of water represents the minimum quantity of water needed to ensure that no solid phase was present in the initial reaction system; the resulting system displayed only liquid-liquid heterogeneity.



Scheme 39. Suzuki coupling of 4-amino-2-bromopyridine under 30.6 atm CO₂

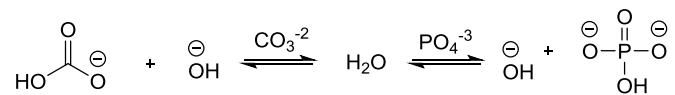
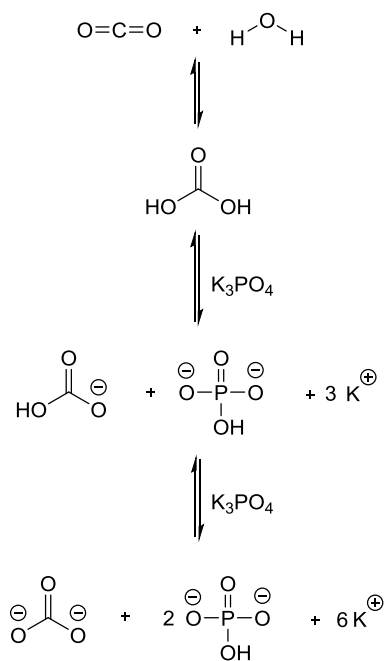
The results from these experiments were compared to the analogous coupling conducted under one atmosphere of nitrogen. The results are shown in Table 10. Significantly lower yields of 4-amino-2-phenylpyridine were obtained in the presence of 30.6 atm of CO₂ compared to 1 atmosphere of N₂.

Table 10. Suzuki coupling under 30.6 atm CO₂ in acetonitrile water at 80°C for 24h

Entry	Atmosphere	Yield (%, HPLC)
1	N ₂ , 1 atm	42±1
2	CO ₂ , 30.6 atm	5±1

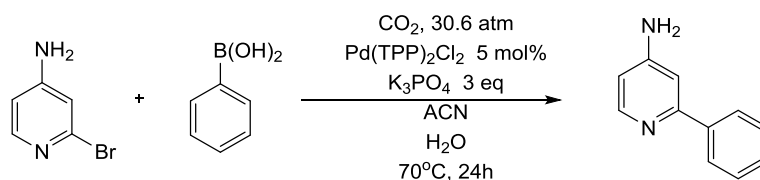
The lower yields in the reactions with CO₂ were attributed to two factors. First, the addition of CO₂ to the acetonitrile-water system led to the formation of large quantities of bicarbonate which is not as strong a base as carbonate and a far less reactive base in Suzuki coupling reactions compared to carbonate. Secondly, the overall hydroxide ion concentration was substantially reduced. The formation of large quantities of bicarbonate resulted in the consumption of water and an accompanying formation of large quantities of solid. The initial liquid-liquid reaction system became a liquid-liquid-solid system. Overall, the phase behavior became more complex, and it was difficult at best to determine the phase location of the reagents necessary for the coupling process. Since the addition of CO₂ decreased the basicity of the reaction medium and since the accompanying acid-base reactions of CO₂ also decreased the amount of water in the

system, it appeared necessary to employ a stronger base and a greater quantity of water in order to facilitate the desired coupling reaction. As mentioned in section 2.4.1.1, water is critical to the promotion of reasonable rates of reaction because it serves as a solvent for the inorganic base and as a source of hydroxide for the transmetallation step. The literature contains several examples of potassium phosphate as an effective base for promoting Suzuki coupling reactions. Its conjugate acid, K_2HPO_4 , is two orders of magnitude more basic than bicarbonate— pK_a 's 12.3 and 10.3, respectively. As a consequence, potassium phosphate was used as the inorganic base for this particular Suzuki coupling reaction. It is important to point out that, in the presence of CO_2 , the resulting base system will be quite complex. An equilibrium mixture comprised of tribasic phosphate, dibasic phosphate, bicarbonate, carbonate, water, and hydroxide (Scheme 40) will be present. In addition, the concentration of each of the bases in this complex mixture will be a function of CO_2 pressure.



Scheme 40. Potassium phosphate-carbonic acid equilibrium

In order to maximize the yield and increase the rate of reaction in the formation of 4-amino-2-phenylpyridine, and to enable a better appreciation for the effect of CO₂, five mole percent of Pd(PPh₃)₂Cl₂ was used in place of two mole percent of palladium tetrakis. The coupling of 4-amino-2-bromopyridine with phenylboronic acid under 30.6 atm of CO₂ was evaluated as a function of time and volume percent of water. The quantity of water investigated was 2.5 vol% and 25 vol% (Scheme 41). The progress of the reaction was quantitatively monitored by GC/MS. Figure 73 graphically summarizes the results.



Scheme 41. Suzuki coupling of 4-amino-2-phenylpyridine using K₃PO₄

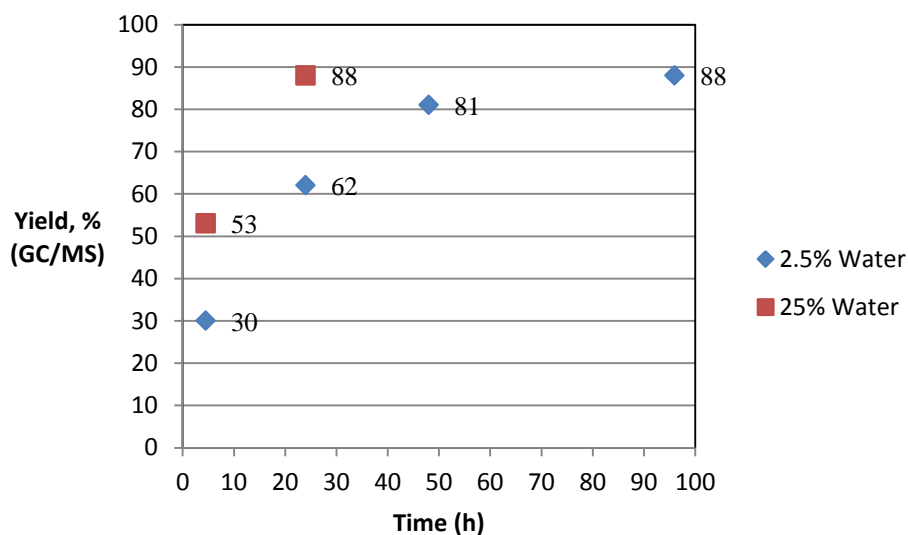


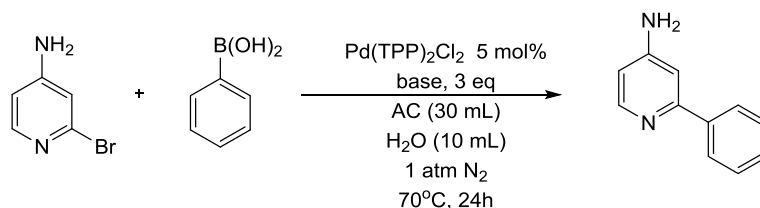
Figure 73. Yield of 4-amino-2-phenylpyridine as a function of time and % water

The reaction with 25% water displayed liquid-liquid heterogeneity; whereas, the reaction using 2.5% water displayed solid-liquid heterogeneity. As can be seen in Figure 72, the reaction proceeds much faster with 25% water than with 2.5% water. Both reactions achieved an 88% yield of product; however, it took the reaction with 2.5% water four times as long. This observation is consistent with trends observed in the water effect study reported in section 2.4.1.1. More importantly, these reactions demonstrate that K_3PO_4 is a highly effective base for Suzuki coupling reactions in the presence of CO_2 and water.

2.4.2.2 Evaluating mono-, di-, and tribasic potassium phosphates

Potassium phosphate was identified as the best base for the Suzuki coupling of 4-amino-2-bromopyridine with phenylboronic acid in the presence of CO_2 under pressure.

Because of the complex mixture of bases present in the reaction system, it was instructive to evaluate the three basic forms of the phosphate system independently and in the absence of CO₂. This would provide valuable information concerning the effectiveness of each of these bases in the Suzuki coupling reaction. Thus, the potassium salts of phosphate (PO₄⁻³), monohydrogen phosphate (HPO₄⁻²), and dihydrogen phosphate (H₂PO₄⁻¹) were evaluated in the coupling of 4-amino-2-bromopyridine with phenylboronic acid under one atmosphere of nitrogen at 70°C in the presence of 5 mol% Pd(TPP)₂Cl₂ in acetonitrile-water (75/25) for twenty-four hours (Scheme 42). The results are summarized in Table 11.



Scheme 42. Suzuki coupling of 4-amino-2-bromopyridine with phenylboronic acid

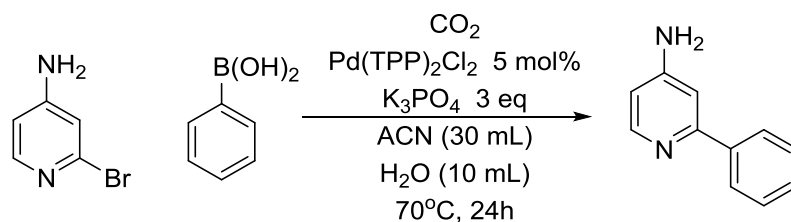
Table 11. Effect of potassium phosphate bases on product yield under 1 atm N₂

Entry	Base	Yield,% (GC/MS)
1	K ₃ PO ₄	29
2	K ₂ HPO ₄	37
3	KH ₂ PO ₄	2

The results clearly show that potassium dihydrogen phosphate was not a good base for the coupling reaction; only a 2% yield was realized in twenty-four hours. Potassium hydrogenphosphate and potassium phosphate both proved to be more effective bases resulting in yields of 29% and 37%, respectively. These results provided valuable insights into the possible effectiveness of potassium phosphate in the presence of CO₂. The addition of CO₂ decreases the basicity of the system resulting in the formation of monohydrogen phosphate which, as indicated in Table 11, is an effective base for this specific Suzuki coupling reaction. It should be emphasized that the use of CO₂ with potassium phosphate not only produces monohydrogen phosphate but also carbonate and bicarbonate. The above experiments merely illustrate that both phosphate and monohydrogen phosphate are catalytic bases. In reality, it could be that it is the complex mixture which represents the effective base system for the successful Suzuki coupling reaction.

2.4.2.3 Suzuki couplings with 4-amino-2-bromopyridine as a function P_{CO2}

The effect of CO₂ pressure on the yield of 4-amino-2-phenylpyridine from 4-amino-2-bromopyridine was investigated. Three pressures were evaluated: 30.6 atm, 17 atm, and 6.8 atm; and compared to a control reaction under 1 atm of N₂. The reaction conditions were as follows: 25% water in acetonitrile, 5 mol% Pd(TPP)₂Cl₂ and three equivalents of base (K₃PO₄) at 70°C for twenty-four hours (Scheme 43).



Scheme 43. Suzuki couplings as a function of CO_2 pressure

Figure 74 clearly shows that as the pressure of CO_2 increased an increase in isolated yield was observed.

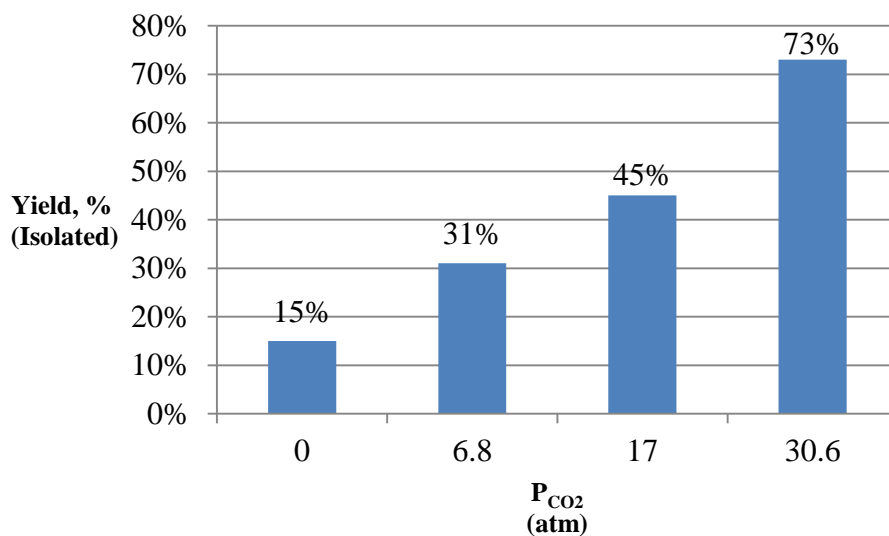


Figure 74. Suzuki coupling of 4-amino-2-phenylpyridine as a function of P_{CO_2}

In the absence of CO_2 , the isolated yield of the coupled product was only 15%. As the pressure increased from 6.8 atm to 30.6 atm the isolated yield continually increased from

31% to 45% to 73%, respectively. Therefore, it has been concluded that the presence of CO₂ does enhance the production of 4-amino-2-phenylpyridine under the conditions outlined, and the increase in yield is significant at 30.6 atm.

2.4.2.4 Suzuki couplings with 4-amino-2-chloropyridine at 30.6 atm CO₂

It is well-known that chloro substrates are much less reactive than the corresponding bromo substrates in Suzuki coupling reactions. As a consequence, 4-amino-2-chloropyridine was reacted with phenylboronic acid under 30.6 atm of CO₂ under the same reaction conditions as those corresponding to the bromide counterpart (Table 12).

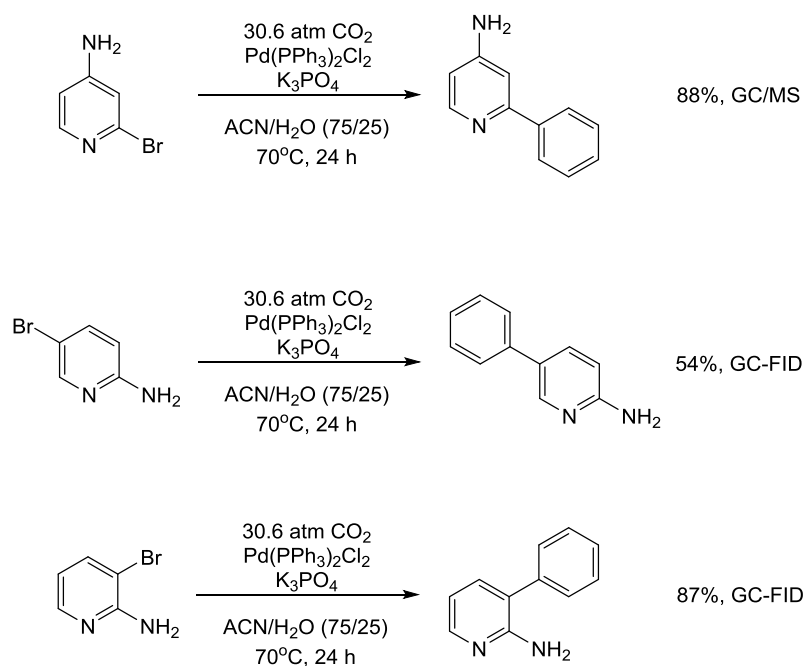
Table 12. Effect of CO₂ on the coupling of 4-amino-2-chloropyridine with phenylboronic acid

<u>Atmosphere</u>	<u>Yield,% (GC/MS)</u>
1 atm N ₂	34
30.6 atm CO ₂	58

The yield of 4-amino-2-phenylpyridine increased from 34% to 58% under 30.6 atm of CO₂. The increase is substantially less than that observed from the reaction using 4-amino-2-bromopyridine, 58%, as the starting substrate. Interestingly, the initial control experiment using 1 atm N₂ for the coupling from 4-amino-2-chloropyridine afforded twice the yield as compared to 4-amino-2-bromopyridine, 34% compared to 15%.

2.4.2.6 Effect of amino-bromopyridine ring substitution pattern on yield

While the 4-amino-2-bromopyridine produced interesting results with respect to the yield of the Suzuki coupling product as a function of CO₂ pressure, it was of interest to determine if the substitution pattern on the pyridine ring influenced the product yield. Thus, yields from three isomeric amino-bromopyridines were compared. Suzuki couplings employing 2-amino-3-bromopyridine and 2-amino-5-bromopyridine with phenylboronic acid under 30.6 atm of CO₂ were compared to the results of the previously discussed coupling of 4-amino-2-bromopyridine with 5 mol% Pd(TPP)₂Cl₂ and three equivalents of K₃PO₄ at 70°C for twenty-four hours (Scheme 44).

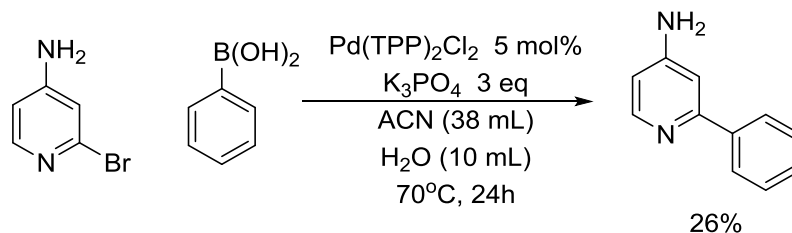


Scheme 44. Effect of substitution pattern about amino-bromopyridines

The 2-amino-3-bromopyridine and the 4-amino-2-bromopyridine substrates each produced excellent yields of coupled product, 87% and 88%, respectively. However, the coupling with 2-amino-5-bromopyridine resulted in a much lower yield, 54%. At this juncture it is not clear as to why there is this rather dramatic difference in product yield. In all three substrates, the amino group and pyridine nitrogen are conjugated. Two of the substrates have the nitrogens in an *ortho* relationship, but the yields were very different. No simple steric or electronic rationalizations are evident at this juncture. These three examples highlight the complex relationship between the substrate structure and accompanying reactivity.

2.4.2.7 Role of CO₂ in Suzuki coupling: Volume Expansion and Dielectric Constant

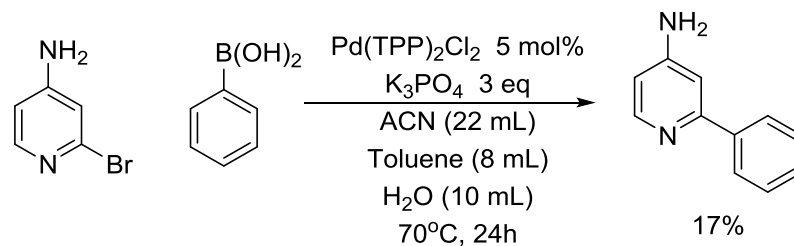
The addition of carbon dioxide to the Suzuki reaction medium has two major effects on the system: the reaction volume is increased and the dielectric constant (ϵ) of the reaction medium decreases. The volume expansion and dielectric constant of the system are a function of the mole fraction (e.g. pressure) of CO₂ in the gas expanded liquid. To decouple these general effects from specific CO₂ interaction, we designed two control experiments to mimic each of these effects. The first experiment evaluated the dilution effect caused by the dissolved CO₂. At 30.6 atm of CO₂, the CO₂-expanded acetonitrile phase was calculated to be an additional eight milliliters more than the acetonitrile with no CO₂. This corresponded to a volume expansion of $\approx 27\%$ with respect to the acetonitrile (20% with respect to acetonitrile and water) and a change in overall concentration of 0.40M to 0.33M with respect to the aminopyridine (Scheme 45).



Scheme 45. Suzuki coupling volume expansion simulation

Experimentally it was found that the yield of the more dilute reaction was 26%, slightly less than the reaction under our standard conditions with no CO₂ (30%). This result indicated that the volume expansion does not play a major role in the increased yields observed at elevated pressure.

The decrease in dielectric constant was simulated by replacing some of the acetonitrile with toluene while maintaining the reaction concentration of 0.40 M. The number of moles of CO₂ in solution at 70°C and 30.6 atm was estimated to be 0.075 mole. A 0.075 molar equivalent of toluene ($\epsilon = 2.38$) was used in place of the acetonitrile. This corresponded to eight milliliters of toluene or 20% of the total amount of water and acetonitrile. Although hydrocarbons such as hexane (1.88) and pentane (1.84) have dielectric constants closer to carbon dioxide (1.0), they are each immiscible with acetonitrile. It was necessary, therefore, to use the miscible toluene instead of the preferred solvents of lower dielectric constant. With the exception of toluene, the reaction parameters were identical to those previously described (Scheme 46).



Scheme 46. Suzuki coupling, decreased dielectric constant simulation

A 17% yield was obtained which is less than the reaction of the 4-amino-2-bromopyridine in the absence of CO₂. It can be concluded that the decrease in dielectric constant appears to have a negative effect on the product yield. It was concluded that the two control experiments suggest that CO₂ or species produced by the presence of CO₂ enhance the Suzuki coupling process.

2.5 Conclusions

Control experiments first evaluated the effects of water and organic and inorganic bases on Suzuki coupling reactions containing no nitrogen centers and in the absence of CO₂ pressure. It was found that (1) the use of small amounts of water, e.g. 2.5 vol%, significantly improves the rate and yield of Suzuki coupling reactions; (2) the presence of water is critical to having an efficient Suzuki coupling reaction in reaction media that exhibit solid-liquid heterogeneity, liquid-liquid heterogeneity, or homogeneity; and (3) K₂CO₃, K₃PO₄, and TEA were the most effective bases.

The results of the application of CO₂ in Suzuki coupling reactions of 4-amino-2-bromopyridine with phenylboronic acid to form 4-amino-2-phenylpyridine are as follows: (1) The yield of 4-amino-2-phenylpyridine is lower in the presence of CO₂ than in the absence of CO₂ when K₂CO₃ is employed as the base probably due to the formation of bicarbonate and the accompanying decrease in the amount of hydroxide and water. Therefore, careful selection of the base is essential. (2) K₃PO₄ was found to be the most effective base in the presence of CO₂. It was emphasized that the presence of CO₂ with phosphate produces a complex mixture of bases which may be responsible for the observed positive effects. (3) The yield of product in the Suzuki coupling of 4-amino-2-bromopyridine with phenylboronic acid was evaluated as a function of CO₂ pressure. Compared to reactions in the absence of CO₂, the yield of product increased at all pressures of CO₂ (6.8, 17, and 30.6 atm)—from 15% with no CO₂ to 73% with 30.6 atm of CO₂. (4) The changes in the reaction volume and the reaction medium's dielectric constant imparted by CO₂ were independently evaluated and were determined not to be responsible for the observed yield increases. Even though the concept of CO₂ protection/activation is demonstrated on Suzuki coupling reactions this principle could also be applicable to other reactions as well (e.g. Heck cross couplings, selective Buchwald-Hartwig cross couplings, condensation reactions, or Michael additions).

2.6 Recommendations

The rates and yields in Suzuki coupling reactions are substrate dependent and sensitive to changes in reaction parameters such as base, palladium source, ligand, solvent(s), temperature, and concentration. Therefore, it is very important to systematically evaluate these parameters as a function of substrate and pressure of CO₂. Future experiments should address the following: (1) establish the substrate scope by investigating pyridines, anilines, and aminopyridines; (2) establish the range of effective CO₂ pressures for the various substrates; and (3) identify and understand the origins of the effects of CO₂. In particular, spectroscopic studies (e.g. NMR, IR, and UV-VIS) investigating the interaction of CO₂ with pyridines, anilines, and aminopyridines as a function of CO₂ pressure may provide insight as to the role of CO₂. It will also be very important to compare the effectiveness of CO₂ in classical amine protection strategies such as *tert*-butylcarbamate (*N*-Boc), acetamide (*N*-Ac), or as a phenylimine.

As pointed out in the main body of this thesis, the presence of CO₂ creates a complex mixture of basic species in the reaction system. It would be advantageous to investigate synthetic mixtures of these bases to determine if it is a synergy of these base combinations that is responsible for the effects observed with CO₂. Additionally, other bases should be evaluated as well. Two specific bases would be potassium fluoride and potassium citrate. The pK_a of carbonic is 6.4, and the pK_a of hydrogen fluoride 3.2; therefore, one would expect little bicarbonate formation from the deprotonation of carbonic acid by fluoride. Thus, the use of fluoride could significantly alter the equilibrium species present in the reaction. Potassium citrate would be an interesting

base to evaluate because it is tribasic like potassium phosphate. The pK_a 's of the citrates are 3.1, 4.8, and 6.4; the pK_a 's of the phosphates are 2.12, 7.21, and 12.32.

2.7 Experimental

2.7.1 General Information

All reagents were purchased from commercial sources as “reagent” grade and were used without further purification. Solvents were degassed by sparging with N_2 or Ar, or by conducting three cycles of freeze-pump-thaw. GCMS data were obtained from a HP6890 gas chromatographer and a HP5973 mass spectrometer. HPLC data were obtained from an HP1100 HPLC-UV instrument. All chromatographic data were quantified by calibration curves. Nuclear magnetic resonance spectra were measured on a 400 MHz Varian relative to $CDCl_3$, δ ppm.

2.7.1.1 Reactions with $Pd(OAc)_2$

Phenylboronic acid (1.3 g, 11 mmol), $Pd(OAc)_2$ (68 mg, 3 mol%), K_2CO_3 (2.7g, 20 mmol) were combined in a three-neck round bottom flask. The flask was purged with Ar for thirty minutes. A total of 25 mL of degassed solvent was added to the reaction flask in the appropriate ratio of THF:water. Bromobenzene (1.5g, 9.5 mmol) was added to the reaction mixture which was then heated to 50°C. After 4-24 hours, the reaction mixture was cooled and an aliquot (100 μ L) was taken for GCMS analysis. The reaction mixture was extracted with ethyl acetate (2 x 25 mL). The combined fractions were washed with

brine (2 x 15 mL), dried over MgSO₄, filtered, and concentrated *in vacuo*. The crude organic product was analyzed by ¹H and ¹³C NMR.

2.7.1.2 Reactions with Pd(PPh₃)₄.

Phenylboronic acid (1.3 g, 11 mmol), Pd(PPh₃)₄ (0.550 g, 5 mol%), K₂CO₃ (3.8g, 30 mmol), 4-bromotoluene (1.6g, 9.5 mmol) were combined in a three-neck round bottom flask. The flask was purged with N₂ for thirty minutes. A total of 25 mL of degassed solvent was added to the reaction flask in the appropriate ratio of THF:water and was then heated to 50°C. After 4-24 hours, the reaction mixture was cooled and an aliquot (100 μL) was taken for HPLC analysis. The reaction mixture was extracted with ethyl acetate (2 x 25 mL). The combined fractions were washed with brine (2 x 15 mL), dried over MgSO₄, filtered, and concentrated *in vacuo*. The crude organic product was analyzed by ¹H and ¹³C NMR.

2.7.1.3 General procedure for Suzuki reactions in a Parr reactor

Phenylboronic acid (2.1 g, 17 mmol), catalyst Pd(PPh₃)₄ (0.37g, 2 mol%) or Pd(PPh₃)₂Cl₂, haloarene (2.7g, 14 mmol), and base were combined in the Parr reactor. The vessel was then sealed and purged with N₂ or CO₂ for thirty minutes. Degassed acetonitrile was added to the vessel which was then heated to 50°C or 70°C. After 24 hours, the reaction mixture was cooled and an aliquot (100 μL) was taken for GC-FID or GC/MS analysis. The remaining reaction mixture was extracted with ethyl acetate (2 x 25 mL). The organic fraction was washed with brine (2 x 15 mL), dried over MgSO₄,

filtered, and concentrated *in vacuo*. The crude organic product was analyzed by ^1H and ^{13}C NMR.

2.7.1.5 Calibration Curves of Starting Materials and Products

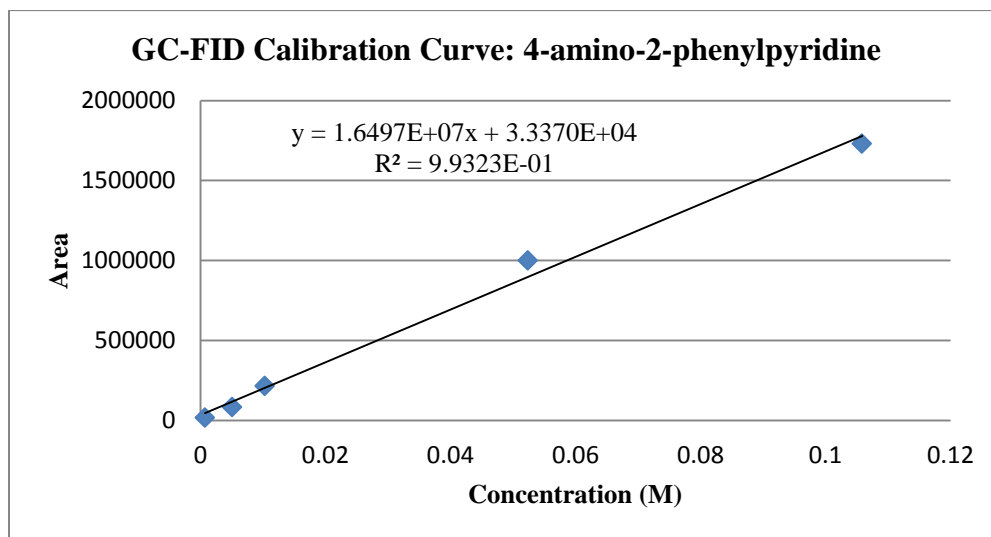


Figure 75. GC-FID Calibration Curve: 4-amino-2-phenylpyridine

GC-FID Calibration Curve: 4-amino-2-bromopyridine

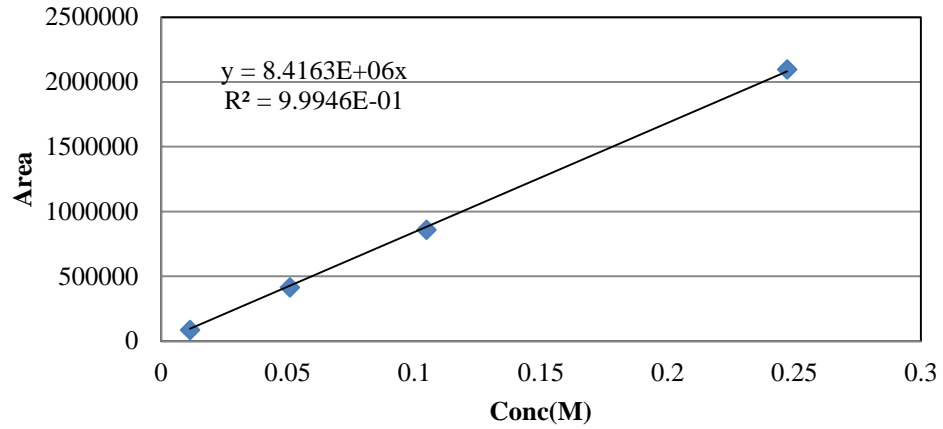


Figure 76. GC-FID Calibration Curve: 4-amino-2-bromopyridine

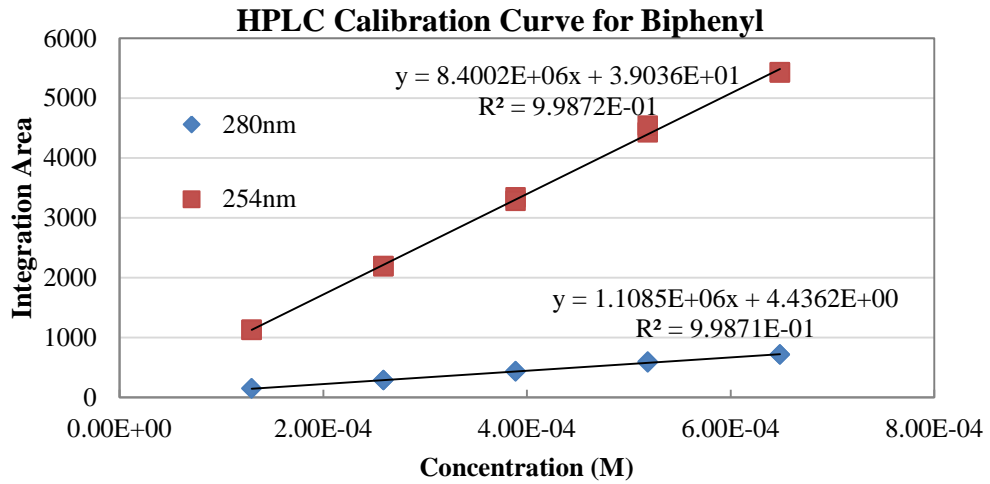


Figure 77. HPLC Calibration Curve: Biphenyl

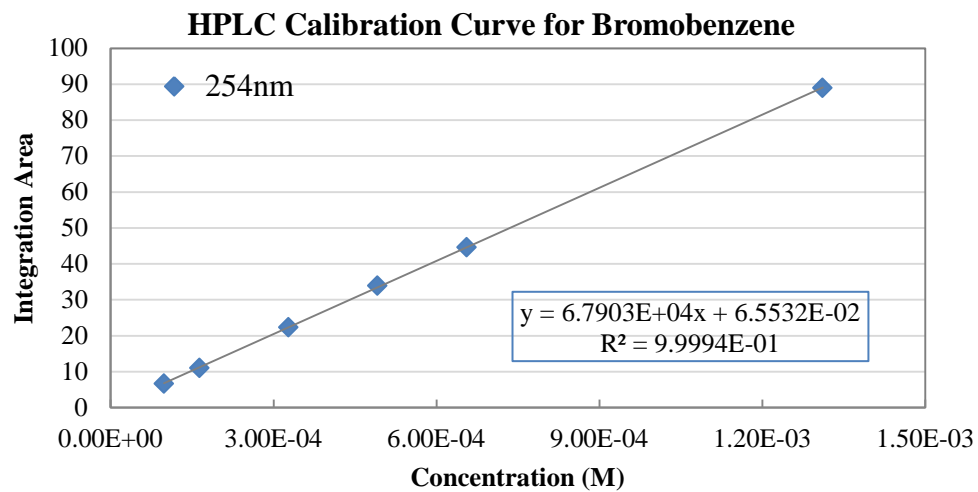


Figure 78. HPLC Calibration Curve: Bromobenzene

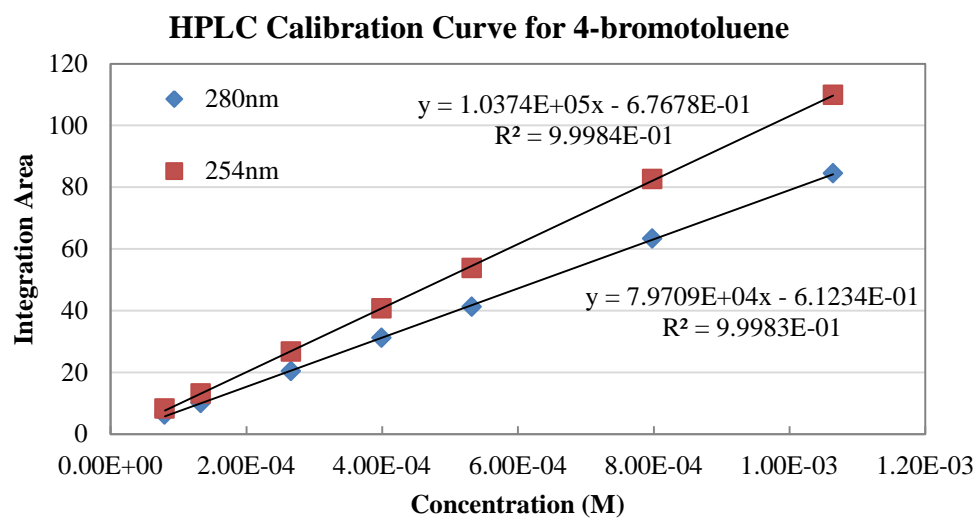


Figure 79. HPLC Calibration Curve: 4-Bromotoluene

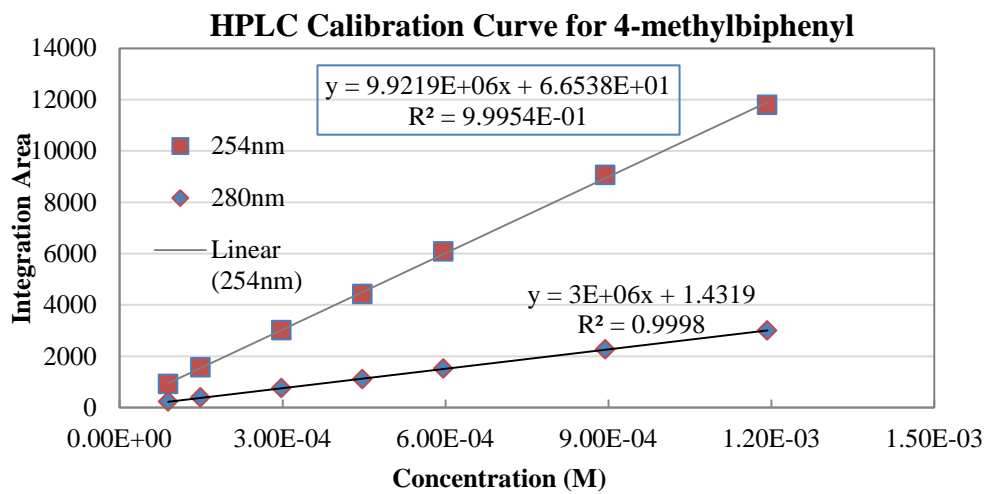


Figure 80. HPLC Calibration Curve: 4-Methylbiphenyl

Chapter 3

3.1 Ligand free Suzuki coupling reactions in aqueous systems

3.1.1 Introduction and motivation

Given the importance and widespread use of the Suzuki coupling, there has been an increased interest in developing sustainable and/or *green* protocols. For the most part, these efforts have focused on replacing phosphine derived ligands with nitrogen ligands,¹⁰⁹⁻¹¹¹ eliminating the use of any ligand,^{88,98,112,113} and/or using water as the only or dominant solvent.^{88,97,101,114} Nevertheless, some of these methods require the use of phase transfer catalysts, surfactants, ligands, and/or microwaves. Many of these approaches are not scalable in chemical manufacturing. Leadbeater et al. have published several reports of ligand free couplings using microwave heating with or without a phase transfer catalyst in water.^{85,87-89,96-100,109,112,115-118} In light of these reports it was of interest to explore aqueous Suzuki couplings as a function of organic solvent content in the absence of a ligand. Our investigation focused in two areas. First we investigated aqueous Suzuki couplings containing basic nitrogen centers. Second, we evaluated the yield of product as a function of percent organic solvent. In both cases the results were compared to substrates not containing nitrogen functionalities.

3.1.2 Ligand free Suzuki couplings in water

A variety of bromo- and chloroarenes were subjected to Suzuki coupling conditions with phenyl boronic acid in water and in the absence of a ligand. The substrates employed in this study are shown in Figure 81. Substrates with and without basic nitrogen centers were included; it was of interest to compare these results with those involving CO₂.

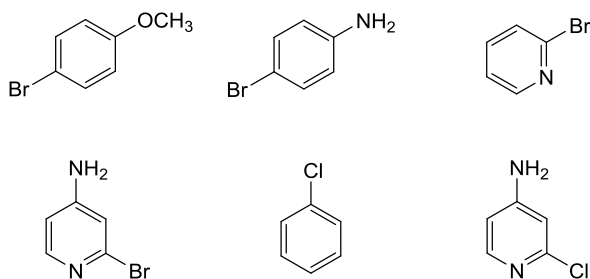
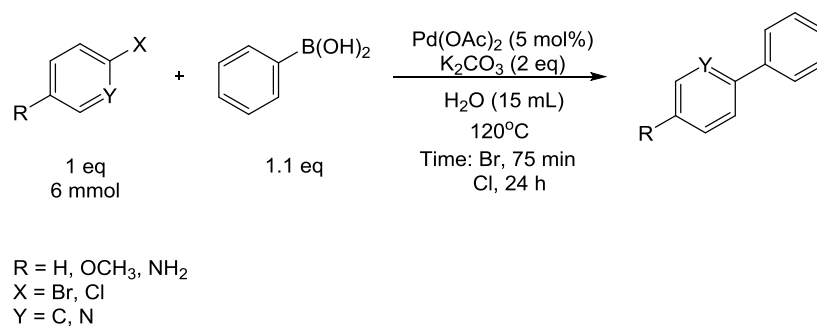


Figure 81. Substrates employed in ligand free Suzuki couplings in water

The preliminary reactions were conducted at 120°C with five mole percent Pd(OAc)₂ and two equivalents of K₂CO₃ in 15 mL of water (Scheme 47). The bromo- substrates were heated for seventy-five minutes and the chloro- substrates for twenty-four hours. The reactions were conducted in AceGlass pressure tubes which were sealed by a Teflon® screw cap, and submerged into a preheated silicone oil bath. The haloarene,

phenylboronic acid, K_2CO_3 (2 eq), and $\text{Pd}(\text{OAc})_2$ (5 mol%) were combined in an AceGlass pressure tube and submerged into a preheated silicone oil bath at 120°C .



Scheme 47. Ligand free Suzuki couplings in water

The appearance of these reactions varied greatly, but they were all heterogeneous. Table 14 summarizes the yield, determined from quantitative HPLC, as well as the phase behavior and colors observed. Palladium black formation was observed in all of the reactions, and all of products of reaction were accompanied by 5-10% homocoupling of the phenyl boronic acid as evidenced by biphenyl in the ^1H NMR.

Table 13. Yield and appearance of aqueous, ligand free Suzuki couplings

Entry	Haloarene	Appearance of liquid(s)	Appearance of solids <i>other than Pd-black</i>	% Yield
1	4-bromoanisole	Beige	Grey/white	94%,
2	4-bromoaniline	White, opaque	Brown	86%
3	4-amino-2-chloropyridine	Beige	Yellow, grey, brown	33%
4	chlorobenzene	Colorless	none	37%
5	2-bromopyridine	Yellow	none	90%
6	4-amino-2-bromopyridine	Yellow-orange	Orange, grey, brown	60%

The reaction of 4-bromoanisole with phenylboronic acid produced a 94% yield of 4-methoxybiphenyl. The formation of grey-white solids was observed in this reaction. 4-Bromoanisole is a liquid; however, the product of the reaction, 4-methoxybiphenyl, is a solid. The grey-white solids were analyzed by ^1H NMR and were found to be predominantly product with traces of starting material. The origin of the grey color was believed to be derived from finely dispersed palladium-black within the white solids. All of the other bromo- substrates also exhibited excellent yields within 75 minutes with the exception of 4-amino-2-bromopyridine which yielded 60% of the desired 4-amino-2-phenylpyridine product. Both chloro- substrates (chlorobenzene and 4-amino-2-chloropyridine) gave poor yields of their desired biaryl products even though they were allowed to react over a 24 hour time period. Chlorobenzene yielded 37% of the biphenyl product after 24 hours; it is conjectured that some of this product was probably a result of homocoupling of the phenylboronic acid. 4-amino-2-chloropyridine yielded 33% of 4-amino-2-phenylpyridine—also a rather poor yield. The reaction with 4-amino-2-chloropyridine had significant amounts of light yellow, grey, and brown particles. The reaction had the appearance of finely dispersed beach sand. In general, it can be

concluded that the bromo substrates provided Suzuki coupled products in good to excellent yields in reasonably short reaction times without the need for a ligand.

3.1.2.1 Temperature optimization

The effect of temperature on the efficiency of the Suzuki coupling of 2-bromopyridine with phenylboronic acid was investigated. The results are shown in Table 15. The yield of 2-phenylpyridine marginally decreased from 90% to 85% when the temperature was lowered from 120°C to 100°C over a 75 minute time period. Reduction of the temperature to 60°C required longer reaction times but still produced product in excellent yields. Even reaction at room temperature produced a reasonable yield within 24 hours. In this case, however, the phenylboronic acid was only sparingly soluble in the aqueous medium.

Table 14. Temperature optimization, isolated yields by column chromatography

Substrate	Temp. (°C)	Pd(OAc) ₂ (mol %)	% Yield isolated	time
2-bromopyridine	120	4.1	90	75 m
2-bromopyridine	100	5	85	75 m
2-bromopyridine	60	5.1	83	24 h
2-bromopyridine	25	4.9	48	24 h

There was a significant amount of this white solid throughout this reaction. The successful coupling of 2-bromopyridine with phenylboronic acid in water at elevated

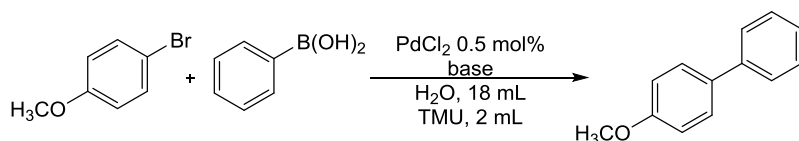
temperatures and in the absence of a ligand suggests that strong solvation by water of a substrate containing a basic nitrogen center adequately competes with the Pd catalyst-substrate interactions to provide good to excellent yields.

3.1.3 Ligand free Suzuki couplings in water:co-solvent systems

While water alone showed some promise as a medium for ligand-free Suzuki coupling reactions, it was of interest to investigate the effects of organic co-solvents in promoting the reaction at temperatures substantially lower than 100°C within a reasonable period of time. Three co-solvents were selected for this investigation: isopropyl alcohol (*i*PrOH), dimethylformamide (DMF), and tetramethylurea (TMU). Isopropyl alcohol was selected as the protic co-solvent candidate. Dimethyl formamide and tetramethylurea were selected as the polar-aprotic co-solvents.

3.1.3.1 Ligand free Suzuki coupling of 4-bromoanisole with phenylboronic acid with tetramethylurea (TMU) co-solvent

The coupling of 4-bromoanisole and phenylboronic acid in 10% TMU, 90% H₂O in the presence of 0.5 mol % PdCl₂ was evaluated using K₂CO₃, K₃PO₄, or KF as the base over a one hour time period (Scheme 48). The yields of were determined by the ¹H NMR ratio of the methoxy signals in the product and starting material.



Scheme 48. Suzuki coupling of 4-bromoanisole in water:TMU

The PdCl₂ was stirred in 2.0 mL of tetramethylurea for fifteen minutes, and a fine suspension was observed. After adding the water (18 mL) only one phase was visible. The 4-bromoanisole, phenylboronic acid, and base were added to the solution of catalyst. The reaction mixture was initially heterogeneous, but after ten minutes the reaction system became homogeneous. The first experiments, performed at ambient temperature with K₂CO₃ and K₃PO₄, only yielded 15% and 11% product (Table 16).

Table 15. Base screening in water:TMU Suzuki coupling with 4-bromoanisole

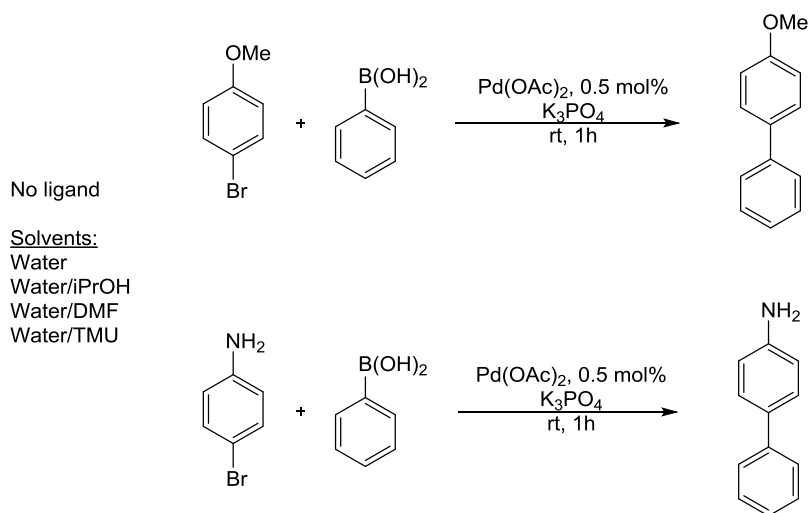
Temperature	Base	Time	% Yield
rt	K ₂ CO ₃	1 h	15%
rt	K ₃ PO ₄	1 h	11%
50°C	K ₃ PO ₄	1 h	68%
50°C	KF	24 h	22%
rt	K ₃ PO ₄	1h	30%* *(PdOAc) ₂

When the temperature was increased to 50°C, the yield increased to 68% when K₃PO₄ was employed. The reaction with KF was allowed to run for twenty-four hours; however, only 22% of 4-methoxybiphenyl was formed. When Pd(OAc)₂ was used in a reaction employing K₃PO₄ at room temperature, a 30% yield was achieved—nearly triple

the yield when PdCl₂ and K₃PO₄ were used at room temperature. Thus, Pd(OAc)₂ and K₃PO₄ were selected as the catalyst and base in the following investigation dealing with the effects of co-solvent on the ligand-free Suzuki coupling reaction.

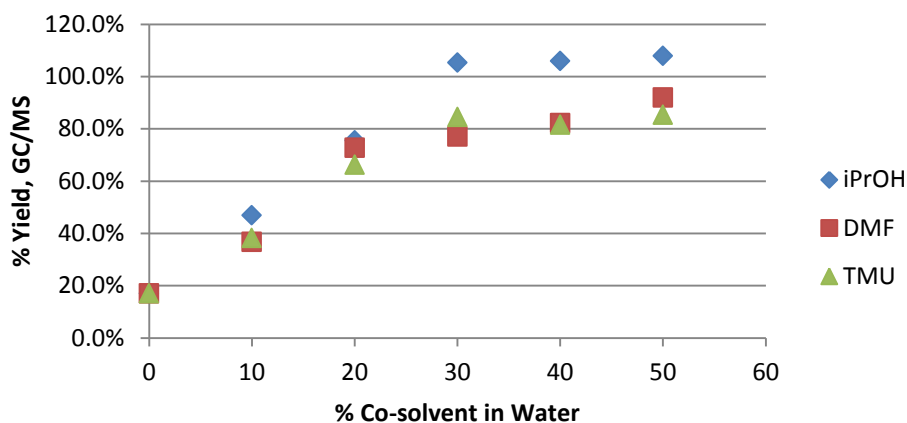
3.1.3.2 Evaluation of the effects of co-solvents and co-solvent ratios on ligand-free Suzuki coupling reactions in aqueous systems

*i*PrOH, DMF, and TMU were evaluated as co-solvents for the Suzuki coupling reaction of 4-bromoanisole and 4-bromoaniline with phenylboronic acid. The amounts of co-solvent were varied from 0%-50% (v/v) in 10% increments. The reactions were performed using 0.5 mole % Pd(OAc)₂ and two equivalents of K₃PO₄ at room temperature, in a total of 15 mL of solvent for a period of one hour (Scheme 49).



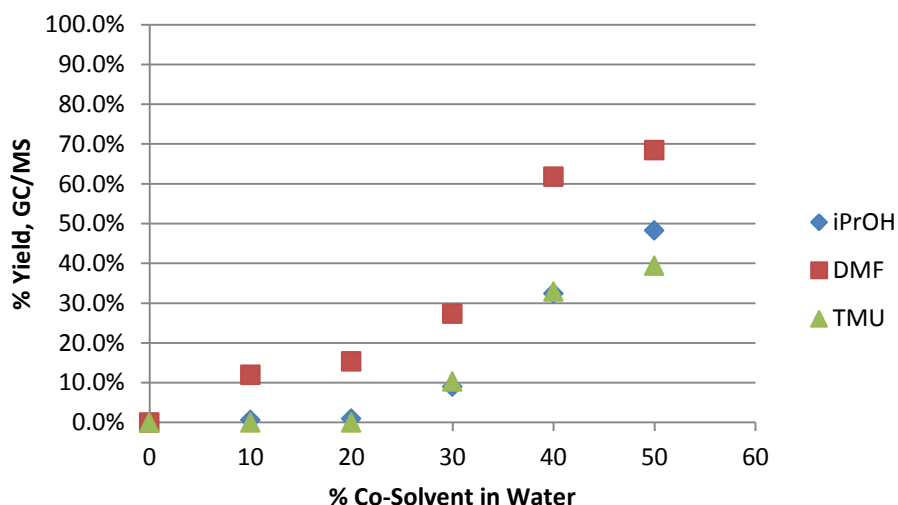
Scheme 49. Suzuki couplings as a function of co-solvent

Table 16. Yield of 4-methoxybiphenyl as a function of co-solvent, average of 2 trials



The effect of the amount of co-solvent in the reaction of 4-bromoanisole with phenylboronic acid is graphically displayed in Table 16. In the absence of a co-solvent, a 17% yield was obtained; whereas near quantitative yields were obtained with fifty percent co-solvent. Clearly, iso-propyl alcohol produced the best results. In contrast to the results for 4-bromoanisole, 4-bromoaniline shows a substantially different behavior with accompanying reduced yields. The results are graphically displayed in Table 17. In this particular series of reactions, DMF proved to be the superior co-solvent. No product was detected from reactions using 10% *i*PrOH or 10% TMU; whereas, 12% product was formed in DMF. The differences in yield between *i*PrOH or TMU compared to DMF increased from 12% to 28% to 38%, respectively, as the percent co-solvent was increased to 50%. Comparing 4-bromoanisole to 4-bromoaniline it was found that 4-bromoanisole reactions led to high product formation at each interval of co-solvent ratio. This indicates that under these conditions 4-bromoaniline is a less reactive substrate than 4-bromoanisole perhaps due to competitive coordination of the amine functionality with the Pd catalyst.

Table 17. Yield of 4-aminobiphenyl as a function of co-solvent



3.1.4 Conclusions and Recommendations

The preliminary results of ligand free, aqueous Suzuki couplings with basic nitrogen containing arenes indicate that the efficacy of this protocol is substrate dependent. Chlorobenzene and 4-amino-2-chloropyridine both performed poorly in water at 125°C with 5% Pd(OAc)₂ yielding 37% and 33% respectively. The bromoarenes performed substantially better than the chloroarenes (4-bromoaniline, 86% yield and 2-bromopyridine, 90% yield).

The evaluation of DMF, TMU, and *i*PrOH as organic co-solvents in ligand free, room temperature Suzuki reactions of 4-bromoanisole or 4-bromoaniline with phenylboronic acid at a low catalyst loading (0.5% Pd(OAc)₂) led to the following conclusions: (1) as the volume percent of co-solvent increased the rate of reaction

increased; (2) as the volume percent of co-solvent increased the yield increased. With respect to the reactions of 4-bromoanisole these two observations were most pronounced between 0-30 vol% of co-solvent. Coupling reactions with 4-bromoaniline in DMF :H₂O produced 15-20% more product than the reactions in *i*PrOH:H₂O or TMU:H₂O. In fact, no 4-aminobiphenyl product was detected when less than 20% *i*PrOH or TMU were used.

Since the reaction mixture is heated in most Suzuki couplings, it would be valuable to investigate Suzuki couplings as functions of both percent co-solvent and temperature.

3.1.5 Experimental Procedures

3.1.5.1 Suzuki Reactions in Water

Haloarene (6 mmol), phenylboronic acid (6.6 mmol) and K₂CO₃ (12 mmol) were combined in a 3-neck round bottom flask (reactions ≤ 100°) or an ace pressure tube (reactions >100°C). HPLC grade water (15 mL) was added and the reaction mixture was while stirring. A reflux condenser was used for the reactions in round bottom flasks. After the requisite time, the reaction mixture was cooled, and the organic products were extracted with dichloromethane or ethyl acetate (1 x 15 mL). An HPLC sample was prepared from the organic fraction. An aliquot (100 uL) was taken and diluted to 5 mL with acetonitrile. An aliquot (100 uL) was taken of the new solution and further diluted to 1 mL with HPLC grade acetonitrile. This sample was analyzed by HPLC from calibration curves. The organic and aqueous phases were separated. The organic phase was dried over MgSO₄, filtered, then concentrated *in vacuo* and analyzed using ¹H and

^{13}C NMR. The crude organic was purified by silica gel column chromatography, increasing the polarity of the mobile from 100% hexanes to 80/20 hexanes:ethylacetate. The isolated yields were determined by mass.

3.1.5.2 General Procedure for Suzuki Reactions in Water, Water:TMU, Water:iPrOH, Water:DMF performed in the Carousel

These reactions were performed in a Radleys CarouselTM. Separate stock solutions of 4-bromoanisole (1.25 M) or 4-bromoaniline (1.25 M) with phenylboronic acid (1.50 M) were prepared in 12 mL of the appropriate organic solvent. If no organic solvent was being used, the substrates were weighed directly in the carousel tube. A 100-mL stock solution of K_3PO_4 (1.3 M) was prepared in HPLC grade water. $\text{Pd}(\text{OAc})_2$ (14 mg, 0.5 mol%), was weighed into each Carousel tube. A 2-mL aliquot of the base stock solution and a 1-mL aliquot of the substrates' stock solution were transferred into each tube. Depending upon the ratio of organic solvent to water being evaluated, an appropriate amount of each was then added to the reaction mixture with stirring. After one hour, 25 mL of dichloromethane were added to each reaction mixture. The aqueous layer was decanted and the volume of the organic layer was measured in a 25 ± 0.25 mL TC graduated cylinder. An aliquot of the organic fraction was taken for GC/MS analysis.

3.1.5.3 Calibration Curves

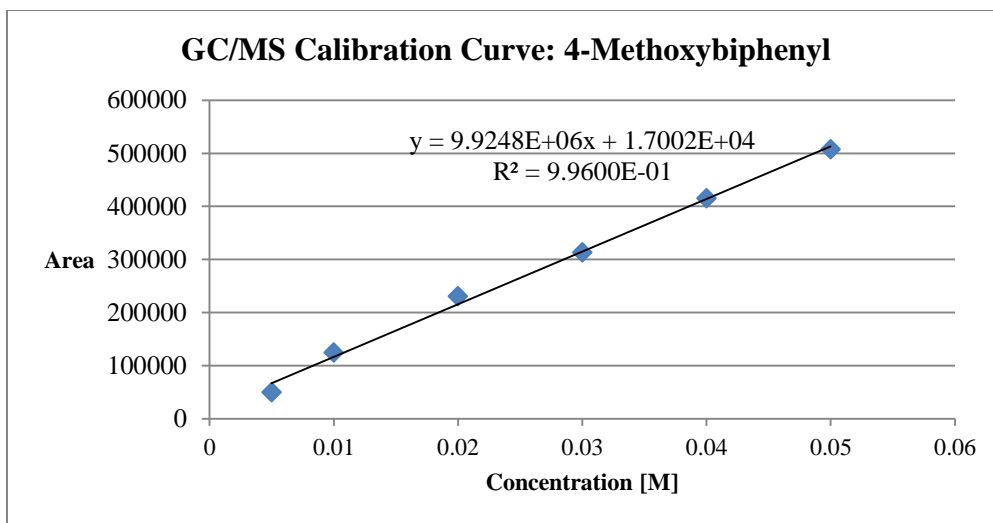


Figure 82. GC/MS Calibration Curve: 4-Methoxybiphenyl

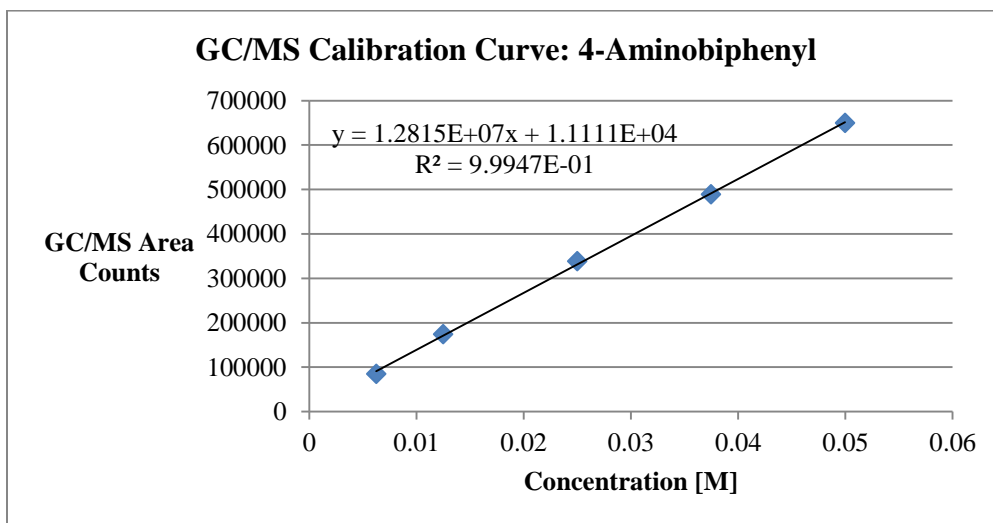


Figure 83. GC/MS Calibration Curve: 4-Aminobiphenyl

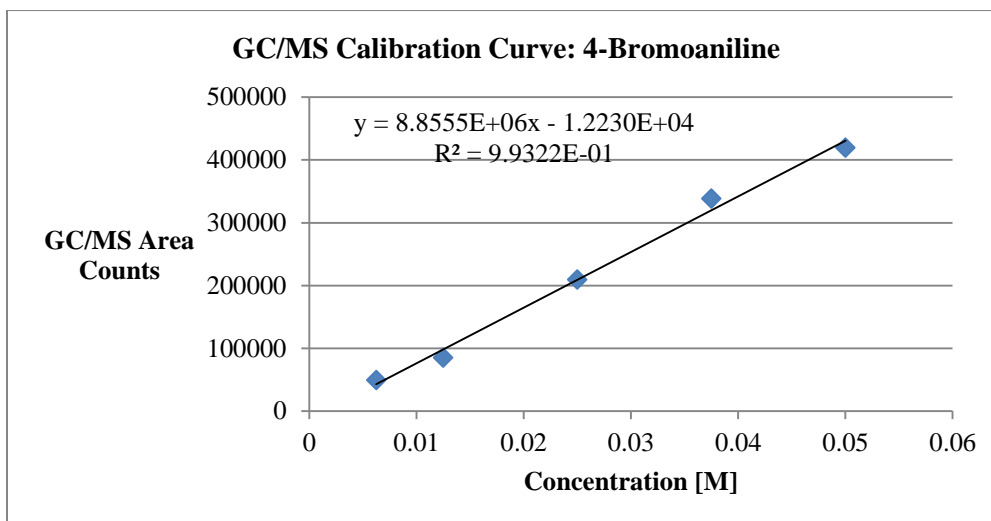


Figure 84. GC/MS Calibration Curve: 4-Bromoaniline

REFERENCES

- (1) Barden, T. In *Heterocyclic Scaffolds II*; Gribble, G. W., Ed.; Springer Berlin Heidelberg: 2011; Vol. 26, p 31.
- (2) Inman, M.; Moody, C. J. *Chemical Science* **2013**, *4*, 29.
- (3) Patil, S. A.; Patil, R.; Miller, D. D. *Current Medicinal Chemistry* **2011**, *18*, 615.
- (4) Clinic, M. http://www.mayoclinic.com/health/melatonin/NS_patient-melatonin, 2012; Vol. 2013.
- (5) Young, S. N. J. *Psychiatry Neurosci.* **2007**, *32*, 394.
- (6) AstraZeneca "AstraZeneca Announces Results of Recentin HORIZON II Phase III Trial in Metastatic Colorectal Cancer," 2010.
- (7) Gerstner, E. R.; Chen, P.-J.; Wen, P. Y.; Jain, R. K.; Batchelor, T. T.; Sorensen, G. *Neuro-Oncology* **2010**, *12*, 466.
- (8) Odiott, O.; Prevention, O. o. C. S. a. P., Ed. http://www.epa.gov/pesticides/chem_search/reg_actions/pending/fs_PC-016330_16-sep-11.pdf, 2011.
- (9) <http://www.chem.wisc.edu/areas/reich/pkatable/>
- (10) Humphrey, G. R.; Kuethe, J. T. *Chemical Reviews* **2006**, *106*, 2875.
- (11) Batcho, A. D. L., Willy *Organic Syntheses* **1985**, *63*, 214.
- (12) Hengartner, U.; Batcho, A. D.; Blount, J. F.; Leimgruber, W.; Larscheid, M. E.; Scott, J. W. *The Journal of Organic Chemistry* **1979**, *44*, 3748.
- (13) Larock, R. C.; Yum, E. K.; Refvik, M. D. *The Journal of Organic Chemistry* **1998**, *63*, 7652.
- (14) Houlihan, W. J.; Uike, Y.; Parrino, V. A. *The Journal of Organic Chemistry* **1981**, *46*, 4515.
- (15) Hemetsberger, H. K., D.; Weidmann, H. *Monatsh. Chem.* **1970**, *101*, 161.
- (16) Knittel, D. *Synthesis* **1985**, 186.
- (17) Baldwin, J. E. *Journal of the Chemical Society, Chemical Communications* **1976**, *0*, 734.
- (18) Czako, B. a. K., Laszlo *Strategic Applications of Named Reactions in Organic Synthesis*; Elsevier, 2005.
- (19) Snyder, H. R.; Beilfuss, H. R.; Williams, J. K. *Journal of the American Chemical Society* **1953**, *75*, 1873.
- (20) Heinrich, T.; Böttcher, H. *Bioorganic & Medicinal Chemistry Letters* **2004**, *14*, 2681.
- (21) Wagaw, S.; Yang, B. H.; Buchwald, S. L. *Journal of the American Chemical Society* **1999**, *121*, 10251.
- (22) Newkome, G. R.; Fishel, D. L. *The Journal of Organic Chemistry* **1966**, *31*, 677.
- (23) Siu, J.; Baxendale, I. R.; Ley, S. V. *Organic & Biomolecular Chemistry* **2004**, *2*, 160.
- (24) Katayama, S.; Ae, N.; Nagata, R. *The Journal of Organic Chemistry* **2001**, *66*, 3474.
- (25) Gassman, P. G.; Van Bergen, T. J.; Gilbert, D. P.; Cue, B. W. *Journal of the American Chemical Society* **1974**, *96*, 5495.
- (26) Orlemans, E. O. M.; Schreunder, A. H.; Conti, P. G. M.; Verboom, W.; Reinhoudt, D. N. *Tetrahedron* **1987**, *43*, 3817.
- (27) Worlikar, S. A.; Neuenswander, B.; Lushington, G. H.; Larock, R. C. *Journal of Combinatorial Chemistry* **2009**, *11*, 875.

- (28) One exception is the modified Fischer reaction which used benzophenone hydrazone (Scheme 3).
- (29) The Hemetsberger indolization can be performed at room temperature with a rhodium catalyst.
- (30) Hemetsberger, H. K., D.; Weidmann, H. *Monatsheft fur Chemie* **1969**, *100*, 1599.
- (31) O'Brien, A. G.; Levesque, F.; Seeberger, P. H. *Chemical Communications* **2011**, *47*, 2688.
- (32) Scriven, E. F. V.; Turnbull, K. *Chemical Reviews* **1988**, *88*, 297.
- (33) Bräse, S.; Gil, C.; Knepper, K.; Zimmermann, V. *Angewandte Chemie International Edition* **2005**, *44*, 5188.
- (34) Dequierez, G.; Pons, V.; Dauban, P. *Angewandte Chemie International Edition* **2012**, *51*, 7384.
- (35) Stokes, B. J.; Dong, H.; Leslie, B. E.; Pumphrey, A. L.; Driver, T. G. *Journal of the American Chemical Society* **2007**, *129*, 7500.
- (36) Kemp, J. E. G. In *Comprehensive Organic Synthesis: Selectivity, Strategy, and Efficiency in Modern Organic Chemistry*; Trost, B. M., Ed.; Pergamon: 1991; Vol. 7, p 469.
- (37) Moody, C. J. In *Comprehensive Organic Synthesis: Selectivity, Strategy, and Efficiency in Modern Organic Chemistry*; Trost, B. M., Ed.; Pergamon Press: 1991; Vol. 7, p 21.
- (38) Roy, P. J.; Dufresne, C.; Lachance, N.; Leclerc, J.-P.; Boisvert, M.; Wang, Z.; Leblanc, Y. *Synthesis* **2005**, *2005*, 2751.
- (39) Sparey, T.; Abeywickrema, P.; Almond, S.; Brandon, N.; Byrne, N.; Campbell, A.; Hutson, P. H.; Jacobson, M.; Jones, B.; Munshi, S.; Pascarella, D.; Pike, A.; Prasad, G. S.; Sachs, N.; Sakatis, M.; Sardana, V.; Venkatraman, S.; Young, M. B. *Bioorganic & Medicinal Chemistry Letters* **2008**, *18*, 3386.
- (40) Farnier, M.; Soth, S.; Fournari, P. *Canadian Journal of Chemistry* **1976**, *54*, 1074.
- (41) Lotz, S. L. M., Görls H., Crausea C., Nienaber H., and Olivier A. *Zeitschrift für Naturforschung. B* **2007**, *62*, 419.
- (42) Material Safety Data Sheets should be consulted prior to the use of alky bromoacetates and sodium azide.
- (43) McKenna, C. E.; Kashemirov, B. A.; Błażewska, K. M.; Mallard-Favier, I.; Stewart, C. A.; Rojas, J.; Lundy, M. W.; Ebetino, F. H.; Baron, R. A.; Dunford, J. E.; Kirsten, M. L.; Seabra, M. C.; Bala, J. L.; Marma, M. S.; Rogers, M. J.; Coxon, F. P. *Journal of Medicinal Chemistry* **2010**, *53*, 3454.
- (44) Campbell-Verduyn, L. S.; Mirfeizi, L.; Dierckx, R. A.; Elsinga, P. H.; Feringa, B. L. *Chemical Communications* **2009**, 2139.
- (45) Shi, F.; Waldo, J. P.; Chen, Y.; Larock, R. C. *Organic Letters* **2008**, *10*, 2409.
- (46) Li, H.; Yao, Y.; Han, C.; Zhan, J. *Chemical Communications* **2009**, *0*, 4812.
- (47) Hemetsberger, H. K., D. und Weidmann, H. *Monatshefte fur Chemie* **1970**, *101*, 161.
- (48) Lehmann, F.; Holm, M.; Laufer, S. *Tetrahedron Letters* **2009**, *50*, 1708.
- (49) Unpublished results, American Pacific Fine Chemicals Co.
- (50) Murakami, Y. W., T; et. al. *Chem. Pharm. Bull.* **1997**, *45*, 1739.
- (51) Kondo, K.; Morohoshi, S.; Mitsuhashi, M.; Murakami, Y. *CHEMICAL & PHARMACEUTICAL BULLETIN* **1999**, *47*, 1227.
- (52) Alicyclic aldehydes, cyclohexanecarboxaldehyde and cyclopentanecarboxaldehyde did not react under these conditions.
- (53) Lechter, R. M. a. A., R.M. *Organic Magnetic Resonance* **1981**, *16*, 316.
- (54) Castro, C. E.; Gaughan, E. J.; Owsley, D. C. *The Journal of Organic*

Chemistry **1966**, 31, 4071.

(55) The literature also reports the indolization promoted by a rhodium catalyst. In these reactions quantitative yields are obtained at temperatures ranging from 25°C to 60°C.

(56) Curiel, D.; Espinosa, A.; Mas-Montoya, M.; Sanchez, G.; Tarraga, A.; Molina, P. *Chemical Communications* **2009**, 0, 7539.

(57) Prasad, G. K. B.; Burchat, A.; Weeratunga, G.; Watts, I.; Dmitrienko, G. I. *Tetrahedron Letters* **1991**, 32, 5035.

(58) Samsoniya, S. A.; Chikvaidze, I. S.; Kadzhrishvili, D. O.; Targamadze, N. L. *Chem Heterocycl Comp* **2010**, 46, 536.

(59) Samsoniya, S. A.; Kadzhrishvili, D. O.; Chikvaidze, I. S. *Pharm Chem J* **2011**, 45, 22.

(60) Pyrroloindoles with these core structures have been reported in literature as they are of interest for their biological activity.²³⁻²⁶ Curiel et al. synthesized a pyrroloindole similar to 3i' via the Hemetsberger indolization by having two methoxy substituents between the para-azidoacrylates in 2i.²³

(61) In its most basic form atom economy is defined as the (mass of product)/(mass of all reactants) x 100%.

(62) Hou, J.; Li, Z.; Fang, Q.; Feng, C.; Zhang, H.; Guo, W.; Wang, H.; Gu, G.; Tian, Y.; Liu, P.; Liu, R.; Lin, J.; Shi, Y.-k.; Yin, Z.; Shen, J.; Wang, P. G. *Journal of Medicinal Chemistry* **2012**, 55, 3066.

(63) Tao, B.; Boykin, D. W. *The Journal of Organic Chemistry* **2004**, 69, 4330.

(64) McNulty, J.; Keskar, K. *European Journal of Organic Chemistry* **2011**, 2011, 6902.

(65) Taylor, S. J.; Abeywardane, A.; Liang, S.; Muegge, I.; Padyana, A. K.; Xiong, Z.; Hill-Drzewi, M.; Farmer, B.; Li, X.; Collins, B.; Li, J. X.; Heim-Riether, A.; Proudfoot, J.; Zhang, Q.; Goldberg, D.; Zuvella-Jelaska, L.; Zaher, H.; Li, J.; Farrow, N. A. *Journal of Medicinal Chemistry* **2011**, 54, 8174.

(66) Sudhakara, A.; Jayadevappa, H.; Mahadevan, K. M.; Hulikal, V. *Synthetic Communications* **2009**, 39, 2506.

(67) The 2010 Nobel Prize in Chemistry was shared between Richard Heck, Ei-ichi Negishi, and Akira Suzuki.

(68) Hassan, J.; Sévignon, M.; Gozzi, C.; Schulz, E.; Lemaire, M. *Chemical Reviews* **2002**, 102, 1359.

(69) Suzuki, A. *Angewandte Chemie International Edition* **2011**, 50, 6722.

(70) Amatore, C.; Jutand, A.; Le Duc, G. *Chemistry – A European Journal* **2011**, 17, 2492.

(71) Amatore, C.; Jutand, A.; Le Duc, G. *Angewandte Chemie International Edition* **2012**, 51, 1379.

(72) Carrow, B. P.; Hartwig, J. F. *Journal of the American Chemical Society* **2011**, 133, 2116.

(73) <http://www.chem.wisc.edu/areas/reich/pkatable/index.htm>

(74) Web of Science search results when "Suzuki coupling" is a topic

(75) Billingsley, K. L.; Anderson, K. W.; Buchwald, S. L. *Angewandte Chemie International Edition* **2006**, 45, 3484.

(76) Hanhan, M. E.; Martínez-Máñez, R.; Ros-Lis, J. V. *Tetrahedron Letters* **2012**, 53, 2388.

(77) Thakur, A.; Zhang, K.; Louie, J. *Chemical Communications* **2012**, 48, 203.

(78) Martin, R.; Buchwald, S. L. *Accounts of Chemical Research* **2008**, 41, 1461.

(79) Lamblin, M.; Nassar-Hardy, L.; Hierso, J.-C.; Fouquet, E.; Felpin, F.-X. *Advanced Synthesis & Catalysis* **2010**, 352, 33.

(80) Machnitzki, P.; Tepper, M.; Wenz, K.; Stelzer, O.; Herdtweck, E. *Journal of*

- Organometallic Chemistry* **2000**, 602, 158.
- (81) Western, E. C.; Daft, J. R.; Johnson, E. M.; Gannett, P. M.; Shaughnessy, K. H. *The Journal of Organic Chemistry* **2003**, 68, 6767.
- (82) Zhou, C.; Wang, J.; Li, L.; Wang, R.; Hong, M. *Green Chemistry* **2011**, 13, 2100.
- (83) Fleckenstein, C. A.; Plenio, H. *Chemistry – A European Journal* **2008**, 14, 4267.
- (84) Itoh, T.; Mase, T. *Tetrahedron Letters* **2005**, 46, 3573.
- (85) Arvela, R. K.; Leadbeater, N. E.; Mack, T. L.; Kormos, C. M. *Tetrahedron Lett.* **2006**, 47, 217.
- (86) Han, W.; Liu, C.; Jin, Z. *Advanced Synthesis & Catalysis* **2008**, 350, 501.
- (87) Leadbeater, N. E.; Williams, V. A.; Barnard, T. M.; Collins, M. J. *Organic Process Research & Development* **2006**, 10, 833.
- (88) Liu, C.; Ni, Q.; Bao, F.; Qiu, J. *Green Chemistry* **2011**, 13, 1260.
- (89) Liu, C.; Ni, Q.; Hu, P.; Qiu, J. *Organic & Biomolecular Chemistry* **2011**, 9, 1054.
- (90) Mondal, M.; Bora, U. *Green Chemistry* **2012**, 14, 1873.
- (91) Turkmen, H.; Can, R.; Cetinkaya, B. *Dalton Transactions* **2009**, 0, 7039.
- (92) Wong, S. M.; So, C. M.; Chung, K. H.; Luk, C. H.; Lau, C. P.; Kwong, F. Y. *Tetrahedron Letters* **2012**, 53, 3754.
- (93) Badone, D.; Baroni, M.; Cardamone, R.; Ielmini, A.; Guzzi, U. *The Journal of Organic Chemistry* **1997**, 62, 7170.
- (94) DeVasher, R. B.; Moore, L. R.; Shaughnessy, K. H. *The Journal of Organic Chemistry* **2004**, 69, 7919.
- (95) Štěpnička, P.; Krupa, M.; Lamač, M.; Císařová, I. *Journal of Organometallic Chemistry* **2009**, 694, 2987.
- (96) Arvela, R. K.; Leadbeater, N. E. *Org. Lett.* **2005**, 7, 2101.
- (97) Leadbeater, N. E.; Marco, M. *Org. Lett.* **2002**, 4, 2973.
- (98) Leadbeater, N. E.; Marco, M. *J. Org. Chem.* **2003**, 68, 888.
- (99) Liu, C.; Han, N.; Song, X.; Qiu, J. *European Journal of Organic Chemistry* **2010**, 2010, 5548.
- (100) Liu, C.; Yang, W. *Chemical Communications* **2009**, 0, 6267.
- (101) Liu, C.; Zhang, Y.; Liu, N.; Qiu, J. *Green Chemistry* **2012**, 14, 2999.
- (102) Thompson, A. E.; Hughes, G.; Batsanov, A. S.; Bryce, M. R.; Parry, P. R.; Tarbit, B. *The Journal of Organic Chemistry* **2004**, 70, 388.
- (103) Caron, S.; Massett, S. S.; Bogle, D. E.; Castaldi, M. J.; Braish, T. F. *Organic Process Research & Development* **2001**, 5, 254.
- (104) Peeters, A.; Ameloot, R.; De Vos, D. E. *Green Chemistry* **2013**, 15, 1550.
- (105) Rohan, A. L.; Switzer, J. R.; Flack, K. M.; Hart, R. J.; Sivaswamy, S.; Biddinger, E. J.; Talreja, M.; Verma, M.; Faltermeier, S.; Nielsen, P. T.; Pollet, P.; Schuette, G. F.; Eckert, C. A.; Liotta, C. L. *ChemSusChem* **2012**, 5, 2181.
- (106) Shannon, M. S.; Bara, J. E. *Separation Science and Technology* **2011**, 47, 178.
- (107) Carrow and Amatore reported on the role of palladium-hydroxy complexes in the transmetallation step, see section.
- (108) Reactions at elevated pressure require extra safety measures, so these reactions were performed in Parr reactors behind blast shields.
- (109) Leadbeater, N. E.; Resouly, S. M. *Tetrahedron* **1999**, 55, 11889.
- (110) Zhang, L.; Wang, L.; Li, H.; Li, P. *Synthetic Communications* **2008**, 38, 1498.
- (111) Peng, Y.-Y.; Liu, J.; Lei, X.; Yin, Z. *Green Chemistry* **2010**, 12, 1072.
- (112) Leadbeater, N. E.; Schmink, J. R. *Tetrahedron* **2007**, 63, 6764.
- (113) Wan, J.-P.; Wang, C.; Zhou, R.; Liu, Y. *RSC Advances* **2012**, 2, 8789.
- (114) Leadbeater, N.; American Chemical Society: 2005, p 52.

- (115)Leadbeater, N.; American Chemical Society: 2005, p 613.
(116)Leadbeater, N. E.; American Chemical Society: 2004, p 42.
(117)Leadbeater, N. E. *Chem. Commun. (Cambridge, U. K.)* **2005**, 2881.
(118)Leadbeater, N. E.; Smith, R. J. *Org. Biomol. Chem.* **2007**, 5, 2770.